VEGF signalling toward MRTF/SRF-mediated transcriptional activation in endothelial cells

Dissertation

der Mathematisch-Naturwissenschaftlichen Fakultät

der Eberhard Karls Universität Tübingen

zur Erlangung des Grades eines

Doktors der Naturwissenschaften

(Dr. rer. nat.)

vorgelegt von

Dongjeong Park

aus Jeongseon, Südkorea

Tübingen

2016

Gedruckt mit Genehmigung der Mathematisch-Naturwissenschaftlichen Fakultät der Eberhard Karls Universität Tübingen.

Tag der mündlichen Qualifikation:	22.04.2016
Dekan:	Prof. Dr. Wolfgang Rosenstiel
1. Berichterstatter:	Prof. Dr. Alfred Nordheim
2. Berichterstatter:	Prof. Dr. Reiner Lammers

Acknowledgement

To end up this dissertation, I have a lot of people to convey my appreciation.

To begin with, I sincerely thank Prof. Dr. Alfred Nordheim who gave me an opportunity to work on this interesting topic, especially for the kind discussions and supervision.

I also would like to extend my special thanks to Prof. Dr. Leiner Lammer for having kindly agreed to be my supervisor and for discussions and comments during seminars in GRK.

Dr. Christine Weinl who is my project supervisor and role model, without whom I can never imagine that I could have completed this study. I appreciate her guidance, continuous encourage me and meaningful advises. I will never forget the time with her.

Heidemarie Riehle, a gentle colleague of mine, she helped and advised me with a lot of tips based on her plentiful experience, also the enjoyable coffee break with her. I thank her for the time that I had with her.

Dr. Christine Stritt, I thank for the kind and productive cooperation and discussion. In working with her, I enjoyed the experiments and learnt a lot.

Dr. Stefan Ohrnberger who was my kind colleague who introduced and helped me technically and made a smooth atmosphere in the lab. To Abhishek Thavamani, I would like to say thank to him for making a joyful mood in the lab and helping me.

I am grateful to persons who are engaged in the lab 2.010. To Anke Biedermann, Dr. Siegfried Alberti, Katja Oesterle and Lisa Nill, they also as good colleagues shared nice experiences with me. They helped and advised me during various experiments. Especially, to Anke for the preparation of chemicals, to Katja for the ordering, to Siggi for plasmid and SRF antibodies.

My thanks must go also to Heiderose Kraus for office work and documentations as well as kind greeting to me. My thanks and appreciation to Elena Kullmann. She technically supported and prepared labour apparatus with smiles.

To the group members of autophagy, Tassula, Simon, Mario, Daniela, Zsuzsanna and Ann-Katrin, I express my thanks for the friendly atmosphere and productive discussions during seminars and journal club in the department.

I am going to really miss all the members of the ‘‘molbios’’ and my wonderful memories of Tübingen.

I also would like to thank GRK 1302 and all members. Especially, I need to express my gratitude and deep appreciation to Charles Anton, the coordinator of GRK who oriented me into the programs and supported my desk works.

Finally, I would like to say all my heart-felt thanks to my dear family who always support me and are there for me. Even though they are far from me, they always encourage and believe in me. This dissertation is dedicated to them.

Table of contents

Keywords:

Serum Response Factor (SRF), Myocardin Related Transcription factor (MRTF), Actin dynamics, small RhoA GTPase, Endothelial cells (ECs), Vascular endothelial growth factor (VEGF), Angiogenesis

1. INTRODUCTION

1.1 Serum Response Factor (SRF)

Serum response factor is a ubiquitously expressed transcription factor that regulates numerous genes involved in various cellular activities such as proliferation, migration, differentiation, apoptosis, and angiogenesis. Based on the data in 2010, approximately 300 human genes contain an SRF binding site, called Serum Response Element (SRE) (Chai and Modak, 2010). This accounts for 1% of the entire human genome. Moreover, 960 SRF-linked genes and more than 3100 SREs were recently identified (Esnault et al., 2014). Among them, at least 196 genes are involved in cytoskeleton remodelling.

1.1.1 Discovery of SRF

In 1984, activation of the *c-fos* and *β-actin* genes was detected in serum-stimulated NIH 3T3 cells (Greenberg and Ziff, 1984). This activation of c-fos was very rapidly (peak at 10 min) and transiently (decrease by 15 min) observed and was not effectively induced by other growth factors or hormones.

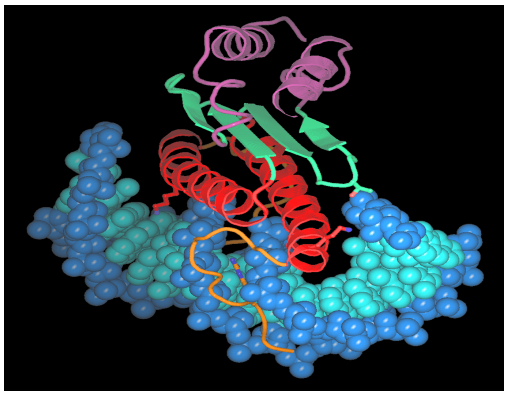

Figure 1.1: The structure of SRF core and SRF-DNA complex

Crystal structure shows that SRF binds to DNA (Source of figure: Prof. T. Richmond, ETH Zurich).

By searching of the *c-fos* promoter region, a transcription factor that binds to specific DNA sequence of *c-fos* was identified and this transcription factor was named serum response factor (SRF) (Treisman, 1986 and 1987). By isolation and characteristics studies of SRF cDNA clones, properties of SRF were further understood. SRF is required for transient activation of genes activated by growth factors and SRF is confirmed as an evolutionary conserved nuclear protein (Norman et al., 1988).

1.1.2 The SRF structure

In the chromosome, the SRF gene is located at 17C region in mouse (*Mus musculus*) and at 6p21.1 in human (*Homo sapience*). The length of the SRF transcript is 4093 bp in mouse, 4343 bp in human, respectively. In both species, the SRF gene consists of 7 exons (Fig. 1.2).

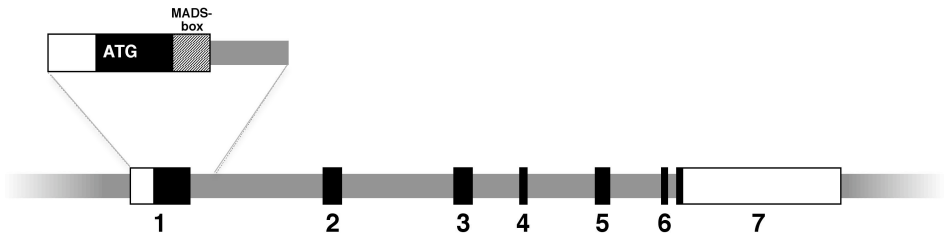

Figure 1.2: The structure of the SRF gene

7 exons of SRF are schematically represented. Each number indicates SRF exons. Protein coding regions are marked as black and non-coding regions are shown in white (Angstenberger, 2007).

The SRF gene generates transcriptional variants as a result of alternative splicing (Kemp and Metcalfe, 2000). Hence, different types of SRF proteins are generated as tissue-specific forms (Fig. 1.3). The full length SRF (SRF-L) is a 67 kDa SRF protein that contains all of the seven SRF exons. It is composed of three district domains: a DNA binding domain, a transactivation domain, and multiple phosphorylation sites. The DNA binding domain is an evolutionary highly conserved homologous domain (about 93% identity between fruit fly and human) that is associated with dimerization and interaction with accessory proteins. SRF-M (62 kDa) is a dominant negative form of SRF protein, which lacks exon 5 (Belaguli et al., 1999). Both of these SRF isoforms have a DNA binding affinity. SRF-S (52 kDa) lacks exon 4 and 5 and this

isoform is only detected in the aorta. The smallest isoform of SRF-I (48 kDa), which lacks exon 3, 4 and 5, is selectively detected in embryos (Chai et al., 2002; Modak and Chai, 2010).

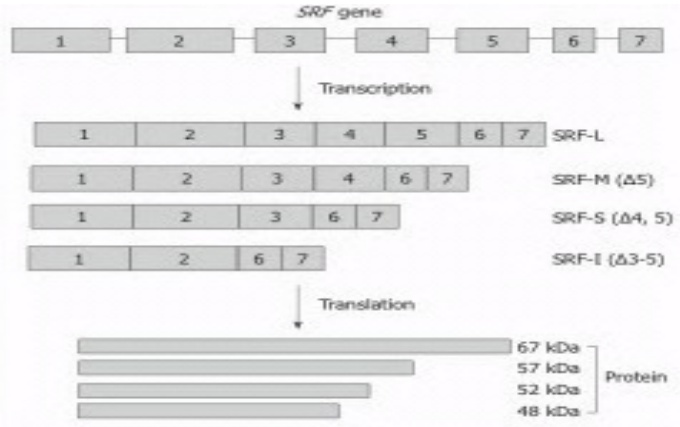

Figure 1.3: SRF splicing variants

The splicing variants of SRF are generated from 7 SRF exons. 4 transcriptional variants were detected by RT-PCR, protein isoforms confirmed by western blotting (Modak and Chai, 2010).

1.1.3 DNA binding of SRF

SRF belongs to the MADS-box transcription factor family. MADS-box genes are ubiquitously conserved 55 to 60 amino acids that encode a DNA binding domain at the N-terminus, named MADS-domain. The acronym MADS originates from the initials of identified proteins in each species: MCM1 (*Saccharomyces cerevisiae*), AGAMOUS (*Arabidopsis thaliana*), DEFICIENS (*Antirrhinum majus*), and SRF (*Homo sapiens*) in mammals (Schwarz-sommer et al., 1990).

SRF binds to DNA as a *cis*-homo dimer form (Norman et al., 1988). This binding site for SRF is known as SRE (serum response element) and also designated as the CArG box. The CArG box is the decamer, which consists of $CC(A/T)_6GG$ sequences (Fig. 1.4). The CArG box was first detected in the evolutionary conserved upstream region of cardiac actin genes in vertebrates (Minty and Kedes, 1986). The CArG box sequence is the critical factor that determines binding of SRF to the DNA. The binding affinity of SRF is mediated by C and G pair in the CArG box, whereas A and T pair do not intrinsically alter the binding affinity (Huet et al., 2005). Due to this characteristic, the CArG box is divided into two classes: the canonical CArG box (no

variation in SRF decamer sequence) and the non-canonical CArG box (with a variation in A and T nucleotide). Changes of the nucleotide sequences in the CArG box influence transcriptional activity as well as specificity of binding of SRF. For example, mutations on oligonucleotide could result in an unusual monomeric or a tetrameric binding of SRF (Huet et al, 2005). SRF binding sites are cell type-specifically reported, suggesting that SRF cofactors plays an important role in determining cell type-dependent SRF binding (Cooper et al., 2007).

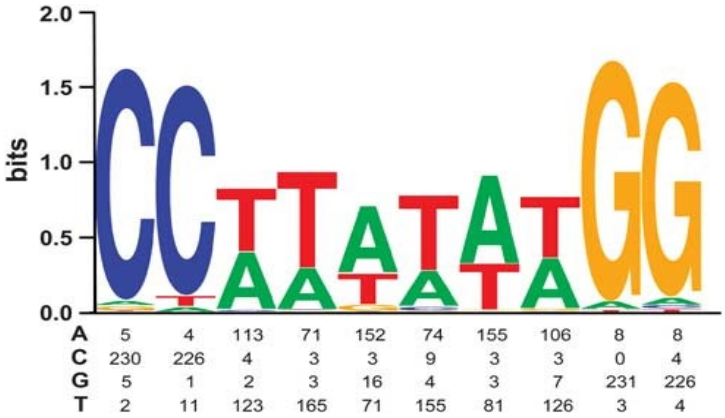

Figure 1.4: The CArG box sequences

CArG box nucleotides are analysed from 242 conserved CArG boxes. Frequencies of each nucleotide are highlighted by the height of each nucleotide (Miano, 2010).

1.1.4 Activation of SRF

Serum- or growth factor-induced activation of SRF is mediated by at least two known pathways: the TCF and RhoA-MRTF pathway. Therefore, SRF target genes are classified into two classes according to signal responsiveness.

1.1.4.1 TCF-dependent activation of SRF

The activity of SRF is modulated through its interaction with accessory proteins. Ternary complex factors (TCFs) were the first identified SRF cofactors (Shaw et al., 1989) that consist of SAP-1 (SRF accessory protein 1, also called Elk-4) (Dalton and Treisman 1992; Dalton et al., 1993), Elk-1 (Ets-like protein 1) (Hipskind et al., 1991), and Net (also termed ERP or SAP-2) (Giovane et al., 1994 and 1997). These proteins bind to Ets-binding site (EBS) of ETS-DNA-binding domain at the N-terminus. Adjacent this domain, TCFs have the SRF binding domains and transcription activation

domains. For transcriptional activation, Elk-1, Net, and SAP-1 form a ternary nucleoprotein complex with SRF/DNA complex over SRF binding domain (Buchwalter et al., 2004), thereby activating class I SRF target genes. IEGs (immediate early gene: transcription occurs immediately upon stimulation regardless of prior protein synthesis), CTGF (connective tissue growth factor or CCN2), BDNF (brain-derived neurotrophic factor), synaptic plasticity associated gene Arc (Knöll, 2011), and Per1 (Esnault et al., 2014) are the members of this group of SRF target genes.

TCFs are regulated by activation of MAPK (mitogen-activated protein kinase). As seen in Figure 1.5, MAPK cascades are followed by serial phosphorylation. The MAP kinases are serine/threonine kinases that finally activate *c-fos*, *c-jun*, *c-myc* via ras small GTPas-Raf–MEK1/2-ERK pathway. The activation of TCFs/SRF complex is implicated in the regulation of cell proliferation.

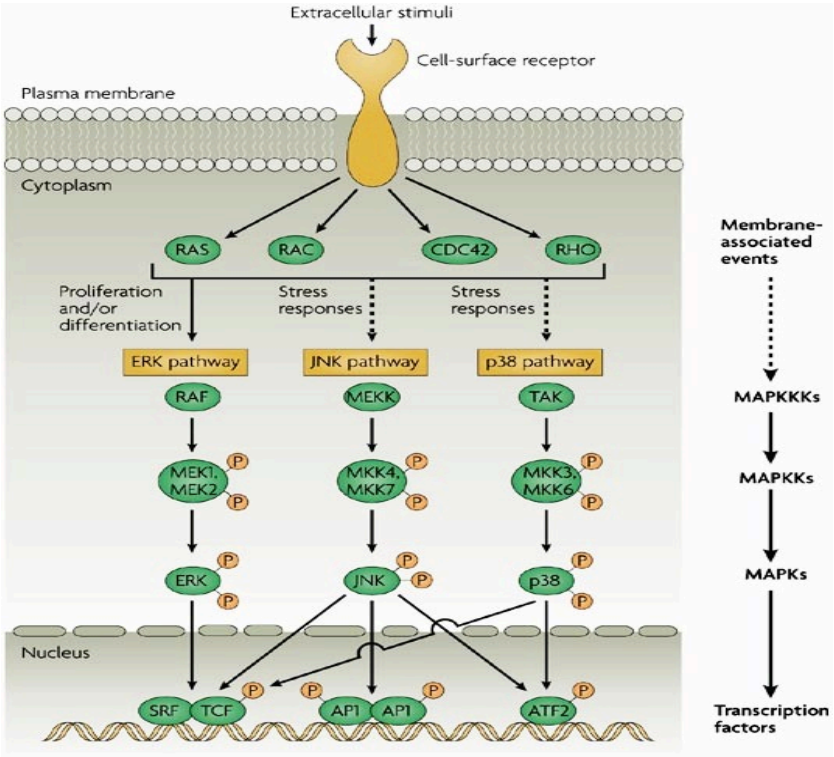

Figure 1.5: Activation of SRF in cooperation with TCFs

Extracellular stimulation by growth factors, cytokines or stress activated membrane associated small GTPases like Ras, Rac, cdc42, or Rho results in activation of MAPKKKs (MAPK kinase kinases) which leads to phosphorylation of MAPKKs (MAPK kinases) on two serine residues. Followed phosphorylation of the MAPKs on threonine and tyrosine residues, then catalytic sites of MAPK are activated. Activated MAPK subsequently translocates into the nucleus and phosphorylates TCFs transcription factors. TCFs form a complex with SRF to regulate IEGs expression/transcription (Liu et al., 2007).

According to a recent study, a 76 TCF-SRF-inducible gene signature was identified (Esnault et al., 2014). However, SRF binding sites for TCF binding sites were a minority among identified binding site for SRF.

1.1.4.2 RhoA/MRTF-dependent activation of SRF

SRF can also be activated by a second class of cofactors, myocardin and Myocardin Related Transcription Factor (MRTF) (Fig. 1.6). In this scenario, SRF controls its class II target gene expression independently of the MAPK pathway-driven TCFs' activation (Gineitis and Treisman 2011; Selvaraj and Prywes 2004; Knöll, 2011).

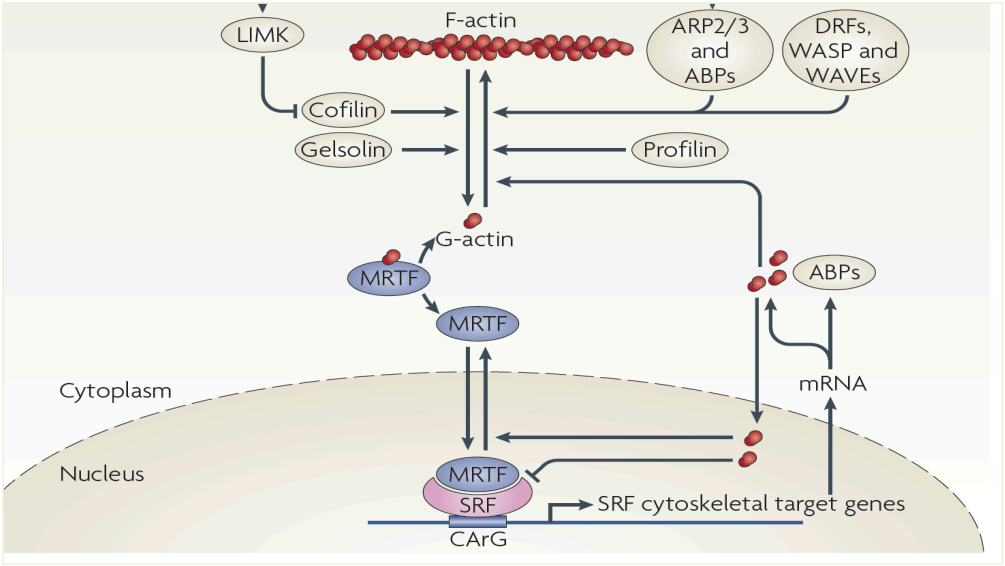

Figure 1.6: SRF activation by its cofactor MRTF

SRF activation is regulated by actin dynamics driven by its cofactors MRTFs. MRTF-A and -B are complexed with G-actin in the cytoplasm, thereby MRTF is held back in the cytoplasm. In this complex, MRTF remains inactive and does not translocate to the nucleus. Upon actin polymerization, the G-actin pool in the cytoplasm is depleted, and then followed translocation of MRTF-A into the nucleus. Therefore, MRTF-driven SRF activation is actin-dependently achieved. In this process, various actin-binding proteins are involved. For example, Profilin, ARP2/3, and WASP can stimulate MRTF activation. On the other hand, Cofilin and Gelsolin suppress MRTF activation. ARP2/3: actin-related proteins (Arp2 and Arp3), WASP: Wiskott–Aldrich-syndrome protein (Olson and Nordheim, 2010).

SRF target genes related to SMC differentiation and the actin cytoskeleton genes are regulated by this mechanism. For instance, actin isomer genes such as Actb (β-actin), Actc (cardiac muscle actin), Actg (γ-actin), Acta (Actin assembly-inducing pro-

tein), actin binding proteins (Gelsolin, Vinculin, Transgelin, Tropomyosin, Myosin) and SM genes (SMα, SM22) are transcriptionally regulated by MRTF-SRF signalling (Knöll, 2011). In addition, some circadian clock-related genes are also regulated by SRF (Balsalobre et al, 1998). Among them, Per2, Nr1d1, Rora, and Nfil3 are identified as MRTF-dependent SRF target genes (Esnault et al., 2014). Since the majority of SRF sites recruits MRTF rather than TCFs, the activation of SRF by MRTF plays an important role in growth factor-mediated signalling. Based on these observations, the MRTF-SRF signalling are key regulators of cell-cell or cell-substrate interaction, ECM components, cytoskeletal dynamics, and gene expression (Esnault et al., 2014).

1.1.4.3 Competition between TCFs and MRTF for regulation of SRF

Since TCFs and MRTFs use the same regions to bind to the DNA, a competitive binding mechanism between both cofactors has been suggested (Fig. 1.7) (Posern and Treisman, 2006). In many cells, competition between TCFs and MRTFs for SRF is likely to happen, because their co-expression is commonly observed. This competition contributes to the binary choice of SRF that is specific to each binding site (Clark and Graves, 2014). The relative levels of two factors are diverse in different cell types, suggesting cell type- or promoter specific binding of SRF cofactors.

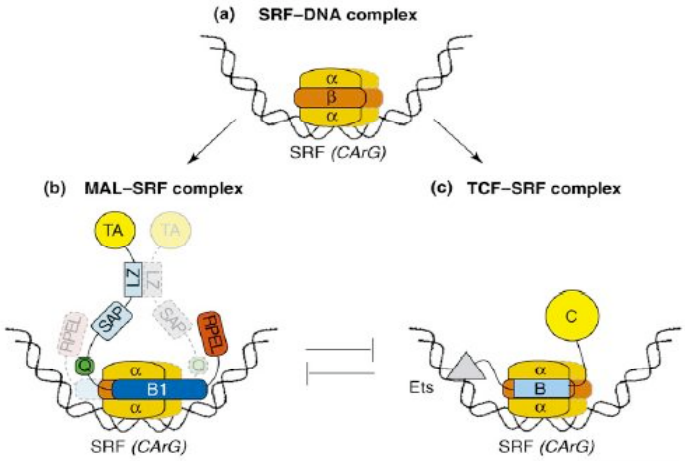

Figure 1.7: Models for SRF-MRTF and SRF-TCFs binding

(**a**): SRF binds to the DNA as a α-β-α sandwich structure on the CArG box. (**b**): MRTF dimer binds to SRF via B1-SRF interaction (one MRTF molecule is designated as shaded colours). (**c**): Ets domain of TCFs interacts with DNA and its B-box interacts with SRF (Posern and Treisman, 2006).

According to recent experimental results, bindings of SRF-MRTF are differently observed from binding of SRF-TCFs (Esnault et al., 2014; Clark and Graves, 2014). For example, SRF-MRTF peaks contain more CArG boxes with a closer match to the consensus than SRF-TCFs peaks. In addition, SRF-MRTF sites have more AP-1 and TEAD motifs. In contrast, more motifs for ETS factors, such as SP-1 and NFY-binding motif, are found near TCFs/SRF peak. Moreover, TCFs prebound already to the DNA and they bound to the SRE via B-box upon phosphorylation. However, upon serum stimulation, nucleosomes near SRF-MRTF binding sites are displaced (Fig. 1.8). Therefore, SRF-MRTF displays higher occupancy than SRF-TCFs after serum stimulation.

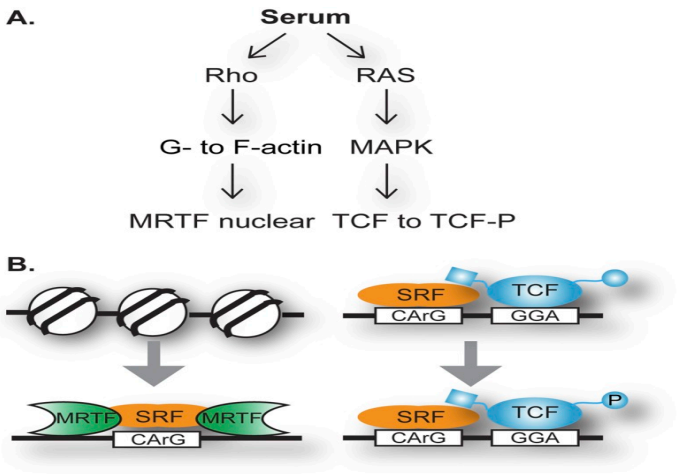

Figure 1.8: Nucleosome coverage of SRF-MRTF and SRF-TCFs complex

SRF target gene expression is mediated by either MRTFs or TCFs with different mechanisms. (**A**): Serum (SRF activator) triggers activation of MRTF via Rho or TCFs via MAPK. (**B**): Response to Rho signalling, SRF binding to DNA is stimulated by nucleosome displacement, therefore DNA binding of MRTF is SRF-DNA binding dependent. Response to Ras/MAPK, TCFs independently bind to DNA and TCFs bind to SRF via B-box (Clark and Graved, 2014).

Among identified SRF genomic binding sites, about 1000 sites are constitutively activated and about 2100 sites are inducible near SRF-binding sites (Esnault et al., 2014). These inducible sites are in most cases MRTF-dependent. Interestingly, the majority of TCF sites are SRF-independent whereas the majority binding sites for MRTF correlate with SRF.

However, there are also 755 solo SRF binding sites, where TCF or MRTF cofactors were not found. This observation suggests constitutively activated SRF transcription or a possibility of an existence of an unidentified cofactor.

1.1.5 The SRF coactivator Myocardin-Related Transcription Factor (MRTF)

Myocardin and MRTF-A/-B are defined as the second class of SRF partner proteins. MRTF-A is also named megakaryoblastic leukemia1 (MKL1), megakaryocytic acute leukemia (MAL), acute megakaryoblastic leukemia (AMKL), MKL/myocardin-like protein 1, BSAC (basic, SAP and coiled-coil), or KIAA1438. MRTF-B is known as megakaryoblastic leukemia2 (MKL2), MKL/myocardin-like protein 2, or Gt4-1 (gene rap insertion site 4-1). In the present work, the terms MRTF-A and MRTF-B will be used.

1.1.5.1 Structure and expression of MRTF

The murine MRTF-A gene consists of 14 exons that distribute up to 37 kb of DNA. The location of murine MRTF-A is on chromosome 15 (Li et al., 2006) and human MRTF-A gene is located on the chromosome 22. MRTF-B is located on the chromosome 16 in both species.

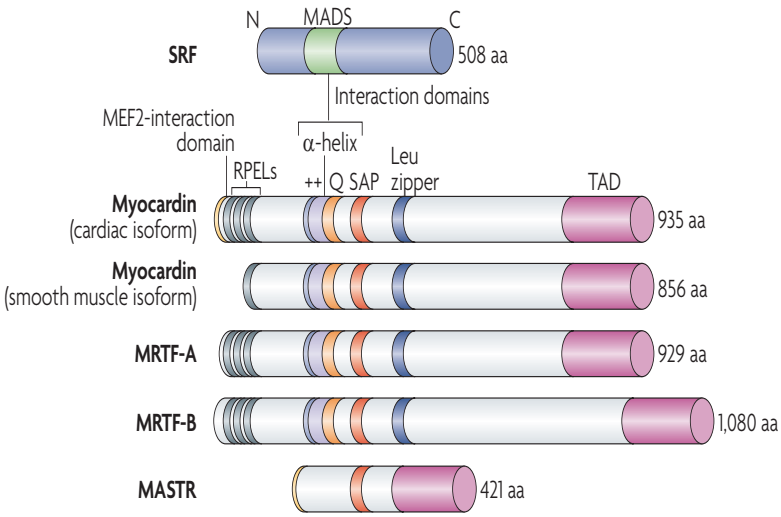

Figure 1.9: Schematic representation of SRF and myocardin family members

The domain structures of the mouse proteins are shown. SRF contains the conserved 57-aa MADS box which mediates homodimerization and has a binding activity to other cofactors and DNA. Myocardin, MRTF-A, and MRTF-B share the following conserved domains: RPEL, basic (++), glutamine-rich (Q), SAP, and LZ domain. The variant MASTR lacks SRF-interacting domains (Olson and Nordheim, 2010).

In Fig. 1.9, sub-domains of MRTF-A and -B are schematically represented (Olson and Nordheim, 2010). Each domain has functional roles in MRTF activity (Wang and Olson, 2004; Olson and Nordheim, 2010). At the N-terminus of myocardin family proteins, RPEL domains (Arg-Pro-X-X-X-Glu-Leu motif) are located. These domains are defined as actin-binding elements of this family (Guettler et al., 2008). Among 3 RPEL domains (from RPEL 1 to 3) in MRTF-A and -B, RPEL1 and RPEL2 have a high binding affinity to actin whereas RPEL 3 has a weak affinity to actin. Within the RPEL domain, MRTF-A contains a bipartite nuclear localization signal (NLS) (Pawlowski et al., 2010). Basic region and glutamine-rich domain are required for binding of MRTF to SRF as well as nuclear translocation of MRTF. Between these two regions, a short α-helical region is located, named B-box, which mediates an MRTF-SRF interaction. The role of Leu zipper domain is known to mediate homo- and hetero-dimerization of MRTF. A SAP (SAF-A/B, Acinus, PIAS) domain is found in some proteins that are known to bind to DNA. This region is responsible for transcriptional control and chromatin remodelling. Deletion of this region disrupts myocardin/SRF-dependent gene expression. A TAD domain (transcriptional activation domain) at the C-terminus mediates transcriptional activity of SRF.

Even though MRTF belongs to the myocardin-family group of transcription factors, the expression pattern of MRTF-A and -B can be distinguished from myocardin (Wang et al., 2002). Myocardin is linage-restricted expressed in the embryo and postnatal stages, and its expression is limited to cardiac myocytes and SMC. In heart, the 935-aa isoform of myocardin is predominantly detected and the 856-aa isoform of myocardin is mainly expressed in SMC-containing tissues. In contrast to myocardin, MRTF-A and -B are widely expressed in broad lineage of cells.

1.1.5.2 Regulatory mechanisms of MRTF

Translocational activity of MRTF

Translocational activity of MRTF was first reported by Miralles and co-workers (Miralles et al., 2003). In serum-starved cells, the location of MRTF-A was predominantly observed in the cytoplasm. However, upon 60 min of serum stimulation, MRTF-A was predominantly detected in the nucleus in murine fibroblast cells (Fig. 1.10).

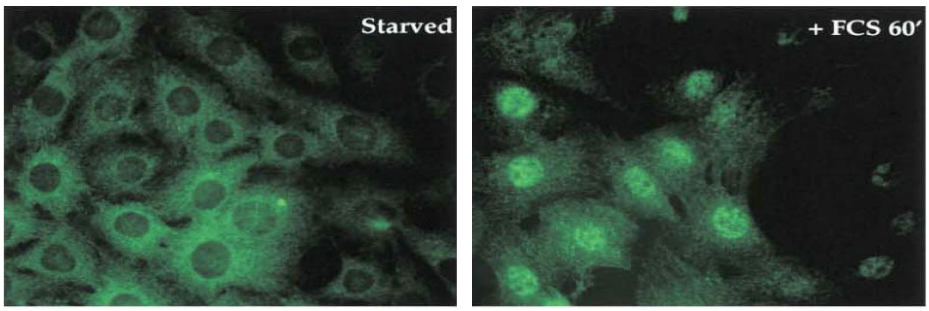

Figure 1.10: Change of sub-cellular location of MRTF-A upon serum stimulation

HA-tagged endogenous MRTF-A was visualized with GFP (green). Stimulation with serum changed sub-cellular location of MRTF-A in NIH 3T3 cells (Miralles et al., 2003).

Miralles' study also identified that RhoA-involved change in actin dynamics is the key mechanism of the translocational activity of MRTF-A. The nuclear accumulation of MRTF-A was not observed in the presence RhoA inhibitor, C3 transferase. However, blockage of MAPK or ROCK (downstream of RhoA), or of PI3K did not affect the nuclear accumulation of MRTF-A. In addition, in cells incubated with actin binding drugs such as Cytochalasin D and Swinholide A, MRTF-A was predominantly detected in the nucleus. These observations suggest that the MRTF-A accumulation in the nucleus is strictly dependent on RhoA and actin dynamics, but not dependent on ROCK or MAPK pathway.

Further, this mechanism was also reported in cancer cells (Medjkane et al., 2009). Interestingly, in two different tumour cells, the location of MRTF-A was observed in different cellular compartments. In human breast carcinoma cell MDA-MB-231, MRTF-A was predominantly seen in the nucleus even under starved condition. In this cell, MRTF-A went back to the cytoplasm with the treatment of Lat B or RhoA inhibitor. In contrast, in starved mouse melanoma cell line B16F2, MRTF-A was predominantly observed in the cytoplasm. Upon treatment of serum, MRTF-A was enriched in the nucleus and treatment with Lat B or RhoA inhibitor abolished this process. Besides, RhoA-dependent MRTF-A accumulation in the nucleus was reported in other cells such as in neuronal cells (Tabuchi et al., 2005) and in megakaryocytes (Smith et al., 2013). These data demonstrate that MRTF-A shuttles between the cytoplasm and the nucleus in most investigated cells.

The translocation of MRTF is regulated by two mechanisms: the balancing between its nuclear import and export, and the G-actin/MRTF interaction. Blockage of nuclear export protein (Exportin) resulted in MRTF-A enrichment in the nucleus and the B2

region (between RPEL domain 2 and 3) of MRTF was required for this process (Vartiainen et al., 2007). Serum is also involved in nuclear export of MRTF. In a resting condition, the export rate of MRTF to the cytoplasm was very high. However, it is dramatically reduced upon serum stimulation since serum blocks nuclear export of MRTF to the cytoplasm.

In the cytoplasm, MRTF-A is promoted to interact with G-actin via its N-terminus RPEL domains. The crystal structure of G-actin/MRTF complex shows that this binding is achieved via either pentavalent or trivalent assembly between G-actin and MRTF (Mouilleron et al., 2011). By binding with G-actin, MRTF-A remains inactive in the cytoplasm. Once actin polymerization is promoted, for example by activation of RhoA, stress fibre formation is accelerated by incorporation of G-actin to F-actin. This results in depletion of G-actin pool in the cytoplasm and reduction in MRTF-A interaction with G-actin. When MRTF is liberated from G-actin/MRTF complex, free MRTF-A can translocate to the nucleus. G-actin also alters in this process. To enter the nucleus MRTF-A uses Importin (Impα/β)-dependent import pathway. G-actin inhibits this pathway since MRTF-A competitively binds to Importin with G-actin. Moreover, another study demonstrated that nuclear actin dynamics also influences MRTF. Nuclear mDia-mediated actin polymerization promotes MRTF-A accumulation in the nucleus and subsequent MRTF-SRF transcription (Baarlink et al., 2013).

Taken together, serum-induced accumulation of MRTF-A in the nucleus is regulated by nuclear transport mechanism (import/export) of MRTF and/or by interaction of MRTF with G-actin controlled by RhoA-driven actin dynamics.

MRTF phosphorylation

Post-translational modifications of MRTF are not much known. Of note, phosphorylation is an important mechanism to regulate MRTF activity. In the nucleus, G-actin-bound MRTF is triggered to export to the cytoplasm and MRTF phosphorylation is required for this process. MRTF can be phosphorylated by serum at the Ser454 residue and mutation at this residue caused constant localization of MRTF in the nucleus (Muehlich et al., 2008). According to a study with a general mass spectrometric technology, EGF-mediated two phosphorylation sites in MRTF-A and one site in MRTF-B were identified in HeLa cells (Olsen et al., 2006). However, the effect of phosphorylation at these sites remains to be elucidated.

1.1.5.3 Biological functions of MRTF

As the synonym of human MRTF-A, MAL (megakaryocytic acute leukemia) suggests, the role of MRTF has been intensively studied in megakaryocytes and platelets. The human MKL 1 (megakaryoblastic leukemia1) gene was identified in infants and children patients with acute megakaryocytic leukemia (Ma et al., 2001). This disease is caused as a result of fusion of MRTF-A (t(1,22)) with RNA-binding motif protein 15 (RBM15) and characterized with frequent fibrosis of the bone marrow resulting in median survival of eight months of age. In megakaryocyte-specific double knockout mice of MRTF-A/B, plate dysfunctions, such as bleeding, decrease in megakaryocyte ploidy, granule complexity, and abnormal cytoskeletal structure, were reported (Smith et al., 2012).

The role of MRTF also has been well elucidated in muscle and cardiac cells. MRTF-A and -B contribute to the TGF-β -driven differentiation of fibroblasts into myoblasts (Crider et al., 2011). Myocardiac differentiation is essential for tissue repair, however, MRTF-A-induced hyperdifferentiation of fibroblasts to myoblasts resulted in myocardial infarction (Velasquez et al., 2013; Small et al., 2011).

Some recent studies demonstrated that MRTF is implicated in some pathological processes. The expression of MRTF-A was highly observed in the injured femoral arteries suggesting that MRTF-A is involved in pathological vascular remodelling (Minami et al., 2012). The role of MRTF-A and -B are also suggested in tumourigenesis since the location of MRTF is consistently observed in the nucleus in some malignant tumour (Medjkane et al., 2009). Consistent with this finding, loss of tumour suppressor protein DLC-1 resulted in consistent nuclear location of MRTF-A (Muehlich et al., 2012). The diverse MRTF target genes with their biological functions of MRTF are summarized in Table 1.1.

In vivo, genetic inactivation of MRTF was introduced in mouse models to understand the role of MRTF. In reported mice models, different roles of MRTF-A and -B have been observed. MRTF-A null mice were viable and born to Mendelian ratio (Li et al., 2006). A marked genetic phenotype of MRTF-A null mice is characterized by disability of the mother to nurse her pups because of defects in myoepithelial cells and mammary gland. Due to this reason, pups showed growth retardation from postnatal day of 4, ultimately causing death at around 20 days of age. This phenotype was compensated when they were fostered by wild type mother.

Table 1.1: Biological functions of MRTF and MRTF-dependent targets

Biological processes	Related MRTF target genes
Muscle cell differentiation	SM22α, SM α-actin, SM MHC, cardiac and skeletal α-actin, skeletal α-MHC, miR-486
Myoepithelial cell differentiation	SM α-actin, MHC, calponin 1, Tpm2
Megakaryocyte differentiation and migration	GATA, GATA2, GP5, MYL9, MMP9
Cardiovascular development and adaptation to stress/myocardial infarction	BNP, SM α-actin, skeletal α-actin, SM22α, Col1a1, Col1a2, Col3a1, elastin, ANF
Remodelling of neuronal networks	Gelsolin, Pctaire1/Cdk16, SM α-actin, slug/Snai2, Tpm3, cdk5
Modulation of actin dynamics and cellular motile functions	SRF, vinculin, Jun-B, Tpm1, Tpm2, zyxin, caldesmon, CTGF, Cyr61, MYL9, MYH9
Epithelial–mesenchymal transition (EMT)	Slug/Snai2, Snail/Snai1, Twist, SMα-actin
Pathogenesis of acute megakaryoblastic leukemia (AMKL)	BPJ-dependent genes (Notch signalling), SRF-dependent genes (c-fos and egr-1)
Tumour cell invasion and metastasis	MYL9, MYH9, β1-integrin, Tpm1[4)]
Antiproliferative effects	tropomyosin, caldesmon
Attenuation of carcinogenesis[1)]	mig6/errfi-1
Regulation of tumour suppressor[2)]	Eplin-α
Induction of proapoptotic protein[3)]	Bok, Noxa/Pmaip
Circadian signal oscillation[5), 6)]	Per2, Nrd1, Rora, Nfil3

MRTFs target genes are categorized according to functions. Table was modified from Scharenberg et al., 2010. [1)]Descot et al., 2009; [2)]Leiter et al., 2010; [3)]Shaposhnikov et al., 2011; [4)] Medjkane et al., 2009, [5)]Gerber et al., 2013, [6)]Esnault et al., 2014.

The phenotypes caused by MRTF-B deletion were more severe than MRTF-A mutant mice. Like MRTF-A, the MRTF-B expression was detected in various cells during development (Wei et al., 2007). Especially, MRTF-B was strongly expressed at E9.5 in the septum transversum mesoderm where generates liver sinusoids, vitelline veins, and yolk sac. Therefore, MRTF-B null mice died by vascular deficiency and liver haemorrhage in the late gestation. In addition, lethality of MRTF-B null mice at E17.5 was also reported due to the cardiac outflow tract defects with an abnormal aortic arch (Li et al., 2005). Moreover, germ-line knockout MRTF-B mice showed cardiovascular abnormalities in bronchial arch arteries and cardiac outflow tact, which was caused by a failure of SMCs differentiation (Oh et al., 2005) and derangement of cytoskeletal organization (Li et al., 2012). These mice died around at E13.5. These

results clearly demonstrate that MRTF-A and -B are deeply implicated in regulation maintenance of various tissues and especially MRTF-B is required during embryonic development.

Phenotypes of MRTF-A and-B double-knockout mice (MRTF bdKO mice) were viable, but significantly smaller than their wild type littermates (Mokalled et al., 2010). These mice showed severe abnormalities in the brain and finally died between P16 and P21. Phenotypes of MRTF bdKO mice phenocopied defects reported in brain-specific SRF-deficient mice (Alberti et al., 2005) suggesting that MRTF-A and-B regulate SRF activity as well as transcription of SRF gene.

Recently, the role of MRTF was suggested in aspect of sprouting angiogenesis (Weinl et al., 2013). After endothelial-specific deletion of MRTF-A/B in mice, severe abnormalities in postnatal retinae, such as reduced vascular outgrowth, aneurysm-like structure formation and lack of formation of deeper capillary networks during retinal angiogenesis, was observed (Fig. 1.11). Interestingly, phenotypes in endothelial-specific Srf deleted mice phenocopied the effects observed in MRTF-A/B endothelial-specific double knockout mice, suggesting that the MRTFs are the important cofactors in signalling in ECs during retinal angiogenesis (Weinl et al., 2013; Franco et al., 2013).

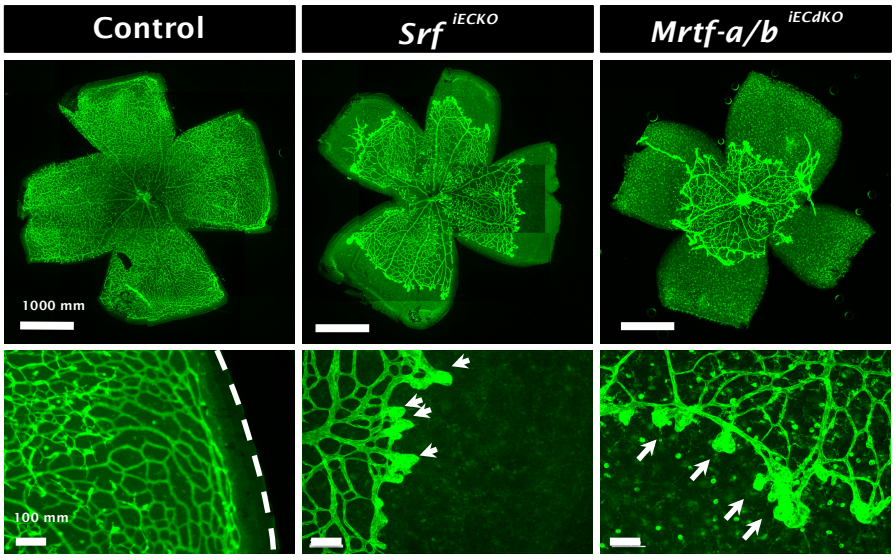

Figure 1.11: The effect of SRF, MRTF-A and -B on murine retinal angiogenesis

Retinal flat mount images of SRF and MRTF-A/B double knockout mice at postnatal day 10. Retinal vasculature is visualized by Isolectin B4 (green). In control retinae, vascularization extends towards the periphery whereas in knockout retinae, avascular zones persist and deep capillary plexi are completely missing. Arrows indicate distal microaneurysms at the abnormal angiogenic fronts, which are absent in control retinae (Weinl et al., 2013).

These results indicate that SRF as well as its cofactor MRTF-A and -B are required for retinal angiogenesis in postnatal stages. However, more detail about the MRTF-dependent regulation for angiogenesis has not been studied in detail yet.

1.1.6 Biological functions of SRF

SRF and its target genes are involved in various biological functions in many aspects. Phenotypes resulting after ablation of Srf in mouse models indicate that SRF plays a pivotal role during development. SRF is required during early embryonic development since SRF-deleted mice ($srf^{-/-}$) showed severe gastrulation defects resulting in early embryonic lethality in the uterus (Arsenian et al., 1998). Using an *in vitro* model, Srf^{-} embryonic stem (ES) cells failed to differentiate into mesodermal cell lines with unusual cell surface morphologies (Weinhold et al., 2000). Another study also evidenced that SRF is required for ES survival since SRF deficiency led to impaired cavitation, reduced Bcl-2 expression, and increased apoptosis (Schratt et al., 2002)

Genetic inactivation studies using tissue-specific knockout mouse models of SRF indicate the important roles of SRF in individual organ systems (Miano, 2010). *In vivo*, SRF expression is seen in the mouse cardiac crescent at E7.75 (Barron et al., 2005). Mice with cardiac muscle-specific inactivation of SRF resulted in embryo demise at E11.5 of development due to poorly developed trabeculations of the ventricular chambers and thin-walled compact zone (Parlakian et al., 2004; Miano et al, 2004).

In blood vessels, phenotypes caused by inactivation of SRF were reported in VSMC (Vascular smooth muscle cell). In VSMC, expression of SRF was detected at up to E10.5 of development (Barron et al., 2005). This time coincides with the expression of contractile gene expression in VSMC (Owens et al., 2004). Therefore, deletion of SRF caused severe defects in vascular system. The knockout of SRF in embryonic VSMC used the Sm22α promoter led to embryonic death at E10.5 due to the dilated heart with defects in the cyto-architecture (Miano et al., 2004). During early embryonic cardiovascular development, vascular progenitor cells are originated from the proepicardium (PE). SRF mediates development of the VSMCs from PE, thereby regulating of genes that are important for assembly and functions of myofibril (Misra et al., 2010). In human adult, knockdown of SRF in coronary artery SMC resulted in

flawed actin cytoskeleton (Miano et al., 2007) and decreases in migration and proliferation of SMC (Werth et al., 2010).

Phenotypes caused by loss of SRF in the skeletal muscle are similar to loss of SRF in the other two muscle types (Miano et al., 2010). Cre-mediated excision of SRF in early embryonic skeletal muscle led to disruption of muscle filament and decrease in contractile gene expression (Li et al, 2005). Finally, these mice died at the perinatal stage due to muscle fibre thinning and orthopnea. In post-mitotic stage, deletion of SRF in the skeletal muscle caused hypotrophy (decrease in muscle mass) and poorly organized sarcomeres (Chavret et al., 2006). Adult skeletal muscle lacking SRF also showed slow and oxidative myofibers (Chavret et al., 2006; Lahoute et al., 2008). In all skeletal muscle-specific knockout model of SRF, the maintenance of a normal contractile cell is lost due to muscle fibre atrophy (Miano et al., 2010). Similarly, smooth muscle cell–specific ablation of SRF in adult mice displayed impaired contractile activity in intestinal smooth muscle, abnormal cytoskeletal organization in colon SMCs, and intestinal obstructions (e.g. massively dilated, obstructed caecum and colon), resulting to lethality (Angstenberger et al., 2007)

In the liver, the expression of SRF by hepatocytes is essential for the maintenance of normal liver function (Sun et al. 2009). SRF-deleted male mice showed abnormal level of glucose, triglyceride, and IGF1 with increase in both hepatocyte proliferation and apoptosis. Another study reported that liver-specific SRF-deleted mice were healthy, but had impaired regenerative capacity of liver after partial hepatectomy (Latasa et al., 2007).

SRF modulates various functions of neuronal cells in the brain. SRF expression in neurons is related with neuronal survival, developmental neuronal migration, axonal outgrowth, and pathfinding of neurites (control of growth cone dynamics and axon guidance) as well as synaptic activity (Knöll and Nordheim, 2009). Expression of SRF has been documented in the postnatal and adult brain neurons in areas except thalamus in mouse (Stringer et al., 2002). The neuronal SRF regulates actin cytoskeleton genes (β-actin and Gelsolin) and phosphorylation of Cofilin that directly influences neuronal actin dynamics, which is required for neuronal migration in the mouse forebrain (Alberti et al., 2005). Therefore, SRF ablation in the early postnatal stage resulted in impaired tangential cell migration, an accumulation of precursor neurons, thereby leading to death by postnatal day 21 (Alberti et al., 2005). In addition, another study reported that forebrain-specific SRF ablation caused abnormally in-

creased oligodendrocyte precursor cells due to inhibition of terminal differentiation of oligodendrocytes (Stritt et al., 2009). Furthermore, neuronal SRF depletion in the mouse brain (cortex, striatum and hippocampus) resulted in death at the age of 3 weeks accompanied with disrupted and fragmented mitochondria (Beck et al., 2012). In neurons, since SRF is an important regulator of anti-apoptotic signal for the survival of dopaminergic neurons, loss of SRF caused an increase in sensitivity to oxidative stress, which may be involved in Parkinson's disease (Rieker et al., 2012). Based on these results it is clear that SRF is required during central nervous system (CNS) development and neuronal functions.

Deletion of SRF in keratinocytes was achieved by two independent groups (Miano, 2010). In one report, keratinocyte-specific SRF-deleted mutant mice died *in utero* due to blistering, edema, and haemorrhage of skin (Koegel et al., 2009). Moreover, postnatal loss of SRF in keratinocytes developed psoriasis-like skin lesions, which are characterized by inflammation, hyperproliferation, and abnormal differentiation of keratinocytes as well as disruption of the actin cytoskeleton. Another group reported a perinatal death of keratinocyte-specific SRF-deleted mice with an impairment of epidermal barrier (Verdoni et al., 2010).

The roles of SRF have been also documented in the hematopoietic system. In adult hematopoietic stem cells (HSCs), SRF ablation affected development of hematopoietic lineage cells. Inactivation of SRF in bone marrow cells caused increased numbers of progenitor cells and SRF-null stem cells showed decreased cell adherence to the ECM due to impaired integrin expression (Ragu et al., 2010). SRF is also required for T-cell maturation due to an observation that peripheral T-cells were significantly decreased in SRF-null mice in T- and B-cells (Fleige et al., 2007). In B-cell specific deleted SRF-null mice, there was a reduction of number of B-cells with a measurable decrease in the expression of IgM. Besides, SRF activity is associated with leukemic process. SRF is essential in megakaryocytic maturation since SRF-deficient mice in megakaryocytes displayed abnormal stress fibres, defect in platelet function as well as enhanced megakaryoblastic progenitor cells (Halene et al., 2010).

In the pancreas, the expression of SRF was detected during embryonic and postnatal stage in both of exocrine and endocrine pancreas in mouse (Miralles et al., 2006). Loss of SRF in the pancreas caused no remarkable effect on endocrine pancreas, however, resulted in pancreatitis and adipogenesis of exocrine pancreas tissue. Furthermore, SRF contributes to the pathogenesis of type II diabetes. In the murine pancreas, the expression of SRF was restricted to murine β-cells and SRF was re-

quired for insulin gene expression (Sarkar et al., 2011). In human type II diabetes, SRF and its cofactor MRTF-A level were highly observed and their expression was inversely related to insulin sensitivity (Jin et al., 2011). This study also demonstrated that hyperactivation of murine SRF or MRTF-A resulted in reduced insulin-stimulated phosphorylation of Akt and Erk. These two studies indicate that SRF is implicated in glucose tolerance in type II diabetes and SRF-involved signalling could be a therapeutic target of type II diabetes.

Interestingly, not only deletion of SRF but also sustained hyperactivation of SRF resulted in severe symptoms. Cardiac-specific SRF-overexpressed transgenic mice died at 6 weeks after birth due to cardiomyopathy characterized by increased heart weight and four-chamber dilation (Zhang et al., 2001). In addition, alterations of microRNAs were reported in these mice (Zhang et al., 2011). In murine retinae, consistently activated expression of SRF (SRF-VP16) caused retinal malfunctions both in young (postnatal day at 20) and adult (six months-old) mice (Sandström et al., 2011). In the liver, hepatocyte-specific expression of SRF-VP16 induced liver cancer (Ohrnberger et al., 2015). These mice developed hyperproliferation of premalignant nodules and progression to full-blown hepatocellular carcinoma (HCC).

As described above, almost every organ system relies on SRF for development and maintenance of functions. A further detail of cell-specific deletion of SRF was summarised in Miano's review (Miano et al., 2010). In future work, SRF signalling and the expression of SRF in less studied cells will be investigated, especially by focusing on human diseases and the role of SRF in the pathogenesis of cancer.

So far, alterations in SRF expression have been reported in some cancers and the role of SRF in carcinogenesis was intensively studied in mouse models of HCC. In these mice models, SRF was highly expressed and the overexpression of SRF itself accelerated growth and proliferation of HCC cells (Kwon et al., 2010) and increased in matrix metalloproteinase activity (Kim et al., 2011). Further evidence indicated that SRF was involved in epithelial–mesenchymal transition associated with E-cadherin expression (Park et al., 2007) and chemo-resistance (Bae et al., 2014). Probably, these observations can be explained by SRF-mediated hyperactivation of the IEGs. In addition, the expression level of miR-122, which targets SRF degradation in the liver, was decleased during tumourigenesis (Bai et al., 2009).

Finally, the recent aspect of SRF's role is control of circadian rhythm (Gerber et al., 2013). The circadian clock is an intrinsic time-sensing system that coordinates in-

ternal physiology and behaviour (Takahashi et al., 2008). Disruption of this rhythm could result in many diseases due to its influence on disease-related pathways. SRF was suggested to align the peripheral clock with the central clock as a transcriptional regulator of IEGs (Zhao et al., 2013). Interestingly, in murine liver, SRF was regulated via diurnal changes of actin dynamics coincident with changes of nuclear accumulation of MRTF (Gerber et al., 2013). According to a gene expression profiling analysis, SRF-induced circadian clock-related genes were signal- and tissue- specifically regulated (Esnault et al., 2014). For instance, SRF activation by Ras-MAPK-TCFs induced *Per1* expression in the brain whereas SRF activation by MRTF induced *Per2* in the liver. More detailed aspects of SRF-regulated circadian clock oscillation remain to be elucidated in future work.

1.1.7 SRF function in ECs (SRF in angiogenesis)

The role of SRF in ECs is first demonstrated by Tarnawski's group. Their study determined the role of SRF as a mediator of VEGF-mediated regulation of endothelial behaviour and angiogenesis *in vitro* (Chai et al., 2004). SRF-deficient HUVECs (human umbilical vein endothelial cells) failed to form capillary-like structure and stimulate sprouting in response to VEGF. In addition, knockdown of RGMECs (rat gastric microvascular endothelial cells) caused reduced VEGF-driven migration and proliferation. Moreover, VEGF-induced actin polymerization was inhibited in SRF-deficient ECs (Fig. 1.12).

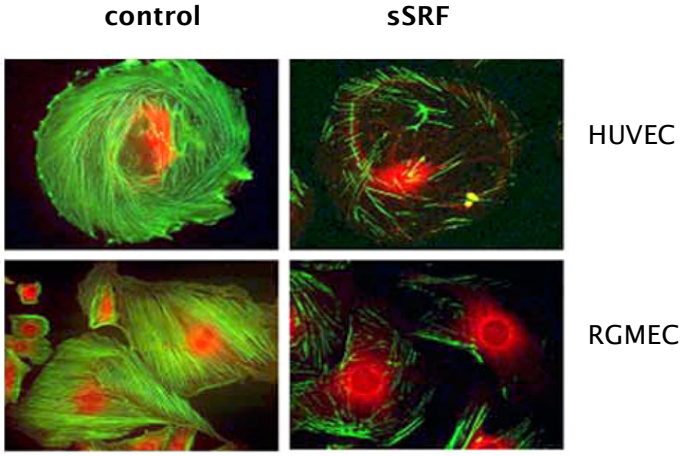

Figure 1.12: Inhibition of VEGF-induced actin polymerization in ECs

Fluorescence images of F-actin (green) and G-actin (red) in control and in SRF-deficient cells (aSRF). VEGF-induced extensive actin polymerization was missing in SRF-deficient ECs. VEGF was treated for 30 min, magnification: x400 (Chai et al., 2004).

The functions of SRF in ECs were further studied using endothelial-specific SRF knockout mice. In these mouse models, genetic loss of SRF resulted in vascular abnormalities with severe phenotypes. Endothelial specific Tie-Cre-driven inactivation of SRF caused embryonic death by E14.5 due to haemorrhage (Franco et al., 2008) (Fig. 1.13). These mice displayed reduction in vascular density and disruption of endothelial junctions that caused vascular defects. Another group also reported that Tie2-Cre$^{+/-}$Srf$^{f/f}$ mice died by E14.5 due to internal haemorrhage, vascular fragmentation, smaller heart, and failure in yolk sac (Holtz and Misra, 2008). These mice also displayed disruption of adhesion molecules on plasma membrane, thereby resulting in failure of cell-cell and cell-matrix contacts at the early phase of vascular development (Misra et al., 2013).

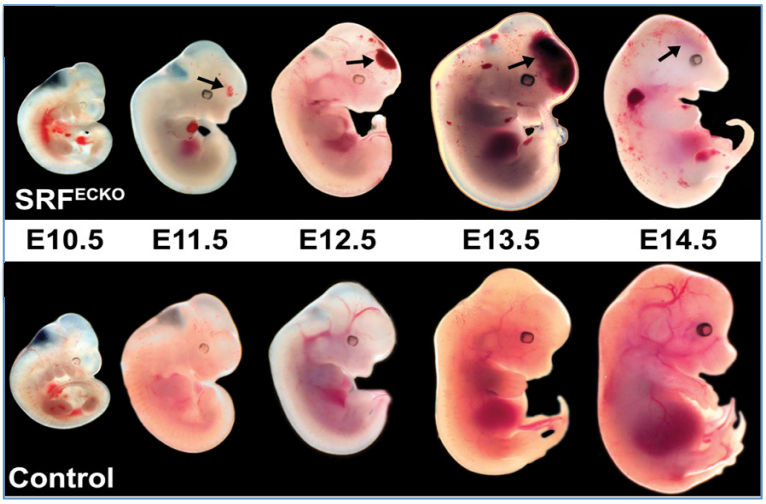

Figure 1.13: Internal hemorrhages in the SRF^{ECKO} embryo

Whole mount images of Tie1-Cre-mediated SRF-deficient (upper panel) and control (lower panel) mouse embryos from E10.5 to E14.5. Arrows indicate hemorrhagic lesions in the forebrain region (Franco et al., 2008).

Endothelial SRF deletion also resulted in vascular abnormalities at postnatal and in adult mice. In the retinae, endothelial-specific SRF-deficient mice displayed impaired endothelial filopodia protrusion, incomplete retinal primary vascular plexus, absence of the deep plexi, and persistence of hyaloid vessels during postnatal angiogenesis (Weinl et al., 2013) (Fig. 1.14). These features correspond with symptoms of human hypovascularization-related vitreoretinopathies. Moreover, morphological changes in vascular sprout as well as impaired tumour angiogenesis were reported in endothelial-specific SRF-deleted mice (Franco et al., 2013). Since SRF is highly ex-

pressed in endothelial tip cells and SRF is involved in tip cell invasion, SRF-null mice lacked vascularization in the deep layer and displayed ballooned sprouts in the retinae. These mice were also poorly vascularized in tumour-implanted mice due to defective tip-cell driven angiogenesis.

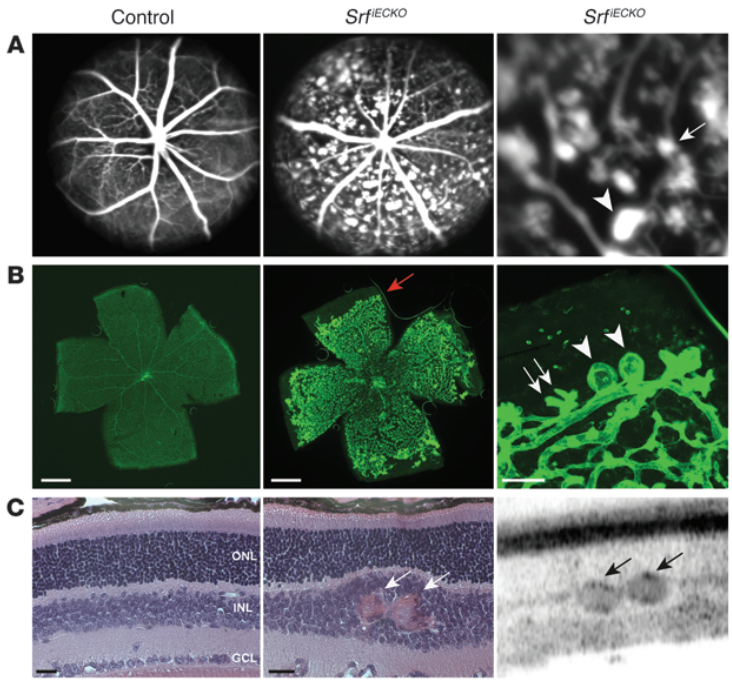

Figure 1.14: Vascular abnormalities in SRF-deficient postnatal murine retinae

Retinal images of control and SRF^{iECKO} mice at P17. At right panel, an enlarged view (x3-fold) of the middle panel is shown. (A): Images of confocal scanning laser ophthalmoscopy (SLO), particularly in fluorescence angiography (FLA) mode (SLO FLA) revealed persistent distal microaneurysms of different sizes and missing of deep plexi in the SRF^{iECKO} mice. (B): ILB4 (isolectin B4) staining on retinal flat-mounts. Distal microaneurysms of small (arrows) and large (arrowheads) size, and recessed angiogenic front of the primary plexus (red arrow) were indicated. (C): Visualization of microaneurysms by H&E staining (left and middle, scale bar:100 μm) and by OCT (optical coherence tomography, right, scale bar: 25 μm). Erythrocyte-filled (white arrows) and distal (black arrows) microaneurysms were present. ONL: outer nuclear Layer, INL: inner nuclear layer, GCL: ganglion cell layer (Weinl et al., 2013).

In contrast, endothelial-specific SRF deletion in adult mice resulted in abnormal intraretinal neovascularization (Fig. 1.15) (Weinl et al., 2013). SRF deletion at 4-6 weeks of age (after the completion of vascular growth and maturation processes) caused abnormal multiple ectopic intraretinal neovascularization structures originated from deep plexi and connected to the retinal pigment epithelium (RPE). This

phenotype was similar to *Vldlr*$^{-/-}$ retinae. This observation strongly indicates that SRF is required for endothelial homeostasis of adult retinal vasculature.

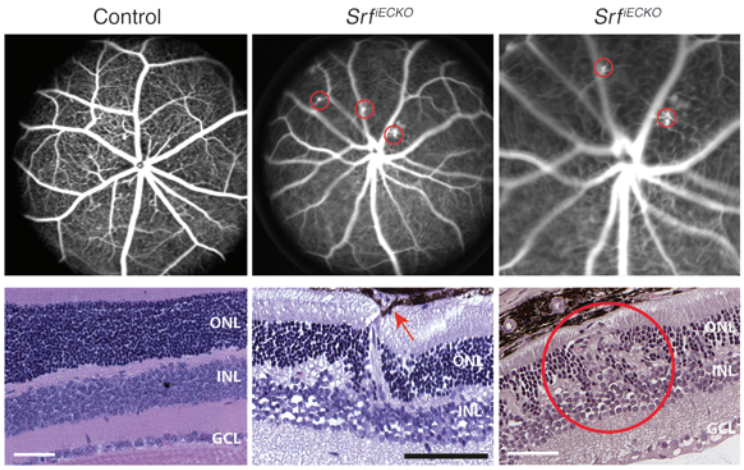

Figure 1.15: Abnormal neovascularization in SRF-deficient adult murine retinae

Retinal images of adult (4-6 weeks of age) control and SRF^{iECKO} mice. (Upper panel): FLA Images of retinal vessels and capillaries indicated that multiple ectopic intraretinal neovascularization in SRF^{iECKO} mice. At right panel, an enlarged view (x3-fold) of the local vascular structures of the middle panel is shown. (Lower panel): H&E staining revealed intraretinal neovascularization in SRF^{iECKO} mice. Red arrow indicates RPE cells that engulf the neovascularization. ONL and INL were distorted in SRF^{iECKO} mice. Scale bars: 50 μm, ONL: outer nuclear Layer, INL: inner nuclear layer, GCL: ganglion cell layer (Weinl et al., 2013).

Furthermore, the role of endothelial SRF was recently identified in the brain vessels (Weinl et al., 2015). Since blood-brain barrier (BBB) is comprised of ECs that are connected via junctions, endothelial-specific deletion of SRF resulted in loss of BBB integrity and intracerebral haemorrhage.

Taken together, these findings demonstrate the pivotal roles of endothelial SRF. Endothelial SRF is required for angiogenic responses as well as maintenance of vessel integrity. Deletion of endothelial SRF resulted in failure of both embryonic and postnatal angiogenesis as well as angiogenesis during adult mice and resulted in vascular disease phenotypes.

1.2 Endothelial cells, VEGF, and angiogenesis

1.2.1 Endothelial cells and vasculature

Endothelial cells (ECs) are flattened cells, which compose the inner lining of blood vessels called endothelium (Berridge, 2012). In the human body, the endothelium is considered the largest endocrine organ. The endothelium consists of approximately $1X10^{13}$ ECs that almost amounts 1 kg (Sumpio et al., 2002). Its surface is calculated to be about a 14,000 square foot surface area, which corresponds to the size of 6.5 tennis courts in square area (Houston et al, 2000).

ECs play critical roles in the control of vascular functions. First, ECs initiate the vascularization. This process is introduced by either vasculogenesis (by differentiation of endothelial precursor cells) or angiogenesis (by sprouting of ECs) upon VEGF (vascular endothelial growth factor) response. This premature vessel, which is introduced by ECs is supported by neighbouring cells such as smooth muscle cells in macrovessels or pericytes in microvessels. Second, ECs are main regulators of blood homeostasis. Blood vessels are selective barriers for molecular transport between blood and tissues. ECs control this molecular transport via the transcellular or the paracellular pathway. They also regulate blood coagulation and platelet functions with expression of anti-coagulants (e.g. thrombomodulon) and anti-platelet agents (e.g. prostacyclin and nitric oxide). Moreover, abnormal endothelial states, such as injury, dysfunctions, or activation of ECs, are deeply implicated in pathological conditions, for example, atherosclerosis (the loss of semi-permeable membrane, haemorrhagic fevers), or viral infection to ECs (e.g. destruction of lung microvascular EC and lung edema by influenza, Hanta, and corona virus) (Voelkel and Rounds, 2009). Third, interaction between ECs and leukocytes is a key event for leukocyte extravasation. During inflammation, migration of leukocytes into the injured or infected tissue is mediated via endothelial junctions. Due to these characteristics of ECs, understanding of endothelial functions is an important aspect for understanding the vascular system and the design of pharmacological treatment targeted for cardiovascular diseases (Sumpio et al., 2002; Michiels, 2003; Keller et al., 2003)

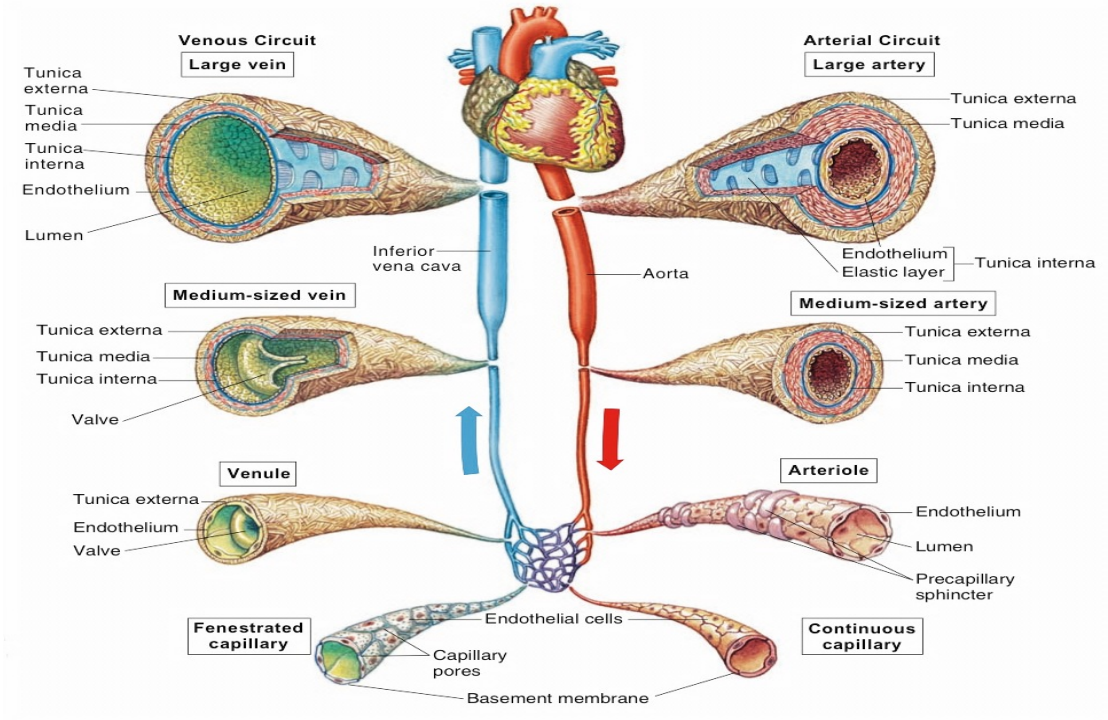

Figure 1.16: Human blood vessel systems and endothelium

The human vascular system consists of three layers termed as tunics. The outer layer is named the tunica externa, the middle one is the tunica media and the inner layer of the blood vessel barrier is the tunica interna. The tunica externa is composed of connective tissue, which is the most abundant connective tissue in the body (Calvino, 2003). The tunica media is the composition of smooth muscle cell layer and the tunica interna consists of three parts: ECs, glycoproteins layer of basement membrane, and elastin (a layer of elastic fibres). In contrast, capillary is a monolayer of ECs without connective tissue and SMCs, thereby permitting rapid exchange of materials between blood vessels and tissues. Capillary is differently organized depending on the local region. Continuous capillary is found in muscles, lungs, adipose tissue, and the CNS. In the CNS, adjacent ECs are closely joined together. Especially, in blood-brain barrier (BBB), intercellular channels between ECs are not found. Discontinuous capillary is observed in the bone marrow, liver, and spleen. In this region, gaps between endothelial cells exist, so capillary looks like little cavities named sinusoids. Fenestrated capillary occurs in kidneys, endocrine glands, and intestines. In these capillaries, mucoprotein supports EC layer and forms wide intercellular pores (800 to 1,000 Å) (Fox, 2010).

1.2.2 Vascular endothelial growth factor (VEGF)

1.2.2.1 Discovery of VEGF

VEGF was discovered, isolated, and termed by various researchers in 1980s. VEGF was originally purified as a tumour-secreted protein that increased microvascular permeability without causing mast cell degranulation or endothelial cell damage

(Senger et al., 1983 and 1986). Thus, VEGF was initially named as tumour-secreted vascular permeability factor (VPF). A few years later, VEGF was identified as a tumour angiogenesis factor and termed as vasculotropin by Plöet (Plöet et al., 1989), and then renamed as VEGF by Ferrara (Ferrara et al., 1989).

1.2.2.2 The VEGF gene

During embryonic development, VEGF plays a pivotal role during vasculogenesis. In addition, VEGF concentration is strictly regulated within a narrow range. A previous study proved that a single *vegf* allele deletion resulted in embryonic lethality at mid-gestation due to lack of a vasculature and absence of blood islands (Carmeliet et al., 1996). Interestingly, two- to threefold overexpression of VEGF from its endogenous locus resulted in severe abnormalities during heart development, then finally led to the embryonic lethality at E12.5-E14 (Miquerol et al., 2000).

In mammals, seven sub-families of VEGFs are reported. They are termed VEGF-A to F and placental growth factor (PIGF). In humans, the *vegf* gene is located on chromosome 6 at the location 6p21.3 (Vincenti et al., 1996). In the mouse, it is positioned on chromosome 17 (De Gregorio et al., 1997). *Vegf-b* and *vegf-c* are located on chromosome 11 at the position q13 in human and on chromosome 4 at the position q34 in mouse, respectively (Paavonen et al., 1996).

VEGF-A

VEGF-A is the most abundant form of VEGF and normally designated as VEGF. The characteristics of VEGF are dependent on its isoforms. The isoforms are derived from 8 exons separated by 7 introns during splicing variants (Fig. 1.17). To date, six isoforms of VEGF are identified with the amino acid length from 121 to 206 (Robinson and Stringer, 2001).

Among six isoforms, VEGF121, 145, and 165 are secreted as dimeric forms of VEGF whereas VEGF189 and 206 are sequestered in the particular matrix upon secretion (Zachary and Gliki, 2001). VEGF121 is the smallest, but the most abundant isoform of VEGF-A (Pradeep et al., 2005). It is a secreted and diffusible isoform due to the lack of a heparin-binding site. VEGF 145 and 165 are also biologically active and abundant forms of VEGF in ECs. In the mouse, VEGF isoforms are designated one less amino acid of matching isoforms in human. For example, VEGF-A188, VEGF-

A164, and VEGF-A120 are the counterparts of human VEGF-A189, VEGF-A165, and VEGF-A121, respectively.

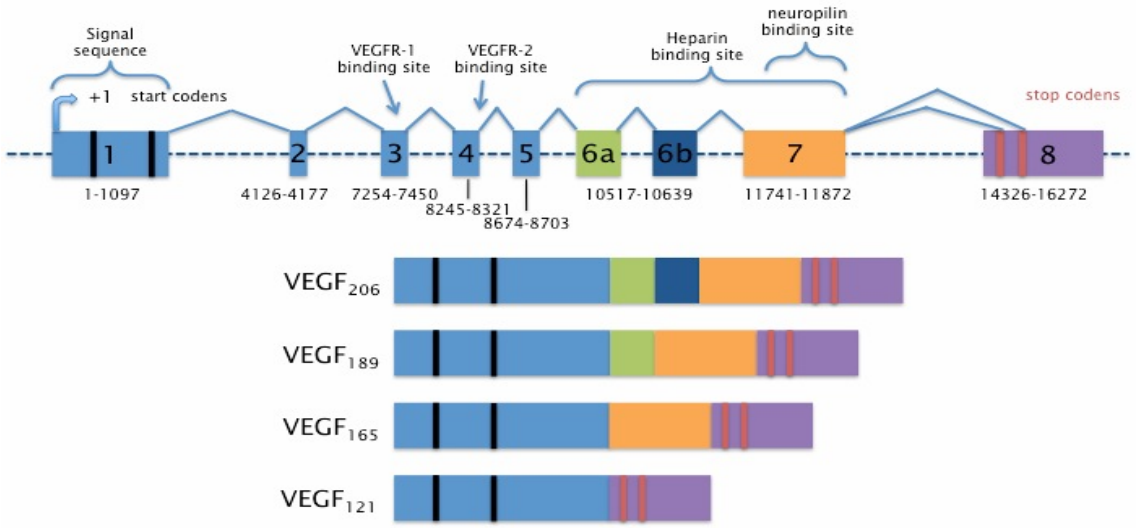

Figure 1.17: Schematic structure of human VEGF-A and its splicing variants

Alternative splicing of VEGF gene occurs during mRNA processing by altering protein-coding region. This generates various protein variants with different amino acid sequence and biological activities. VEGF-A exists as multiple isoforms resulting from pre-mRNA splicing. Names of VEGF isoforms are designated according to its total amino acid number in the mature proteins. In all isoforms, the exon 1 to 5, and 8 (either 8a or 8b) are commonly observed except VEGF148 (Grünewald et al., 2010). Figure was modified from Arcondéguy et al. 2013 and Cross et al., 2003.

The expression of VEGF is regulated by hypoxia that leads to the binding of hypoxia inducible factor (HIF) at the hypoxia-binding element of the VEGF promoter. Moreover, mRNA stability of VEGF is dependent on oxygen condition (Zuchary and Gliki, 2001). In normoxia condition, mRNA of VEGF is rapidly degraded with the half-life 15 to 40 min *in vitro*. However, under hypoxia condition, the stability of VEGF-A mRNA is mediated by the AU rich element (Arcondéguy et al., 2013).

VEGF-B

VEGF-B was discovered as a VEGF homologue (Olofsson et al. 1996). There are fewer studies about VEGF-B because phenotypes of VEGF-B mutants have been modestly observed (Li, 2010). *Vegf-b*$^{-/-}$ mice showed abnormalities of atrial conduction, but

they still live a normal life (Aase et al., 2001). Moreover, the overexpression of VEGF-B resulted in only restricted angiogenic activity (Li et al. 2008), in contrast to the powerful role in both vasculogenesis and angiogenesis of VEGF-A. Therefore, the role of VEGF-B has been focused on as a facilitator of VEGF-A. However, recent studies addressed the new role of VEGF-B as a modulator of fat utilization (Hagberg et al., 2010), and as a potent neuroprotective factor (Poesen et al, 2008).

The expression of VEGF-B is observed largely in heart, brain, and kidney. VEGF-B often forms VEGF-A/B heterodimers by co-expression of VEGF-A. However, its function is still not clear. Probably, VEGF-B can be consistently functional because VEGF-B is not regulated by hypoxia and it has a relative long half-life (mRNA >8 hrs) (Pradeep et al., 2005). Two different isoforms of VEGF-B are reported: A heparin-binding VEGF-B167 (a predominant form) and a diffusible VEGF-B186 isoform.

VEGF-C and lymphangiogenesis

In adult tissues, VEGF-C is prominently expressed in some somatic tissues such as heart, placenta, ovary, and brain. On the other hand, in embryos, VEGF-C is expressed where lymph angiogenesis arises from embryonic veins (Hoeben et al., 2004). The role of VEGF-C is especially emphasized on the lymphatic vessel formation (lymphangiogenesis). 50% of *Vegfc*$^{-/-}$ mice died between E15.5 and 17.5 with phenotypes including a lack of lymph vessels and a fluid accumulation in tissues (Karkkainen et al., 2004).

VEGF-D

VEGF-D is initially described as *c-fos*-induced growth factor (FIGF) (Orlandini et al., 1996) and a few years later designated as VEGF-D based on homology with VEGF-A (Achen at al.1998). VEGF-D, like VEGF-C, is synthesized as pre-protein form, which requires a proteolytic process in both N- and C-terminus to generate the mature form. The immature form of VEGF-D binds to VEGFR-3 whereas the mature form binds to both VEGFR-2 and VEGFR-3 since a binding affinity to VEGFR-2 is increased after cleavage (Achen at al.1998). In mouse models, VEGF-D knockout did not affect lethality and these mice showed normal lymphatics. These observations suggest that the activation of VEGFR-3 can be substituted for VEGF-C or others. In some tu-

mour tissues, the expression of VEGF-D is upregulated and its expression is correlated with lymph node metastasis (Roskoski Jr. 2007).

VEGF-E

VEGF-E is a factor that originates from Orf virus (Ogawa et al., 1998) that affects sheep, goat, and occasionally human. On infection, VEGF-E generates lesion for angiogenesis by stimulating proliferation and sprouting of ECs. VEGF-E has about 25% homology with VEGF and the mitotic effect of VEGF-E is similar with VEGF165 (Hoeben et al., 2004).

Placental growth factor (PIGF)

PIGF is a homodimeric glycoprotein that shares 42% of amino acid homology with VEGF (Roskoski Jr., 2007). PIGF produces 4 transcription variants, namely PIGF131, 152, 203, and 224. These isoforms are formed primarily in placenta, but are also observed in cancer cells and somatic tissues. PIGF does not stimulate endothelial proliferation and migration, but can induce ERK activation and mitogenesis (Landgren et al., 1998).

1.2.2.3 The VEGF receptors (VEGFRs) and VEGF signalling

VEGF signalling is mediated via binding to VEGFRs at the N-terminus in the extracellular receptor domain. So far, three VEGFRs are identified (except four VEGFRs in the zebra fish including KDR-like receptor) (Bussmann et al, 2008). Additionally, neuropilin-1 and -2 are known as VEGFR co-factors. VEGFRs are named differently in different systems. VEGFR-1 is termed Flt1 (fms-like tyrosyl kinase-1) in mouse and Fms in feline McDonough sarcoma virus. VEGFR-2 is also known as KDR (kinase domain-containing receptor) in human and Flk (fetal liver kinase) 1 in mouse. VEGFR-3 has a synonym for Flt4 (fms-like tyrosine kinase 4) (Koch et al., 2011; Roskoski Jr., 2007).

Binding affinity

VEGF-A is known to bind to both VEGFR-1 (De Vires et al., 1992) and VEGFR-2 with high affinity (Millauer et al., 1993). Both of them are widely expressed in ECs. PLGF

and VEGF-B bind only to VEGFR-1, and the binding partner of VEGF-C and VEGF-D is VEGFR-3 (Fig. 1.18).

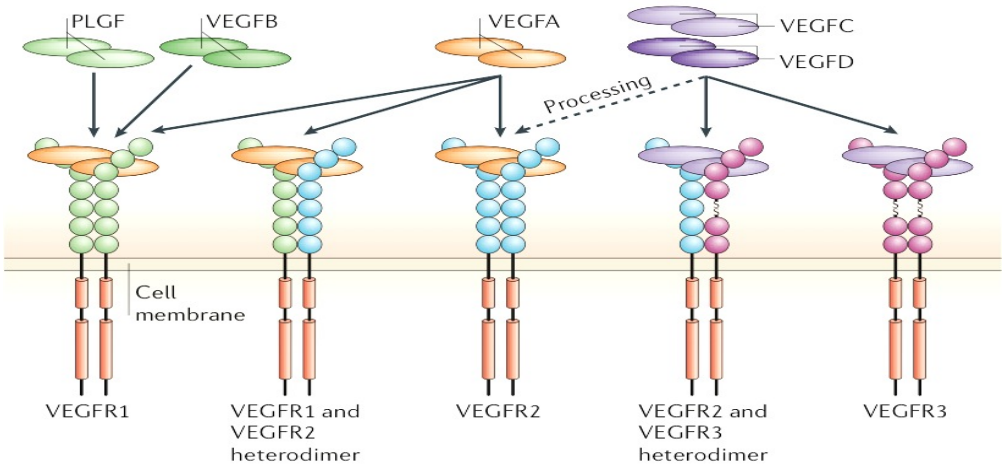

Figure 1.18: Mammalian VEGFs receptors and their ligands

Mammalian VEGFs bind to the different VEGFRs with different binding affinities. This leads to the homo- or heterodimer formation of VEGFRs (Olsson et al., 2006).

VEGF is produced and secreted in various cells such as neighbouring ECs and tumour-associated cells. There was the hypothesis that ECs are not able to express VEGF themselves. However, a study evidenced that ECs are also able to express VEGF. This autocrine signalling is required for endothelial survival (paracrine source of VEGF could not be compensated) by altering apoptotic signal during stress conditions (Lee et al., 2007). By binding of VEGF, VEGFRs are able to form both homo- and heterodimers. The properties of heterodimers are not clearly elucidated yet. The mechanism of VEGFRs dimerization will be described in the following paragraph.

Activation of VEGFR upon VEGF binding

VEGFRs belong to type V receptor tyrosine kinases (RTKs) whose extracellular domain consists of seven Ig-like domains. Activation of VEGFRs is initiated by VEGF-mediated dimerization. VEGF induces dimerization of VEGFR-2 that leads to autophosphorylation. Phosphorylation occurs *in trans*, that is, one kinase of dimer catalyzes phosphorylation of tyrosine at the other dimer and its phosphorylation in turn catalyzes initial phospho-residue (Fig. 1.19).

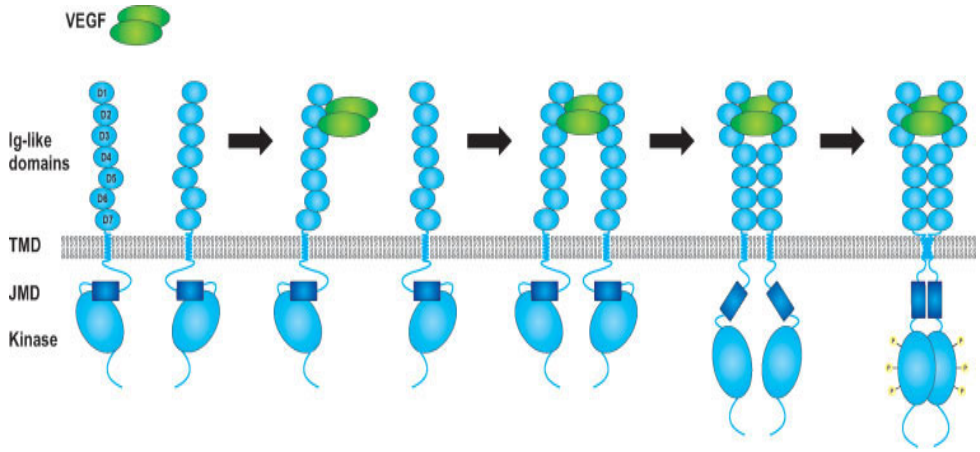

Figure 1.19: Mechanism of VEGFRs dimerization

VEGF receptors are activated upon VEGF binding-mediated dimerization. A covalently linked VEGF dimer binds to VEGFR initiating to dimerization. For activation of VEGFR-1, sub-domain 2 of extracellular Ig-like domain is sufficient for binding at VEGFR whereas VEGFR-2 requires sub-domains 2 and 3. Following binding of VEGF to VEFGR, receptors are stabilized by additional interaction between Ig-like domain 4 and 7. It results in activation of receptor kinase by autophosphorylation at tyrosine residues to initiate downstream signalling. TMD: transmembrane domain, JMD: juxtamembrane domain (Stuttfeld and Ballmer-Hofer, 2009).

After dimerization and phosphorylation, specific downstream cascades are activated via different adaptor molecules and their binding partners, noted as VRAP (VEGF receptor-associated protein). These specific sites are discussed in the following chapter.

VEGFR-1

VEGFR-1 is an approximately 180 kDa protein that can be activated by VEGF-A, -B, and PlGF. The role of VEGFR-1 remains still elusive, however it has been described as a potential negative regulator of VEGFR-2-mediated angiogenic process, since VEGF has a higher affinity to VEGFR-1 (≈ 10 pM) than to VEGFR-2 (75 to 750 pM) (Roskoski Jr., 2007). VEGFR-1 has a week kinase activity due to presence of a suppressor motif in its juxtamembrane domain. This suggests that phosphorylation of intercellular domain of VEGFR-1 can be difficultly achieved (Cébe-Suarez et al., 2006). Therefore, it is suggested that VEGFR-1 may spatially capture VEGF to control VEGFR-2 driven angiogenesis (Kappas et al., 2008).

VEGFR-1$^{-/-}$ mice had normally differentiated ECs. However, these mice displayed disorganized vasculature, then died at E 8.5 to 9 due to the increased number of endo-

thelial progenitor cells and abnormal lumenless vessels (Fong et al., 1995, 1996, and 1999). However, unexpectedly, mice with a dysfunction only at tyrosine kinase domain of VEGFR-1 showed normal vasculature (Hiratsuka et al., 1998).

VEGFR-2

VEGFR-2 is a 210 kDa predominant mediator of VEGF-triggered signalling in EC with its powerful kinase activity that can induce cellular responses. *In vivo* studies proved that VEGFR-2 is required during embryonic development because VEGFR-2$^{-/-}$ mice died at 8.5 and 9.5 due to the aberrant vasculogenesis, which was caused by insufficient functional ECs (Shalaby et al., 1995 and 1997).

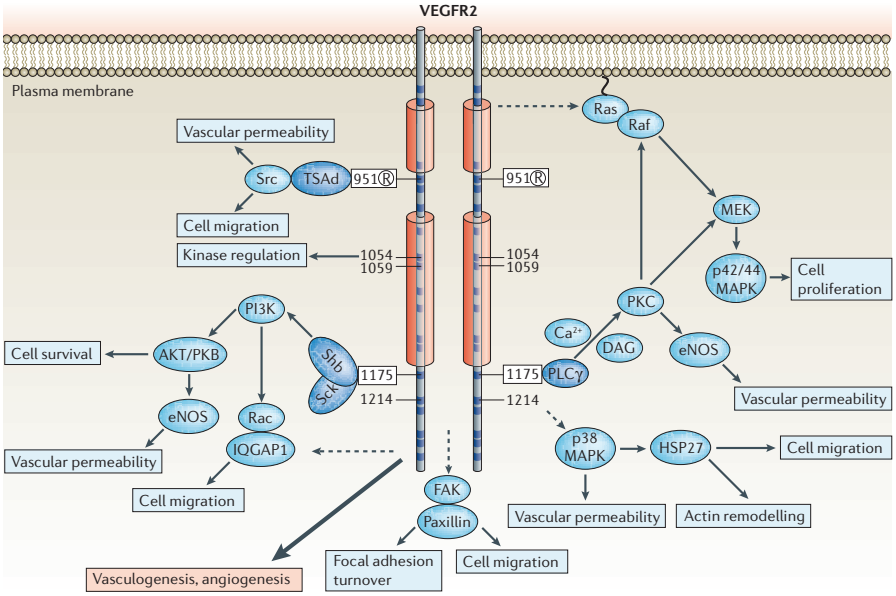

Figure 1.20: Major phosphorylation sites at VEGFR-2 and signal transduction

Tyrosine-phosphorylation residues at intercellular domain of VEGFR-2 and their adaptor molecules are indicated. The sites that are angiogenesis-dependently regulated in ECs are highlighted with tyrosine number with Ⓡ. Abbreviations: DAG (diacylglycerol), eNOS (endothelial nitric oxide synthase), FAK (focal adhesion kinase), HPC (haematopoietic progenitor cell), HSP (heat-shock protein), PI3K (phosphatidylinositol 3 kinase), PKC (protein kinase C), PLCγ (phospholipase Cγ), Shb (SH2 and β-cells), TSAd (T-cell-specific adaptor) (Olsson et al., 2006).

There are major phosphorylation sites at VEGFR-2 (Olsson et al., 2006) (Fig. 1.20). At the phosphorylation site Y951 in the kinase insert domain, binds T cell-specific adapter molecule (TSad). Phosphorylation at this site is observed during development and in tumour vasculature, not in quiescent ECs. Y1054 and 1058 in the ki-

nase domain are probably altered with promotion in kinase activity. Y1175 in the C-terminus domain is binding site for PLCγ and its adapter molecules Shb and Sck as well as ShcA and Grb2 (growth factor receptor-bound protein 2) that recruits Rho-GEF SOS1 (son of sevenless). At the phosphorylated Y1214 binds its adapter protein Nck.

VEGFR-3

VEGFR-3 differs from the other two receptors. It contributes to the formation of a primary capillary plexus in the embryo. VEGFR-3-null mice died at E10 to E11 due to cardiovascular remodelling defects (Dumont et al., 1998). However, the expression of this receptor is observed only in lymphatic ECs in the adults. Mutations on VEGFR-3 are naturally observed unlike other two receptors. This led to chronic and disfiguring swelling of lymphatic vessels, known as human hereditary lymphedema (Milroy's disease).

Using radioactive immunoprecipitation studies, five phosphorylation sites were identified at VEGFR-3 (Y1230, 1231, 1265, 1337 and 1363). Among them, Y1337 recruits Shc and Grb2 where signal transduction of MAPK pathway begins. Another important VEGFR-3 signalling is VEGF-C/VEGFR-3 mediated PI3K/AKT activation and this signalling is involved in lymphatic endothelial migration (Makinen et al., 2001).

1.2.3 Angiogenesis

1.2.3.1 Mechanism of angiogenesis

Angiogenesis is the process of new vessel formation, which is led by ECs from pre-existing blood vessels. ECs are normally in a quiescent (G_0) state with a very low turnover rate (within months to year) (Augustin, 2004). Quiescent ECs highly express transcription factor HOXC9 and this keeps the vasculature in a resting state via inhibition of interleukin-8 production (Stoll and Kroll, 2012). Angiogenesis can be triggered in response to low oxygen (hypoxia), lack of glucose, or by mechanical stress (angiogenic switch). Among them, hypoxia and VEGF are known as major inducers of angiogenesis.

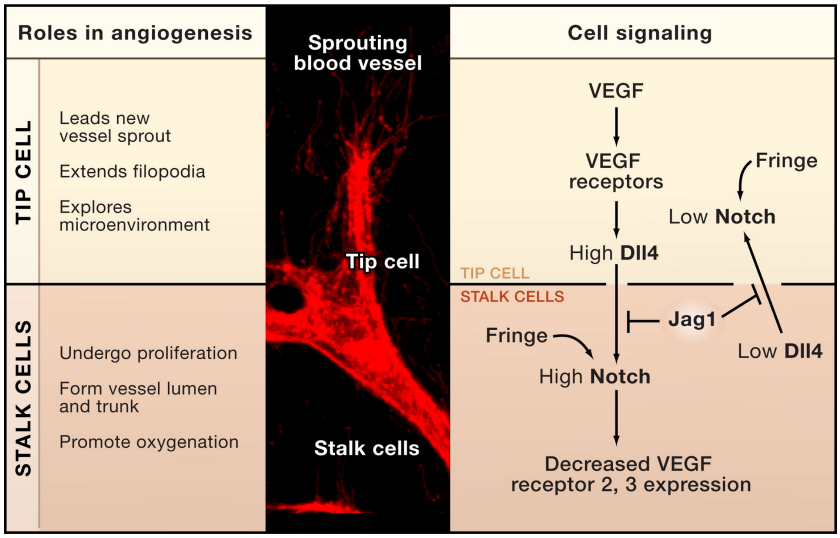

Figure 1. 21: The endothelial tip and stalk cells during angiogenesis

In vivo, ECs begin angiogenesis by forming specialized ECs called tip cells at the leading edge of vascular sprouting. The tip cell is a highly migratory cell that expresses high levels of VEGFR, thereby responding to VEGF by chemotaxis to the avascular zone. Following the tip cell, thick structural ECs named stalk cells support a vascular trunk. They are proliferative rather than migratory. Stalk cells highly express Notch to attenuate VEGFRs (Suchting und Eichmann, 2009).

Angiogenesis can be distinguished from vasculogenesis. Vasculogenesis refers to *de novo* formation of blood vessels by differentiated ECs from precursor cells (hemangioblasts). This process restrictively occurs during early embryogenesis. By contrast, angiogenesis occurs during vascular growth or repair according to the following processes (Berridge, 2012).

1. At a local site of hypoxia or in an avascular zone, HIF (hypoxia-inducible factor) is activated. HIF induces the expression and release of VEGF. VEGF is also produced and secreted at sites of inflammation or damaged tissue. Then, a gradient of VEGF in local region initiates activation of VEGFR2 on ECs.
2. Sensing VEGF, endothelial tip cells begin to express high levels of Delta-like-4 (Dll4), which is a ligand for Notch signalling. Upon VEGF-driven activation of Dll4, tip cells prevent neighbouring ECs from differentiation into another tip cell by activation of Notch pathway, known as lateral inhibition.
3. Neighbouring ECs (stalk cells) activate Notch pathway, thereby decreasing VEGFR-2 expression. By activation of Notch, stalk cells retain responsiveness to VEGF for proliferation.

4. Activated tip cells locally release PDGF (platelet-derived growth factor) that induces proliferation of local ECs to develop the branch. As a new vessel grows, deposition of new ECM (extracellular matrix) begins for external covering of new vessels.
5. The new vessel recruits pericytes by releasing PDGF-β by tip cell. Pericytes sense PDGF-β by their PDGFβ receptor, then migrate to the new vessel.
6. ECs release sphingosine 1- phosphate (S1P) to activate sphingomyelin signalling pathway in pericytes. Pericytes react S1P via Sphingosine-1-Phosphate receptors, thereby modulating the N-cadherin complex that is a channel for ECs-pericytes interaction (Peg-socket junctional complex).
7. ECs and pericytes also interact through an angiopoietin-Tie2 signalling. Pericytes release angiopoietin 1 that targets Tie2 receptor on ECs to control maturation and stabilization of ECs. ECs can release angiopoietin 2 for the contrary regulation to angiopoietin 1.

1.2.3.2 Endothelial extracellular matrix remodelling

Angiogenesis starts with release extracellular proteins, such as matrix metalloproteinase (MMPs), by ECs (Mignatti and Rifkin, 1996). ECs have a high proteolytic activity during remodelling of blood vessels. To hydrolyse endothelial basal membrane or to destabilize endothelial junctions, ECs secrete proteases such as matrix metalloproteinases (MMPs) and a disintegrin and metalloproteinases (ADAMs).

Matrix metalloproteinases (MMPs)

MMPs are proteolytic enzymes that are produced and secreted by most connective tissues including fibroblasts, chondrocytes, ECs, and inflammatory cells (Fig. 1.22) (Kalluri et al., 2003). The numbers of MMPs are determined from 1 to 28 based on their identification and structure. MMPs are divided into two classes, membrane type (MT-MMP) and soluble MMPs. Most MMPs are secreted as inactive properties, so an activation process (proteolytic removal of the pro-domain by plasmin) is required.

The major MMPs involved in tumour angiogenesis are MMP2, 9, and 14 (MT1-MMP). Briefly, MT1-MMP is a collagenase that promotes cellular invasion into type I collagen (Barnes et al., 2009). It also regulates vascular stability in response to injury (Sounni et al., 2010). MMP2 and 9 are gelatinases that degrade denaturated colla-

gen (gelatin) and type IV collagen (Jackson and Nguyen, 1997). MMP9 is slowly expressed, but its mRNA is found in all tissues (Nuttall et al., 2004). It is implicated in angiogenesis in many aspects such as a bioavailability of VEGF, the activation of FGF-2 pathway, and the regulation of anti-angiogenic proteins (Kessenbrock et al., 2010). Notably, these three MMPs are produced by VEGF or TGFβ in ECs (Rundhaug, 2003) and inhibition of them caused the attenuation of both angiogenesis and lymphangiogenesis (Nakamura et al., 2004).

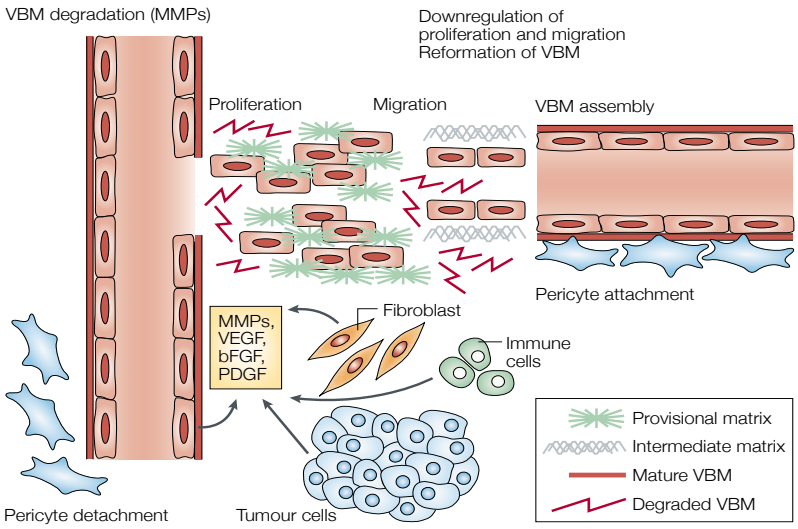

Figure 1.22: Matrix remodelling during angiogenesis

Degradation and reformation of the vascular basement membrane (VBM) is a critical event of angiogenesis. In response to growth factors (VEGF, bFGF, and PDGF), MMPs degrade and form an immature matrix, which allows endothelial cell proliferation and migration. This leads to the formation of an intermediate matrix, then mature VBM (Kalluri et al., 2003).

A disintegrin and metalloproteinases (ADAMs) family

ADAMs are Zn^{2+}-dependent adamakysin members of transmembrane proteins that are related to MMPs, snake venom metalloproteinases (SVMP) and ADAM-TSs (adams with thrombospontin domains). ADAMs cleave various cell surface membrane molecules with their adhesive and proteolytic properties.

Since the targets of ADAMs are both ligands and receptors of membrane molecules, different consequences can arise. In case of ligand shedding, ligand fragments can bind to receptors on the same cell (an autocrine effect), neighbouring cells (a paracrine effect), or even enter the bloodstream (an endocrine effect), thereby mediating signalling. On the other hand, upon cleavage of membrane receptors by ADAMs, the

ectodomain of the receptor is cleaved and released, thereby inhibiting ligand-mediated signalling, for example, Macrophage colony stimulating factor receptor (MCSGR) and VEGFR (Primakoff and Myles, 2000).

So far, 40 ADAMs proteins are reported in mammals and 21 ADAMs are discovered in human. Among them, thirteen ADAMs have proteolytic activities. Of note, ADAM10, 12, 15, and 17 are reported as growth factor shedding enzymes (Gooz, 2010; Duffy et al., 2011). ADAM10 is deeply involved in angiogenesis by shedding of ectodomain of VEGFR2, VE-cadherin, collagen IV, and cMet (angiogenic regulator, RTK) (Claesson-Welsh, 2010; Donners et al., 2010). ADAM15 is involved in pathological angiogenesis such as in ischemic retinae, atherosclerotic plaques, or retinopathies (Duffy et al., 2009). The expression of ADAM17 (CD156b, TACE) is widely observed and it is responsible for the cleavage of VEGFR-2, TNF-α, TGF-α, and Tie2 (Swendeman et al., 2008; Jin et al., 2013).

1.2.3.3 Anti-angiogenic factors

There are also factors that repress angiogenic processes, namely anti-angiogenic factors. The balance between pro-angiogenic and anti-angiogenic factors is critically regulated during tissue development, repair, remodelling, and vascular homeostasis. Excessive angiogenesis is involved in a variety of pathological diseases, such as inflammation, ischemia, and tumour growth, whereas insufficient angiogenesis causes cardiovascular diseases, stroke, and chronic wound due to hypovascularization (Nessa et al, 2009). As angiogenic inhibitors, endostatin, angiostatin, vasostatin, thrombospondin, troponin, and MMP-inhibitors were known (Peter Carmeliet, 2000). In this study, thrombospondin and MMP-inhibitors are dealt with as anti-angiogenic factors.

Thrombospondin-1 (TSP-1)

TSP-1 is a trimeric molecule and a basement membrane component that was isolated as a 142 kDa glycoprotein (Lawler et al., 1978). Among five TSP family members, only TSP-1 and -2 (subgroup A) have anti-angiogenic features (Iruela-Arispe et al., 2004) (Fig. 1.24) and influence on ECs (Armstrong and Bornstein, 2003).

TSP-1 mediates various key events in ECs. The expression of TSP-1 resulted in complete suppression of PECAM-1 (Sheibani et al., 1997). In addition, TSP-1 inhibited

endothelial migration and proliferation by inducing apoptosis (Daly et al., 2003; Ren et al., 2006). This signalling is mediated by CD36 (Asch et al., 1992) or integrin β_1 (Short et al., 2005). Upon binding to CD36, TSP-1 recruits tyrosine kinase p59fyn, thereby enhancing apoptosis via caspase-3 expression (Jiménez et al., 2000).

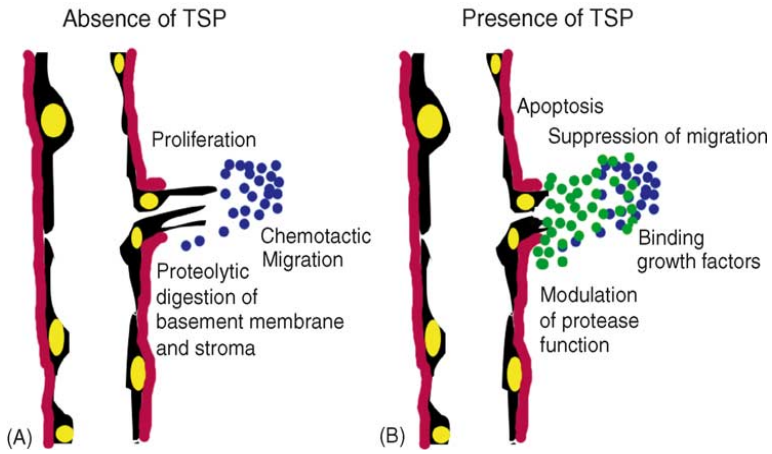

Figure 1.23: The effect of TSP on EC

(A): In the absence of TSP, growth factor (blue dots) induces degradation of basal membrane. (B): In the presence of high levels of TSP (TSP-1 or -2, green dots), growth factor-driven vascular sprouting can be attenuated by activating TGF-β, inhibiting endothelial apoptosis, and suppressing extracellular protease (Iruela-Arispe et al., 2004).

Clinically, TSP-1 has been designed for an anti-cancer therapy due to its functions: upregulation of the tumour suppressor gene p53 (Ren et al., 2006) and suppression of the transforming growth factor-β (TGF- β) in the tumour microenvironment (Lawler, 2002). The overexpression of TSP-1 in tumour cells inhibited tumour growth, which was characterized by decreased number and size of tumour vessels (Streit et al., 1999). *In vivo* findings also indicate that VEGF is highly expressed in high-grade tumours where TSP-1 expression is suppressed (Donmez et al., 2009). With these reasons, the mimic peptide of TSP-1 (Reiher et al., 2002) or the synthetic analogue of TSP-1 (ABT-510) were reported as effective *in vivo* anti-tumour reagents (Markovic et al, 2007; Ebbinghaus et al. 2007).

MMP inhibitors: TIMPs

Tissue inhibitors of metalloproteinases (TIMPs) are the endogenous natural inhibitors of MMPs, as their name suggests. Among 4 identified TIMPs (TIMP-1 to -4),

TIMP-1 and -2 have been intensively studied (Nagase et al., 2006). In ECs, expression of TIMP-1, -2 and, -3 were reported (Groblewska et al., 2012) and TIMP-4 expression is relatively restricted.

TMPs are involved in angiogenesis in many aspects since TIMPs can alter endothelial proliferation and migration (Rundhaug, 2005). TIMP-1 attenuates VEGF-induced endothelial migration and TIMP-2 inhibits bFGF-induced ECs proliferation. TIMP-3 is also reported with its ability for inhibition of endothelial migration and proliferation and TIMP-4 inhibits endothelial tube formation. Moreover, TIMPs inhibit EC vacuole and lumen formation (Davis and Senger, 2005).

TIMPs bind to the active site of MMPs with a 1:1 stoichiometric ratio (Nuttall et al., 2004). The crystal structure of MMP/TIMP indicates that wedge-like four N-terminus amino acid residues of TIMPs slots into the active site of MMPs. TIMP-2 has a longer AB loop and the modification of AB loop or each domains alters its reactivity (Nagase et al., 2006). Due to these structural differences, TIMPs have selective activity for target substrates. According to the reports, TIMP-1 is able to bind to all MMPs except MT-MMPs and ADAM10. In contrast, TIMP-2 selectively inhibits MT1-MMP and ADAM10. TIMP-3 has broad targets in ADAMs family such as ADAM10, 12, and 17 (Murphy, 2011).

1.3 Actin dynamics

Actin is the most abundant 42 kDa single peptide protein in eukaryotic cells. Since the discovery of actin in 1942, it was not understood that actin exists in every eukaryotic cell until 1962 (Saito, 2009). In this chapter, the structure and regulation of actin as well as actin-binding proteins will be introduced.

1.3.1 Structure of actin

The insides of actin, there are four sub-domains (Fig. 1.24). In each corner and the centre, nucleotide-binding sites are located. In cells, three kinds of six actin isoforms exist, namely α-actin (cardiac, smooth, and skeletal), β-actin (cyto), and γ-actin (cyto and skeletal). They are coded from different genes and each isoform has unique cellular functions with only slight variations in amino acid sequence (Perrin and Ervasti, 2010).

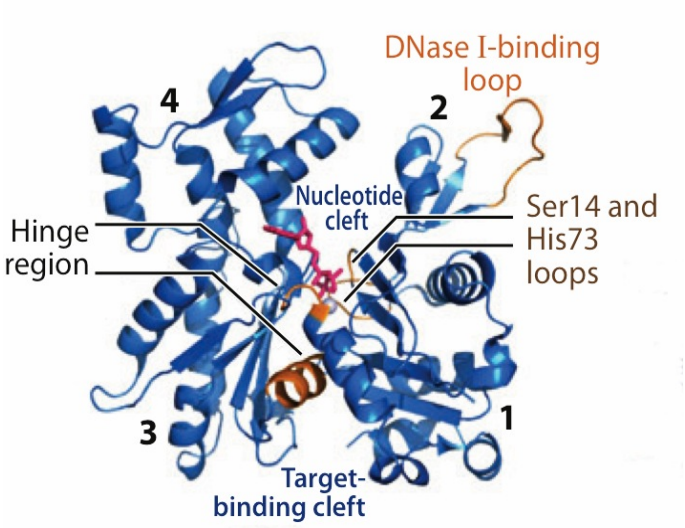

Figure 1.24: Structure of monomeric actin

Monomeric actin contains 4 sub-units, which are shown as ribbon representation. With this structure, ATP-binding cleft is formed in the centre of sub-units. ATP, along with Mg^{2+} docks between sub-unit 2 and 4 named minus end where ATP is hydrolysed to ADP+ Pi (Allingham et al., 2006). Sub-unit 1 and 3 is called plus end (Dominguez and Holmes, 2011).

As a component of the cytoskeleton, actin structures mainly exist three filament forms in cells. They are termed stress fibres, filopodia, and lamellipodia (Fig. 1.25)

and are regulated by Rho family of small GTPases, RhoA, cdc42, and Rac1, respectively (Nobes and Hall, 1995).

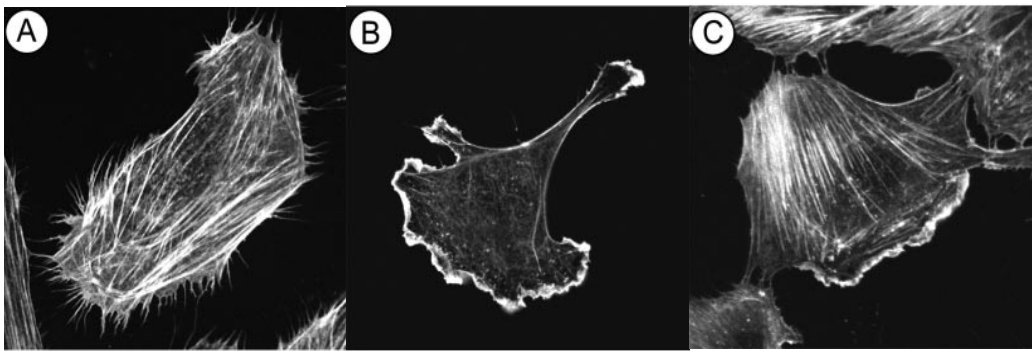

Figure 1.25: Endothelial actin filaments

Three major actin fibres are visualized in HUVECs. (A) The filopodia: Filopodia are niddle-like structures near the periphery formed by protrusions from lamellipodia. (B) The lamellipodia: Lamellipodia are peripheral thick cortical actin found at the leading edge. (C) Stress fibres: They are bundles of actin filaments associated with myosin II and accessory proteins (Lamalice at al., 2007).

1.3.1.1 Stress fibres

Endothelial cells are steadily exposed to mechanical stress due to hydrostatic, cyclic stretch and fluid shear as blood flow over their surfaces. These environments stimulate the development of actin stress fibres in ECs. *In vivo,* the endothelial stress fibres are developed along the direction of blood flow, especially in arteries (Pellegrin and Mellor, 2007). Stress fibres are the cytoskeletal F-actin cables (approximately 10 to 30 actin filaments) (Cramer et al., 1997), which are linked to the cell membrane at focal adhesion at the plasma membrane. They are located towards the leading edge during migration. Fibre bundles are linked with actin-crosslinking proteins such as α-actinin, Fascin, Espin, and Filamin. The formation of stress fibres is diverse in each fibre. Based on their sub-cellular locations, stress fibres are divided into three classes (Fig. 1.26). Ventral stress fibres are most abundant stress fibres that arise along the basal of the cells and attaches to focal adhesion at both ends. Dorsal stress fibres arise from dorsal contacts. At one side they are attached to focal adhesion, the other direction terminates in a loose matrix. Transverse arcs are observed beneath the dorsal surface in migrating cells (Hotulainen and Lappalainen, 2006; Pellegrin and Mellor, 2007).

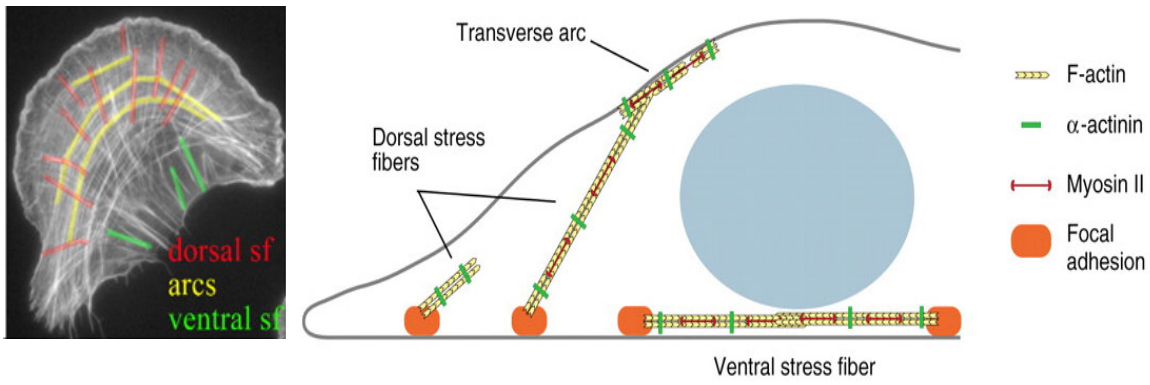

Figure 1.26: The three classes of actin stress fibres

(Left): F-actins were highlighted in U2O2 cells. The three categories of stress fibres are marked with colours (Hotulainen and Lappalainen, 2006). (Right): Schematic representation of sub-cellular location of stress fibres (Pellegrin and Mellor, 2007).

1.3.1.2 Filopodia

Filopodia are rod-shaped protrusions, which are filled with linear actin filaments. Filopodia are evolutionary conserved structure from amoeba to human and their frequency of the formation is strongly dependent on the cell type (Rottner et al., 2011). Filopodia explore adhesive surfaces and sense molecular cues to determine the direction of cell motility. For example, filopodia in neuronal cells recognize attractive and repulsive cues for axon guidance. In endothelial tip cells, filopodia sense the VEGF concentration gradient and guide sprouting of ECs during angiogenesis (Yang and Svitkina, 2011). Structurally, filopodia are formed from 10 or more actin filament bundles mediated by a small cross-linking protein, Fascin (Arjonen et al., 2011).

Regarding the formation of filopodia, two different models have been suggested. The convergent elongation model accounts for the elongation of filopodia from lamellipodia meshwork where is recognized by Arp2/3 complex. On the other hand, the tip nucleation model elucidates this process from cortical actin cytoskeleton by directly nucleating by formin on the plasma membrane (Gupton and Gertler, 2007: Yang and Svitkina, 2011).

1.3.1.3 Lamellipodia

The lamellipodia are surface-attached membrane protrusions that are observed in motile cells. The lamellipodium of motile cells consists of a thin (0.1-0.2 μm) fila-

ment filled with high-density actin filaments (100/μm of leading edge) (Abraham et al., 1999). Lamellipodia can fold towards or backwards onto the cell. This is called ''ruffled'' and this process is known as ruffling (Rottner and Stradal, 2011). The lamellipodia filaments are generated from the plasma membrane by branching mediated by WASP-Arp2/3.

1.3.2 Actin dynamics

In a cell, actin is found as two major forms: the G-actin (monomer form of actin) and the F-actin (helical polymer of actin). Straub and his colleagues reported that monomeric globular actin (G-actin) could transform into fibrous polymers in the presence of salt (Saito, 2009). Between two forms, actin filaments are structurally and kinetically dynamic. During polymerization, actin filaments have an inherent polarity that is termed as the plus end (or barbed end) and the minus end (or pointed end). At the plus end, ATP-G-actins get together and are hydrolysed. The hydrolysed ADP-actin is released at the minus end. Free ADP-actin can be turned into GTP-actin, then can be incorporated at the plus end again (Lambrechts et al., 2004). This process is referred to as actin treadmilling (Fig. 1.27).

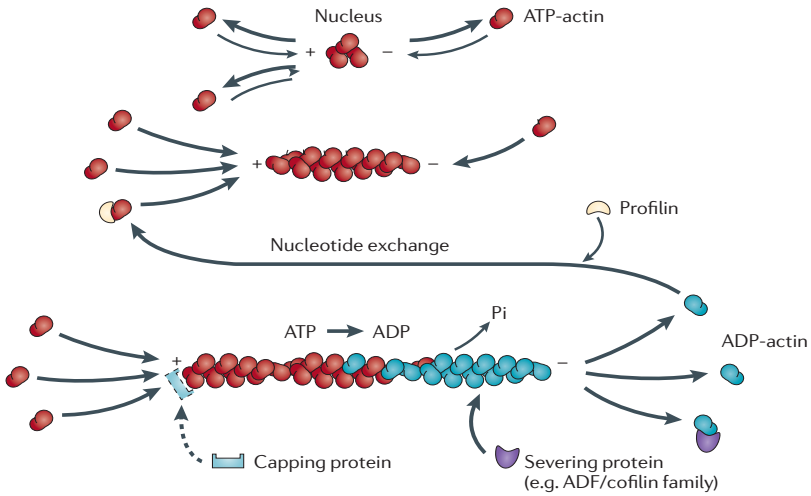

Figure 1.27: Schematic mechanism of actin polymerization

Spontaneous actin polymerization is naturally impeded by the kinetics. Once an actin is nucleated, the incorporation of actin monomers is accelerated in the presence of ATP. When ATP is hydrolysed and dephosphorylated, this brings about destabilization of the filaments. Then, the filament becomes prone to associate with severing proteins such as actin depolymerizing (ADP)/Cofilin (Nürnberg et al., 2011).

The growth of actin filament is initiated by the assembly of actin monomers called nucleation. During assembly of filament, polymerization of three G-actins was much favourably processed. Then, subsequent monomer addition is followed. On the other hand, filament assembly by serial steps from monomers, the dimerization, and trimerization are not favourable (Chhabra and Higgs, 2007). Actually, the growth of actin filament occurs at both ends of the actin filament. However, the elongation at the plus end is faster (five- to tenfold) than at the minus end (Allingham et al., 2006).

1.3.3 Actin-binding proteins

Actin is regulated via various actin-binding proteins. In this chapter, representative proteins that alter actin dynamics and their functions are introduced.

1.3.3.1 Actin nucleating/polymerizing factors - Profilin

Actin polymerization can be stimulated by various mechanisms (Chhabra and Higgs, 2007). Arp2/3 is the first discovered actin nucleating protein that creates *de novo* actin nucleation by branching from existing filament. Formin creates a nucleation of an actin filament, then moves to the barbed end. Spire nucleates an actin filament by stabilizing a longitudinal tetramer. After nucleation spire detaches from the filament.

1.3.3.2 Actin depolymerizing factor (ADF) - Cofilin

Some actin-binding proteins induce severing of actin filaments. Cofilin-1 (non-musical cells), Cofilin-2 (muscle cells), Gesolin, and Twinfilin belong to this group of proteins. The expression of all these proteins is observed in all eukaryotes (Domingguez and Holmes, 2011). As mentioned above, ADP-actin is produced by hydrolysis of ATP in the filament, and ADF factor proteins have high sensibility to ADP-actin. Cofilin binds to actin dimer to stimulate disassembly of the filament. This process is initiated by Gelsolin (Taylor et al., 2011). Cofilin also splits the actin filament without association with the barbed end (Lambrechts et al., 2004).

1.3.3.3 Actin modulators (actin-targeting nature products)

There are some natural chemicals that modulate actin dynamics *in vitro*. These substances alter actin dynamics by different mechanisms.

Latrunculin B (Lat B): ATP binding cleft-binding protein

Lat B is a cytotoxin isolated from Red Sea sponge *Negombata magnifica* (Morton et. al. 2000; Allingham et al., 2006). It exudes a noxious red fluid that kills a fish within minutes. Lat B only binds to actin monomers. The crystal structure shows that Lat B binds within the interface between actin sub-domain 2 and 4, above the actin-binding site. That is, Lat B may interfere by occupying this site and restrict conformational changes, thereby sequestering actin monomers from polymerization.

Jasplakinolide (Jasp): barbed end-binding protein

Jasplakinolide is synthesized by the marine sponge *Jaspis johnstoni* and described as an actin filament stabilizer as well as an *in vitro* inducer of actin polymerization (Bubb et al. 2000). This is achieved by both of increasing of the nucleation rate and of decreasing of the sequestered actin monomers. However, *in vivo* jasplakinolide disrupts a filament formation because of its competition with phalloidin to bind to the actin. This mechanism is still poorly understood.

Cytochalasin D (Cyto D): barbed end-binding protein

Cyto D is a cell permeable fungal toxin purified from *Zygusporium mansonii* (Cooper, 1987). Cyto D promotes actin depolymerization in two ways. First, it binds to the barbed end of the actin filament, then inhibits association of G-actin to the actin filament. A stoichiometry study elucidates that cytochalasin binds to the actin filament with an 1:1 ratio (Wakatsuki et al., 2001). Second, Cyto D stimulates depolymerization of the filament by capping the barbed end as well as ATP hydrolysis of G-actin.

Both Lat B and Cyto D hinder actin polymerization, however, have different effects on the MRTF/SRF activation (Fig. 1.28). Cyto D promotes dissociation of the G-actin-MRTF complex, thereby liberating MRTF-A from G-actin. This contributes to the activation of MRTF/SRF transcription. On the contrary, Lat B supresses the MRTF/SRF

activity by blocking disassociation of MRTF-A from the G-actin-MRTF complex (Miralles et al., 2003).

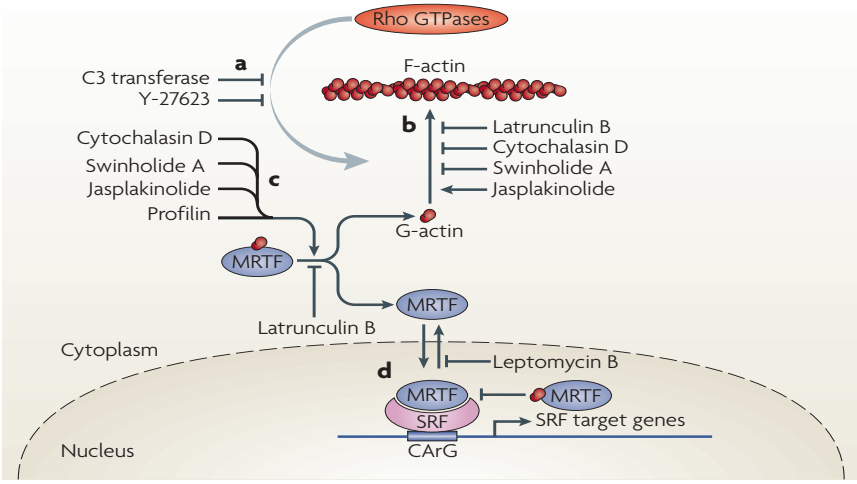

Figure 1.28: The effect of Rho GTPase and actin modulators on MRTF activation

MRTF regulation by actin dynamics can be modulated by actin-binding drugs or activity of the Rho GTPses. (a): Inhibition of RhoA-induced actin polymerization, (b): Alteration in actin polymerization, (c): Influence on MRTF/G-actin complex, (d): Influence on nuclear MRTF/G-actin complex (Olson and Nordheim, 2010).

DNAse I: G-actin binding-protein

DNAs I is an enzyme that hydrolyzes specific single or double strand DNA producing 3′-OH oligonucleotide fragments (Hitchcock, 1980). Since purified pancreatic DNAse I has a high affinity to actin monomer, DNAse I has been used for labelling of G-actin in conjunction with fluorescence markers. DNAse I forms an 1:1 complex with G-actin. In the complex, the activity of DNAse I is inhibited. DNAse I does not tightly bind to the actin filament. However, once bound, DNAse I initiates actin depolymerization and exists 1:1 complex with depolymerized-actin.

Phalloidin: F-actin binding-protein

Phalloidin is a fungal toxin originated from poisonous 'Death Cap' mushroom *Amanita phalloides* (Cooper, 1987). Phalloidin has a much higher affinity to F-actin than to G-actin (Fig. 1.29). Due to this characteristic, conjugation of fluorescence markers to phalloidin enables the visualization of F-actin structure *in vitro*. Additionally, the

functions of phalloidin are known as stabilization of actin filaments and acceleration of actin polymerization.

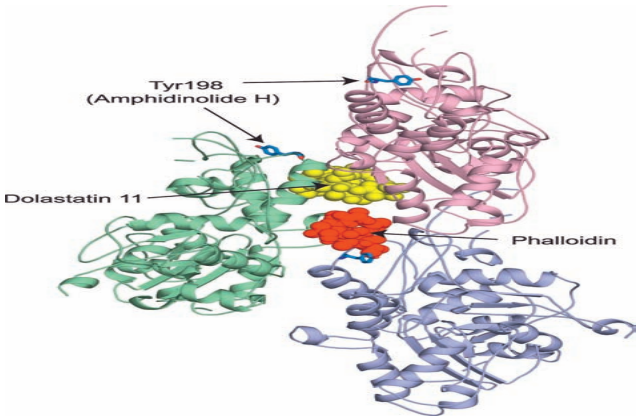

Figure 1.29: Binding site of phalloidin within actin

Schematic image shows that phalloidin interacts with actin. The phalloidin (red spheres) binds to the actin filament and interacts with three actin monomers simultaneously (Allingham et al., 2006).

1.4 The Rho small GTPase

The Rho (Ras homologue) is a Ras superfamily of small GTPase (20 - 30 kDa) that regulates numerous cellular functions such as cytoskeletal dynamics, NADPH oxidase activation, migration, polarity, membrane trafficking, and transcription (Ridley, 2012). Since the first proteins of Rho GTPase, RhoA, has been discovered (Madaule and Axel, 1985), 22 members of mammalian Rho proteins were identified, so far.

1.4.1 The families of Rho GTPases

In the early 1980s, a 21 kDa viral Ha-Ras was identified as the first member of Ras member of small GTPase which was implicated in tumour progression (Andersen et al., 1981). Since then, numerous Ras superfamily proteins were discovered (more than 150 members in mammals). Ras and Ras-related proteins are considered as evolutionally very conserved molecules (the most conserved protein involved in cell signalling among species) due to the fact that they are found in all searched eukaryotes (Boureux et al., 2006).

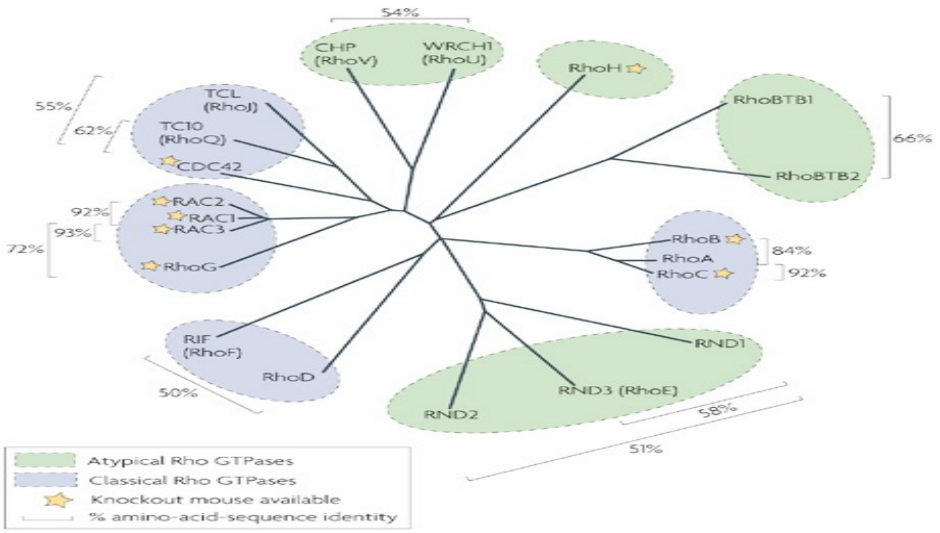

Figure 1.30: Phylogenetic tree of 20 representative Rho family proteins

Rho family proteins are divided into 8 sub-families that are designated with a circle. Rho GTPases within blue circles are the classical Rho GTPases that are regulated by transition between GDP-bound and GTP-bound Rho. The Atypical GTPases in green circles need an additional mechanism for amino acid substitution, therefore are not regulated by GEF and GAP. These 20 GTPase are commonly found in most mammals, some tissue specific splicing variants were reported. Figure is from Heasman and Ridley, 2008 and text is quoted from Boureux et al., 2006.

Ras superfamily is divided into five subgroups: Ras, Rho, Rab, Arf, and Ran (Fig. 1.30). Among them, Rho proteins are distinguished from other Ras proteins with a presence of Rho-specific 12-amino acid insert domain between G4 and G5 boxes (Freeman et al., 1996).

1.4.2 Rho regulators

To regulate Rho pathway, three Rho regulators have been characterized. These factors cause molecular changes of Rho proteins, thereby allowing Rho proteins as a molecular switch in the cell.

1.4.2.1 RhoGEFs (Guanine nucleotide exchange factors)

Rho GEFs are essential factors to activate Rho proteins. GEFs stimulate disassociation of GDP from Rho-bound GDP complex. This process happens step by step (Fig. 1.31). First, GEF binds to Rho-GDP complex with low affinity. This enables GDP to dissociate from Rho-GDP complex. Since in the cytosol, the concentration of GTP is much higher than GDP, GTP easily docks to Rho protein. Then, GEF is quickly liberated from Rho proteins.

Figure 1.31: Exchanges of Rho-bound nucleotides by RhoGEF

The changes of nucleotide from GDP to GTP at Rho proteins are mediated by RhoGEF (Cherfils and Chardin, 1999).

The first identified RhoGEF was Dbl, which is originated in B-cell-lymphoma cells. Since then, 69 members of human Dbl family members proteins have been identified. Among 69 members, Tiam1, LARG (leukaemia-associated Rho GEF), Abr, Bcr, Sos, and Vav families are intensively studied (Rossman et al., 2005).

1.4.2.2 RhoGAPs (GTPase activating proteins)

RhoA mediated signalling can be terminated by RhoGAP-mediated hydrolysis of RhoGTP. RhoGAP stimulates hydrolysis rate of GTP to GDP up to 10^5. Even though

the structures of GAP domains are diverse within GAP families, GAP domains are commonly folded into α-helical structures. RhoGAP domain contains 9 α-helices and conserved arginine residue referred as an arginine finger.

The nucleotide hydrolysis mechanism can be explained by the conventional arginine finger/switch II glutamine mechanism (Hakoshima et al., 2003; Moon and Zheng, 2003; Cherfils and Zeghouf, 2013). In the ground state, RhoGAP-RhoA complex is bound to non-hydrolysable GTP analogue, GMPPNP. Upon a binding of RhoGAP to GDP and Alf (aluminium fluoride, Alf_3 or Alf_4), Alf is used to mimic its transition state. This Rho-GDP-Alf_4 complex reveals a 20° body rotation between RhoA and GAP. In the transited position, GAP interacts with switch I, II regions* via arginine finger and p-loop of Rho, thereby stabilizing partial negative charges at the GTP-binding core. There, the conserved glutamine from the switch II (Gln61 in Ras, Gln 63 in Rho) activates and restricts hydrolytic water molecules that enable nucleophilic attack for the g-phosphate of GTP. The arginine finger also interacts with GTP and Mg^{2+} ion to neutralize the charges in the phosphate group as well as to stabilize phosphate group and ion.

As a negative regulator of Rho pathway, mutations on RhoGAP are able to result in hyperactivatation of Rho signalling. These mutations are oft observed in some cancer models. For instance, the deletion of DLC-1, a GAP for RhoA and cdc42, is widely observed in breast tumour patients and DLC-2 downregulation was observed in a HCC model (Ellenbroek and Collard, 2007). In another GAP, such as RasGAP, mutations on p-loop interferes in attachment of arginine finger of RasGAP, hence Ras activity is continuously activated (Cherfils and Zeghouf, 2013). These mutants were found in cancer patients.

* switch I and II region: Two regions exist in RhoGTPase, which undergo a conformational change in the GTP-bound form. In this region, active GTPases interact with downstream effectors (Garcia-Mata et al., 2012).

1.4.2.3 RhoGDIs (GDP dissociation inhibitors)

RhoGDIs are the first discovered Rho regulators. Their names are designated according to their role, namely inhibition of dissociation of GDP from Rho and prevention the binding of GTPγS to Rho-GDP.

RhoGDI specifically binds with GDP-bound Rho with a ratio 1:1, but not with GTP-bound or nucleotide-free Rho protein (Ueda et al., 1990). Since RhoGDI binds to Rho proteins via its C-terminus prenyl group of Rho, RhoGDI captures Rho proteins from the surface membrane of ER and transfers to the plasma membrane after post-translational modification (prenylation*) of Rho protein (Boulter et al., 2012).

Moreover, Rho GDI controls the concentration of Rho proteins (Boulter et al., 2012). RhoGDI selectively docks to Rho-GDP complexes on the plasma membrane, and induces the detachment from the plasma membrane. In the cytosol, RhoGDI-bound Rho proteins are prevented from proteasomal degradation. Since the number of RhoGDI is restricted in a cell, RhoGDI plays a role in regulation of RhoA concentration.

In contrast to RhoGEFs and RhoGAPs, which have various numbers of proteins (more than 70 GEFs and 80 GAPs) (Marinissen et al., 2005), only three RhoGDI proteins were reported in mammals and plants. RhoGDI1 (RhoGDI or GIIa) is a ubiquitously expressed GDI, which binds to most Rho family proteins. RhoGDI2 (D4-Ly-GDI or RhoGDIb) is a hematopoietic-specific form of GDI that is more specific to Rac1 family of small GTPase. RhoGDI3 (GDIg) is known as a lung-, brain- and testis-specific GDI. Its activity is specifically restricted to RhoG (DerMardirossian and Bokoch, 2005; Dransart et al., 2005).

* Prenylation: the process that adds hydrophobic prenyl groups (3-methyl-2-butane-1-yl) to the protein by transferring either a farnesyl or a geranyl-geranyl moiety to the C-terminus cysteine of the target protein. Most of the Ras GTPases undergo various lipid modifications during PTM. In case of Rho, isoprenylation is used for the protein maturation (Boulter et al., 2012).

1.4.3 Biological functions of the RhoA-ROCK cascade

The importance of RhoA-ROCK-mediated signalling has been diversely elucidated. The role of RhoA has been studied both *in vivo* and *in vitro,* demonstrating its pivotal role during development and in cytokinesis, respectively. Endothelial-specific Rho GTPase-deleted mice died *in utero* due to vascular defects (Heasman and Ridley, 2008; Jin et al., 2013). In cells, disruption of RhoA by siRNA or chemical inhibitors induced abnormal cortical contractility and furrow formation (Piekny et al., 2005).

The Rho-ROCK pathway also plays an important role in gene regulation of cell cycle proteins and proliferation. ROCK is the regulator of cyclin D, cyclin D1, and p27Kip1

(Croft and Olson, 2006). ROCK (ROCK II) also interacts with the nuclear phosphoprotein, Nucleophosmin (NPM-1) (Hanashiro et al., 2011). This association is required for centrosomal duplication during S-phase.

RhoA-ROCK-mediated cell proliferation is regulated by focal adhesions (FAs). FAs are the site where integrin clustering forms a physical link between the actin cytoskeleton and the ECM (Provenzano et al., 2011). FA signalling is activated in response to the extracellular contraction. The stiffness of ECM transmitted via the actin cytoskeleton leads to the promotion of FA assembly. This leads to the activation of RhoA, thereby stimulating cell proliferation. In ECs, blockage of FAK inhibits Rho-mediated proliferation.

With these reasons, Rho pathways are able to contribute to the progression of cancer. High protein level and signalling activity of RhoA and -C are detected in various tumour types. RhoGTPases contribute to cancer by loosening of cell-to-cell contacts, by alteration of the plasticity of cell (epithelial-mesenchymal transition, EMT), and by regulation of MMPs expression involved in cancer cell invasion and metastasis (Parri and Chiarugi, 2010). Additionally, another study reported that a consistent activation of RhoA stimulated cancer cell transformation (Jaffe et al., 2005).

In ECs, RhoA-ROCK-induced cell contraction regulation is underlined in aspect of paracellular permeability. The vascular permeability is defined as a property of the capillary wall to impede movement of substances driven by physical force (Bates, 2010). Paracellular pathway is the passage between two endothelial cells through endothelial junctions, which is regulated by contraction of the cytoskeleton. Abnormally increased endothelial cell contraction is closely related to pathological conditions (Chen et al., 2010). Therefore, the equilibrium between endothelial junctions and actinmyosin-based centripetal tension is tightly controlled.

Phosphorylation of the myosin light chain (MLC) is the primary contributor to this equilibrium and regulated by MLC Phosphatase and MLC kinase (MLCK). It is achieved by two different mechanisms: an initial contraction by Ca^{2+}-calmodulin in muscle cells and a transient contraction by RhoA-ROCK in non-muscle cells (Fig. 1.32). In vascular ECs, ROCK phosphorylates myosin-binding sub-unit of myosin phosphatase, thereby resulting in inactivation of myosin phosphatase (Spindler et al., 2010).

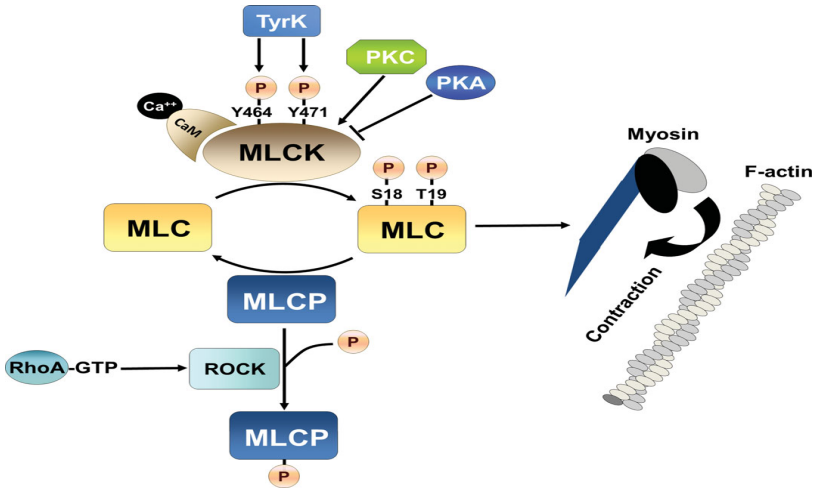

Figure 1.32: MLC-dependent regulation of cytoskeletal contraction in ECs

Phosphorylation of MLC at Ser-18 and Tyr-19 is increased in response to MLCK activation or inhibition of myosin light chain phosphatase (MLCP). In endothelium, actin-myosin contraction is regulated by MLCK. The activity of MLCK is increased in response to the Ca^{2+}-calmodulin binding, phosphorylation by protein kinase C (PKC), or tyrosine kinase phosphorylation at Tyr-464 and Tyr-471 whereas decreased in response to protein kinase A (PKA). RhoA activation is also involved in phosphorylation of MLC since ROCK activation inhibits MLCP, resulting in phosphorylation-dependent inhibition of MLCP (Rigor et al., 2013).

1.4.4 RhoA signalling

The classically activated Rho signalling is mediated by binary switch between GTP-bound (Turn on) and GDP-bound (Turn off) as mentioned above. Once activated, GTP-bound Rho recruits various effectors to initiate following cascades. These cascades are mediated by different Rho effector proteins (Fig. 1.33).

1.4.4.1 Rho effectors: ROCK and mDia

So far, more than 70 effector proteins have been described. They are mostly serine/threonine kinases (Ellenbroek and Collard, 2007). Among them, there are two most intensively studied effectors: ROCK (Rho-associated coiled-coil-containing kinase) and mDia (mammalian homolog of Drosophila diaphanous).

ROCK is the representative serine/threonine kinase that belongs to the AGC (PKA/PKG/PKC) family. Under resting conditions, the activity domain of ROCK is autoinhibited with a segment of ROCK by itself. Both ROCK isoforms, ROCK1 (ROKβ or p160ROCK) and ROCK2 (ROKα), are ubiquitously expressed. However, the dominancy of each isoform is differently observed in different tissues (Amin et al., 2013).

Two isoforms share overall 65% identity, 92% homology in the kinase domain, suggesting that they have similar specificity to the substrate targets.

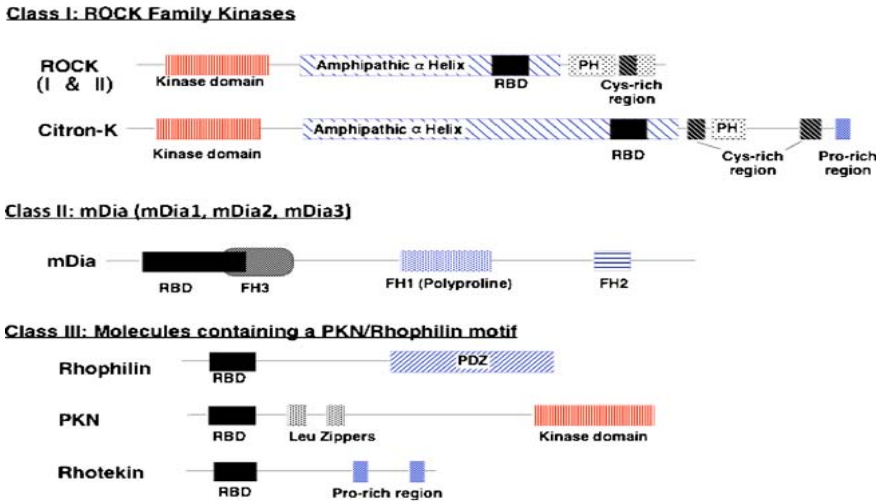

Figure 1.33: The Rho effectors

Rho effectors are divided by based on homology of domain structure. RBD: Rho binding domain, PH: pleckstrin homology domain, FH: formin homology domain (Narumiya et al., 2009).

The C-terminus domain of ROCK consists of RBD and PH domain (Fig. 1.33). This region is responsible for negative regulation of kinase activity. Interference of this site, such as site deletion or neutralization by antibody, resulted in consistently activated of ROCK (Amano et al., 2010). ROCK plays a critical role in modulation of the cytoskeleton (stress fibres), actin-myosin contraction (tension), and MLCP activity by increasing phosphorylation of MLC (Fig. 1.34).

ROCK also regulates microtubule dynamics by phosphorylating tubulin polymerization promoting protein 1 (TPPP1/p25), thereby controlling cellular migration and invasion at the microtubule level (Schofield et al., 2012). However, microtubule regulation by Rho has been more elucidated by cooperation with its other effector mDia. mDia is a Formin family of actin-binding protein that induces actin polymerization by microtubule stabilization and creates actin nucleation. mDia localized at the leading front of migrating cells. There, it induces cellular polarization and adhesion. Since ROCK antagonizes mDia-mediated Rac activation and membrane ruffle formation, the regulation of cell morphogenesis, adhesion, and motility can be determined by the balance between mDia and ROCK (Narumiya et al., 2009).

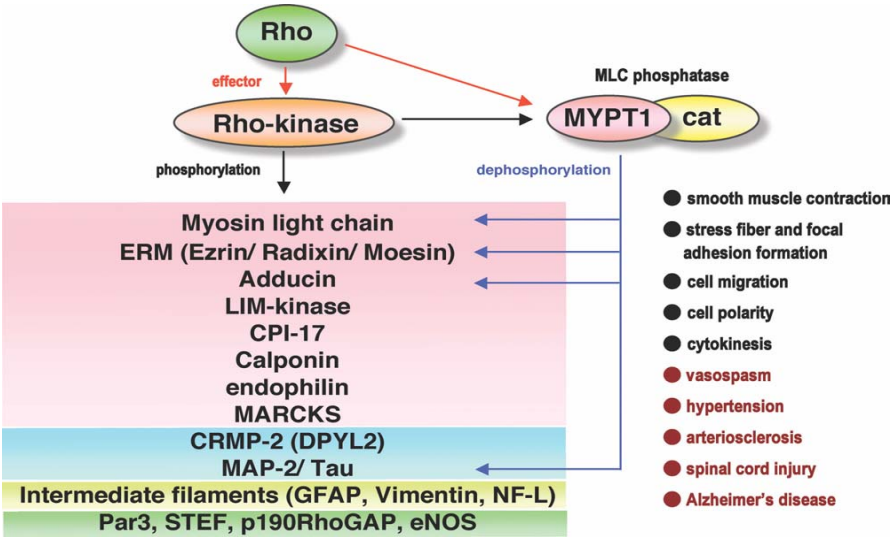

Figure 1.34: Targets of ROCK and biological processes

ROCK mediates phosphorylation of various substrates. (Red): actin binding proteins, (Blue): microtubule binding proteins, (Yellow): intermediate filaments, (Green): proteins involved in other pathways. At the right, physiological (black) and pathological (red) processes by ROCK are designated (Amano et al., 2010).

1.4.4.2 RhoA pathway inhibitors

RhoA inhibitor: C3 transferase (CT04)

CT04 is the commercial name of purified C3 transferase of Cytoskeleton, Inc. Its inhibitory effect against RhoA is already proven in various studies (Kakudo et al, 2011; Kim et al, 2012). CT04 is the exoenzyme C3 transferase originated from *Clostridium botulinum*. According to the product datasheet, C3 transferase is covalently attached to a proprietary cell-penetrating moiety via disulfide bond. Through this modification, CT04 can be directly given to the cell and rapidly transported through the plasma membrane. In a cell, the cell-penetrating moiety is released in the cytosol, thereby free-liberated C3 transferase specifically inhibits RhoA, B, and C proteins (Kakudo et al, 2011). The inhibitory mechanism of CT04 is achieved by ADP-ribosylation on asparagine 41 in the effector-binding domain of the Rho protein, thereby inactivating GTP-binding proteins (Sehr et al., 1998). It does not alter other small GTPases such as Rac1 and cdc42 (Kakudo et al., 2011).

RhoA signalling inhibitor: CCG-1423

CCG-1423 (Center for Chemical Genomics core facility at the University of Michigan-Ann Arbor) was recently identified as a RhoA and RhoC signalling inhibitor (Evelyn et al., 2007 and 2010) (Fig. 1.35). In order to identify a new RhoA inhibitor, more than 2,000 compounds from the Maybridge Diverse Chemical Compound Collection were screened and finally two novel chemicals (CCG-977 and CCG-1423) that specifically inhibit the RhoA pathway were identified. By SRE.L Luciferase assays, the inhibitory activity was confirmed without specific cellular toxicity in HEK 293. CCG-1423 does not influence SRF binding on the SRE and does not alter ROCK activity. Clearly, CCG-1423 inhibits Gα-LARG (Leukemia-associated RhoGEF)-RhoA triggered MRTF-SRF transcription. However, this mechanism is not clarified yet.

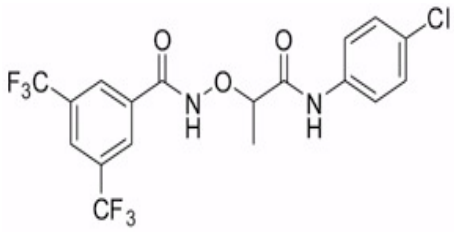

Figure 1.35: The structure of CCG-1423

Chemical structure of CCG-1423 is shown. CCG-1423 has an aliphatic linker linking six atoms between R1 (3,5-bis-trifluoromethylphenyl) and R2 (p-chlorophenyl) group, whereas CCG-977 contains an aromatic linker with eight atoms between them (Evelyn et al., 2007 and 2010).

ROCK inhibitor: Y-27632

Y-27632, (+)-(R)-*trans*-4-(1-aminoethyl)-N-(4-pyridyl)cyclohexanecarboxamide dihydrochloride, is now widely used as a specific inhibitor of Rho kinase, ROCK. Y-27632 has a much higher affinity (at least 20 to 30 times) and inhibitory effect (100 times more powerful) to the both ROCK isoforms than other ROCK effectors (Ishizaki et al., 2000; Rafferty et al., 2012).

The mechanism of inhibition is introduced by blocking the catalytic site of ROCK by competing with ATP for binding (Ishizaki et al., 2000). The effect is against both of ROCK isoforms, however, due to the fact that ROCK can inhibit other kinases at high concentration, Y-27632 has not permitted the adaption for use in human studies (Surma et al., 2011).

Previous reports showed that Y-27632 altered endothelial behaviour such as endothelial cell attachment, proliferation, and inhibition of apoptosis (Okumura et al., 2009). In addition, Y-27632 is involved in eNOS production and NO release from ECs (Nunes et al., 2010). Moreover, blocking of ROCK by Y-27632 delayed stress fibre formation and reduced VEGF-mediated vascular permeability (Curry and Admson, 2010). In other cells, Y-27632-mediated G1 to S cell cycle transition was also reported (Ishizaki et al., 2000).

1.5 Aim of this study

Our recent study proved that endothelial-specific genetic depletion of SRF resulted in embryonic lethality when induced during embryogenesis, and in defects in murine retinal vascularization when induced at postnatal and adult age (Weinl et al., 2013). We identified endothelial MRTF to be required for proper murine retinal vascularization at postnatal age. In addition, genes, which are deeply involved in angiogenesis, such as *Vegfr2*, VE-cadherin (*Cdh5*), and β-actin (*Actab*), were confirmed as endothelial MRTF/SRF target genes. Based on these observations, we hypothesize an endothelial specific role of SRF in cooperation with MRTF to be essential for angiogenesis.

To investigate the role of SRF and MRTF in endothelial cells in more detail, this work focused on endothelial cells *in vitro*. Experiments were designed to identify transcriptional activation of SRF-MRTF, which is driven by VEGF. First, VEGF-driven SRF target gene expression was investigated. Furthermore, luciferase assays were applied to prove SRF-mediated transcriptional activation by VEGF.

Of note, the main idea of this study was to identify the effect of VEGF on endothelial MRTF. Since nuclear localization of MRTF is a key event for MRTF-driven SRF gene expression, sub-cellular location of MRTF was examined upon VEGF stimulation. In accordance with other reports, RhoA-mediated signalling was chosen as a target of this signalling. Because RhoA-mediated changes in actin dynamics is the regulatory mechanism of MRTF, various RhoA inhibitors as well as *in vitro* actin modulators were used. At the same time, VEGF and RhoA inhibition-caused changes in endothelial actins were also explored.

Additionally, novel endothelial SRF/MRTF target genes were analysed by siRNA strategy. Potential genes that are involved in angiogenesis were chosen and their expression was studied upon SRF depletion. Besides, siMRTFs were screened for further studies.

By this approach, VEGF-induced changes of SRF and its target gene expression as well as its effect on MRTF in endothelial cells can be elucidated. With these results, regulatory mechanisms of SRF/MRTF in ECs can be better understood.

2. MATERIALS AND METHODS

2.1 Materials

2.1.1 Technical equipment

Device	Manufacturer
Bench top centrifuges	Heraeus Pico 17, Thermo Scientific
Centrifuge for cell culture	Megafuge 2.0R, Thermo Scientific
Clean bench	Integra biosciences
DNA speed Vac, DNA110	Savant Instruments
Deep freezer	Thermo Scientific
Densitometer	Molecular Dynamics, Inc
Electrophoresis power supply	Pharmacia Biotech
Fluorescence microscope	Axiovert 200M, Zeiss
Ice crusher	Wessamat
Incubator	Heraeus Instruments
Incubator, CO_2	Thermo Scientific
Incubator shaker	New brunswick scientific
Luminometer	Lumat LB 9507, Berthold
Magnetic stirrer	Heidolph
NanoDrop	NanoDrop 1000, Thermo Scientific
Optical microscope	Axiovert 25, Zeiss
pH meter	Hanna instruments
Real-Time PCR Instrument	Applied Biosystems
Refrigerated incubator shaker	New Brunswick Scientific
Rotating shaker	GFL
Scale	Sartorius
SDS-PAGE and blotting apparatus	Bio-Rad
Sonicator	Branson Sonifier® 250
Sprout minicentifuge	Biozym
Thermomixer	Eppendorf

UV/visible spectrophotometer	Pharmacia Biotech
Vortexer	Neolab
Water bath	GFL
Water purification system	Millipore

2.1.2 Chemicals

Chemical	Purchased from
Acrylamide (40%, Mix 19:1)	AppliChem
Adenosine triphosphate (ATP)	AppliChem
Ammonium persulfate	Genaxxon
Bovine serum albumin (BSA)	AppliChem
Bovine serum albumin (BSA, purified)	New England Biolabs
CCG-1423	Calbiochem
Chelex100	Bio-Rad
Coomassie Brilliant Blue	Sigma-Aldrich
CT04	Cytoskeleton, Inc.
Cytochalasin D	Calbiochem
DNAse I (Alexa Fluor® 488-conjugated)	Invitrogen
DNase I recombinant, RNase-free	Roche
DAPI (4',6-Diamidino-2-phenylindol)	AppliChem
Dimethyl sulfoxide (DMSO)	AppliChem
Ethanol	Sigma-Aldrich
Fetal calf serum	PAN Biotech
Gelatin from porcine skin	Sigma-Aldrich
L-glutamine	Invitrogen
Glycine	AppliChem
Glycerin	AppliChem
Hydrogen chloride (HCl), 37%	Fluka
IFN-γ recombinant murine	Peprotech
Immersion oil	Zeiss
Isopropanol	Fisher scientific
Jasplakinokide	Calbiochem
Latrunculin B	Calbiochem
Lipofectamine® 2000 transfection reagent	Invitrogen
Lipofectamine® RNAiMAX transfection reagent	Invitrogen

D-luciferin	AppliChem
MEM Non-Essential Amino Acids Solution	Invitrogen
β-Mercaptoethanol	AppliChem
Methanol	Sigma-Aldrich
Mowiol	Carl Roth
MTT (3-[4,5-dimethylthiazol-2-yl]-2,5- diphenyltetrazolium bromide; thiazolyl blue)	Sigma-Aldrich
M-MLV Reverse Transcriptase 5X buffer	Promega
M-MLV Reverse Transcriptase RNase H Minus	Promega
Nitric acid (HNO_3)	Fluka
Nonfat dry milk (skim milk)	AppliChem
Penicillin-streptomycin (Pen/Strep)	Invitrogen
Phalloidin, sulforhodamine 101 (Texas-Red)-conjugated	Biotium Hayward
Phosphatase Inhibitor Cocktail PhosSTOP	Roche
Phosphate buffered saline (PBS)	PAA
n-Propyl gallate	Sigma-Aldrich
Protease inhibitor (complete, EDTA free)	Roche
PromoFectin-HUVEC transfection reagent	PromoCell
Protein A-Agarose beads	Santa Cruz
Proteinase K	Genaxxon
Rabbit serum	Vector Laboratories
Random Hexamers	Sigma-Aldrich
RiboLock RNase Inhibitor	Thermo Scientific
Sodium azide (NaN_3)	Merck
Sodium chloride (NaCl)	Sigma-Aldrich
Sodium dodecyl sulfate (SDS)	AppliChem
Sodium hydroxide (NaOH)	AppliChem
Sodium pyruvate	Invitrogen
Sucrose	AppliChem
SYBR Green master	Roche
Tetramethylethylendiamine (TEMED)	AppliChem
Triton® X-100	AppliChem
Trizma® base	Sigma-Aldrich
Trypan Blue	Sigma-Aldrich
Tween® 20	AppliChem
$VEGF_{120}$ recombinant mouse	R&D Systems

$VEGF_{165}$ recombinant human	Peprotech
Y-27632 in Solution™	Calbiochem

2.1.3 Cell culture

2.1.3.1 Endothelial cell lines (ECs)

mECs (immortalized mouse ECs) were used mainly for this study. They are kindly provided by Prof. Ralf Adams at the Max Planck Institute in Münster and described in a previous study (Benedito et al., 2009). For additional studies, HRMVECs (Human Retinal Microvascular Endothelial Cells) were purchased from Cell Systems, HUVECs (Human umbilical vein endothelial cells) were purchased from Lonza.

2.1.3.2 Cell culture media

For mECs

DMEM containing 10% (v/v) heat-inactivated FCS, 1% (v/v) L-glutamine (200 mM), 1% (v/v) MEM non-essential amino acids (100x), 1% (v/v) penicilin/Streptomycin, 1% (v/v) sodium pyruvate (100 mM), 50 U/ml IFN-γ, 5 ng/ml VEGF

For HRMVECs

EGM-2 MV: EBM-2 containing ascorbic acid, hEGF, 25 ml FBS, hFGF-B, GA-1000 (gentamicin, amphotericin-B), hydrocortisone, R3-IGF-1, VEGF

For HUVECs

EGM-2: EBM-2 containing ascorbic acid, hEGF, 10 ml FBS, hFGF-B, GA-1000 (gentamicin, amphotericin-B), heparin, hydrocortisone, R3-IGF-1, VEGF

For Transfection

Opti-MEM® Reduced Serum Medium, GlutaMAX™

2.1.3.3 Cell culture chemicals

FCS (fetal calf serum)	Heat inactivation at 56°C, 30 min, PAA Laboratories

Gelatin solution	0.2% (w/v) gelatin in PBS Sterilization by autoclave
Mycoplasma detection kit	Venor®GeM Classic Mycoplasma PCR Detection Kit, Minerva Biolabs
PBS (phosphate buffered saline)	Dulbecco's PBS (1x) without Ca & Ma, PAA Laboratories
Trypan Blue solution	0.2% (w/v) Trypan Blue in PBS
Trypsin-EDTA solution	0.5% Trypsin-EDTA (1x), Gibco®

2.1.4 Oligonucleotides

Oligonucleotides used for qRT-PCR experiments were ordered from Sigma-Aldrich. For siRNA study, siSRF797 and siGL2 were synthesized and purchased from Purimex. siMRTF-A, siMRTF-B, and all star negative control siRNA were purchased from Qiagen Science.

2.1.4.1 Oligonucleotides for qRT-PCR

Gene	Direction	Sequence	Reference
β-actin	Forward Reverse	5'-AGAGAGGTATCCTGACCCTGAAGT-3' 5'-CACGCAGCTCATTGTAGAAGGTGT-3'	Ohrnberger, 2010
Adam10	Forward Reverse	5'-TCTCCGGAATCCGTAACATC-3' 5'-TCCAGGAACTTCTCCACACC-3'	Franzke et al., 2009
Adam15	Forward Reverse	5'-AAAACTGCTGCTACCGAGGA-3' 5'-GGATCCGAGAAATGACAGGA-3'	Xie et al., 2008
Adam17	Forward Reverse	5'-CAGCAGCACTCCATAAGGAAA-3' 5'-TTTGTAAAAGCGTTCGGTA-3'	Franzke et al., 2009
Cofilin1	Forward Reverse	5'-TCTGGGCCCCCGAGAAT-3' 5'-TTGATGGCATCCTTGGAGC-3'	Alberti et al., 2005
c-fos	Forward Reverse	5'-CTTGCCCCTTCTCAACGA-3' 5'-GCTCCACGTTGCTGATGCT-3'	Angstenberger, 2007
Gapdh	Forward Reverse	5'-TGGATCTGACGTGCCGC-3' 5'-TGCCGTCTTCACCACCTTC-3'	Ohrnberger, 2010
Mmp2	Forward	5'-GTCGCCCCTAAAACAGACAA-3'	Yin et al., 2006

	Reverse	5'-GGTCTCGATGGTGTTCTGGT 3'	
Mmp3	Forward Reverse	5'-TGGAGATGCTCACTTTGACG-3' 5'-GCCTTGGCTGAGTGGTAGAG-3'	Urso et al., 2010
Mmp9	Forward Reverse	5'-CGTCGTGATCCCCACTTACT-3' 5'-AACACACAGGGTTTGCCTTC-3'	Yin et al., 2006
Mmp14 (MT1-MMT)	Forward Reverse	5'-ATGGGCAGTGATGAAGGTGAGTG-3' 5'-AGCTTGGCAGAGTGGAAAGACTGA-3'	Barnes et al., 2009
Mrtf-a	Forward Reverse	5'-CACTGTGACCAATAAGAGTGC-3' 5'-GCCTGTGGAGGTCATCAATG-3'	Saha et al., 2009
Mrtf-b	Forward Reverse	5'-GCCATCCCAAGAATCCAAACGAC-3' 5'-GTCATCCAAGCTGGAGGGCAGCG-3'	Saha et al., 2009
OAS1	Forward Reverse	5'-CGTGCTGCCAGCCTATGATTT-3' 5'-TTGGTTGGGCGACAGTTCAG-3'	Zhou et al., 2007
Pak1	Forward Reverse	5'-CGTATTGCGGGTGTTTGCTA-3' 5'-CACAGCAGGAGAACCAAAACC-3'	Thuy le et al., 2011
Srf (exon 1/2)	Forward Reverse	5'-CACGACCTTCAGCAAGAGGAA-3' 5'-CAAAGCCAGTGGCACTCATTC-3'	Angstenberger, 2007
Stat1	Forward Reverse	5'-GCTGGGCGTCTATCCTGTGGT-3' 5'-GCTCAGCTGGTCTGCGTTCA-3'	Zhou et al., 2007
Timp1	Forward Reverse	5'-TGGGCTCTGAGGACTACCAG-3' 5'-CTAGGGGAAGGCTTCAGGTC-3'	Urso et al., 2010
Timp2	Forward Reverse	5'-GTAGTGATCAGGGCCAAAG-3' 5'-TTCTCTGTGACCCAGTCCAT-3'	Barnes et al., 2009
Tsp-1	Forward Reverse	5'-TCGGCCTTTAACGAATGAGAA-3' 5'-AGCGGGCACCTTCCTAGTG-3'	Moon et al., 2005
Vegfr-1	Forward Reverse	5'-AGCCTACCTCACCGTGCAAG-3' 5'-AAAAGAGGGTCGCAGCCAC-3'	Tham et al., 2006
Vegfr-2	Forward Reverse	5'-GATGCCCGACTCCCTTTGA-3' 5'-CGAAAGACCACACATCGCTCT-3'	Jackson et al., 2002

2.1.4.2 Oligonucleotides for ChIP qRT-PCR

Oligonucleotides for ChIP qRT-PCR were selected by Dr. Christine Stritt.

Gene	Direction	Sequence
β-actin, +0.8 kb (CCTTTTATGG)	Forward Reverse	5'-TCTGGCTTCCTGCCCTAGGT-3' 5'-CCGGCCGCATTATTAGGAT-3'
TSP-1, −1.2 kb (CCTTATTTGG)	Forward Reverse	5'-TGCCAAGATCCTTATTTGGTGAT-3' 5'-CCAGGGATCCAGGTAAAAGCA-3'

Pak 1, control	Forward	5'-GCCCTAACTGTTAAAGGTCCTACCA-3'
	Reverse	5'-GCCCATGTGTTAAACGCCTG-3'

2.1.4.3 Oligonucleotides for siRNA

Sequences for siGL2 and siSRF were adapted from Konjer (Konjer, 2009) and sequences for siMRTFs were aquired from Qiagen Science as commercially available siRNA products.

Target gene	Direction	Sequence
siGL2	Sense	CGU ACG CGG AAU ACU UCG AdTdT
	Antisense	UCG AAG UAU UCC GCG UAC GdTdT
siSRF797	Sense	GAU GGA GUU CAU CGA CAA CAA
	Antisense	GUU GUC GAU GAA CUC CAU CUU
siMRTF-A1	Target	CAG GTA AAT TAC CCA AAG GTA
	Sense	GGU AAA UUA CCC AAA GGU ATT
	Antisense	UAC CUU UGG GUA AUU UAC CTG
siMRTF-A2	Target	CCC ACT CAG GTT CTT TCT CAA
	Sense	CAC UCA GGU UCU UUC UCA ATT
	Antisense	UUG AGA AAG AAC CUG AGU GGG
siMRTF-A3	Target	CTG CAT TTC ATG AGC AGA GAA
	Sense and antisense sequence are unknown	
siMRTF-A4	Target	CGA GGA CTA TTT GAA ACG GAA
	Sense and antisense sequence are unknown	
siMRTF-B1	Target	AAC GAC AAA CAC CGT AGC AAA
	Sense	CGA CAA ACA CCG UAG CAA ATT
	Antisense	UUU GCU ACG GUG UUU GUC GTT
siMRTF-B2	Target	AAG AGG AAA CTG GAA CAA GAA
	Sense	GAG GAA ACU GGA ACA AGA ATT
	Antisense	UUC UUG UUC CAG UUU CCU CTT
siMRTF-B3	Target	CAC TTC GAG GAT AGA AAT AAA
	Sense and antisense sequence are unknown	
siMRTF-B4	Target	CTC ATG GAA TAC TGC ACT TAA
	Sense and antisense sequence are unknown	

2.1.5 Plasmids

2.1.5.1 Plasmid constructs for luciferase reporter gene assay

The TSm and Tmm plasmids that contain the SRE of the *c-fos* promoter were designed and generated by Dr. Sebastian Raimundo (Ergin, 2008).

TSm

TSm plasmid is referred as *c-fos* construct that has an intact TCF-binding site (Ets-binding site), an intact SRF binding site (a CArG box) and a mutated AP-1 binding site. AP-1 binding site was mutated in order to exclude any effects of AP-1 on luciferase activity.

Tmm

Tmm construct was deciphered as *c-fos* construct with an intact TCF-binding site, a mutated SRF, and a mutated AP-1 binding site.

Sequences of each clone *(mutated sequences are underlined)*

Ets-binding site: 5'-AGGCCTTACACAGGA-3'

Ets-binding site (mutation): 5'-AGGCCTTACAACTAA-3'

CArG box: 5'-TGTCCATATTAGGA-3'

CArG box (mutation): 5'-TGTCCCAATCGGGA-3'

AP-1 binding site (mutation): 5'-CATCGTCGTACGCAT-3'

Schematic overview of the c-fos reporter plasmid variants TSm and Tmm

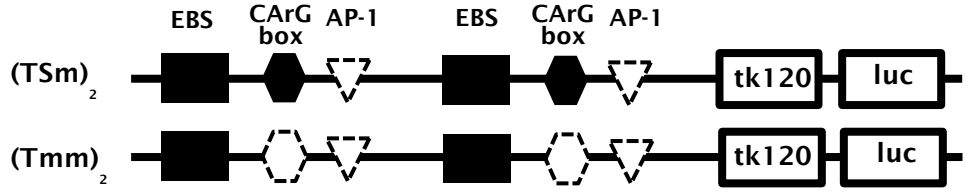

pCS2+ (Dave Turner and Ralph Rupp)

Mammalian expression vector contains sCMV-promoter and two polylinkers. For selection, ampicillin resistance gene is included. This vector was used as a negative control in this study.

2.1.5.2 Plasmid constructs for Immunofluorescence

MRTF-GFP in pEGFP-N3

Full-length MRTF is cloned into pEGFP-N3 with an antibiotics selection marker for kanamycin. This plasmid was kindly provided by Richard Treisman and described in a previous report (Vartiainen et al., 2007).

2.1.6 Antibodies

2.1.6.1 Primary antibodies

Antigen	Isotype	Manufacturer	Dilution	Application
GAPDH	Mouse	Acris Acr001P	1:10000	WB
GFP	Rat	Santa Cruz	1:200	IF
IgG	Rabbit	Cell signaling	1:40	ChIP
MRTF-A	Mouse	Chiquet's Laboratory	1:10 1:30	IF WB
MRTF-A	Rabbit	Santa Cruz	1:1000	IF, WB
MRTF-A	Rabbit	Sigma	1:1000	WB
MRTF-B	Rabbit	Bethyl	1:3000	IF, WB
p-Cofilin	Rabbit	Cell signaling	1:1000	WB
p-MLC	Rabbit	Santa Cruz	1:500	WB
RhoA	Mouse	Santa Cruz	1:500	WB (IP)
RhoA-GTP	Rabbit	New East	1:500	IP
SRF (2C5)	Rat	Nordheim's Laboratory	1:10 1:5	IF WB
SRF (sc-335)	Rabbit	Santa Cruz	1:200	IF
VEGFR-2	Rabbit	Cell Signaling	1:100 1:1000	IF WB

2.1.6.2 Secondary antibodies

Antigen	Label	Isotype	Manufacturer	Dilution	Application
Mouse IgG	Alexa Fluor® 488	Goat	Invitrogen	1:1000	IF
Mouse IgG	Alexa Fluor® 546	Goat	Invitrogen	1:1000	IF
Rabbit IgG	Alexa Fluor® 488	Goat	Invitrogen	1:1000	IF
Rabbit IgG	Alexa Fluor® 546	Goat	Invitrogen	1:1000	IF
Rat IgG	Alexa Fluor® 488	Goat	Invitrogen	1:1000	IF
Rat IgG	Alexa Fluor® 546	Goat	Invitrogen	1:1000	IF
Goat IgG	HRP	Donkey	GE-Healthcare	1:10000	WB
Mouse IgG	HRP	Sheep	GE-Healthcare	1:10000	WB
Rabbit IgG	HRP	Donkey	GE-Healthcare	1:10000	WB
Rabbit IgG	HRP	Mouse	abcam	1:1000	WB (IP)
Rat IgG	HRP	Goat	GE-Healthcare	1:10000	WB

2.1.7 Reagents and technical equipment

2.1.7.1 Luciferase reporter gene assay

ATP stock solution	0.5 M ATP in water, store at -20°C
Firefly-Luc measuring buffer	25 mM Glycylglycin 15 mM $MgSO_4$ 10 mM Tris-Base Sterilization by autoclave Before use add 5 mM ATP
Luc-assay lysis buffer	25 mM Tris-PO_4 (pH 7.8) 2 mM EDTA (pH 8.0) 10% (v/v) Glycerin 1% (v/v) Triton X-100 2 mM DTT
Luciferin stock solution	25 mM Firefly D-Luciferin in water
Luciferin solution	250 µM Firefly D-Luciferin

	250 μM NaOH

2.1.7.2 Transformation

TFB (transformation buffer) I	30 mM KAc, pH 5.8
	50 mM $MnCl_2$
	100 mM $Rbcl_2$
	10 mM $CaCl_2$
	15% glycerine (v/v)
	Sterile filtration
TFB (transformation buffer) II	10 mM MOPS, pH 7
	75 mM $CaCl_2$
	10 mM $Rbcl_2$ (may be substituted to KCl)
	15% glycerine (v/v)
	Sterile filtration, store in darkness

2.1.7.3 Immunofluorescence

Blocking solution	2% BSA in PBS
DNAse I (Alexa 488-conjugated)	5 mg/ml in pH 7.4 PBS containing
	50% v/v glycerol
DAPI	2 μg/ml in PBS, store in darkness
Fixation solution	4% PFA/5% Sucrose in PBS
	pH 7.3, store at -20 °C
Immersion oil	Zeiss
Mowiol	25 g Mowiol in 100 ml PBS
	Stirr O/N at RT
	Add 50 ml glycerol, stir O/N at RT
	Centrifuge for 15 min at 4000 rpm
	Transfer supernatant and add a spatula

	tip of n-propyl-gallate
	Centrifuge for 15 min at 4000rpm
	Store at -20˚C
	Pre-heat before use at 37˚C
Permeabilization solution	0.1% Triton-X 100 in PBS
Phalloidin	300 Units in 1.5ml MeOH (6.6 μM)

2.1.7.4 SDS-PAGE gel

Buffers

2x stacking gel buffer (pH 6.8)	Tris-Base (0.25 M) 3 g
	Add H_2O to 90 ml
	Adjust pH 6.8 with HCl
	Add 2 ml 10% SDS
	Add H_2O to 100 ml
4x running gel buffer (pH 8.8)	Tris-Base (0.25 M) 16.95 g
	Add H_2O to 90 ml
	Adjust pH 8.8 with HCl
	Add 4 ml 10% SDS
	Add H_2O to 100 ml
SDS electrode buffer (10x)	144 g Glycin
	30.25 g Tris-Base
	Add H_2O to adjust volume to 1000 ml
	During dilution adjust 0.1% SDS

Gel composition

Stacking gel composition (per plate)

Stacking gel	**5%**	**7%**	**8%**	**10%**	**12%**	**15%**
H_2O	6 ml	5.75 ml	5.5 ml	5 ml	4.5 ml	3.7 ml
4x Gel buffer	2.5 ml					

40% PAA	1.25 ml	1.75 ml	2 ml	2.5 ml	3 ml	3.8 ml
10% SDS	100 µl					
	Mixing					
TEMED	7.5 µl					
10% APS	100 µl					

Running gel composition

Running gel	**Volume**
H_2O	3.9 ml
2x gel buffer	5.0 ml
40% PAA	1.0 ml
10% SDS	100 µl
	Mixing
TEMED	10 µl
10% APS	100 µl

Protein molecular weight marker	PageRuler™ Prestained Protein Ladder, Fermentas

2.1.7.5 Western blot

2x Protein loading buffer	125 mM Tris, pH 7.5 0.1% Bromphenolblue 20% Glycerin 5% β-ME 2.5% SDS Add H_2O to adjust volume 10 ml
6x Protein loading buffer	300 mM Tris pH 6.8 6% SDS 60% Glycerin 600 mM β-ME

	A tip of spatula Bromphenolblue
	Add H_2O to adjust volume
Blocking solution	5% (w/v) BSA or skim milk in TST
Blotting papers	Whatman 3MM Chr paper
Bradford reagent	Bio-Rad protein assay
	1:5 dilution in H_2O
Coomassie Brilliant Blue	2 g Coomassie Brilliant Blue dissolved in 1000 ml H_2O
	Add 55.5 ml H_2SO_4, stir for 3 hrs
	Filter through Whatman Chr paper
	Add 220 ml 10 M NaOH
	Add 310 ml TCA (100%) slowly on ice
Coomassie Blue destaining solution	Tap water
ECL substrate	Immobilon™ Western, Millipore
Lysis buffer (RIPA, 10x)	500 mM Tris-HCl, pH 8
	1.5 M NaCl
	10% NP40
	5% Sodium Deoxycholate
	1% SDS
	10 mM EDTA
	Add H_2O to adjust volume 100 ml
Membrane	Immobilon®-p transfer membrane
	Filter type: PVDF
	Pore size: 0.45 μm
Stripping buffer (500 ml)	2% SDS
	62.5 mM Tris-Cl, pH 6.7
	Add H_2O to adjust volume
Transfer buffer (10x)	144 g Glycin
	30.25 g Tris-Base

	Add H_2O to adjust volume to 1000 ml
TST buffer (10x)	100 mM Tris-HCl, pH 7.5
	1 M NaCl
	1% Tween 20
	10 mM EDTA, pH 8
	Add H_2O to adjust volume to 1000 ml
X-ray films	CEA medical x-ray screen film

2.1.7.6 siRNA transfection

RNAse-free water	Qiagen
siRNA hybridization buffer	40 µl 5 M NaCl
	50 µl 1M Tris-Cl, pH 7.5
	1910 µl RNAse-free water

2.1.7.7 RhoA activation assay

Lysis buffer (5x)	250 mM Tris-HCl, pH 8.0
	750 mM NaCl
	50 mM $MgCl_2$
	5 mM EDTA
	5% Triton X-100
	Store at -20°C, add phosphatase and protease inhibitors before use
Protein beads	Protein A-Agarose, Santa Cruz

2.1.7.8 ChIP assay

IP buffer	150 mM NaCl
	50 mM Tris-HCl, pH 7.5
	5 mM EDTA

	0.5% (v/v) NP-40 1% (v/v) Triton X-100 Add phosphatase and protease inhibitors before use
Protein beads	Protein A-Agarose, Santa Cruz

2.2 Methods

2.2.1 Cell culture

Cell culture protocol was performed routinely. Every second or third day cells were split or medium was changed according to cellular confluence. Trypsin-EDTA was used to detach cells from the tissue culture plate. For HRMVECs and HUVECs 0.2%, gelatine-coated plates were prepared to enhance cellular attachment. Thawing and freezing of cells were also done in accordance with general protocols.

2.2.2 Luciferase reporter gene assay

Reporter gene assay monitors expression of target gene by its enzymatic-linked luminescent or fluorescent read-outs (Cheng et al., 2010). The luciferase gene is one of the most popularly used reporter gene that yields a fluorescent product in the presence of ATP, Oxygen, and Mg^{2+} by oxidizing D-luciferin. This fluorescent product can be quantified by measuring the released light. In this work, firefly (*Photinus pyralis*) luciferase was used in order to monitor *c-fos* expression.

2.2.2.1 Purification of reporter plasmids

Preparation of competent bacteria

For the transformation of competent bacteria (XL1-blue) with Tsm or Tmm, calcium chloride-based method was used. One colony of competent cells was picked and suspended in LB medium containing 10 μg/ml tetracycline. The bacteria were amplified by incubating O/N with vigorous shaking. After adding of 100 ml LB medium containing tetracycline to the bacterial solution, the bacteria were further cultivated. The cultivation was stopped when optical density of the bacteria was reached at 0.35 to 0.5 (logarithmic phase of bacterial growth). After centrifuge 10 min, 3000 rpm, at 4˚C, the bacteria were collected into 2 tubes. Then, each of the bacterial pellets was resuspended in 10 ml TFB I buffer 10 min on ice. The pellet was spun down 10 min at 4˚C. The bacteria were again suspended in 2 ml ice-cold TFB II buffer. 200 μl of bacteria was aliquoted and frozen on dry ice and stored at -70˚C.

Transformation

Frozen competent bacteria were thawed on ice. The Plasmids were extracted either with 10 µl water from 3M paper containing plasmid DNA or by directly taking 0.5 µl from plasmid stock, and added to the bacteria. The bacteria were serially incubated for 20 min on ice, for 90 sec at 42˚C, and for 2 min on ice, then 300 µl LB medium was added. Afterwards, the bacteria were spread and cultivated O/N on LB plates in the presence of selective antibiotics Penicillin/Streptomycin.

Plasmid preparation

A single colony of competent bacteria was picked and suspended in 5 ml LB media with selective antibiotics then incubated at 37˚C with vigorous shaking. After O/N incubation, 150 µl bacterial solution was diluted in 300 ml LB media containing antibiotics, then cultivated again O/N on a shaker at 37˚C. The bacterial pellets were collected by centrifuging for 20 min, at 6000 rpm, at 4˚C. Plasmids were purified with Qiagen's Endofree® plasmid Maxi kit according to the manufacturer's protocol. After purification, the DNAs were precipitated with isopropanol by centrifuging (10000 rpm, 30 min, 4˚C). After decanting of the supernatants, the DNA pellets were washed with 70% EtOH and air-dried. Finally, the plasmid DNAs were resolved either in water or in TE buffer and stored at -20˚C. The concentration of the plasmid was spectrophotometrically measured by Nanodrop at 260 nm.

2.2.2.2 Transfection of plasmids

For transfection of reporter plasmids into HRMVECs, cells were seeded into 24 well plates as duplicates at a density of $1.5X10^5$. After 24 hrs, culture medium was changed to serum-, antibiotics- and growth factor-free medium. For a duplicate, 400 ng plasmids (200 ng of TSm or Tmm plasmid with 200 ng of full-length MRTF-A plasmid and 200 ng of pCS2+ plasmid, respectively) and 6 µl of PromoFectin-HUVEC transfection reagent were prepared and pipetted into a tube containing 150 µl culture medium, then thoroughly mixed to homogenate. This mix was incubated at room temperature for 20 min. After incubation, 75 µl of the plasmid-transfection reagent mixture in medium was added per well by dropping. After 5 hrs of transfection, the transfection process was stopped by changing medium to antibiotics- and VEGF-free complete medium containing 0.2% serum. After 48 hours of incubation,

cells were harvested. To investigate the effect of VEGF on Tsm, Tmm, and MRTF expression, VEGF stimulation was designed. In case of VEGF stimulation, 100 ng/ml of VEGF was added to the medium for 2 hrs before cell lysis.

2.2.2.3 Measurement of luciferase activity

Two days after transfection, culture medium was removed and cells were lysed with 200 µl Luc-assay lysis buffer per well in order to release intracellular enzymes. Cell culture plates were incubated at least for a day at -80˚C. On the day of experiment, frozen cell lysates were slowly thawed on ice. Then, each of the 50 µl cell lysates were transferred into two transparent 5 ml glass tubes (Sarstedt). Just before measurement, 300 µl of Firefly-Luc measuring buffer containing 5 mM ATP and 50 µl of Luciferin solution were added and homogenised by short vortexing. The luminescence was measured for 10 seconds in a Luminometer as quadruplicates.

2.2.3 mRNA analysis: semi-quantitative real-time PCR

2.2.3.1 RNA isolation, cDNAse treatment, and cDNA synthesis

Whole RNA from cells was obtained by using RNeasy mini kit (Qiagen) according to manufacturer's protocol. Cell lysates were obtained by adding RLT buffer containg β-Mercaptoethanol (600 µl for 10 cm dish, 350 µl for 6 cm dish). 30 µl of RNA eluate was obtained for each sample according to the kit's manual. Subsequently, DNase I in RNA samples was treated. For 30 µl of RNA eluate, 3 µl of 10x DNAse I buffer, 1µl of RNase-free recombinant DNAse I were added, followed by incubation for 30 min at 37˚C and 20 min at 65˚C. Afterwards, the RNA eluate was kept on ice. After digestion of DNase I, the concentration of RNA was photometrically measured by NanoDrop at 260 nm. The ratios 260/280 and 260/230 were referenced as an indicator of purity.

For reverse transcription of RNA to cDNA, random hexamers (dN6) were used. The advantage of random hexamers in comparison to oligo dNT is that synthesis of cDNA can be more stably progressed to the end of 5' exon.

cDNAs were synthesized as described. RNAse-free water was added to 1 µg of RNA and the volume was adjusted to 20 µl. After adding 5 µl random hexamers (dN6),

the mixes were incubated 10 min at 70 ˚C to denaturize secondary structure of RNA and cooled down on ice. After that, 10 μl of master mixes were supplemented. Each master mix was prepared with 7 μl M-MLV reverse transcriptase 5x reaction buffer, 2 μl dNTPs, 0.5 μl RNAse inhibitor and 0.5 μl Reverse transcriptase. Then, cDNA was synthesized by serial incubation for 10 min at RT, for 45 min at 42˚C, and 3 min at 99˚C. On ice, 15 μl RNase-free water was supplemented. Finally, 50 μl of cDNA was produced through these processes. The synthesized cDNAs were stored at -20˚C.

2.2.3.2 qRT-PCR reaction

To quantify mRNA expression of target genes, primers and cDNA were prepared as a master mix. A master mix for one sample contained:

Primer mix (3 μl per well)	0.3 μl forward primer
	0.3 μl reverse primer
	2.4 μl water
cDNA mix (7 μl per well)	5 μl SYBR Green
	2 μl cDNA

In total, 10 μl of the master mix was pipetted into a 96 well plate as triplicates. As a housekeeping gene, *Gapdh* was used in order to normalize relative expression of target genes in each sample. Primer sequences are displayed in chapter 2.1.4.1. cDNAs were amplified by the following programme in qRT-PCR machine (The ABI PRISM® 7000 Sequence Detection System or the ABI PRISM® 7500 FAST Sequence Detection System was used, Applied Biosystems).

Segment 1	0˚C	2 min
	5˚C	10 min
Segment 2: repeats 40 cycles	5˚C	15 sec
	0˚C	1 min
Segment 3: melt/dissociation curve	5˚C	15 sec
	0˚C	20 sec
	5˚C	15 sec

2.2.3.3 Quantification of mRNA level

To analyse qRT-PCR data, 7000 system SDS 1.2.3 software and 7500 software were used for ABI PRISM® 7000 and 7500 equipment, respectively. Data were analysed based on relative gene expression with CYBR® Green technology and analysed by C_T method. CYBR® green is a fluorescent dye that incooperates into double strand DNA. Prior to binding DNA, CYBR® green emits week fluorescent signals. With amplification of DNA, CYBR® fluorescent intensity of CYBR® green is proportionally amplified to the DNA amount. When the signal intensity of CYBR® green become significant, the quantitative cycle has endpoint named cycle threshold, C_T (Schmittgen and Livak, 2008). The C_T value is an important indicator to define gene expression. For qRT-PCR, it is assumed that all cycle reactions run with the same efficiency for all gene amplifications. Target gene expressions were calculated as a mean of the triplicates and normalized to the internal control gene *Gapdh* (ΔC_T value).

$$\Delta C_T = C_T \text{ gene of interest} - \Delta\, C_T \text{ internal Gapdh}$$

Relative expression of RNA can be calculated as follows,

$$\text{relative RNA (concentration)} = 2^{-\Delta CT}$$

because PCR reaction was doubled via each cycle according to logarithms. Finally, RNA amount in each sample can be compared between treatment groups.

$$\text{Fold change} = 2^{-\Delta CT} \text{ (treated group)} \,/\, 2^{-\Delta CT} \text{ (untreated group)}$$

2.2.4 Western blot

2.2.4.1 Protein isolation

To lyse proteins, RIPA (Radio-Immunoprecipitation Assay) buffer was mainly used for this study. Concentrated RIPA buffer was diluted into water with one tablet of protease and phosphatase inhibitor cocktail to preserve proteins in the cell lysates. Cells were harvested on ice. Cell culture media was aspirated and washed with cold PBS twice. PBS was completely removed and ice-cold RIPA lysis buffer was added to the cells (120 µl to per 6 cm, 250 µl per 10 cm tissue culture plate). Culture plates were placed on ice for 20 min. Cells were detached from the plate by scraping with a cell scraper. The lysates were transferred into Eppendorf tubes and shortly vor-

texed. The tubes were centrifuged for 10 min, 13000 rpm at 4˚C, then only the supernatants were collected. For future use, lysates were snap frozen and stored at -80˚C.

The concentration of the lysates was measured with Bradford Reagent (Bio Rad). The Bradford Reagent was diluted 1:5 in water on ice freshly before use. 2 µl of each protein lysate was mixed with 998 µl reagent and subsequently incubated for 5 min at RT. The standard curve was set by using BSA (1 mg/ml concentration) previously before protein concentration was measured. Absorption was determined at 595nm and the protein concentration was calculated per µg/µl.

2.2.4.2 SDS-PAGE (sodium dodecylsulfate polyacrylamide gel electrophoresis)

In order to separate proteins according to their molecular mass, SDS-PAGE was used (Laemmli, 1970). Therefore, Bio-Rad Mini-PROTEAN® system was employed. Proteins were separated in 8 to 15% SDS-PAGE gel according to protein sizes in an electrical field of 80 to 120 V.

2.2.4.3 Protein transfer

Separated proteins on the PAGE-gels were transferred to the membrane. Transfer was done in wet condition (sponge/ paper/ gel/ membrane/ paper/ sponge) in transfer buffer. The proteins on the gels move from negative-charged field to positive-charged electrode where membranes are installed. For transfer to the PVDF membrane, pre-treatment of PVDF membrane in methanol is required, thereby increasing the attachment of proteins from SDS-PAGE gel by enhancing hydrophilicity of the membrane surface. The gels run approximately 1 hr at 100 V, with modifications of time and voltage according to target protein size.

2.2.4.4 Antibody detection

After transfer of proteins, membranes were incubated at least 1 hr at RT in either 5% BSA or skim milk (for non-phosphorylated proteins) in TST-buffer in order to inhibit non-specific binding of proteins. Subsequently, membranes were incubated in primary antibodies of interest. After overnight incubation at 4˚C, membranes were

washed at least three times with TST-buffer, followed by HRP-conjugated secondary antibody incubation at RT for 1 hr. Then membranes were again washed with TST-buffer. HRP-conjugated antibodies on the membrane were detected with chemiluminescent HRP substrate on X-ray films.

2.2.4.5 Stripping

In case of reprobing of membranes, which were already used in western blot, membranes were stripped to get rid of the attached antibody. Dried membrane were shortly submerged into 100% MeOH solution and washed in TST-buffer, then incubated in stripping buffer containing β-Mecaptoethanol (35 µl β-Mecaptoethanol in 5 ml TST-buffer) on a shaker (35 rpm) for 30 min at 50°C. Afterwards, membranes were washed twice with TST-buffer for 10 min and blocked with 5% BSA or skim milk solution. Therefore, membranes could be used for detection of other proteins by different antibodies.

2.2.4.6 Quantification of protein bands

In all experiments, GAPDH was used as a loading control to normalize target protein expression. Due to the fact that most of actin related housekeeping genes could be potential SRF target gene, the usually employed β-actin or Tubulin could not be used as loading controls in this work. For quantitation, band intensities per volume were measured using a densitometer (Molecular Dynamics, Inc) and resulting values were normalized to the GAPDH values.

2.2.5 Immunofluorescence

2.2.5.1 Cover glasses preparation

For immunofluorescence staining, cover classes were treated as follows to remove attached pollutants and to enhance cellular attachment. For a start, cover glasses were submerged in 2 M NaOH for 1hr and washed with H_2O three times. Then, they were merged in 70% HNO_3 for at least 3 days on gentle shaker and washed with H_2O three times. Followed the cover glasses were soaked in 9 M (37%) HCl for at least 1

hr, then washed with H_2O ten times in 24 hrs O/N. After washing, cover glasses were drenched with 100% EtOH shortly, followed in H_2O shortly. Finally, the cover glasses were stored in 70% EtOH. After drying, cover glasses were stored and handled under sterile conditions.

2.2.5.2 Immunofluorescence procedure

$2X10^4$ cells were seeded onto gelatin-coated cover glasses in a 4-well plate. The next day, cells were starved from VEGF and FCS for 18 hrs. In a subset of experiments, actin-binding drugs (Lat B and Cyto D: 400nM for 30 min, Jaspk: 200 nM 2 hrs) or pharmaceutical inhibitors of RhoA (Y-27632: 50 μM for 2 hrs, CT04: 2μg/ml for 4 hrs, and CCG-1423: 20μM for 4hrs) were applied. Subsequently, cells were stimulated with serum and VEGF, respectively. Then cells were fixed with 4% PFA/5% sucrose solution either 1hr at RT or at 4˚C O/N. Fixed cells were washed with PBS at least three times, then permeabilized with 0.1% Triton X-100 for 15 min. After that, blocking was performed with 2% BSA for 1hr at RT. Primary antibody was diluted in BSA, and cells were incubated with antibody solution at 4˚C O/N. After washing three times with PBS, cells were treated with secondary antibody which is conjugated with Alexa Fluor® together with Texas-Red conjugated phalloidin to visualize F-actin. This process was performed for 1 hr at RT in darkness. DAPI solution was added to cells to stain cell nuclei after washing from secondary antibody solution. Finally, cells were again washed and embedded into pre-warmed Mowiol on cover slides and dried overnight. Fluorescence was imaged by using a Zeiss Axiovert 200M microscope.

Fluorescent dye	Absorption wavelength	Emission wavelength
DAPI	345 nm	455 nm (blue)
FITC/ Alexa Fluor® 488/ GFP	499 nm	519 nm (green)
Texas red/ Alexa Fluor® 546	589 nm	615 nm (red)

2.2.6 Gene knockdown by siRNA

2.2.6.1 siRNA preparation

Each sense strand of siRNA (SRF797) was hybridized before use. For this process, 20 µl of each siRNA sense and antisense strand was dissolved in 160 µl siRNA hybridization buffer. The siRNA solution was slowly heated to 95°C, then cooled down to 37°C, afterwards at RT. siRNA was aliquoted in RNAse-free water and stored at -20°C. The concentration of siRNA stock solution was kept at 20 µM.

2.2.6.2 siRNA transfection

siRNA was used at a concentration of 166 pmol regarding to the highest efficiency in knock-down as shown in a previous study (Konjer, 2009). $2x10^5$ mECs were seeded in 6 cm plates in complete medium without antibiotics. On the next day, culture medium was changed to Opti-MEM® after once washing with PBS. 17 µl Lipofectamine® RNAiMAX Transfection Reagent and siRNA were diluted in 0.5 ml Opti-MEM® and roughly homogenized by pipetting followed by incubation for 20 min. Afterwards, Lipofectamine® reagent-siRNA mixture was added to the cells. Transfection continued for 5 hrs. Transfection was stopped and cells were grown again in complete medium excluding antibiotics for 2 days for RNA extraction and for 3 days for protein extraction. For protein extraction, medium was changed to new culture medium on the second day of post-transfectional incubation. AllStars Negative Control siRNA (Qiagen) proven as a reliable control siRNA was used as control siRNA in this study.

2.2.7 MTT assay

In this study, MTT assay was performed to quantify cellular proliferation. It is based on a colorimetric measurement using the cell-permeable chemical MTT ((3-(4,5-dimethylthiazol-2-yl)-2,5-diphenyl tetrazolium bromide) that incorporates into mitochondria. There, the tetrazolium ring, which presents a yellow colour, is cleaved by mitochondrial enzymes to reduced MTT formazan. The violet formazan is crystalized in the cells that can be resolved by cell lysis. This MTT-dependent reaction occurs only in living active cells, so it has been used as a tool for cellular viability or

proliferation measurement (Mosman, 1983). For the experiment, 5 mg/ml MTT solution was dissolved in PBS and sterile filtered and dealt in darkness. Cells were cultivated in 24 well plates as duplicates. On the day of measurement, cells were washed one time with PBS. Culture medium containing 20 µl/ml MTT was given to the cells for 3 hrs in darkness. After that, cells were carefully washed with PBS twice in order to remove unincorporated MTT. Cells were lysed with 250 µl purified DMSO and incubated for 30 min. Two times 100 µl of these cell lysates were taken from a well, thereby optical density was measured as a quadruplicate. The values of optical density were obtained in a Microplate reader at 570 nm.

2.2.8 Immunoprecipitation (IP) assay for active-RhoA

2.2.8.1 Cell lysate preparation

For immunoprecipitation of active RhoA, $1X10^6$ mouse ECs were seeded into 10 cm tissue culture plates. The next day, cells were starved from FCS and VEGF for 18 hrs. Stimulation was done with 100 ng/ml VEGF for either 10 min or 60 min. Control cells were simultaneously treated with equal amounts of cell culture medium only. After stimulation, plates were moved onto ice and washed twice with ice-cold PBS. Non-ionic detergent (Triton X-100) containing RhoA lysis buffer was used in order to gain the native form of proteins and minimize denaturation of antibody binding site.

2.2.8.2 Pre-clearing of cell lysates

Acquired cell lysates were centrifuged in order to homogenize and remove the nuclear fraction. Supernatants were collected in new Eppendorf tubes. Protein concentration was measured by Bradford assay (chapter 2.2.4.1). For IP, 0.5 ml of 1 mg/ml lysate was prepared. Pre-clearing step was designed to decline non-specific binding of proteins to proteinA agarose beads. Cell lysates were incubated with 25 µl rabbit serum for 1hr on ice. Then, 50 µl of protein A-Agarose beads were added to the lysates. Lysate-serum-beads mixtures were incubated for 30 min at 4°C on a rotator. Next, lysates were centrifuged at 13000 rpm for 30 min. Supernatants were transferred into new tubes for further IP reactions. To measure the amount of total RhoA, the protein lysates were also prepared for western blot.

2.2.8.3 Immunoprecipitation (Pull-down)

Pre-cleared lysate samples were immunoprecipitated O/N with 1 µl of anti-active RhoA antibody that is able to specifically recognize the GTP-bound form of RhoA. Then, 20 µl Protein A-Agarose beads were added to the lysates and incubated for 4 hrs with gentle shaking. Non-bound proteins were removed by washing with lysis buffer three times with very gentle rpm (3000 rpm). At final washing, lysates were centrifuged and supernatants were discarded and beads were immediately frozen at -20˚C.

2.2.8.4 Western blot and detection

Immunoprecipitated Rho-GTP was detected with RhoA antibody. Frozen lysates were thawed on ice. Proteins were denaturated and separated from the beads by heating for 5 min at 95˚C with 20 µl 2x loading buffer, then samples were centrifuged and 20 µl supernatants were loaded in 15% SDS-PAGE gel. Then transfer was performed at 100 V for 50 min. Blocking and antibody incubation was done with 5% skim milk. The antibody against RhoA and HRP-conjugated secondary antibody were incubated O/N and for 1 hr, respectively. The amount of GTP-RhoA was normalized to total RhoA bands.

2.2.9 Chromatin Immunoprecipitation (ChIP)

The Chromatin immunoprecipitation assay monitors whether a target protein binds to a specific DNA sequence and estimates the amount of protein-DNA complex on this region. This experiment was done in kind cooperation with Dr. Christine Stritt.

2.2.9.1 Cell lysate preparation

mECs were seeded at a density of $2.5X10^6$ cells per 10 cm culture plate and grown for 3 days. The day before stimulation, cells were washed and starved from VEGF and FCS for 18 hrs. Stimulation was performed with 15% FCS for 1 hr. Non-stimulated cells were treated with the same volume of culture medium to normalize the effect of cellular stress caused by this process. The following ChiP procedure was performed by Dr. Christine Stritt as described in the publication (Nelson et al., 2006). After stimulation, cells were fixed with 1.42% fresh formaldehyde for 15 min

to crosslink DNA-protein complex. Thereafter, 125mM glycerine was added for 5 min to quench the fixation. After washing of cells with ice-cold PBS, cell lysates were collected by scraping and centrifuging and can be stored at -80˚C for further use.

2.2.9.2 Immunoprecipitation

On the day of experiment, cell lysate were thawed on ice with 1 ml of IP buffer containing protease inhibitors. The nuclear pellet was obtained after centrifugation and aspiration of the supernatant. Again, the pellet was resuspended in IP buffer and sonicated to shear the chromatin. Sonication was carried out by Branson Sonifier®250 with 3 X 15 sec-pulses, 90% duty cycle, putout level 3 and 2 min rests between rounds. The size of DNA fragments was confirmed between 100 and 600 bp by a 1% agarose gel. After centrifugation, supernatants were pre-cleared with 50 µl Protein A-Agarose beads for 45 min. For IP, 200 µl of sheared DNA was incubated with 5µl anti-SRF antibody or rabbit IgG for mock IP control on a rotator at 4˚C O/N. After centrifugation, 90% of supernatant was transferred and incubated with 50 µl of Protein A-Agarose beads for 1 hr at 4˚C. Agarose beads were then washed with IP buffer three times, high salt IP buffer (including 500 mM NaCl) three times and again with IP buffer twice. Fragmented DNA was isolated by adding 100 µl of 10% Chelex 100 and boiled for 10 min. 1µl of Proteinase K (20 µg/µl) was added to each sample and incubated at 55˚C for 30 min with 1000 rpm. After boiling and centrifugation, supernatant was collected. 120 µl water was added to beads and combined with supernatant, To normalize ChIP samples, 40 µl of input DNA was precipitated with 100 µl 100% EtOH O/N at -20˚C. Input samples were centrifuged and pellets were washed with 70% EtOH and then prepared by the Chelex method as described before. The data was analysed and quantified by qRT-PCR. The sequences of primers are indicated in chapter 2.1.4.2.

2.2.10 Statistical analysis

Data are presented as mean ± SEM. To determine significance between two groups, experimental groups are normalised to respective control groups. Statistical significance was analysed by *2-tailed students t-test* and indicated in figures by an asterisk. Statistical significance was assumed when *p*-values were less than 0.05. In the

following graphs, significance values are presented as follows: * $p<0,05$, ** $p<0,01$, *** $p<0,001$, ns $p>0,05$ not significant.

3. RESULTS

3.1 The effect of VEGF on SRF target gene expression in ECs

3.1.1 SRF is expressed in the endothelial nucleus

SRF is known as a ubiquitously expressed transcription factor. At first, the expression and location of SRF in ECs, which are used for this study, were examined. By qRT-PCR, the mRNA expression of SRF was confirmed (detected by exon 1,2 primer of SRF, data not shown). Then, the endothelial SRF expression was visualized with two different SRF antibodies. One is the commercially purchased anti-SRF from Santa Cruz (sc-335) and the second SRF antibody is anti-SRF named 2C5 produced in our laboratory according to a reference (Koegel et al., 2009).

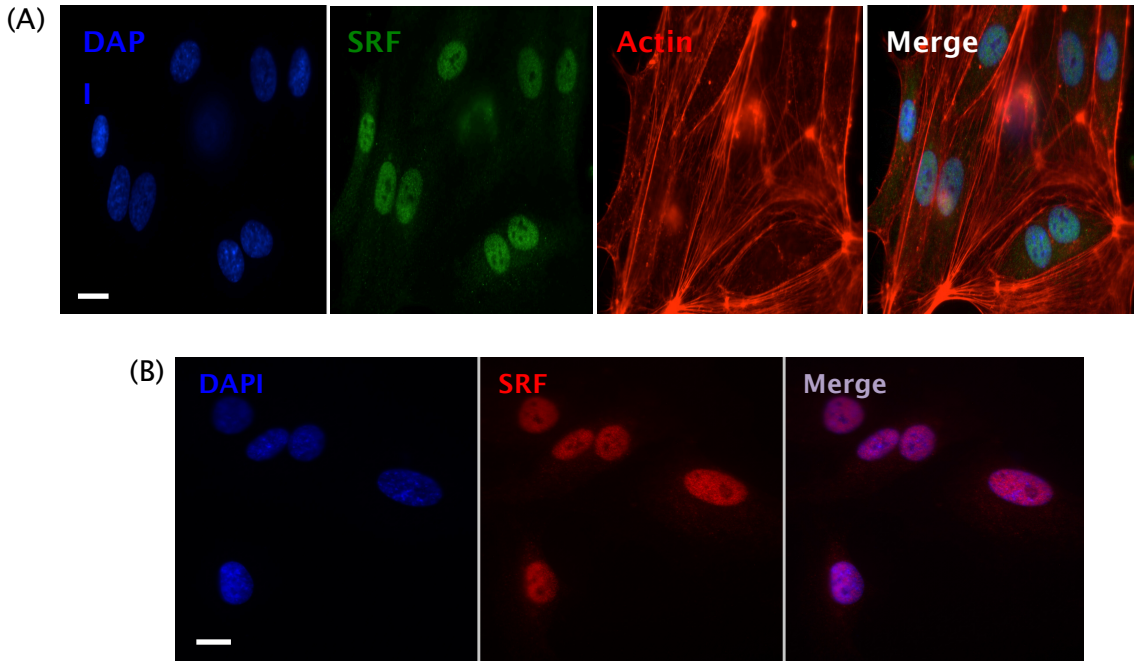

Figure 3.1: SRF expressions in HUVECs

(**A**): HUVECs were stained with DAPI for nucleus (blue), Alexa Fluor®488 for anti-SRF (Santa Cruz sc-335, green), and Texas Red-conjugated phalloidin for F-actin. (**B**): HUVECs were costained with DAPI for nucleus (blue) and Alexa Fluor®546 for anti-SRF (2C5, red). Scale bar = 10 μm.

In HUVECs (human umbilical vein endothelial cells), the sub-cellular location of SRF was confirmed in the nucleus. Both SRF antibodies indicate that SRF is strongly expressed in the nucleus of HUVECs (Fig. 3.1). In other mECs (primary mouse endothelial cells) that were mainly used in this work, SRF expression was also observed in the nucleus where it co-localizes with DAPI (nuclear marker).

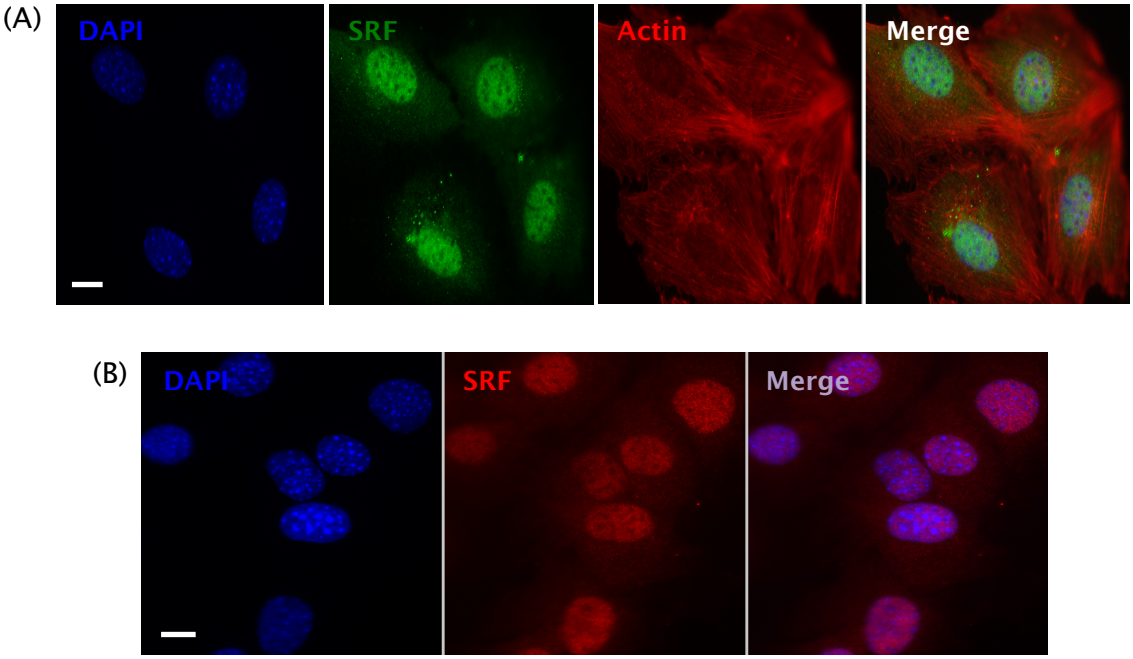

Figure 3.2: SRF expressions in mECs

(**A**): mECs were stained with DAPI for nucleus (blue), Alexa Fluor®488 for anti-SRF (Santa Cruz sc-335, green), and Texas Red-conjugated phalloidin for F-actin. (**B**): mECs were costained with DAPI for nucleus (blue) and Alexa Fluor®546 for anti-SRF (2C5, red). Scale bar = 10 μm.

In two different EC types (HUVECs and mouse ECs), the sub-cellular localization of SRF was detected in the nucleus (Fig. 3.2) where it can act as a nuclear transcription factor in ECs.

3.1.2 VEGF induces SRF target gene expression

As a transcription factor, SRF is regulated by various extracellular stimuli including growth factors. Since it has not been determined yet, whether SRF-mediated transcriptional activation is influenced upon VEGF stimulation in ECs, expression of representative SRF target genes were examined after VEGF stimulation of mECs.

To investigate the effect of VEGF on SRF target gene expression, mECs were starved from serum and VEGF, then treated with 100 ng/ml VEGF for 1hr. Cells were also starved from serum to exclude any effect of serum on SRF activation.

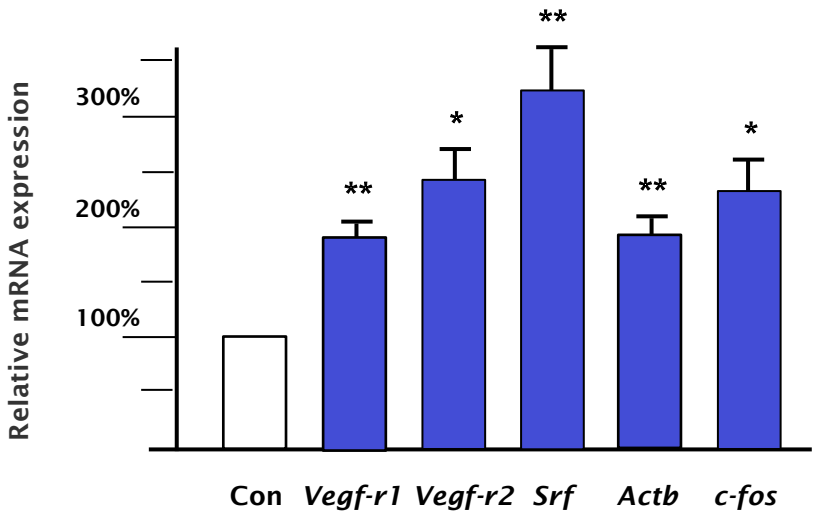

Figure 3.3: Expression of SRF target genes upon VEGF stimulation

Relative mRNA expression was analysed by qRT-PCR upon VEGF stimulation in mECs. Data are normalized to *Gapdh* and presented as mean ± SEM of 4 experiments of *Vegfr-1*, *Srf* and *β-actin,* and 3 experiments of *Vegfr-2* and *c-Fos*. $*p < 0.05$, $**p < 0.01$.

Treatment of VEGF induced the expression of VEGF receptors (*Vegfr-1, Vegfr-2*) as well as well-known SRF target genes such as β-actin, c-fos, and SRF itself (Fig. 3.3). This result demonstrates that VEGF activates SRF and its target genes, indicating VEGF-mediated control of SRF target gene expression in ECs is induced.

3.1.3 VEGF-driven SRE activation is CArG box-dependent

With the confirmation that VEGF induces SRF target genes in ECs, as a next step, a study was conducted to determine whether VEGF utilizes SRE for transcriptional activation. *c-fos* is a well-studied SRF target gene that is composed of 3 major binding sites for transcription factors, namely an Ets binding site for TCFs, an SRE for SRF, and an AP-1 binding site. For the experiment, modified *c-fos* plasmids, which were generated and tested in the previous report (Ergin, 2008), were administrated. The reporter plasmids, TSm and Tmm, were designed for monitoring of SRE with a selective luciferase activity. Each plasmid construct was a double construct in order to

produce more intense signalling effect and thymidine kinase promoter was inserted in front of the luciferase gene to enhance transcriptional activity. More details about structure of the plasmids are described in 2.1.5.1.

The transfected HRMVECs (human retinal microvascular endothelial cells) were additionally co-transfected with full-length MRTF-A plasmid to know any effect of MRTF-A on VEGF-mediated luciferase activity. After transfection, cells were cultivated for 2 days in complete medium excluding VEGF, serum, and antibiotics. For VEGF stimulation, 100 ng/ml of VEGF was applied for 2 hrs, then cells were lysated and harvested.

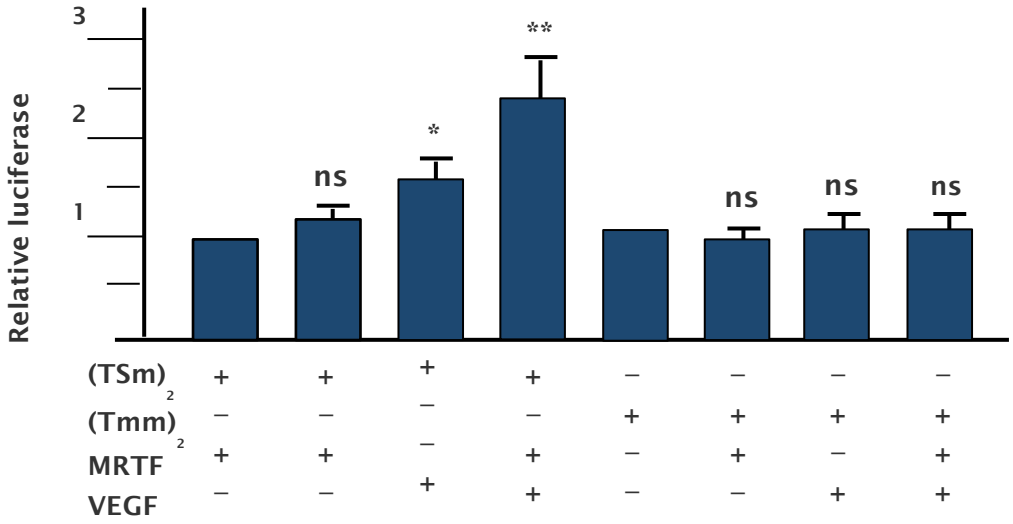

Figure 3.4: VEGF-driven luciferase activity *c-fos*

(**A**): Schematic overview of the *c-fos* reporter plasmid variants TSm and Tmm. (**B**): Results of relative luciferase activity. HRMVECs were co-transfected with TSm or Tmm plasmid (800 ng) together with full-length MRTF-A plasmid (200 ng) and mock plasmid (pCS2+, 200 ng), respectively. Luciferase activity was normalized to the control transfected with mock plasmid. Data are presented as the mean ± SEM of 8 experiments. $*p < 0.05$, $**p < 0.01$, ns: not significant vs. respective control.

After co-transfection of full-length MRTF-A plasmid, luciferase activity was slightly increased (Fig. 3.4). Of note, upon stimulation with VEGF, the luciferase activity was significantly enhanced. Moreover, together with MRTF-A transfection and VEGF stimulation, the luciferase activity increased even more. This indicates a synergistic effect of VEGF and MRTF-A on transcriptional activation of SRF. Interestingly, this effect was totally abolished, when an SRF-binding site is mutated. In cells, which

were transfected with Tmm, no induction of luciferase activity was observed. These data demonstrate that VEGF-induced activation of luciferase activity was SRE-dependently induced.

3.2 Regulation of MRTF by VEGF

3.2.1 Serum induces MRTF-A accumulation in the nucleus in ECs

As a cofactor of SRF, MRTF-A binds to SRF on SRF-DNA complex in the nucleus, thereby inducing MRTF-dependent SRF target genes. Due to this characteristic, the key mechanism of MRTF/SRF target gene expression is the sub-cellular localization of MRTFs in the nucleus and binding of SRF on DNA. Since the effect of serum on the sub-cellular localization of endothelial MRTF has not been reported yet, serum-mediated translocation of MRTF was studied in ECs.

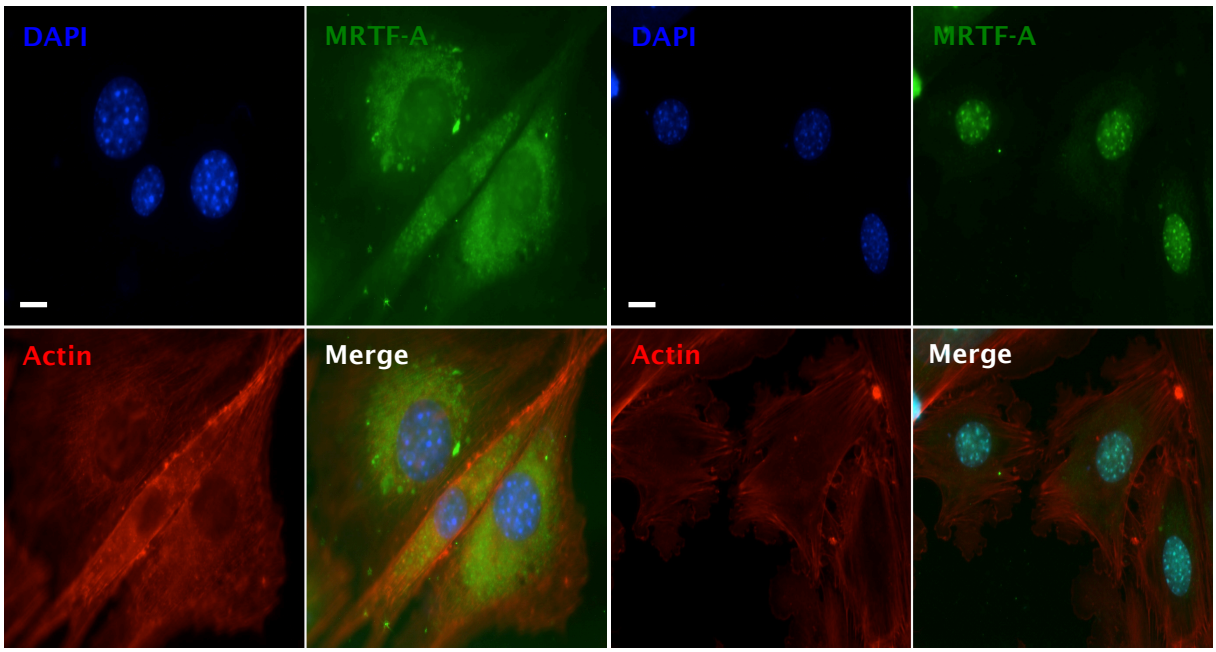

Figure 3.5: Effect of serum on the sub-cellular localization of endogenous MRTF

Immunofluorescent images of MRTF-A in control (left panel) and serum-treated mECs (right panel). Serum and VEGF-starved cells were cultured in the presence and absence of 15% serum for 60 min, respectively. Then cells were fixed and incubated with antibodies against MRTF-A, followed by Alexa 488-conjugated secondary antibody (green). The nuclei were visualized with DAPI (blue) and F-actin was visualized with Texas Red-conjugated phalloidin (red). Scale bar: 10 μm.

In mECs, endogenous MRTF-A was predominantly observed in the cytoplasm during starving conditions (94% in the cytoplasm, 4% in both regions, and 1.5% in the nucleus). However, after serum stimulation, sub-cellular distribution of MRTF-A was significantly rearranged, thereby MRTF-A is significantly observed in the nucleus (48.2%, statistically significant by t-test: $p<0.05$) (Fig. 3.5).

Furthermore, GFP-tagged full-length MRTF-A was introduced into mECs and the ratio of MRTF-A in the nucleus and cytoplasm was compared. The sub-cellular localization of MRTF-A was mainly restricted to the cytoplasm in starved mECs (88% in the cytoplasm, 5% are diffuse, 4% in the nucleus). In comparison with starved cells, MRTF-A was predominantly detected in the nucleus in the serum-stimulated mECs (16% in the cytoplasm, 11% are diffuse, 73% in the nucleus, statistically significant: $p<0.05$) (Fig. 3.6).

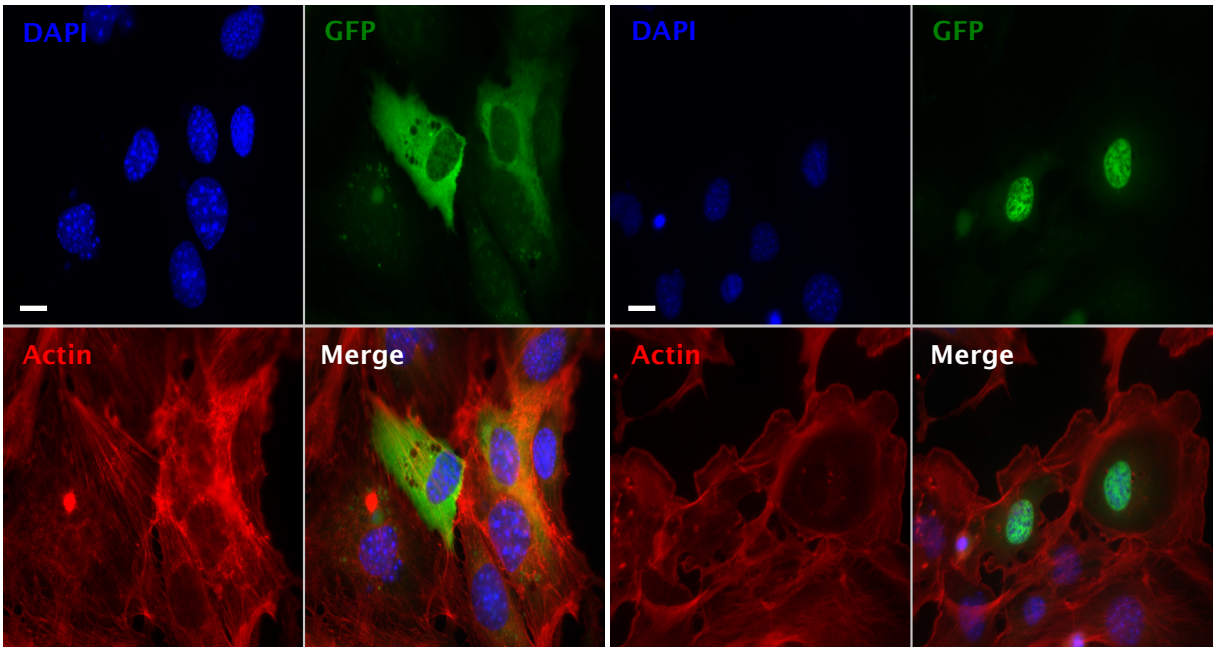

Figure 3.6: Effect of serum on sub-cellular localization of transfected MRTF-A

Immunofluorescent images of GFP-tagged MRTF-A in control (left panel) and serum-treated mECs (right panel). mECs were transfected with full-length MRTF-A, then starved from serum and VEGF. Serum stimulation was performed with 10% serum for 60 min. Then cells were fixed and incubated with antibodies against GFP, followed by Alexa 488-conjugated secondary antibody (green). The nuclei were visualized with DAPI (blue) and F-actin was visualized with Texas Red-conjugated phalloidin (red). Scale bar: 10 μm.

From the experimental results, it was confirmed that serum-induced enrichment of MRTF-A in the nucleus was shown both for endogenous MRTF-A and MRTF-A introduced by transfection. These two results strongly suggest that serum triggers MRTF-A translocation to the nucleus in ECs. Regarding actin filament appearance, stress fibres within the cells were missing upon serum stimulation. However, a ruffling structure of actin near the periphery was developed (Fig. 3.6, right panel). This

lammelipodia structure was visualized with F-actin staining in the microscopic images.

3.2.2 VEGF promotes nuclear accumulation of endothelial MRTFs

As a next step, VEGF was introduced to investigate its influence on MRTF activity in ECs. VEGF (VEGF120) was added to starved-mECs and incubated either 30 min or 60 min, then the sub-cellular localization of MRTF was examined. Upon 30 min of VEGF treatment, MRTF-A was observed in the endothelial nucleus (data not shown). Upon 60 min of VEGF stimulation, MRTF-A was significantly observed in the nucleus in mECs (nucleus: 15.3% in VEGF-stimulated cell versus 1.6% in starved cells; diffused: 33.4% in VEGF-stimulated cell versus 4.7% in starved cells, statistically significant by t-test: $p<0.05$) (Fig. 3.7). Besides, VEGF resulted in a change in endothelial stress fibres. Thick stress fibres crossing through the whole cell was observed upon VEGF-stimulation (Fig. 3.7, right panel) suggesting that VEGF regulates endothelial MRTF-A by modulating stress fibres.

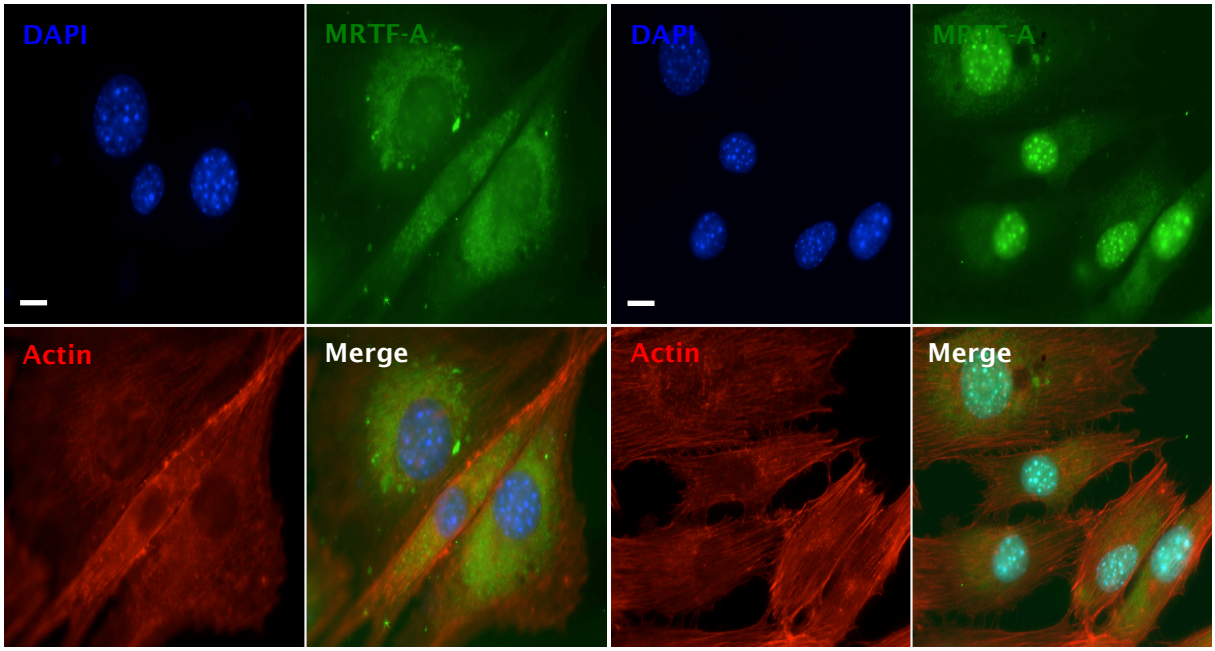

Figure 3.7: Effect of VEGF on sub-cellular localization of endogenous MRTF-A

Immunofluorescent images of MRTF-A in control (left panel) and VEGF-treated mECs (right panel). Serum and VEGF-starved cells were cultured in the presence and absence of 100 ng/ml VEGF for 60 min, respectively. Then cells were fixed and incubated with antibodies against MRTF-A, followed by Alexa 488-conjugated secondary antibody (green). The nuclei were visualized with DAPI (blue) and F-actin was visualized with Texas Red-conjugated phalloidin (red). Scale bar: 10 μm.

3.2.3 VEGF-induced translocation of endothelial MRTF-A is actin dynamics-dependent

Previous studies proved that MRTF is strictly dependent on RhoA-regulated actin dynamics. Since VEGF-induced development of endothelial stress fibres was observed in mECs, representative actin-modulating drugs were introduced.

3.2.3.1 Latrunculin B (Lat B) treatment

Lat B has been used as an *in vitro* modulator of actin dynamics. To understand the effect of actin dynamics on VEGF-induced MRTF activation, cells were incubated with Lat B, followed by VEGF application.

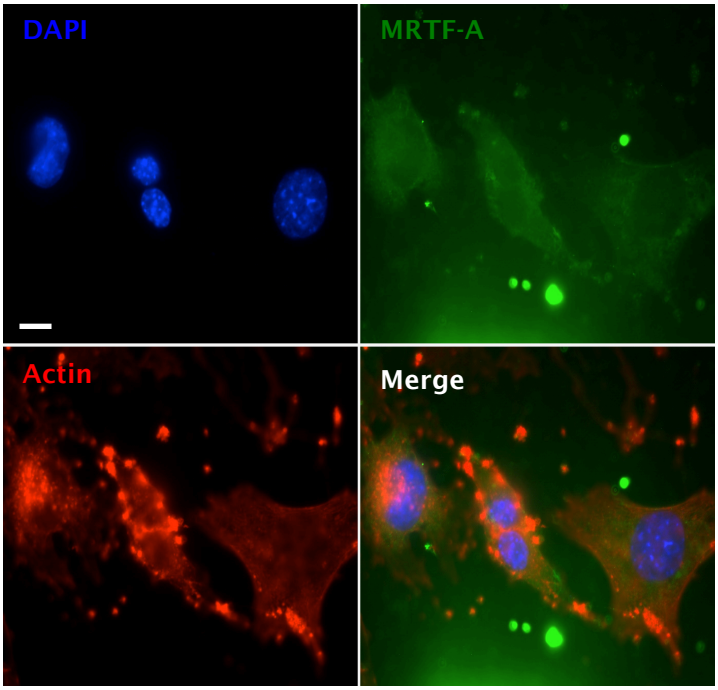

Figure 3.8: Blockage of VEGF-mediated MRTF-A accumulation in the nucleus by Lat B

Immunofluorescent image of endogenous MRTF-A in mECs. Serum and VEGF-starved cells were cultured in the presence of 400 nM Lat B for 30 min. Subsequently, 100 ng/ml VEGF was applied. Cells were stained with DAPI (nucleus, blue), MRTF-A (green), and F-actin (red), respectively. Scale bar: 10 μm.

Interestingly, Lat B totally disrupted F-actin bundles and these disrupted fibres could not be recovered by VEGF stimulation. Thus, VEGF-induced actin fibre structure was

totally missing in the presence of Lat B. Notably, VEGF-triggered MRTF-A enrichment in the nucleus was also abolished in the presence of Lat B (Fig. 3.8). This observation demonstrates that VEGF-modulated MRTF-A regulation is dependent on Lat B-regulated actin dynamics and MRTF-A/G-actin complex.

3.2.3.2 Cytochalasin D (Cyto D) treatment

Cytochalasin D (Cyto D) is a barbed end-binding drug that attenuates actin polymerization. However, unlike Lat B, Cyto D promotes dissociation of MRTF-A from G-actin, thereby inducing MRTF-A liberation. Therefore, it was expected that treatment of Cyto D could induce MRTF-A accumulation in the nucleus.

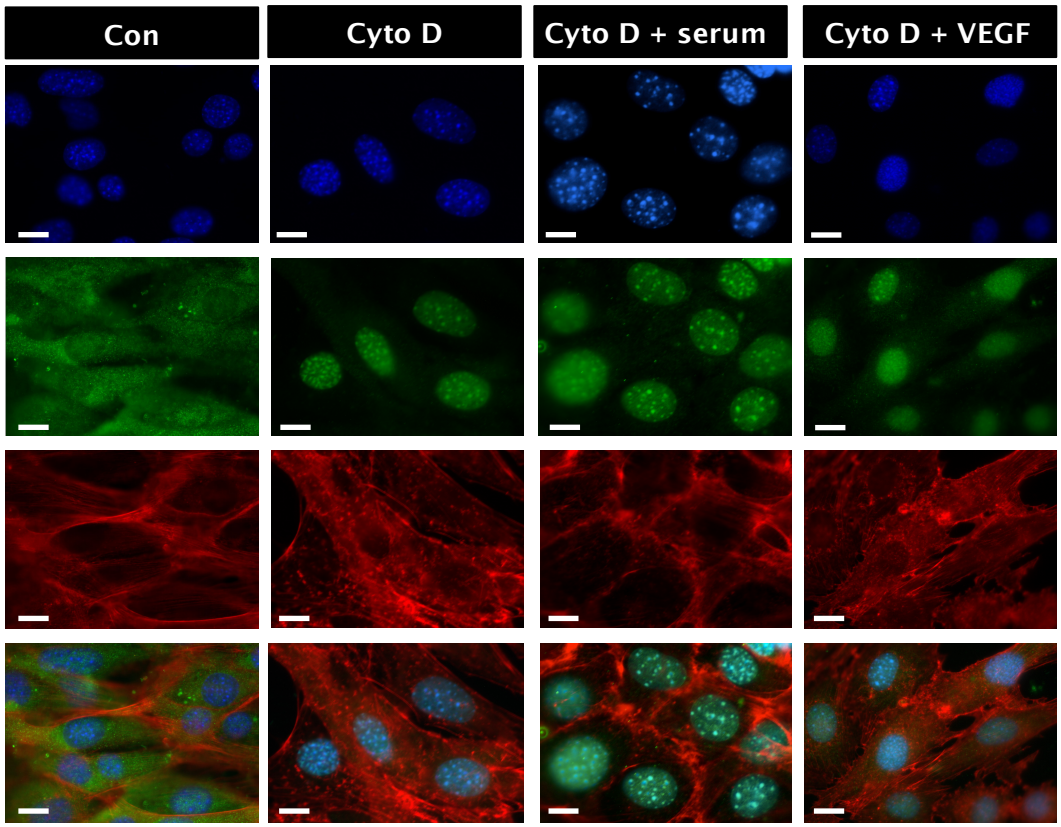

Figure 3.9: Effect of Cyto D on sub-cellular localization of endogenous MRTF-A

Immunofluorescent images of MRTF-A in control and Cyto D-treated mECs. Serum and VEGF-starved cells were cultured in the presence and absence of 400 nM Cyto D for 30 min, respectively. Subsequently, 15% serum or 100 ng/ml VEGF was applied for 60 min, respectively. Then, cells were fixed and incubated with antibodies against MRTF-A, followed by Alexa 488-conjugated secondary antibody (green). The nuclei were visualized with DAPI (blue) and F-actin was visualized with Texas Red-conjugated phalloidin (red). Scale bar: 10 μm.

Upon Cyto D treatment, MRTF-A was significantly observed in the endothelial nucleus, as expected (Fig. 3.9). After co-stimulation with serum or VEGF, MRTF-A was also predominantly observed in the nucleus suggesting that actin alteration by Cyto D was efficiently able to drive MRTF-A to the nucleus.

3.2.3.3 Jasplakinolide (Jasp) treatment

The other actin modulator used in ECs was Jasplakinolide (Jasp). Jasp stimulates actin polymerization by docking at the barbed end of actin filaments, thereby exhibiting F-actin bundles in a dose- and time-dependent manner. In mECs, after treatment with 200 nM Jasp for 2 hrs, endothelial stress fibres were replaced by large F-actin masses. At this concentration, the localization of MRTF was investigated.

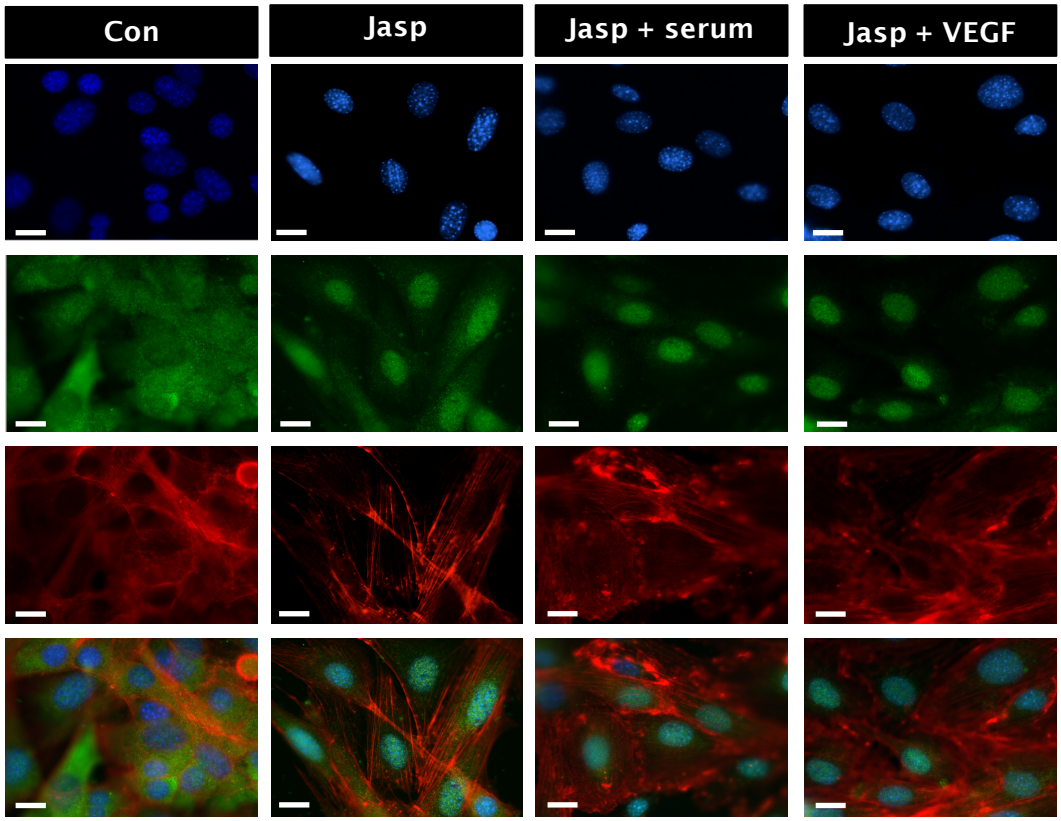

Figure 3.10: Effect of Jasp on sub-cellular localization of endogenous MRTF-A

Immunofluorescent images of MRTF-A in control and Jasp-treated mECs. Serum and VEGF-starved cells were cultured in the presence of 200nM Jasp for 2 hrs. Subsequently, 15% serum or 100 ng/ml VEGF was applied for 60 min, respectively. Then, cells were fixed and incubated with antibodies against MRTF-A, followed by Alexa 488-conjugated secondary antibody (green). The nuclei were visualized with DAPI (blue) and F-actin was visualized with Texas Red-conjugated phalloidin (red). Scale bar: 10 μm.

After stimulation with Jasp, MRTF-A was predominantly observed in the nucleus in mECs (Fig. 3.10). Serum- and VEGF-induced MRTF-A enrichment in the nucleus was also confirmed in the presence of Jasp.

3.2.4 VEGF drives MRTF-B to the nucleus in cooperation with Jasp

In the next set of experiments, MRTF-B was stained to investigate the VEGF-driven effect on sub-cellular localization of MRTF-B. VEGF could induce nuclear accumulation of MRTF-B after co-treatment with Jasp (Fig. 3.11). Besides, as observed on microscopic images, the suc-cellular localization of MRTF-A and MRTF-B was different. MRTF-A was distributed in the whole cytoplasm whereas MRTF-B was stained in the cytoplasm but rather concentrated near the nucleus.

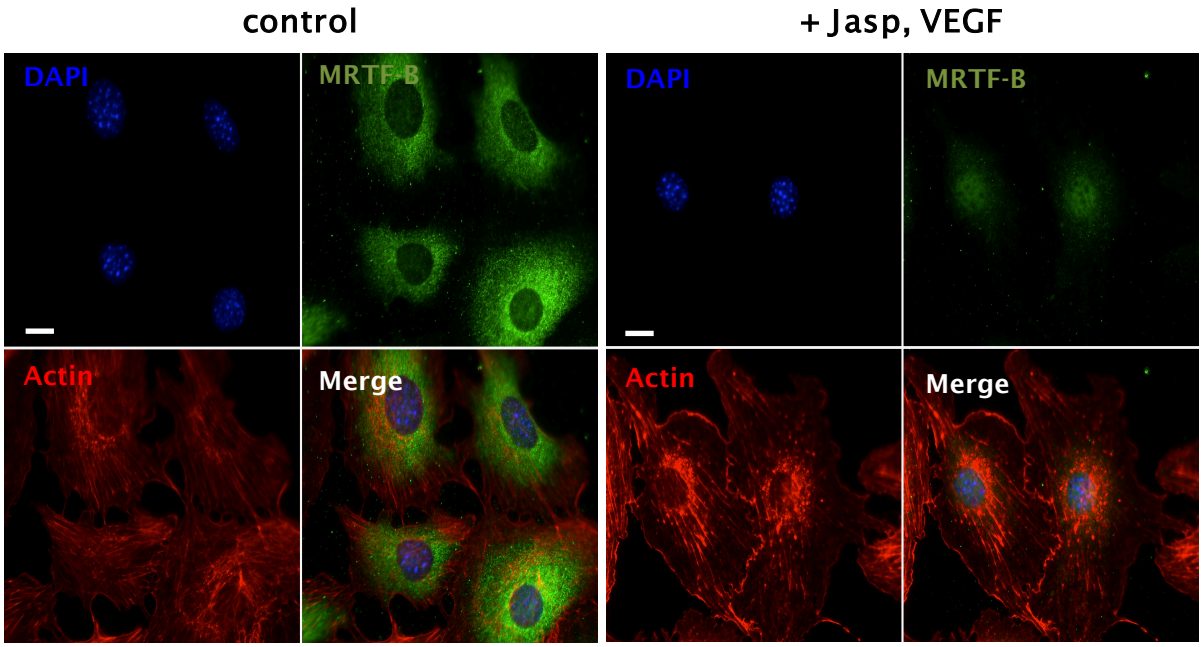

Figure 3.11: Effect of co-treatment of VEGF with Jasp on localization of MRTF-B

Immunofluorescent images of endogenous MRTF-B in control (left panel) and VEGF, Jasp-cotreated mECs (right panel). Serum and VEGF-starved cells were cultured with 200 nM Jasp for 2 hrs. Subsequently, 100 ng/ml VEGF was applied for 60 min. Then, cells were fixed and incubated with antibodies against MRTF-B, followed by Alexa 488-conjugated secondary antibody (green). The nuclei were visualized with DAPI (blue) and F-actin was visualized with Texas Red-conjugated phalloidin (red). Scale bar: 10 μm.

To sum up, these observations demonstrate that serum as well as VEGF regulates sub-cellular translocation of MRTFs in ECs. VEGF triggers MRTFs enrichment in the

nucleus and this process was strictly dependent on endothelial actin dynamics regarding the disruption of the MRTF/G-actin complex shown for both MRTF-A and -B.

3.2.5 VEGF-driven MRTF accumulation in the nucleus is dependent on RhoA-mediated actin dynamics

The small GTPase RhoA is a major regulator of actin dynamics, especially stress fibres. Since it was proven that serum-mediated accumulation of MRTF-A in the nucleus is regulated by RhoA-mediated signalling in a fibroblast model (Miralles et al., 2003), next experiments were designed with RhoA inhibitors to identify the role of RhoA in VEGF-induced nuclear accumulation of MRTFs in ECs.

3.2.5.1 ROCK inhibition by Y-27632

Rho-associated coiled-coil containing protein kinase (ROCK) is a major downstream effector of RhoA. To disrupt ROCK activity, the selective pan-ROCK inhibitor Y-27632 was introduced. To begin with, the effect of blockage of ROCK on endothelial actin was studied. Upon of Y-27632 treatment, stress fibres were missing in mECs, but no effect on peripheral actin was observed (Fig. 3.12).

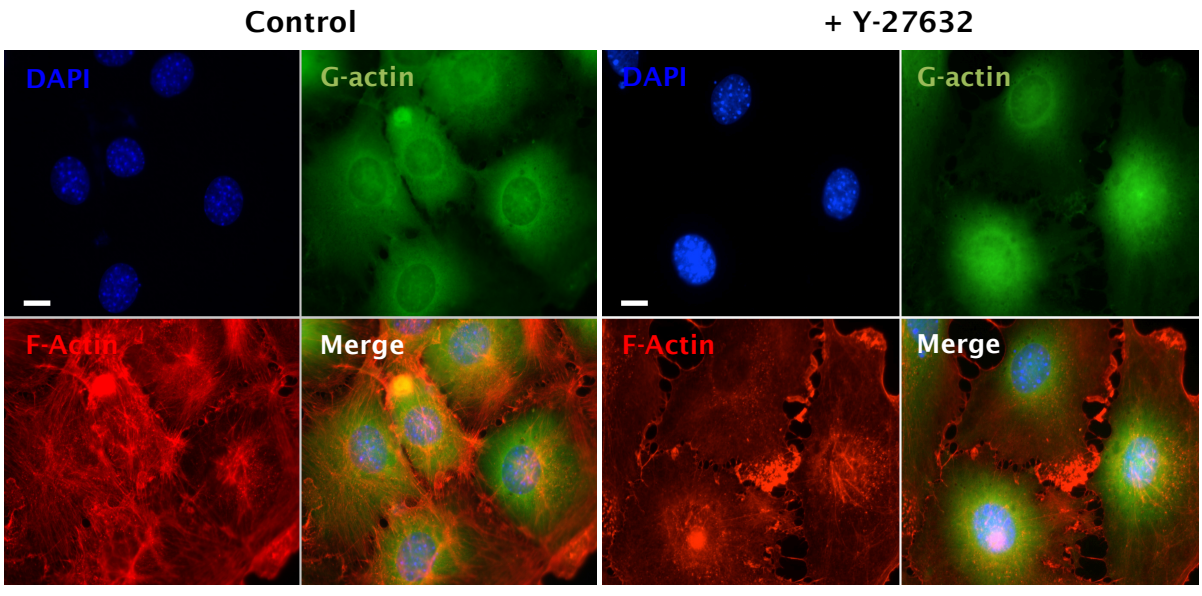

Figure 3.12: Alteration of endothelial actin by Y-27632

Immunofluorescent images of actin staining in control (left panel) and Y-27632-treated mECs (right panel). Serum and VEGF-starved cells were fixed and stained with DAPI (nucleus, blue), F-actin with Texas Red-conjugated phalloidin (red) and G-actin with Alexa 488-conjugated DNAse I (green). Scale bar: 10 μm.

Next, the localization of MRTF-A was analyzed upon ROCK blockage. The sub-cellular localization of MRTF-A was predominantly observed in the cytoplasm with Y-27632 treatment. The remarkable difference between control and Y-27632-treated cells was that MRTF-A was diffused in the cytoplasm in control cells whereas MRTF-A was more condensedly distributed near nuclei in cells treated with Y-27632 (Fig. 3.13).

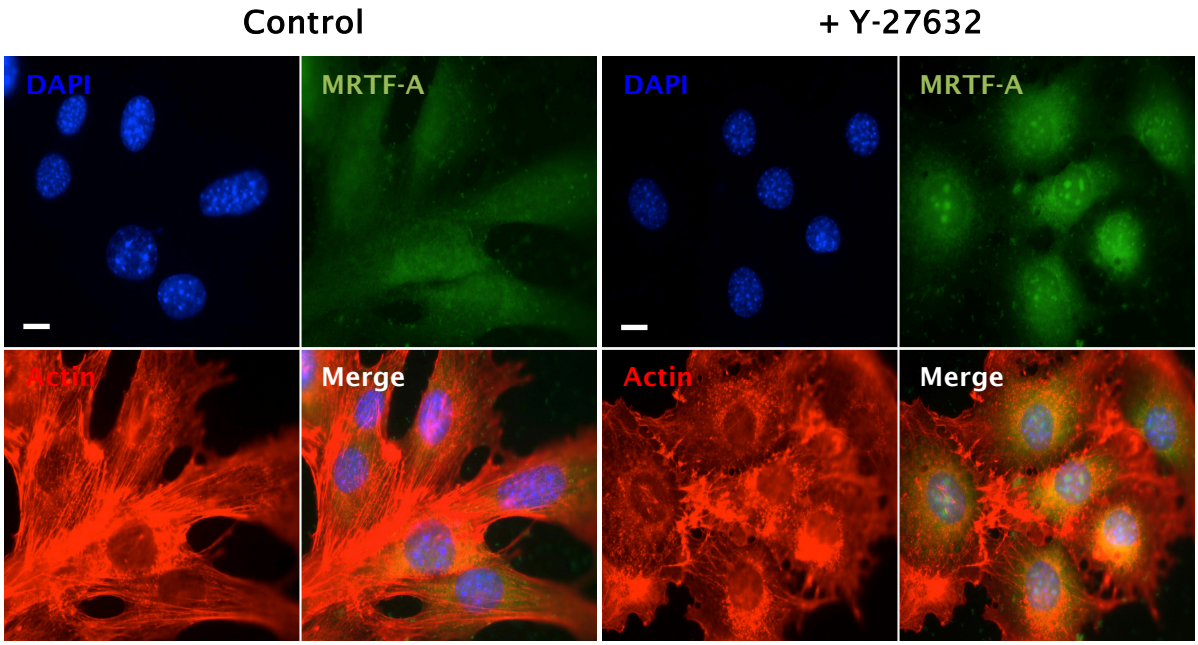

Figure 3.13: Effect of Y-27632 on sub-cellular localization of endogenous MRTF

Immunofluorescent images of endogenous MRTF-A in control (left panel) and Y-27632-treated mECs (right panel). Serum and VEGF-starved cells were cultured in the presence and absence of 50 μM Y-27632 for 2 hrs, respectively. Then cells were fixed and incubated with antibodies against MRTF-A, followed by Alexa 488-conjugated secondary antibody (green). The nuclei were visualized with DAPI (blue) and F-actin was visualized with Texas Red-conjugated phalloidin (red). Scale bar: 10 μm.

Next, cells were stimulated with serum or VEGF in the presence of Y-27632. In serum- or VEGF-stimulated cells, MRTF-A was predominantly detected in the cytoplasm upon Y-27632 stimulation (Fig. 3.14). The localization of MRTF-A in the cells was observed in the cytoplasm near nuclei, which was similar with Y-27632-incubated cells. These observations indicate that serum and VEGF-induced accumulation of MRTF is dependent on the major RhoA effector, ROCK.

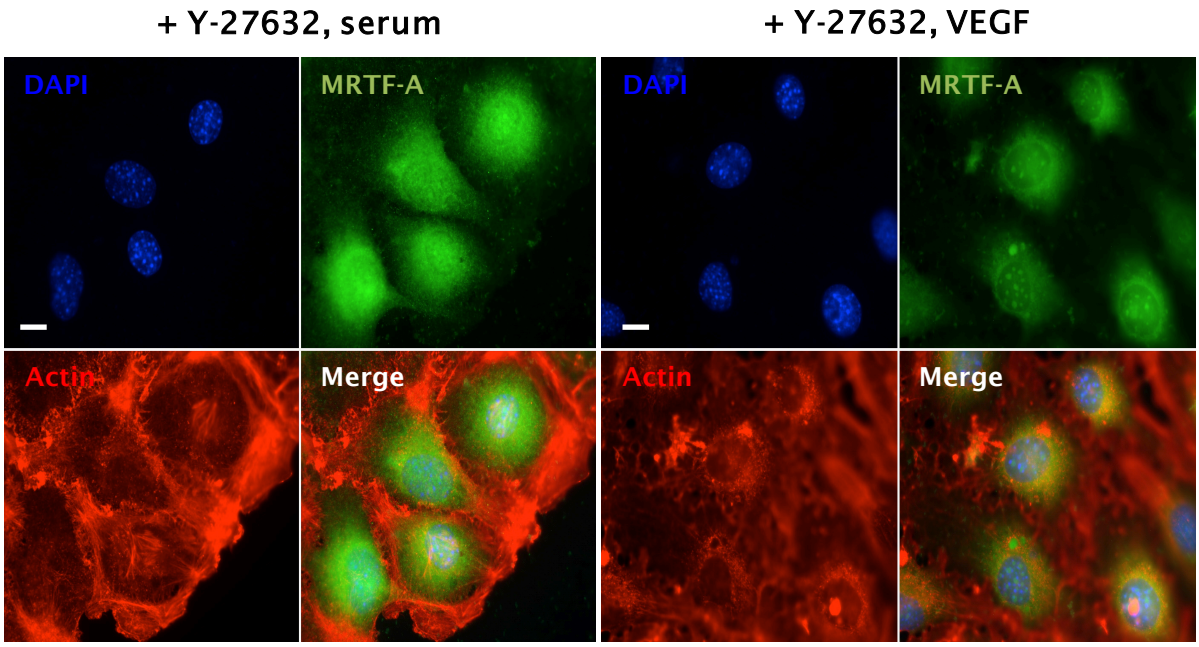

Figure 3.14: Effect of co-treatment of Y-27632 with serum or VEGF on location of MRTF-A

Immunofluorescent images of endogenous MRTF-A in Y-27632, serum-treated (left panel) and Y-27632, VEGF-treated mECs (right panel). Serum and VEGF-starved cells were cultured in the presence of 50 μM Y-27632 for 2 hrs. Subsequently, 15% serum and 100 ng/ml VEGF was applied for 60 min, respectively. Then, cells were fixed and incubated with antibodies against MRTF-A, followed by Alexa 488-conjugated secondary antibody (green). The nuclei were visualized with DAPI (blue) and F-actin was visualized with Texas Red-conjugated phalloidin (red). Scale bar: 10 μm.

3.2.5.2 RhoA inhibition

RhoA inhibition by CT04

The following experiment was designed for a RhoA disruption. Initially, cells were treated with CT04, the substance of the RhoA inhibitor C3 transferase, then serum or VEGF was applied in the presence of CT04, respectively. As it was seen in the previous chapter, MRTF-A was largely observed in the nucleus upon serum stimulation (Fig. 3.15, left panel). However, in the presence of CT04, serum-induced nuclear accumulation of MRTF-A was inhibited, thereby MRTF-A was predominantly observed in the cytoplasm.

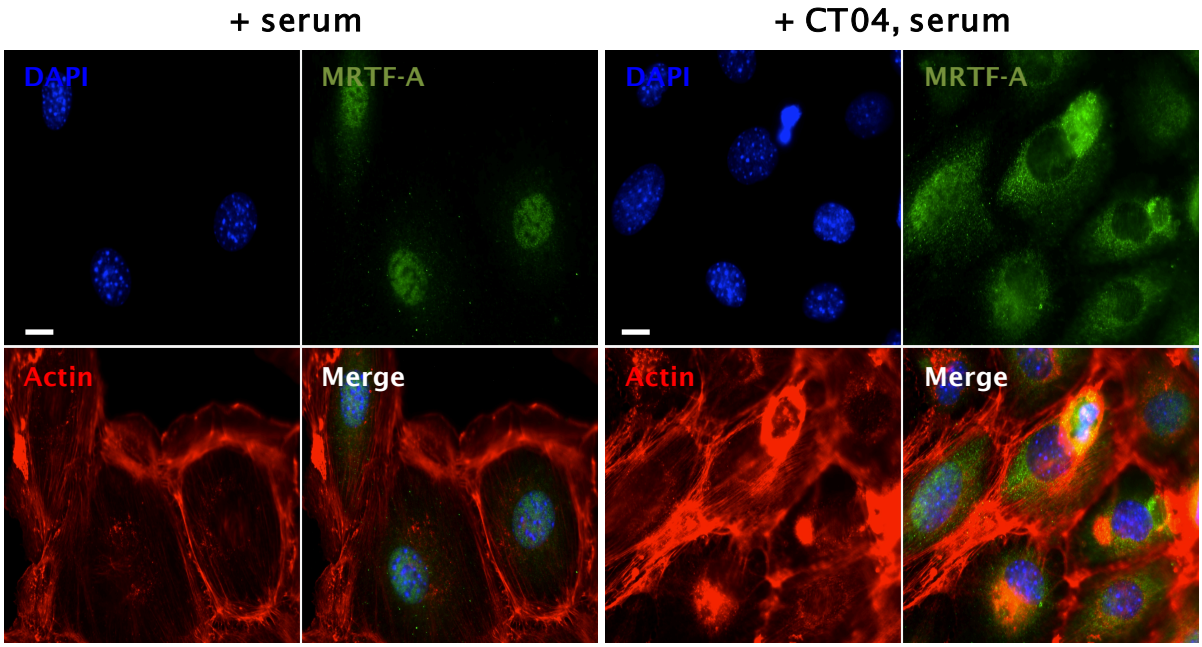

Figure 3.15: Effect of CT04 on serum-driven nuclear location of MRTF-A

Immunofluorescent images of endogenous MRTF-A in serum-treated (left panel) and CT04, serum co-treated mECs (right panel). Serum and VEGF-starved cells were cultured in the absence or presence of 2 μg/ml CT04 for 4 hrs. Subsequently, 15% serum was applied for 60 min. Then, cells were fixed and incubated with antibodies against MRTF-A, followed by Alexa 488-conjugated secondary antibody (green). The nuclei were visualized with DAPI (blue) and F-actin was visualized with Texas Red-conjugated phalloidin (red). Scale bar: 10 μm.

Notably, in VEGF-stimulated cells, MRTF-A was held back in the cytoplasm in the presence of CT04 (Fig. 3.16). CT04 blocked VEGF-induced nuclear accumulation of MRTF-A. In addition, CT04-treated cells could not display VEGF-induced stress fibres. The results suggest a pivotal role of RhoA in regulation of endothelial actin dynamics, which influences on sub-cellular localization of MRTF-A.

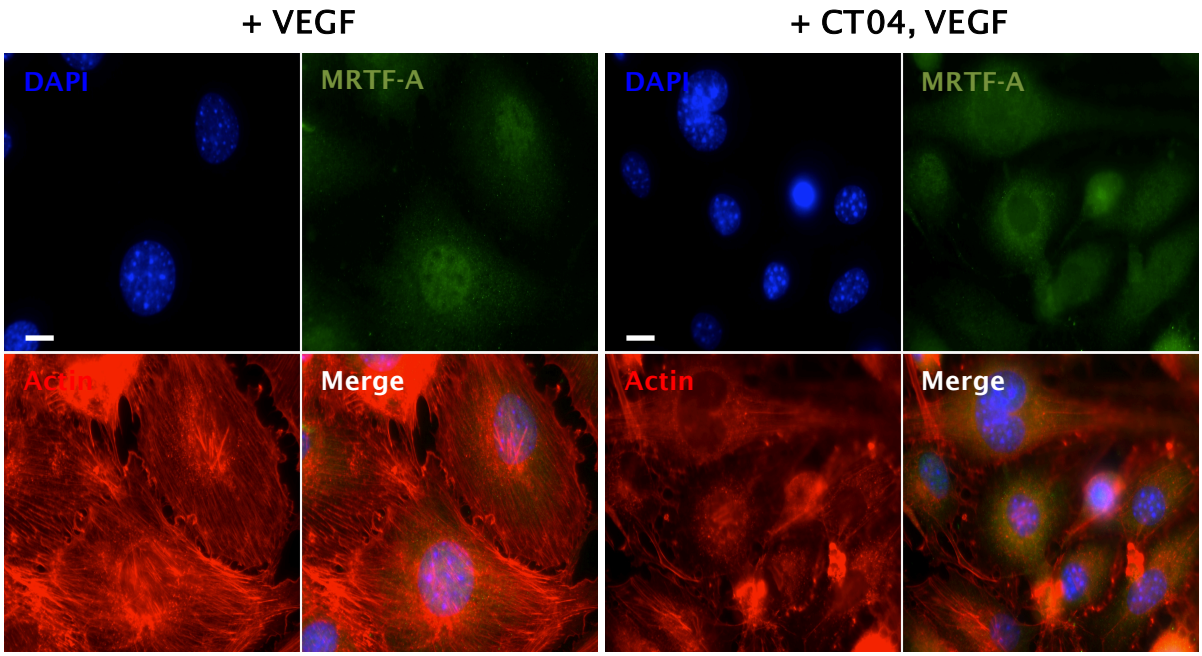

Figure 3.16: Effect of CT04 on VEGF-driven nuclear localization of MRTF-A

Immunofluorescent images of endogenous MRTF-A in serum-treated (left panel) and CT04, VEGF co-treated mECs (right panel). Serum and VEGF-starved cells were cultured in the absence or presence of 2 μg/ml CT04 for 4 hrs. Subsequently, 100 ng/ml VEGF was applied for 60 min. Then, cells were fixed and incubated with antibodies against MRTF-A, followed by Alexa 488-conjugated secondary antibody (green). The nuclei were visualized with DAPI (blue) and F-actin was visualized with Texas Red-conjugated phalloidin (red). Scale bar: 10 μm.

RhoA pathway inhibition by CCG-1423

Since the inhibitory effect of CCG-1423 against RhoA signalling has been reported in other cells, but not ECs (Evelyn et al., 2007 and 2010; Lundquist et al., 2014), cytotoxicity of CCG-1423 was initially tested in mECs. In mECs, CCG-1423 caused cellular toxicity at a concentration higher than 20 μM (Cytotoxicity was measured by the MTT test, data not shown). In addition, the F-actin structure was examined upon CCG-1423 treatment because the typical phenotype of RhoA inhibition is the disruption of stress fibres. In investigated mECs, CCG-1423 resulted in no remarkable change in actin stress fibres up to the sub-lethal concentration of CCG-1423 in cells (Fig. 3.17).

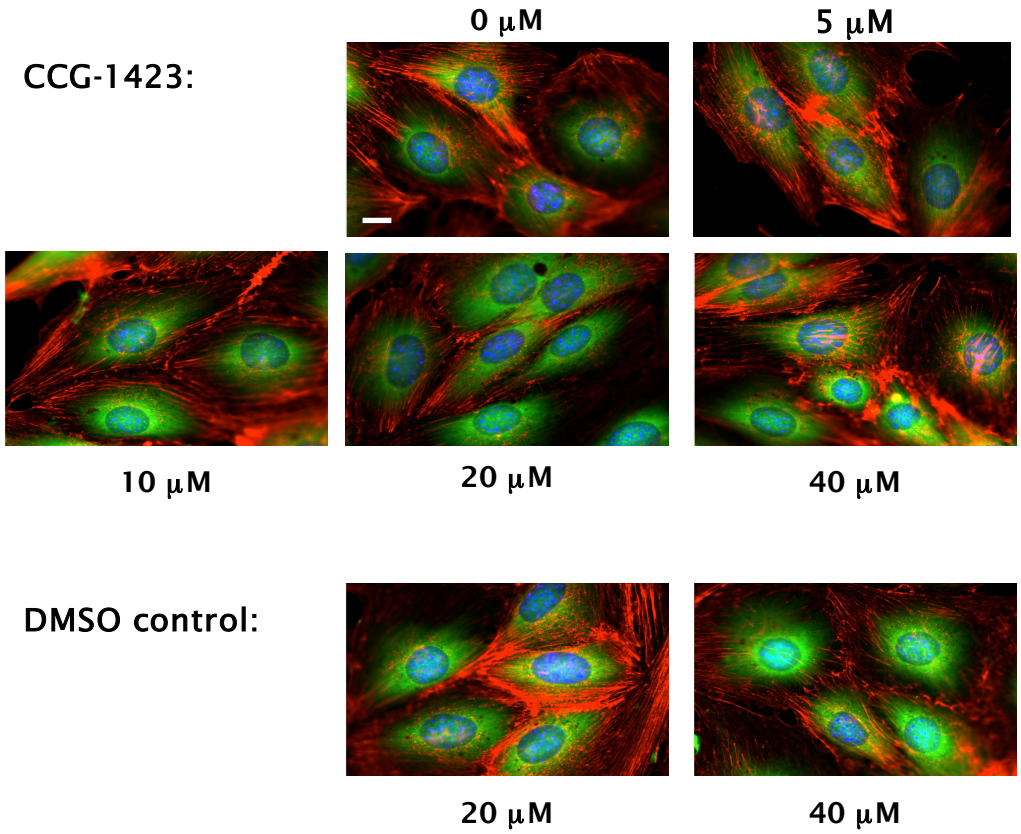

Figure 3.17: The effect of CCG-1423 on endothelial actin

Immunofluorescent images of actin staining in CCG-1423-treated (upper panel) and control (lower panel) mECs. mECs were treated with various concentrations of CCG-1423, and then stained with DAPI (nucleus, blue), G-actin (Alexa 488 conjugated-DNAse I, green), and F-actin (Texas red conjugated phalloidin, red). Scale bar: 10 μm.

As a following step, sub-cellular localization of MRTF-A was investigated in the presence of CCG-1423. Interestingly, CCG-1423 did not alter RhoA-induced stress fibre formation as well as serum- or VEGF-triggered nuclear accumulation of MRTF-A in mECs (Fig. 3.18). These results demonstrate that CCG-1423 does not alter RhoA-induced stress fibres formation. In addition, translocation of MRTF-A cannot be regulated by CCG-1423-driven activation of RhoA signalling.

Based on these studies with ROCK and RhoA inhibitors Y-27632 and CT04, respectively, it can be demonstrated that RhoA-ROCK dependent actin rearrangement plays a pivotal role in VEGF-induced MRTF-A enrichment in the nucleus in ECs.

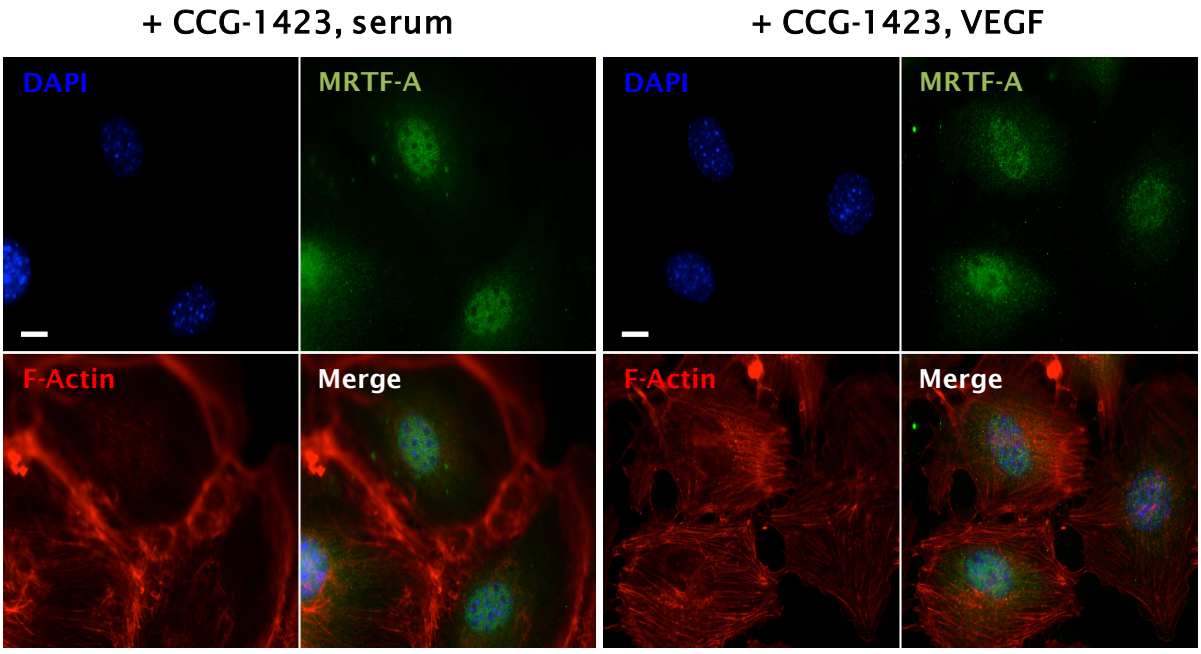

Figure 3.18: Effect of co-treatment of CCG-1423 with serum or VEGF on localization of MRTF-A

Immunofluorescent images of endogenous MRTF-A in CCG-1423, serum-treated (left panel) and CCG-1423, VEGF-treated mECs (right panel). Serum and VEGF-starved cells were cultured in the presence of 20 μM CCG-1423 for 4 hrs. Subsequently, 15% serum and 100 ng/ml VEGF was applied for 60 min, respectively. Then, cells were fixed and incubated with antibodies against MRTF-A, followed by Alexa 488-conjugated secondary antibody (green). The nuclei were visualized with DAPI (blue) and F-actin was visualized with Texas Red-conjugated phalloidin (red). Scale bar: 10 μm.

Interestingly, regarding actin structure, endothelial actin displayed different F-actin structure by incubating with different RhoA inhibitors (Fig. 3.19). The remarkable change induced by Y-27632 was the lack of F-actin bundles. By CT04, ECs lacked stress fibres as well as lamellipodia. After incubation with CCG-1423, there was no significant change on endothelial actin. These observations suggest that endothelial actin can be differently regulated by RhoA or its regulators.

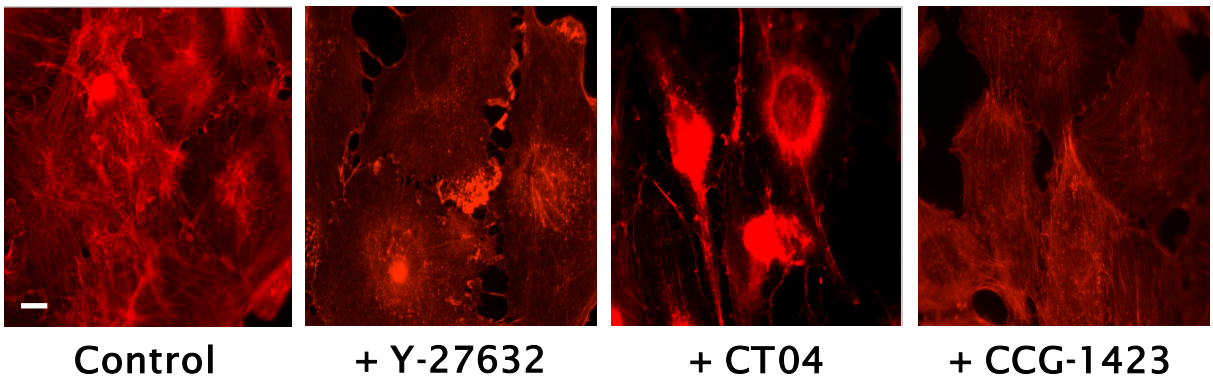

Figure 3.19: Changes of endothelial actin by RhoA inhibitors

Immunofluorescent images of F-actin staining in control and RhoA -treated mECs. Serum and VEGF-starved cells were cultured in the presence and absence of 50 μM Y-27632 for 2 hrs, respectively. Then, cells were fixed and F-actin was stained with Texas Red-conjugated phalloidin (red). Scale bar: 10 μm.

3.3 Endothelial RhoA activation by VEGF

Immunofluorescent data described in the previous chapter clearly suggested that nulclear localization of MRTF-A is regulated by VEGF via RhoA-ROCK-dependent signalling. In the following, a RhoA activation assay was performed to analyse whether VEGF influences RhoA level in mECs. Activation of RhoA was measured by quantitating an active form (RhoA-GTP) of RhoA in control and VEGF-stimulated cells. In VEGF-stimulated cells, the level of RhoA was increased after 10 min stimulation with VEGF, then decreased in cells cultured with VEGF for 60 min (Fig. 3.20). Therefore, activation of RhoA by VEGF was rapid and transiently in mECs.

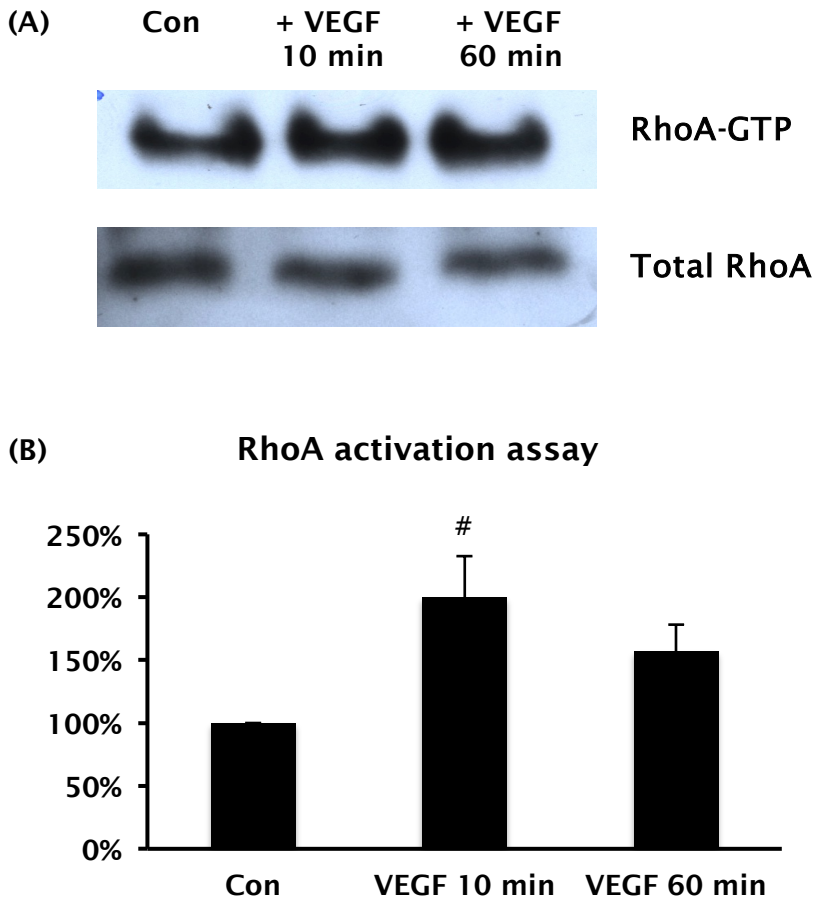

Figure 3.20: VEGF-induced RhoA activation in ECs

(**A**): Western blotting of immunoprecipitated active-RhoA level. (**B**): Quantitative analysis of RhoA activation assay. Protein levels were normalized to total RhoA and presented as percent of control. Data are presented as the mean ± SEM (4 experiments for 10 min stimulation, 3 experiments for 60 min VEGF stimulation). $^{\#}p = 0.05$.

3.4 SRF knockdown *in vitro* and analysis of endothelial target genes

Even though more and more SRF target genes, which are involved in various cellular signallings have been identified, endothelial SRF target genes and their role in angiogenesis are still poorly understood. As next set of experiments, SRF knockdown induced by siRNA treatment of endothelial cells *in vitro* was performed to screen for potential endothelial SRF target genes involved in angiogenesis.

3.4.1 siSRF797 effectively downregulated SRF in mECs

In a previous study, two potential siSRF sequences against SRF have been designed and named siSRF797 and siSRF820, respectively (Konjer, 2009). Comparing these two siRNAs, siSRF797-mediated downregulation of SRF levels was more efficient, therefore, siSRF797 was introduced in mECs. Even though siSRF797 was tested in human and porcine smooth muscle cells, it was expected that siSRF797 could be functional in mECs since siSRF797 recognizes the sequence within the MADS box of SRF (Konjer, 2009), which is highly conserved in mammals.

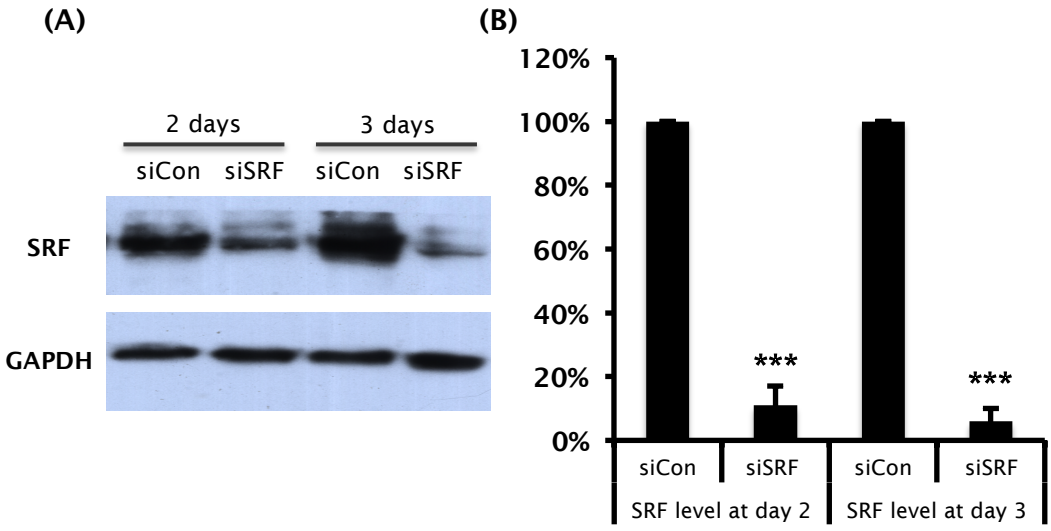

Figure 3.21: Knockdown of SRF protein upon siSRF797 transfection

(**A**): Representative Western blot image shows protein levels of SRF upon siSRF797 transfection for 2 or 3 days in mECs compared to control cells. Full length of SRF (SRF-L) protein was shown at 67 kDa and the loading control GAPDH was detected at 37 kDa. (**B**): Quantitative analysis of SRF expression. Protein levels were normalized to GAPDH and presented as percent of control. Data are presented as the mean ± SEM of 5 experiments. ***$p < 0.001$.

By siSRF797, SRF expression was dramatically decreased in mECs at the mRNA level as well as at the protein level. mRNA was downregulated approximately 60 to 80% on the second day after siSRF797 transfection (data not shown) At the protein level, SRF expression was decreased about 90% on the second day after siSRF 797 transfection and approximately 95% on the third day after transfection (Fig. 3.21). Based on this result of efficient downregulation of SRF, siSRF797 could be used in mECs for further studies.

3.4.2 VEGFR-2 was confirmed as an SRF target gene

VEGFR is a widely expressed key receptor for angiogenesis. Based on the observation that VEGF induced SRF target genes and CArG boxes are present in the VEGFR-2 promoter (Franco et al., 2008), the level of VEGFR-2 was investigated after siRNA-mediated knockdown of SRF.

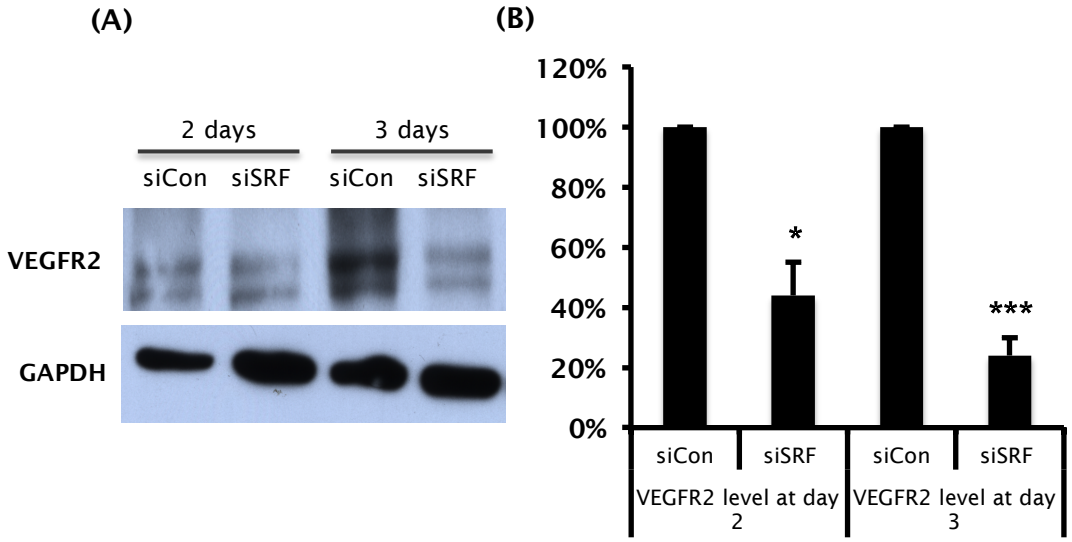

Figure 3.22: Protein level of VEGFR-2 upon siSRF797 transfection

(**A**): Representative Western blot image shows protein levels of VEGFR-2 upon siSRF797 transfection for 2 or 3 days in mECs. One set of VEFGR-2 double band was shown at 210 and 230 kDa and the loading control GAPDH was detected at 37 kDa. (**B**): Quantitative analysis of VEGFR-2 expression. Protein levels were normalized to GAPDH and presented as percent of control. Data are presented as the mean ± SEM of 4 experiments. $*p < 0.05$, $***p < 0.001$.

Upon transfection of siSRF797, the VEGFR-2 level was significantly downregulated and the effect was even more significant in cells cultivated for 3 days (Fig. 3.22).

Fig. 3.22 shows full-length VEGFR-2 as one set of double band that were detected at 210 and 230 kDa. This finding demonstrates that VEGFR-2 is under the control of SRF and SRF depletion can result in defects of VEGF signalling due to the loss of VEGFR-2.

3.4.3 SRF regulated endothelial Cofilin

Previous evidences indicate that SRF activity is regulated by actin dynamics (Sotiropoulos et al., 1999; Geneste et al., 2002). However, SRF is capable to regulate actin dynamics by altering actin components, *vice versa*. SRF is involved in regulation of actin dynamics via LIM kinase (LIMK), which catalyzes phosphorylation of Cofilin. Cofilin is an actin depolymerizing factor (ADF) that severs filamentous actin-to-actin fragments, thereby inducing actin depolymerization. Phosphorylation at the residue Ser3 is the major mechanism of inhibition of Cofilin function (Morgan et al., 1993). Phosphorylation at this site was dramatically increased in forebrains of SRF-deficient Mice, which displayed impaired neuronal migration (Alberti et al., 2005). Therefore, a change at Ser3 of Cofilin was studied in order to understand the effect of SRF on Cofilin regulation. Upon siSRF transfection, phosphorylated Cofilin level was significantly enhanced which has not been reported in ECs (Fig. 3.23).

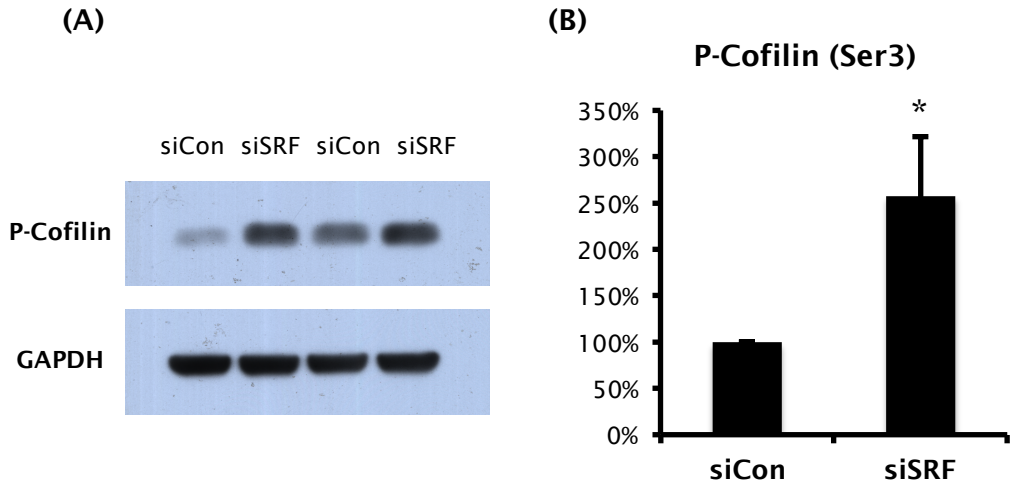

Figure 3.23: Protein level of P-Cofilin upon siSRF797 transfection

(**A**): Representative Western blot image shows protein levels of phosphorylated Cofilin at the Ser3 upon siSRF797 transfection for 3 days in mECs. Phosphorylated Cofilin was shown at 19 kDa and the loading control GAPDH was detected at 37 kDa. (**B**): Quantitative analysis of P-Cofilin expression. Protein levels were normalized to GAPDH and presented as percent of control. Data are presented as the mean ± SEM of 9 experiments. $*p < 0.05$.

This result suggests that the activity of Cofilin is regulated by SRF in ECs. Depletion of SRF results in hyperphosphorylation of Cofilin, thereby inactivating Cofilin.

3.4.4 Phosphorylation of MLC was regulated by SRF in ECs

Next, a potential influence of SRF on myosin light chain (MLC) was analysed. In a previous study, it was shown that endothelial-specific SRF-deleted mice displayed defects at endothelial junctions with abnormally increased vascular permeability (Franco et al., 2008). Endothelial junctions are bound to actomyosin actin filaments and phosphorylation of MLC contributes to disassembly of endothelial junctions. Therefore, an experiment was designed to investigate whether the phosphorylation level of MLC is controlled by SRF.

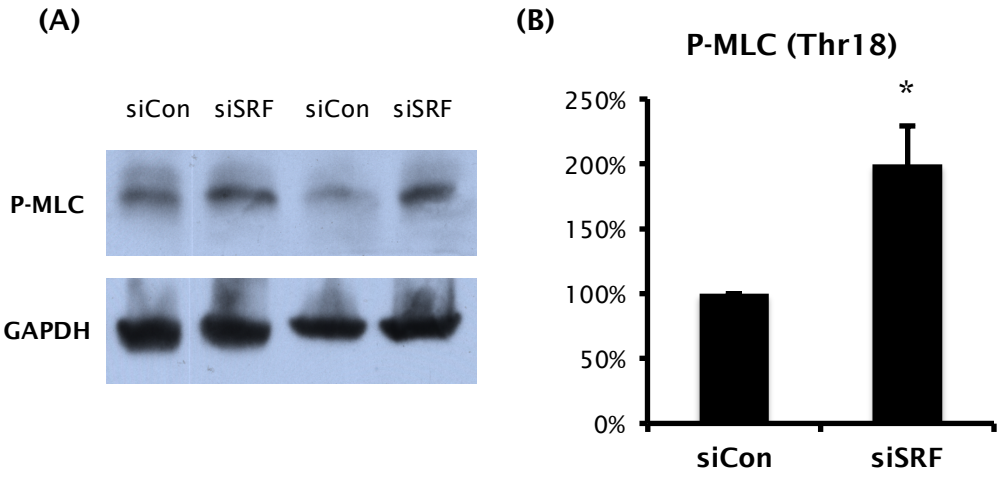

Figure 3.24: Protein level of P-MLC upon siSRF797 transfection

(**A**): Representative Western blot image shows protein levels of phosphorylated Myosin light chain (MLC) at the Thr18 upon siSRF797 transfection for 3 days in mECs. Phosphorylated MLC was shown at 19 kDa and the loading control GAPDH was detected at 37 kDa. (**B**): Quantitative analysis of P-MLC expression. Protein levels were normalized to GAPDH and presented as percent of control. Data are presented as the mean ± SEM of 7 experiments. *$p < 0.05$.

ECs, which lack SRF by siSRF transfection, showed hyperphosphorylation of MLC at the residue Thr18 (Fig. 3.24). This result demonstrates that SRF is involved in control of the balance between cellular contraction and release by altering phosphorylation of myosin light chain.

3.4.5 Membrane proteases were identified as potential SRF target genes

The matrix metalloproteinases (MMPs) and their related proteases a disintegrin and metalloproteases (ADAMs) are the enzymes that degrade membrane components of the ECM and membrane-bound proteins. They are required for extracellular remodelling such as tissue remodelling, wound healing, developmental processes, and angiogenesis. So far, there was no evidence for SRF regulation of MMPs' expression in ECs. Moreover, expression and regulation of ADAMs by SRF have not been reported yet. To investigate the role of SRF in regulation of proteases, representative proteins of MMPs and ADAMS as well as their inhibitor the tissue inhibitors of metalloproteinases (TIMPs) were selected according to their described roles in ECs, and their expression levels were analysed after SRF knockdown by siSRF transfection.

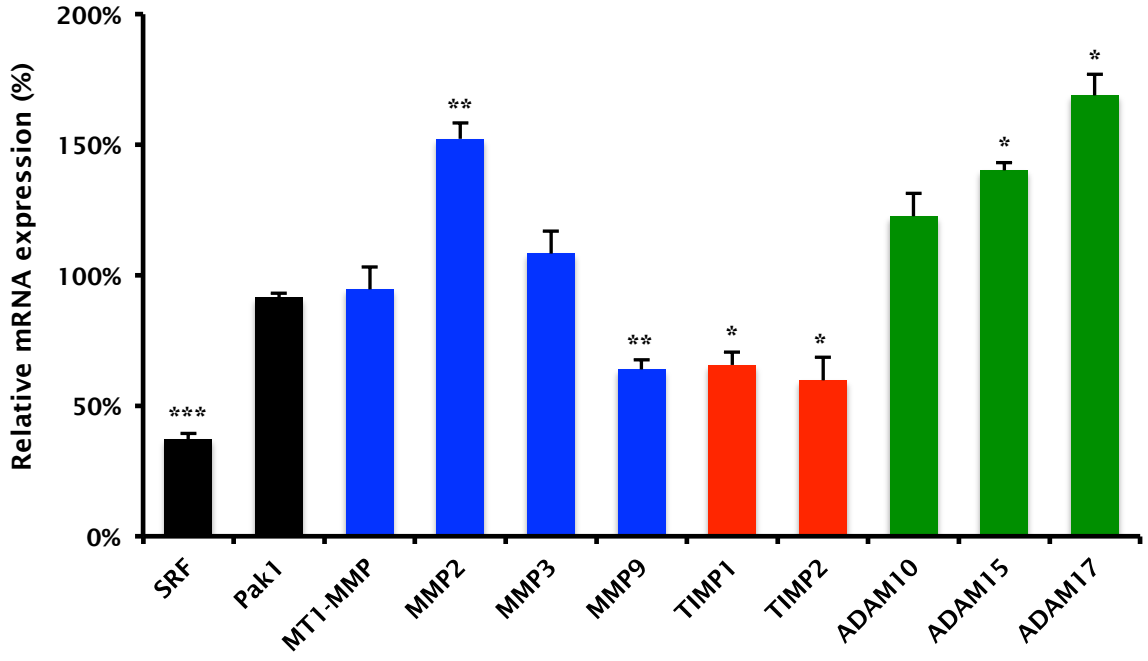

Figure 3.25: The effects of SRF depletion on membrane proteases

qRT-PCR analysis shows mRNA level of MMPs (blue), TIMPs (red), and ADAMs (green) upon SRF depletion. SRF depletion was introduced by transfection of siSRF797 and expression level was normalized to *Gapdh*. Pak1 was used as a negative control known not to be regulated by Srf. Data are presented as the mean ± SEM of 6 experiments. $*p < 0.05$, $**p < 0.01$, $***p < 0.001$.

The results show that the MMPs levels were differently shown upon SRF depletion (Fig. 3.25). The membrane type of MMP, MMP14 (MT1-MMP) was not significantly changed by SRF depletion. The expression level of MMP2 was elevated and SRF target gene MMP9 was significantly downregulated upon SRF depletion. The level of MMP12 was also investigated, however, due to its very low expression level, it was barely detectable (data not shown). The representative two MMP inhibitors, Timp1 and 2 were dramatically downregulated by SRF depletion, suggesting that SRF probably controls TIMPs in ECs. Adam10 was not significantly changed. Interestingly, Adam15 and 17 were significantly increased upon SRF depletion. To understand these effects better, CArG boxes were screened in the tested membrane proteases.

Table 3.1: CArG boxes in the murine membrane protease genes

Gene	Position	Sequence
MT1-MMP (Mmp14)	- 5kb	CCTTATCTGG
	+11kb	**CCTTAAAAGG**
Mmp2	- 6.4kb	CCATACAGGG
	+1kb	CCACAAAAGG
	+11kb	CCAAATGAGG
Mmp3	- 9kb	CCATGAAAGG
	- 8.2kb	CCATGAAAGG
	+ 4.2kb	**CCTAAAATGG**
Mmp9	- 7.4kb	**CCATATAAGG**
Mmp12	- 11kb	**CCATATATGG**
	- 10.5kb	CCATCTATGG
	- 1.3kb	**CCTATTAAGG**
Timp1	- 6.7kb	**CCATATTTGG**
	- 4.4kb	CCAAACAGGG
	+ 0.9kb	GGCCATGTAAGC
Timp2	- 3.3kb	**CCAAAAATGG**
	- 0.2kb	CCTTTCAGGG
	+ 2.4kb	CCAAATAGGG
Adam10	- 12.3kb	CCAGATATGG
	- 7.9kb	CCTATCATGG
	+ 1.9kb	CCTAGCAAGG
	+ 3.2kb	**CCTAATAAGG**
Adam15	- 6.1kb	**CCTAATTTGG**
	+ 4kb	CCATTATGGG

	+8.9kb	**CCTTTAATGG**
Adam17	- 10kb	**CCTTAAAAGG**
	- 8.2kb	CCCTTTTTGG
	- 3kb	CCAATCTTGG
	+ 1kb	CCATCTAAGG
	+ 8kb	CCTTGTTTGG

CArG box sequences were screened by representative membrane proteases in murine genes. Sequences were founded via NCBI blast and direction of upstream and downstream is designated plus and minus. The canonical CArG boxes are highlighted in bold. The screening of CArG box via NCBI blast was carried out by Dr. Stritt.

All membrane protease genes investigated in this study contain at least one CArG box (Table 3.1). Among them, canonical CArG boxes were detected in some genes. The location of CArG boxes exists at various loci. Based on this observation, it seems that SRF can be involved in regulation of ECM and basal membrane modulation at least by altering membrane proteases.

3.4.6 SRF-altered endothelial proliferation and siMRTF screening

3.4.6.1 Screening of different siMRTF sequences

After confirmation of the knockdown model of SRF by siSRF797, experiments for siMRTFs were designed to identify potential endothelial MRTF target genes. In a first step of siRNA experiments, several siRNAs were selected in order to find effective siMRTF. By NCBI screening (www.ncbi.nlm.nih.gov/blast), two transcription variants of MRTF-A were found in murine (Table 3.2).

Table 3.2: Murine MRTF-A transcriptional isoforms

Mrtf-a (murine)	Reference sequence	Size
Transcription variant 1	NM 153049	4111bp
Transcription variant 2	NM 001082536	4266 bp

Both transcription variants share functional key domains of MRTF-A that are involved in MRTF activity. For experiments, four different siMRTF-A sequences, which target both variants are chosen and named siMRTF-A1 to -A4.

In the murine MRTF-B gene, 3 transcriptional variants were screened (Table 3.3).

Table 3.3: Murine MRTF-B transcriptional isoforms

Mrtf-b (murine)	Reference sequence	Size
Transcription variant 1	NM 153588	8295 bp
Transcription variant 2	NM 181860	714 bp
Transcription variant 3	NM 001122667	8281 bp

Among 3 isoforms of MRTF-B, the transcription variant 1 and 3 contain functional MRTF-B domains whereas transcription variant 2 lacks SAP and RPEL domains. Moreover, the transcription variant 2 is significantly smaller than other transcription variants. For siMRTF-B sequences screening, 4 different siMRTFs, which have different transcriptional targets, were selected and named siMRTF-B1 to B4. siMRTF-B1 targets transcription variant 3 of MRTF-B gene and siMRTF-B2 targets transcription variant 1. Both siMRTF-B3 and -4 were designed against MRTF-B transcription variant 2. With these siMRTFs, the efficiency of the siRNA sequences was tested in mECs.

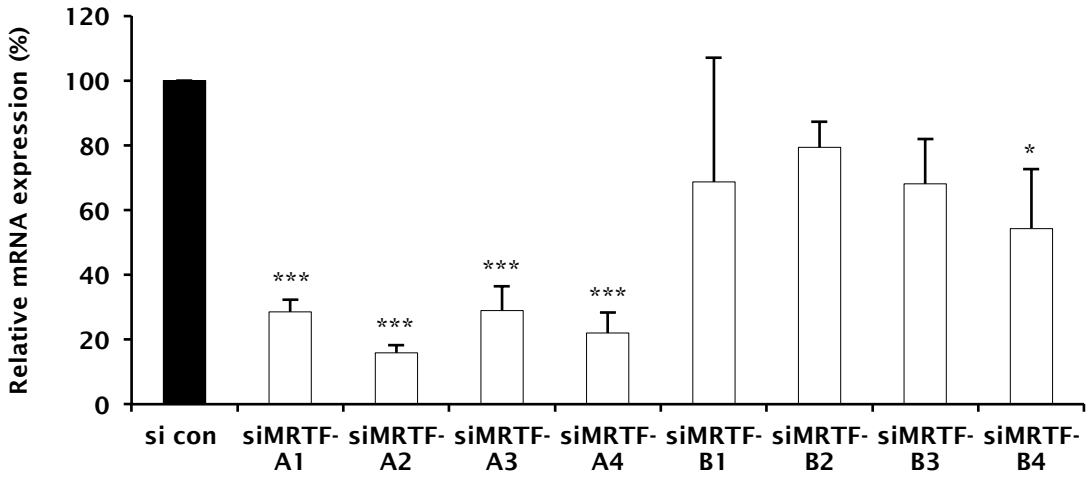

Figure 3.26: MRTF-A knockdown by different siRNAs

qRT-PCR analysis shows mRNA level of MRTF-A after transfection of various siMRTF-A in mECs. Expression level was normalized to control siRNA (si con). Data are presented as the mean ± SEM of 3 experiments. $^{*}p < 0.05$, $^{***}p < 0.001$.

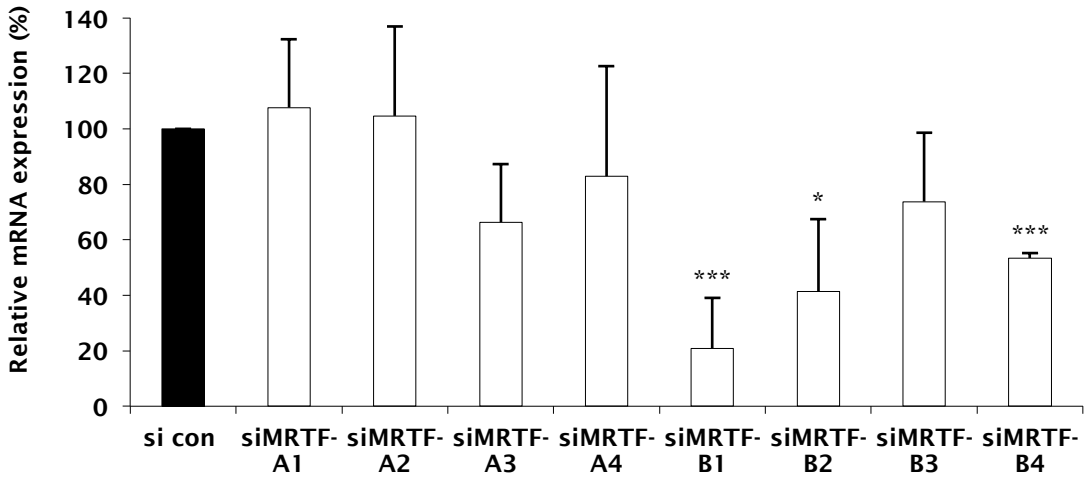

Figure 3.27: MRTF-B knockdown by different siRNAs

qRT-PCR analysis shows mRNA level of MRTF-B after transfection of various siMRTF-B in mECs. Expression level was normalized to control siRNA (si con). Data are presented as the mean ± SEM of 3 experiments. $*p < 0.05$, $***p < 0.001$.

Fig. 3.26 and Fig. 3.27 showed that different siRNA sequences had different knockdown efficiency on MRTF gene. According to experimental results, all of siMRTF-As effectively downregulated MRTF-A level without alteration of MRTF-B expression (Fig. 3.26). At the protein level, the result was similar to results of RNA, but siMRTF-A1 was slightly more efficient (data not shown). siMRTF-B sequences were also able to effectively downregulate MRTF-B expression. Among them, siMRTF-B1- and -B2-induced downregulation of MRTF-B expression did not alter MRTF-A expression (Fig. 3.27).

3.4.6.2 Depletion of SRF, MRTF and endothelial proliferation

As the efficiency of siSRF and siMRTFs was confirmed, siRNAs mediated knockdown was applied to investigate the influence on endothelial proliferation. For proliferation assay, equal numbers of mECs were seeded and transfected with each of siRNAs. After transfection, cell numbers were quantitatively measured by MTT-based method on the second and third day after transfection. Control siRNA (siCon) was used to normalize the effects that can be caused during transfection.

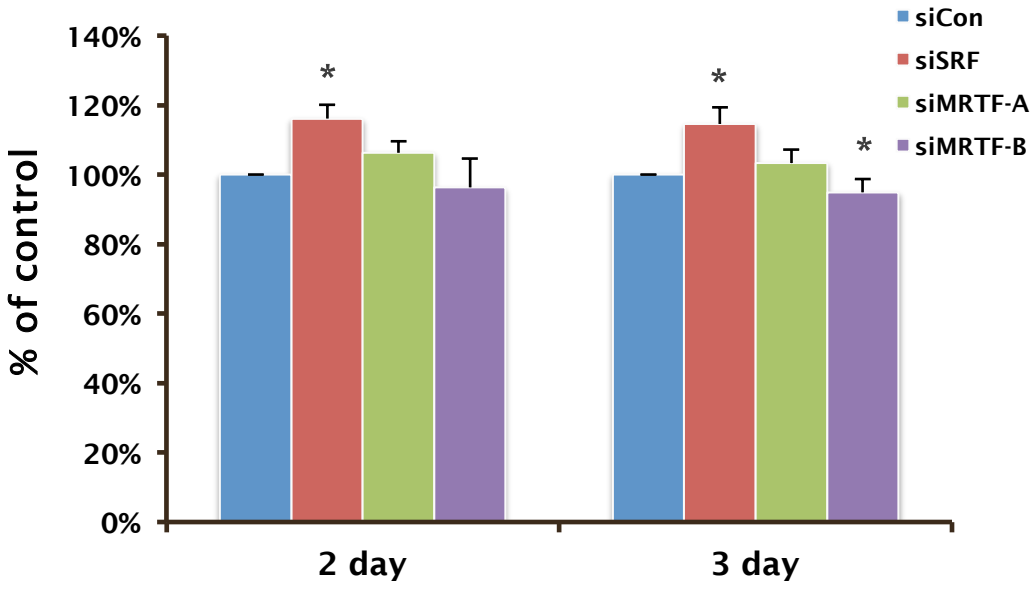

Figure 3.28: Endothelial proliferation upon siSRF and siMRTF transfection

Proliferation assay shows relative proliferation of mECs upon SRF, MRTF-A and -B depletion. Gene depletion was introduced by transfection of siRNAs and expression level was normalized to GAPDH. Data are presented as the mean ± SEM of 5 experiments. $*p < 0.05$.

Experimental results showed that SRF depletion caused hyperproliferation of ECs (Fig. 3.28). This effect is small but significant on the second and the third day after transfection. MRTF-A depletion caused no remarkable effect on endothelial proliferation whereas MRTF-B depletion induced modest inhibition of cellular proliferation on the third day. These results indicate that SRF depletion could alter endothelial proliferation by promoting proliferation. MRTF-A and -B showed different effects on proliferation, highlighting their different biological role in ECs.

3.4.7 TSP-1 was identified as a novel endothelial SRF target gene

3.4.7.1 Regulation of TSP-1 expression by SRF in ECs

TSP-1 is an anti-angiogenic factor derived from endothelium (Reed et al., 1995). It diminishes angiogenic process, thereby playing an important role in balancing between pro- and anti-angiogenesis. Since control of anti-angiogenic proteins by SRF is still poorly understood, TSP-1 was selected as a representative anti-angiogenic factor and TSP-1 level was studied upon SRF depletion.

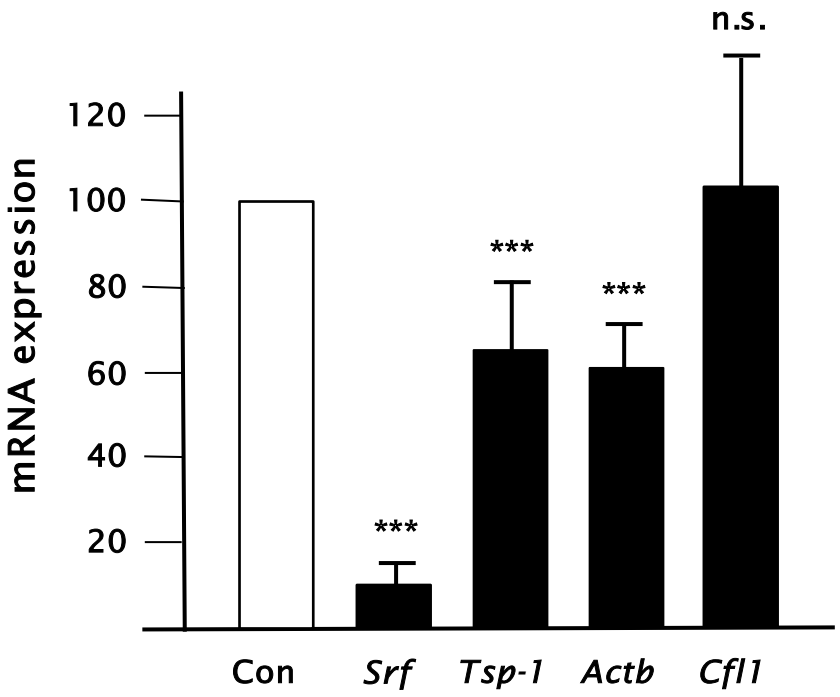

Figure 3.29: TSP-1 expression upon SRF depletion

qRT-PCR analysis indicated that siSRF797-induced SRF depletion exhibited downregulation of SRF (*Srf*), β-actin (*Actab*) as well as TSP-1 (*TSP-1*) level. Cofilin 1(*Cfl1*) was used as a negative control. Data were normalized to *Gapdh*. Data are shown as the mean ± SEM of 5 experiments. Data were analysed by Dr. Christine Stritt. ****p* < 0.001, ns: not significant vs. respective control.

mRNA analysis by qRT-PCR revealed that TSP-1 expression level was significantly downregulated upon siSRF797 transfection (Fig. 3.29). This result demonstrated that endogenous TSP-1 expression is under control of SRF in ECs.

3.4.7.2 Recruitment of SRF to the TSP-1 promoter

From the mRNA study described above, it could be hypothesized that SRF may bind to the TSP-1 promoter, thereby transcriptionally controlling TSP-1 gene. To prove this hypothesis, ChIP assay of SRF to TSP-1 promoter was performed by Dr. Christine Stritt. In cultivated mECs, fragmented chromatins were immunoprecipitated with SRF antibody, and then the intensity of binding signal to each promoter was analyzed by qRT-PCR. For TSP-1, the promoter region -1,2kb with the sequence CCTTATTTGG was examined and for β-actin, at + 0,8kb promoter region with the sequence CCTTTTATGG was investigated. Pak1 was considered as a negative control since it does not contain any CArG box sequences.

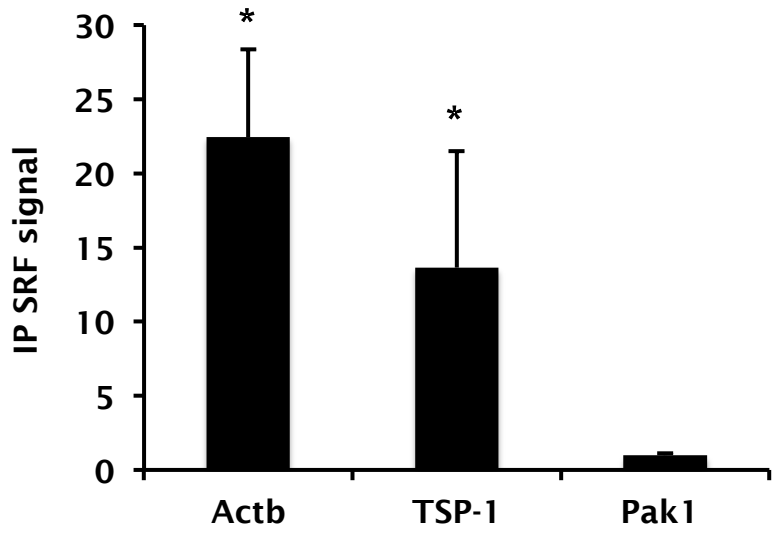

Figure 3.30: SRF ChIP assay to TSP-1

SRF chip signal of different target genes are shown. The ChiP signal of SRF antibody (SC 335) to TSP-1 was compared with β-actin (Actb) and Pak1. IgG control was performed and confirmed that no ChIP signal was detected. Data are shown as the mean ± SEM of 5 experiments. Data were analysed by Dr. Christine Stritt. $*p < 0.05$, ns: not significant vs. respective control.

The findings from SRF ChIP assay indicate that SRF ChIP signal was strongly detected on the endothelial TSP-1 promoter (Fig. 3.30). This result demonstrates that SRF directly binds to the TSP-1 promoter, thereby regulating endothelial TSP-1 expression. Based on the two studies with TSP-1, it is strongly suggested that TSP-1 is a novel endothelial target gene of SRF.

4. DISCUSSION

4.1.1 VEGF regulates SRF target genes in ECs

Previous reports demonstrated that SRF-mediated angiogenesis is required during murine embryonic development (Franco et al., 2008) as well as at postnatal development (Weinl et al., 2013). Moreover, the SRF cofactor MRTF was also proved as an important regulator of retinal angiogenesis in murine model of retinal vascularization (Weinl et al., 2013). Nevertheless, SRF/MRTF-mediated transcriptional activation is still poorly understood, especially in ECs.

At first, this study demonstrates that VEGF activates SRF target genes. Two representative SRF target genes including the class I target gene, *c-fos* and the class II target gene, *β-actin* as well as VEGF receptors (*Vegfr-1 and Vegfr-2*), and SRF itself (*Srf*) were investigated upon VEGF stimulation. The expressions of these genes were significantly increased in VEGF-stimulated mECs (Fig. 3.3). This observation strongly suggests that endothelial SRF expression is under control of VEGF. In addition, a previous study reported that VEGF controls endothelial proliferation, migration by controlling a SRF target gene, *Egr-3* (Suehiro et al., 2011). Notably, the results of luciferase reporter gene assays show that this effect is dependent on SRE, but not on ETS-binding sites (TCFs). VEGF significantly induced transcriptional activity of *c-fos*. Furthermore, transfection with MRTF-A resulted in even higher luciferase activity, suggesting cooperative roles of MRTF-A and VEGF for activation of SRF (Fig. 3.4).

To determine VEGF-mediated SRF activation in ECs, sub-cellular localization of SRF was examined. In two different ECs (mECs and HUVECs), the localization of SRF was observed in the nucleus (Fig. 3.1 and 3.2). Even though SRF has been known as a nuclear factor, previous studies reported that SRF was predominantly observed in cytoplasm of ECs and SRF can be translocated by VEGF stimulation in rat ECs (Chai et al., 2004) and in HUVEC (Suehiro et al., 2011). This discrepancy could be explained by different culture conditions such as media composition, or due to different EC lines, or cellular density. However, except of these two reports, SRF expression is mainly observed in the nucleus, therefore SRF is regarded as a ubiquitously expressed nuclear transcription factor.

4.1.2 VEGF controls sub-cellular localization of MRTFs and endothelial actin dynamics

The activity of MRTFs is dependent on the sub-cellular localization of MRTFs that is regulated by actin dynamics. In cultured mECs, different sub-cellular localization of MRTFs was observed depending on culture conditions, demonstrating MRTF can shuttle between the cytoplasm and the nucleus as it was shown in a fibroblast model (Miralles et al., 2003). Serum, a positive regulator of SRF, induced endothelial actin rearrangement as well as MRTF-A accumulation in the nucleus (Fig. 3.5 and 3.6). Interestingly, VEGF also significantly induced MRTF-A accumulation in the nucleus upon 1 hr of stimulation (Fig. 3.7). Of note, this effect was abolished when F-actin of cells was disrupted. In the presence of Lat B, VEGF could not drive MRTF-A into the nucleus, demonstrating that VEGF-induced MRTF-A rearrangement is dependent on the actin dynamics between G- and F-actin (Fig. 3.8).

Analysing the F-actin structure, VEGF-stimulated ECs exhibited thin but well-developed stress fibres (Fig. 3.7). This observation is consistent with previous studies. From publications, VEGF rapidly (within 10 min upon stimulation) induces thin stress fibre formation in ECs that at least persist for 3 hrs (van Nieuw Amerongen et al., 2003). This effect is thought to be more sustainable, due to the fact that VEGF modulates endothelial junctions via phosphorylation of VEGFR-2, PLCγ, paxillin, and stress fibres are observed until 45 hrs after VEGF stimulation (Cohen et al., 1999). This may be caused by VEGF-induced RhoA activation, which results in actin polymerization. Interestingly, ECs stimulated with serum lacked stress fibres (rather disappeared) but well-developed lamellipodia were observed (Fig. 3.5 and 3.6). Serum is known as an inducer of actin polymerization, however, its effect on actin appeared different. Probably, serum liberates MRTF-A from a G-actin/MRTF complex in ECs by actin polymerization leading to lamellipodia formation.

Besides VEGF, the factors that regulate accumulation of MRTF-A in nucleus were reported. For example, low calcium (Sebe et al., 2008), Oxidized low-density lipoprotein (Ox-LDL) (Fang et al., 2011), and pathogenic bacterial infection such as EPEC (enteropathogenic E. coli) (Heath et al., 2011)-induced MRTF-A enrichment in the nucleus were reported in various cell lines. In addition, cardiac and skeletal muscle-specific factor STARS also promotes MRTF-A localization in the nucleus (Kuwahara et al., 2005) suggesting sub-cellular localization of MRTF-A can be regulated by various mechanisms.

Regarding MRTF-B localization, MRTF-B was also regulated by VEGF stimulation in cultured mECs. The distribution of MRTF-B was seen near peripheral regions of the nucleus in the cytoplasm. It differed from MRTF-A, which was distributed in the whole cytoplasm. Moreover, the localization of MRTF-B seemed to more correlate with G-actin. Unlike MRTF-A, VEGF could not induce MRTF-B accumulation in the nucleus (data no shown). However, co-stimulation with the actin-polymerizing drug Jasplakinolide, VEGF led to increased MRTF-B localization in the nucleus (Fig. 3.11). This may indicate that MRTF-B is strongly linked to G-actin, thus for the disruption of this complex, actin modulators are required for VEGF-induced MRTF-B activation. Indeed, the affinity study in VSMCs indicates that MRTF-B binds more strongly to G-actin than MRTF-A and disruption of G-actin induced more strongly accumulation of MRTF-B than -A (Nakamura et al., 2010). Moreover, a different regulatory mechanism between MRTF-A and -B was also reported in another study. Upon stimulation of TGF-β, nuclear accumulation of two MRTFs was observed to be different in lens epithelial cells (Gupta et al., 2013). In these cells, MRTF-A accumulation in the nucleus was induced by TGF-β whereas MRTF-B remained in the cytoplasm despite TGF-β treatment. In this issue, TGF-β-induced MRTF-A regulation was blocked after co-treatment with an MMP2/9 inhibitor. These results suggest that MRTF-A and -B are differently regulated in response to growth factors and MMP activation may act somewhere in signalling that is involved in MRTF-A translocation to the nucleus.

To sum up, this study is the first report to show that VEGF controls MRTF in ECs. In addition, this study extends previous findings, the correlation of MRTF with actin dynamics, to endothelial cells.

4.1.3 VEGF controls MRTF-A in ECs via the Rho-ROCK pathway

As outlined above, VEGF-induced sub-cellular movement of MRTF is controlled by stress fibre arrangement. Since the formation of stress fibre is regulated by small GTPase RhoA, involvement of RhoA in this event can be expected. Indeed, many studies from literatures support MRTF-A activation by actin dynamics, notably by RhoA activation. Thus, it was tested whether VEGF activates MRTF-A via RhoA-involved signalling.

In this study, three different Rho inhibitors were used with different inhibitory mechanisms: CT04 is a modified C3 transferase which is inhibitory against RhoA, -B and –C. CCG-1423 is a RhoA pathway inhibitor and ROCK is a selective Rho effector

Rho kinase (ROCK) inhibitor. As a result, inhibition of RhoA by CT04, ECs lacked stress fibres and VEGF-induced as well as serum-induced MRTF-A accumulation in the nucleus was abolished (Fig. 3.14 and 3.15). This is strong evidence that VEGF or serum-induced actin polymerization and consequent translocation of MRTF-A into the nucleus is dependent on RhoA activation. This is coincident with previous studies performed in other cells (Miralles et al., 2003).

Regarding the downstream effector ROCK, both isoforms of ROCK stimulate endothelial stress fibre and the pan-ROCK inhibitor Y-27632 supresses both of ROCK isoforms. In the presence of Y-27632, ECs lacked stress fibres and MRTF-A was seen in the cytoplasm, but near the nucleus (Fig. 3.13). Interestingly, Y-27632 blocked serum- or VEGF-driven MRTF-A accumulation in the nucleus as it was seen via RhoA inhibition by CT04 (Fig. 3.14). Therefore, these two results demonstrate that VEGF as well as serum triggers endothelial MRTF-A enrichment in the nucleus via activation of RhoA and its effector ROCK. However, disruption of MRTF-A activation by ROCK is different from the finding of MRTF-A enrichment in the nucleus by serum in a fibroblast model (Miralles et al., 2003). In this study, serum-induced MRTF-translocation was dependent on Rho-mDia pathway, but not dependent on ROCK. In this model, ROCK inhibition did not alter sub-cellular localization of MRTF-A. mDia and ROCK are representative RhoA effectors and both of them are crucial regulators of RhoA-induced actin cytoskeletal arrangement. However, functions of mDia and ROCK are differently reported. mDia polymerizes actin via nucleation and it especially effects microtubule formation. In contrast, ROCK induces actin polymerization by phosphorylating of LIMK, thereby promoting stress fibres. Interestingly, these two kinases are cell-type specifically regulated (Geneste et al., 2002). In ECs, many studies demonstrate the involvement of ROCK as a RhoA effector rather than mDia suggested that ROCK plays a critical role in ECs as a main downstream effector of RhoA activation.

The third substance that was used as a RhoA inhibitor was CCG-1423. CCG-1423 is designated as a RhoA pathway inhibitor, more exactly RhoA-induced SRF/MRTF transcription inhibitor. This compound was screened as an anti-cancer targeting drug and its inhibitory effect on Rho-induced luciferase assay and proliferation was confirmed in cancer cell lines (Evelyn et al., 2007). The effect of CCG-1423 was just investigated in restricted number of cell types such as prostate carcinoma (Evelyn et al., 2010) and skeletal muscle cells (Jin et al., 2011).

CCG-1423 treatment showed no remarkable effect on actin structure in ECs. Disruption of RhoA pathway typically shows impaired stress fibres. Disruption of RhoA by CT04, endothelial stress fibres and peripheral F-actin disappeared. ROCK also caused stress fibre disruption but lamellipodia were observed. However, cells incubated with CCG-1423 showed no remarkable changes in endothelial stress fibres (Fig. 3.17). Of note, in the presence of CCG-1423, MRTF-A was largely observed in the nucleus in serum- or VEGF-treat cells. This result was different from the Y-27632- or CT04-treated cells. This observation may suggest that CCG-1423 cannot directly inhibit RhoA and it may not be involved in translocation of MRTF. However, according to a previous study, it showed inhibitory effect on RhoA-activated SRF/MRTF transcriptional activation (Evelyn et al., 2007).

In this aspect, one of the possible targets of CCG-1423 is a nuclear protein MICAL-2 (Lundquist et al., 2014). CCG-1423 enhances nuclear MRTF-A by catalyzing depolymerization of nuclear actin. In the nucleus, CCG-1423 directly binds to MICAL, thereby supressing catalytic activity of MICAL-2. Besides, Evelyn and his co-workers suggested possible inhibitory mechanisms of CCG-1423 in their publication (Evelyn et al., 2007). Probably, GGC-1423 may alter MRTF at the posttranslational level such as enhancing sumoylation that causes transcriptional repression. Alternatively, it may supress MRTF-A by inhibiting interaction between MRTF and SRF or may disrupt function of MRTF co-activator. With this study, it turned out that CCG-1423 does not prevent the release of MRTF-A from G-actin/MRTF-A complex or block nuclear accumulation of MRTF-A.

Of note, this study first proved VEGF-driven regulation of MRTF-A and some other studies also supported this observation. For instance, VEGF-induced accumulation of MRTF-A in the nucleus was also proved by quantification (Franco et al., 2013). A study demonstrated that VEGF-induced MRTF-A activity is required during differentiation from mesenchymal stem cells (MSCs) to endothelial (Oswald et al., 2013). ECs are not normally differentiated from MSCs but from endothelial stem cells in bone marrow. Surprisingly, since decades it has been established that MSCs are able to differentiate into ECs in the presence of VEGF. MRTF-A activation is required for this process. Another study indicated that MRTF-A is involved in VEGF-induced differentiation of ECs from MSCs *Cyr61* and CArG box dependently and RhoA signalling is involved in this process (Wang et al., 2013).

In addition, this study also showed that VEGF-activated GTP-bound RhoA was rapidly (within 10 min of VEGF stimulation) detected and decreased at the 60 min of stimu-

lation in investigated mECs (Fig. 3.20). This pattern was similarly described in previous reports (van Nieuw Amerongen et al., 2003).

Recently, it was shown that activation of VEGF recruits some RhoGEF to the VEGFR such as Syx (Synectin-binding RhoA exchange factor) (Ngok and Anastasiadis, 2013). The RhoAGEF Syx and TEM4 (Tumour Endothelial Marker 4) (Ngok et al., 2013) are found at the endothelial junctions and play an important role in VEGF-induced RhoA for endothelial junction maintenance, suggesting that activation of RhoA by VEGF is mediated by specific RhoGEFs. However, which GEFs are involved remains to be elucidated.

Despite the important finding about VEGF/RhoA/ROCK-mediated MRTF-A activation, further studies must address the following questions. First, the cascade upstream of RhoA activation was not analysed, for example the activation of VEGFR-2 and interaction of VEGFR-2 and Rho regulators, especially Rho GEF. Second, it is obvious that VEGF activates VEGFR-2 by phosphorylating of special tyrosine residue. There are many specific sites for phosphorylation, but it has to be explained at which site and which kind of adaptor proteins are responsible for VEGF-driven RhoA activation. Furthermore, for activation of RhoA, Rho-GEF is a prerequisite. It is still not clear which Rho GEFs or GAPs are involved in endothelial SRF/MRTF-A regulation. In addition, this study focused on MRTF-A activation by VEGF-RhoA pathway. However, MRTF-A activity may be influenced by other pathways that can alter actin dynamics such as other small GTPases Rac1, cdc42 or by PI3K pathway, probably.

4.1.4 Knockdown of Srf using siRNAs in ECs

4.1.4.1 Confirmation of siSRF797 efficiency in ECs

RNA interference (RNAi) is a useful tool to monitor roles of the gene by loss-of-function. siRNA-mediated gene depletion is introduced by specific double strand RNA sequence and its mechanism is well elucidated. For SRF siRNA studies, one of the most efficient SRF sequences was adapted from a previous study (Konjer, 2009). As shown in this study, siSRF797 was effectively functioning in mECs. It significantly downregulated SRF both on mRNA and protein level (Fig. 3.20).

It is known that transfection of siRNA can cause off-target effects. This leads to unspecific degradation of mRNAs. To avoid this problem, the concentration of siRNA was strictly controlled to be below 20 nmol. Additionally, mRNA level of OAS1 (2'-5'-

oligoadenylate synthetase 1) and STAT-1 (Signal Transducers and Activators of Transcription) were also investigated to check for possible interferon-(IFN) γ activation. These genes are known to be regulated by interferon-γ, thus they are markers of activation of IFN-γ-mediated unspecific mRNA downregulation. qRT-PCR analysis showed that there was no induction of OAS-1 and STAT-1 level upon siRNA transfection (data not shown). In addition, control genes, *Pak1* or *Cfl1*, which do not contain CArG boxes, were not changed in their expression levels in the experimental set-up. These results strongly suggest that siSRF797-mediated downregulation was effective and selective with no side effects.

4.1.4.2 VEGFR-2 expression upon SRF depletion

To determine endothelial SRF target genes involved in VEGF signalling, VEGFR-2 expression was investigated. In a previous paper, 4 CArG boxes were found in the VEGFR-2 promoter suggesting that VEGFR-2 could be under control of SRF (Franco et al., 2008). However, no matching results on proteins level upon SRF deletion was reported. *In vivo* in the retina, endothelial-specific SRF deletion caused downregulation of VEGFR-2 at the protein level (Weinl et al., 2013). Correspondingly, SRF depletion results in a loss of VEGFR-2 receptor *in vitro* in ECs (Fig. 3.21) suggesting that downregulated VEGFR-2 by SRF could alter SRF-mediated angiogenesis. One possible mechanism to explain this observation can be SRF-mediated hyperactivation of ADAMs, which can result in cleavage of VEGER2. More details about this hypothesis would be discussed in the chapter 4.1.4.7.

4.1.4.3 SRF depletion induced phosphorylation of Cofilin

SRF induces RhoA activation, thereby activating LIMK-1. LIMK-1, in turns, activates SRF via F-actin polymerization (Sotiropoulos et al., 1999). Elevated levels of Cofilin phosphorylation can be interpreted as production of inactive Cofilin caused by inactivation of LIMK. Thus, inhibition of SRF may result in hyperphosphorylation of Cofilin. Indeed, this work proved that SRF depletion upon siSRF797 transfection resulted in enhanced phosphorylation of Cofilin in ECs (Fig. 3.23). This observation was also reported in previous studies as a result of SRF depletion. In a murine model, in the central nervous system (CNS) (Alberti et al., 2005), in neurons (Beck et al., 2012),

and in retinae (Weinl et al., 2013), loss of SRF correlated with hyperphosphorylation of Cofilin.

The mechanism of SRF/MRTF-mediated regulation of phosphorylated Cofilin is well elucidated in neuronal cells (Mokalled et al., 2010). In the neurite outgrowth model, MRTF/SRF activation leads to the expression of *Pctaire 1*, thereby controlling neurite outgrowth. In contrast, MRTF/SRF activates *Cdk5*, which inactivates *Pak1* by phosphorylation under normal conditions. Reduced *Pak1* activity curtails LIMK activity, which induces phosphorylation of Cofilin.

However, since *Pctaire-1* and *Cdk5* are specifically expressed in neurons, this mechanism might not be adaptable to the endothelial model. Probably, in ECs, SRF depletion may result in suppression of RhoA-mediated LIMK activation, thereby increasing phosphorylation of Cofilin.

4.1.4.4 Phosphorylation of MLC upon SRF depletion

Endothelial junctions are primary regulators of vascular permeability by interacting with the actin/myosin filament of the cytoskeleton. Junction proteins bind to actin filaments via adaptor proteins. At the other end of the filament, integrin receptors are bound which sense extracellular signalling (Berridge, 2012). The key regulatory mechanism of disassembly of endothelial junctions is phosphorylation of myosin light chain (MLC) and phosphorylation can be achieved at two residues; Thr18 and Ser19.

These two sites are regulated by different mechanisms. In platelets, phosphorylation of both residues on MLC was observed (Getz et al., 2010). Interestingly, inhibition of ROCK by Y-27632 abolished the phosphorylation at Thr18, but did not alter the phosphorylation at Ser19. This indicates the selective phosphorylation of MLC by different regulators.

In this work, hyperphosphorylation of MLC at Thr18 was detected upon SRF depletion (Fig. 3.24). Additionally, the antibody that specifically recognizes phosphorylation of MLC at Ser19 and the antibody that recognizes both sites of MLC were adapted to this experiment. However, with these antibodies phosphorylation of MLC could not detect. This can be interpreted by either low phosphorylation at Ser19 residue in mECs (or probably, no phosphorylation at this site in mECs) or some pos-

sible problems of the antibody. Nevertheless, depletion of SRF caused significant elevated phosphorylation of MLC at Thr18 in mECs.

Since hyperphosphorylation of MLC can result in increase in the endothelial paracellular permeability, this result could explain why loss of SRF resulted in abnormalities including enhanced vascular permeability.

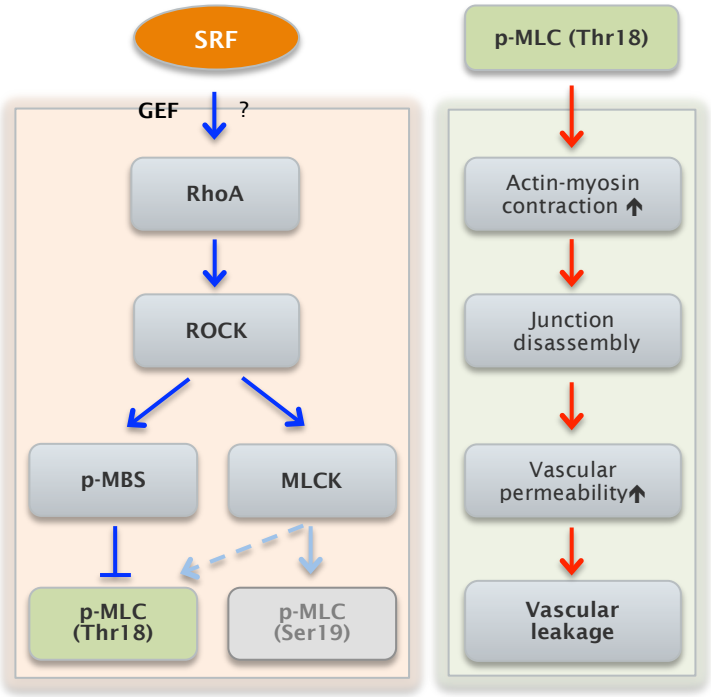

Figure 4.2: Suggested model for SRF-mediated control for vascular integrity

Based on the observation from enhanced phosphorylation upon SRF depletion, the following SRF-mediated vascular integrity model is suggested. SRF activated RhoA by unknown mechanism. The RhoA effector ROCK phosphorylates myosin-binding subunit (MBS) of myosin phosphatase at Thr696 or Thr697, thereby phosphorylated myosin phosphatase is unable to phosphorylate MLC. Upon SRF depletion, RhoA/ROCK level is decreased, thus, MBS cannot be phosphorylated by ROCK leading to inactivation of myosin phosphatase (light blue arrows), thereby phosphorylation of MLC is enhanced. The phenotype that loss of SRF causes junction disassembly and increasing vascular permeability was reported in conditional knockout model of ECs (Franco et al., 2008) (red arrows).

In mouse embryos, endothelial SRF deletion resulted in downregulation of integrin as well as tight and adherent junction proteins (Franco et al., 2008). Elevated phosphorylation of MLC at Thr18 may explain abnormally increased endothelial junction disassembly (Fig. 4.2).

4.1.4.5 Screening of different siMRTF sequences

To understand endothelial targets of MRTF, siMRTFs were screened and their effects on MRTF expression was measured. For depletion of MRTF-A, all screened siRNAs effectively downregulated MRTF-A without alteration of MRTF-B levels (Fig. 3.26). siMRTF-Bs also downregulated MRTF-B, but due to different targets for isoforms, the efficiency was different (Fig. 3.27).

Protein levels of MRTF-A and -B upon siRNA were also analysed (data not shown). However, the specificity of MRTF-A and MRTF-B antibodies must be proven. It was difficult to clarify the specificity of MRTF-A and MRTF-B antibodies because of several reasons. First, there is a high genetic homology between murine MRTF-A and MRTF-B. According to NCBI Blast data, 67% of homology between two genes was elucidated (data not shown). MRTF-A and -B share conserved functional key domains, thereby making it hard to distinguish them from each other. Second, MRTF-A and B can form a heterodimer (Esnault et al., 2014). This mechanism is still poorly understood. Third, the splicing variant isoforms of MRTFs have not been well established.

Nevertheless, the efficiency of siMRTFs was confirmed at least on mRNA level. With these results, selected siMRTFs can be adapted for future work for various purposes.

4.1.4.6 SRF and endothelial proliferation

Proliferation of ECs is also an important feature of angiogenesis to form new vasculature. *In vivo*, proliferation is especially required in stalk ECs to form mature vessels. So far, SRF depletion-induced hyperproliferation *in vitro* ECs has not been reported yet. This study demonstrated that after depletion of SRF, ECs were more proliferative. Although the result was statistically significant, the increase in proliferation of ECs was relatively small. This can be explained with endothelial characteristics such as very low turnover rate (hundreds of days), genetic stability (Félétou, 2011), or their large size.

Previous reports described endothelial hyperproliferation *in vivo* after SRF depletion. This can be explained by loss of SRF target proteins (Holtz and Misra, 2011). A failure of junction protein-mediated-signalling by SRF depletion can result in sustained proliferation due to the loss of integrin signalling. Another study found that VEGF-

induced endothelial proliferation was inhibited upon SRF depletion (Chai et al., 2004). This is caused due to the failure of VEGF-induced IEGs expression.

In other cells, the effect of SRF knockdown on proliferation was cell line specifically observed. In murine embryonic stem cells, SRF depletion showed no effect on proliferation (Schratt et al., 2001). The same result was observed in heart muscle cells (Miano et al., 2004). In contrast, in VSMCs, SRF depletion by shRNA resulted in hyperproliferation with increased c-Jun expression (Kaplan-Albuquerque et al., 2005).

These different observations are controversial and are believed that SRF contributes to cellular proliferation by altering the cell cycle transition of G0 to G1 phase with IEGs expression (Poser et al, 2001). Probably, SRF-mediated cell proliferation is controlled in a cell-type and signalling specific manner.

4.1.4.7 SRF and matrix proteases

Extracellular proteolysis is mediated by membrane-bound or secreted matrix proteases. MMPs, TIMPs, and ADAMs are representative matrix proteases that are implicated in cleavage of the extracellular matrix (ECM), basal membrane, junction proteins, membrane receptors, and their ligands. ECs require this process during angiogenesis to detach from the basal membrane as well as to allow physical path into the ECM (Rundhaug, 2003).

MMPs not only contribute to angiogenesis degrading ECM components, but also promote angiogenesis by releasing ECM-bound growth factors such as bFGF and VEGF. Moreover, fragments of ECM components, which are produced by MMPs, can initiate integrin-mediated signalling. This signalling is involved in endothelial survival and proliferation (Rundhaug, 2003). However, despite the important roles of MMPs, the regulatory mechanisms of MMPs in ECs remain to be investigated.

So far, 23 members of human MMPs are discovered. Among them, some MMP proteins are intensively studied. This study focused on screening of MMPs as potential SRF target genes that are involved in SRF-mediated angiogenesis.

siRNA-mediated depletion of SRF caused different effects on four representative MMPs (Fig. 3.25). qRT-PCR results showed that SRF depletion caused downregulation of MMP9 which was not reported in ECs. In contrast, the level of MMP2 was increased and the levels of MT1-MMP and MMP3 were not significantly changed upon

SRF depletion. A previous study indicated that MMPs can be differently regulated in response to growth factors, for example by VEGF (Heo et al., 2010).

In a previous study, the role of MMP9 was reported as an MRTF-dependent SRF target in megakaryocyte (Gilles et al., 2009). Additionally, this study identified the SRF binding sites on MMP9 promoter and proved binding of SRF to these loci. Many studies demonstrated that MMP9, rather than MMP2, is implicated in angiogenesis, at least in tumour angiogenesis models (Bergers et al., 2000). In mouse, MMP9 level is critical for tumour carcinogenesis that elevated MMP9 expression induced VEGF expression. Due to this fact, urinary MMP9 (uMMP) level is used as an indicator for cancer progression and metastasis (Yan et al., 2001; Mohammed et al., 2013).

The MT1-MMP was selected and investigated in this study due to its known role in ECs. It plays an important role at the leading edge of protrusion of endothelial tip cells in conjunction with $\alpha v\beta 3$ integrin (Friedl and Gilmour, 2009). Additionally, MMP12 level was also investigated but the mRNA level was so low that it was hard to detect. Probably, MMP12 is expressed at very low level in the mECs tester here or generally in all ECs. However, for confirmation, protein levels of each protease and activity assays of proteases, such as gelatin zymography (for MMP2 and -9), have to be performed in future work.

Two investigated MMP inhibitors, TIMP-1 and -2, were significantly downregulated upon SRF depletion. This finding suggests that TIMP-1 and TIMP-2 can be SRF target genes in ECs. Downregulated TIMP activity can result in hyperproteolysis of membrane and ECM proteins since TIMP binds to MMP with 1:1 ratio, thereby inhibiting MMPs activity. Indeed, in many pathological conditions, many studies proved that TIMP level was significantly downregulated (Sharma et al., 2004; Chen et al., 2010; Sun 2010).

The ADAMs family proteins are MMP-related membrane proteases, which regulate various membrane-associated ligands, receptors and junction proteins. Among members of ADAMs, especially, ADAM9, 10, 15, and 17 play an important role in angiogenesis in ECs due to the fact that they shed endothelial junctional proteins and VEGFR (Claesson-Welsh, 2010). Interestingly, in SRF-depleted ECs, overexpression of ADMAMs, namely ADAM15 and 17 were observed (Fig. 3.25) that could cause degradation of VEGFR (Gooz, 2010; Duffy et al., 2011). sVEGF (soluble VEGF) is a 75 kDa that is produced via VEGFR from full-length VEGFR. It is an extracellular sub-unit of VEGFR-2, which is shed and released by ADAM10, 15, or 17 (Jin et al.,

2013). sVEGF binds to VEGFR with high affinity, thereby antagonizing VEGF signalling. According to results of siSRF797, depletion of SRF induced downregulation of VEGFR-2 level and increased expression of ADAM15 and 17. This may lead to degradation of VEGFR-2 that may cause the obstruction of VEGF signalling due to the loss of VEGFR or antagonizing of signalling by sVEGF. In addition, ADAMs alters endothelial behaviour, for example, overexpression of ADAM17 affects endothelial proliferation, pathological vascularization (Duffy et al, 2011).

In this study, the level of TIMP-3 and -4 was not investigated. From the results of other studies, TIMP-3 can inhibit some ADAMs family including ADAM10, 12, and 17 by regulation of TIMP-3 (Murphy, 2011). Therefore, examination of the level of TIMP-3 and -4 is also necessary to understand the biological roles of TIMPs and ADAMs in ECs. To sum up, these data demonstrate that SRF controls membrane proteases such as MMPs, TIMPs, and ADAMs, thereby SRF may contribute to degradation of ECM, adhesion molecules, and membrane receptors.

4.1.5 TSP-1 is an endothelial SRF target gene

Thrombospondin-1 (TSP-1) is one of the first identified natural anti-angiogenic factors. The level of TSP-1 is downregulated in many tumours, where angiogenic activity is highly observed in correlation with p53 (Ren et al., 2006). A recent report suggests that TSP-1 is expressed in ECs and plays an important role in the regulation of dormancy of sprouting neovasculature in the tumour cell niche (Ghajar et al., 2013). In the TSP-1 promoter, serum response elements are detected (Lee and Iruela-Arispe, 2008). This finding demonstrates that TSP-1 could be a target gene of SRF. Indeed, TSP-1 was reported as an inducible gene by serum, but an MRTF-independent SRF target gene in NIH 3T3 cells (Selvaraj and Prywes, 2004). Nevertheless, regulation of TSP-1 by SRF has not been investigated in ECs.

In this study, it was shown that TSP-1 is controlled by SRF. siRNA-mediated downregulation of SRF caused downregulation of TSP-1 level (Fig. 3.29). In addition, ChIP results showed that TSP-1 binds to the SRF promoter either in the absence (data not shown) or in the presence of serum (Fig. 3.30). Serum stimulation triggered binding of TSP-1 to SRF more efficiently (data not shown) suggesting that TSP-1 is under control of SRF and a serum inducible factor in ECs. Moreover, upon downregulation of MRTF-A, TSP-1 level is also downregulated, suggesting that TSP-1 is an MRTF-A dependent SRF target gene in ECs (data not shown).

Recently, it was reported that TSP-1 attenuates angiogenesis by antagonizing VEGF signalling from extracellular matrix, thereby influencing endothelial cell migration, proliferation, survival, and apoptosis (Lawler and Lawler, 2012). This result demonstrates TSP-1 plays important roles in endothelial behaviour by balancing VEGF signalling. Correspondingly, endothelial-specific loss of SRF resulted in downregulation of TSP-1, which leads to pathological neovascularizations in the adult retina (Weinl et al., 2013).

These findings demonstrated that SRF controls pro-angiogenic factors such as VEGF as well as anti-angiogenic factors, like TSP-1 and TIMPs. Therefore, loss of SRF may result in loss of the balance between anti- and pro- angiogenic signalling by altering both pro- and anti-angiogenic functions.

4.1.6 Suggested model of VEGF-induced MRTF/SRF activation in ECs

Taken together, VEGF controls MRTF-A-dependent SRF target genes via activation of RhoA-ROCK-involved actin polymerization (Fig. 4.2).

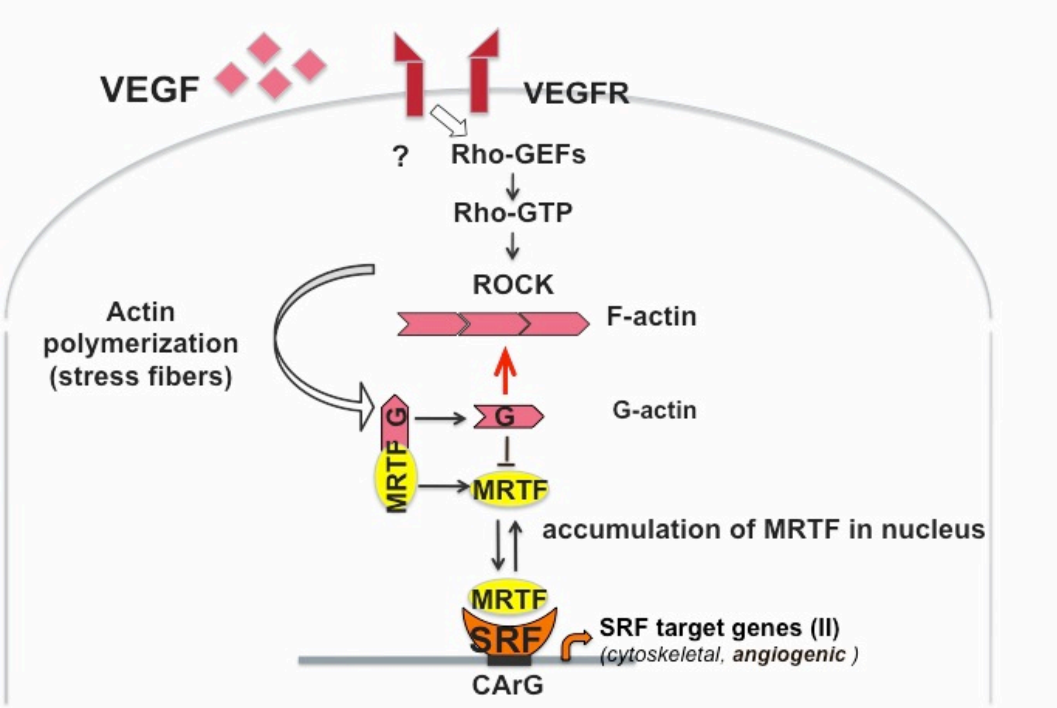

Figure 4.2 Suggested model for VEGF-mediated MRTF/SRF induction in ECs

VEGF-induced activation of MRTF leads to the activation of MRTF-dependent SRF target genes, which is dependent on RhoA/ROCK activation-driven actin polymerization. Figure was designed by Prof. A. Nordheim.

VEGF (mainly by paracrine secretion) activates VEGFR-2 receptors by dimerization. Then, phosphorylation of VEGFR-2 recruits adaptor proteins followed by RhoGEF-mediated RhoA activation. Activated-Rho induces actin polymerization, thereby inducing formation of endothelial stress fibres by ROCK. MRTF, which is bound to G-actin and held back in the cytosol, is liberated from the MRTF/G-actin complex, therefore able to translocate to the nucleus. In the nucleus, MRTF binds to SRF on the CArG of DNA. This, in turn, leads to activation of SRF target genes that are widely involved in angiogenic processes such as VEGFR-2, TSP-1, and metalloproteases (MMPs, TIMPs, ADAMs) as well as phosphorylation of Cofilin and MLC in ECs.

5. SUMMARY

5.1 Summary in English

The transcription factor SRF controls numerous cellular activities in response to extracellular signalling. The SRF cofactor, MRTF (Myocardin Related Transcription Factor) is known for its regulating role in cooperation with SRF. Recent observations (Weinl et al., 2013) indicated that endothelial-specific SRF- as well as MRTF-deleted mice exhibited impaired retinal angiogenesis suggesting that SRF/MRTF signalling is involved in endothelial cell (EC)-mediated angiogenesis. Since the role of transcriptional activation of SRF/MRTF is still poorly understood in ECs, this study focuses on functions of endothelial SRF/MRTF regarding angiogenesis driven by VEGF.

The major finding of this study is the activation of SRF/MRTF by VEGF and its effects on ECs. The experimental results indicated that VEGF induced representative SRF target genes in ECs. VEGF-driven *c-fos* expression was dependent on SRE (SRF binding site, CArG box). Interestingly, the accumulation of MRTF-A in the nucleus induced by serum as well as by VEGF was confirmed in ECs.

Especially, the VEGF-induced accumulation of MRTF in the nucleus was accompanied by the development of stress fibres and associated with an enhancement of the active level of small GTPase RhoA. The accumulation of MRTF-A in the nucleus was also observed after treatment with actin-binding drugs such as cytochalasin D and Jasplakinolide. Of note, VEGF-driven enrichment of MRTF-A in the nucleus was not observed in the presence of either Lat B or RhoA/ROCK inhibitor. These results demonstrate that MRTF-A can be activated by the VEGF-RhoA pathway, which is strictly regulated by actin dynamics.

Using siRNAs studies, SRF target genes involved in angiogenesis were found in ECs. With the well-established siRNA model, it was confirmed that VEGFR-2 is under control of SRF. Anti-angiogenic Protein, TSP-1 (Thrombospondin-1) was also confirmed as an endothelial SRF target gene. In addition, SRF-depleted ECs showed hyperphosphorylation of Cofilin and myosin light chain (MLC). Moreover, SRF altered the expression of matrix metalloproteases. The effect of SRF on MMPs was different in the studied individual MMPs. TIMP-1 and -2 were downregulated as a consequence of

SRF depletion. Interestingly, the level of ADAMs (ADAM15 and ADAM17) was significantly increased upon SRF depletion. This highlights the important roles of SRF regarding control of membrane receptors and junction proteins.

Taken together, SRF/MRTF are activated by actin dynamics-dependent VEGF-RhoA-ROCK and they control various genes involved in angiogenesis in ECs. They are versatile regulators and their functions are important in regulation of ECs.

5.2 Summary in German

Der Transkriptionsfaktor SRF (Serum Response Factor) steuert zahlreiche zelluläre Aktivitäten als Reaktion auf extrazelluläre Signale. Der SRF Cofaktor MRTF (Myocardin Related Transcription Factor) ist für seine regulierende Wirkung in Zusammenarbeit mit SRF bekannt. Beobachtungen (Weinl et al., 2013) an endothelspezifische SRF- sowie MRTF-defizienten Mäusen zeigten defekte retinale Angiogenese, was darauf hindeutet, dass SRF/MRTF Signalgebung in Angiogenese-Prozessen involviert ist. Da die Funktion der Transkriptionsaktivierung von SRF/MRTF in ECs bislang noch weitgehend unbekannt ist, konzentriert sich diese Arbeit auf die Funktionen von SRF/MRTF in Bezug auf VEGF (Vascular Endothelial Growth Factor) und SRF/MRTF gesteuerte Angiogenese.

Das wichtigste Ergebnis dieser Studie ist die durch VEGF-gesteuerte Aktivierung von SRF/MRTF und ihre Auswirkungen auf ECs. Die Versuchsergebnisse zeigten, dass repräsentative SRF Zielgene in ECs durch VEGF induziert wurden. Darüber hinaus konnte eine Abhängigkeit der untersuchten VEGF-gesteuerten c-fos-Expression von SRE (SRF-Bindungsstelle, CArG Box) nachgewiesen werden.

Interessanterweise wurde eine Akkumulation von MRTF-A im Kern nach Stimulation mit Serum oder VEGF in ECs bestätigt. Vor allem, die VEGF-induzierte Akkumulation von MRTF im Kern wurde durch die Entwicklung von Stressfasern und durch die Steigerung des Niveaus der aktiven kleinen GTPase RhoA begleitet. Die Akkumulation von MRTF-A im Kern wurde ebenfalls nach der Behandlung mit Actin-bindenden Wirkstoffen wie Cytochalasin D und Jasplakinolide beobachtet. Bemerkenswert war weiterhin die Blockade der durch VEGF-gesteuerten Anreicherung von MRTF-A im Zellkern bei Zugabe von Lat B bzw. RhoA/ROCK-Inhibitoren. Diese Ergebnisse zeigten, dass MRTF-A durch VEGF-RhoA Kaskade aktiviert werden kann, wobei dieser Prozess streng durch Aktindynamik reguliert wird.

Mit siRNAs Studien wurden an der Angiogenese beteiligten SRF Zielgene in ECs gefunden. Mit dem etablierten siRNA Modell wurde festgestellt, dass VEGFR-2 durch SRF kontrolliert wird. Das anti-angiogene Proteine TSP-1 (Thrombospondin-1) wurde als ein endotheliales SRF Zielgen bestätigt. Zusätzlich verursachte die Depletion des SRF in ECs Hyperphosphorylierung von Cofilin und MLC (Myosin-leichte-Kette). Darüber hinaus veränderte SRF die Matrix-Metalloproteasen MMPs und ADAMs. Die Wirkung von SRF auf MMPs war für die einzelnen untersuchten MMPs unterschiedlich. TIMP-1 und -2 wurden als Folge der SRF Depletion herunterreguliert. Inter-

essanterweise wurde das Niveau der ADAMs (ADAM15 und ADAM17) deutlich nach Depletion von SRF erhöht. Dies zeigte die wichtige Funktion von SRF in Bezug auf Kontrolle der Membranrezeptoren und Junction-Proteine.

Zusammenfassend wurden SRF/MRTF durch aktindynamik-abhängige VEGF-RhoA-ROCK aktiviert und sie steuern verschiedene bei der Angiogenese beteiligte Gene in ECs. Sie sind also vielseitige Regulatoren und ihre Funktionen sind bei der Regulierung von ECs wichtig.

6. ABBREVIATIONS

aa	Amino acid
Actb	Beta-actin
ADAM	A disintegrin and metalloproteinase
APS	Ammonium peroxodisulfate
ATP	Adenosine-tri-phosphate
BSA	Bovine serum albumin
CArG-Box	Cytosin Adenosin rich Guanosin
CCG	Center for Chemical Genomics core facility at the University of Michigan – Ann Arbor
CD31	Cluster of differentiation 31 (PECAM)
cDNA	Complementary DNA
cFOS	FBJ (Finkel, Biskis, and Jinkins) osteosarcoma oncogene
ChIP	Chromatin Immunoprecipitation
Chr	Chromatography
CO_2	Carbon dioxide
C-Terminus	Carboxyl-terminus
Cyto D	Cytochalasin D
DAPI	4',6-diamidino-2-phenylindole
DMEM	Dulbecco's Modified Eagle Medium
DMSO	Dimethyl sulfoxide
DNA	Desoxyribonucleic acid
DNAse	Deoxyribonuclease
dNTP	Deoxy nucleotide-triphosphate
DTT	Dithiothreitol
EBM-2	Endothelial basal medium-2
EBM-2MV	Endothelial cell growth medium -2

EC(s)	Endothelial cell(s)
ECL	Enhanced chemiluminescence
ECM	Extracellular matrix
EDTA	Ethylenediaminetetraacetic acid
EGM-2	Endothelial cell growth medium-2
EGM-2MV	Microvascular endothelial cell growth medium-2
ES cell	Embryonic stem cell
EtOH	Ethanol
F-actin	Filamentous actin
FCS	Fetal calf serum (Fetal bovine serum, FBS)
FLT-1	Fms-related tyrosine kinase 1(VEGF-R1)
G-actin	Globular actin
GAP	GTPase-Activating Protein
GAPDH	Glyceraldehyde 3-phosphate dehydrogenase
GDP	Guanosine diphosphate
GEF	Guanine nucleotide exchange factor
GFP	Green fluorescent protein
GPCRs	G-protein coupled receptors
G protein	Heterotrimeric guanosine nucleotide binding protein
GTP	Guanosine triphosphate
GTPγS	Guanosine 5'-o-(3-thiophosphate), a non-hydrolyzable analog of GTP
H_2O	Dihydrogen monoxide, water
HEK 293	Human Embryonic Kidney 293 cells
HCl	Hydrochloric acid
HNO_3	Nitric acid
hr(s)	Hour(s)
HRMVEC	Human retinal microvascular endothelial cells
HRP	Horseradish peroxidase
HSP 90	Heat shock protein 90

HUVEC	Human umbilical vein endothelial cells
IF	Immunofluorescence
IFN-γ	Interferon-gamma
IgG	Immunoglobulin G
IP	Immunoprecipitation
Jasp	Jasplakinolide
KD	Knock down
kDa	Kilo dalton
KDR	Kinase insert domain receptor (VEGFR-2)
KO	Knock out
L	Liter
Lat B	Latrunculin B
M	Mole
m	Milli (10^{-3})
μ	Micro (10^{-6})
MADS	MCM1, Agamous, Deficiens and SRF
MAPK	Mitogen-activated protein kinase
mDia1	Mammalian Diaphanous-related formin 1
mEC(s)	Mouse endothelial cell(s)
MEM	Minimal Essential Medium
MeOH	Methanol
MKL	Megakaryoblastic leukemia (MRTF)
MMP	Matrix metalloproteinase
mRNA	Messenger RNA
MRTF	Myocardin related transcription factor
MTT	3-(4,5-Dimethylthiazol-2-yl)-2,5-diphenyltetrazoliumbromide
n	Nano (10^{-9})
NaCl	Sodium chloride
NaOH	Sodium hydroxide

N-Terminus	Amino-Terminus
O/N	Overnight
p	Pico (10^{-12})
PAA	Polyacrylamide
PAGE	Polyacrylamide gel electrophoresis
P-Cofilin	Phospho-Cofilin
PECAM-1	Platelet endothelial cell adhesion molecule (CD31)
PFA	Paraformaldehyde
pH	Potentia hydrogenii
P-MLC	Phospho-Myosin Light Chain
PVDF	Polyvinylidene difluoride
qRT-PCR	Quantitative real time polymerase chain reaction
Rho A	Ras homologous A protein
Rho GDI	Rho GDP dissociation inhibitor
RNA	Ribonucleic acid
ROCK	Rho-associated coiled-coil kinase
RPM	Rounds per minute
RT	Room temperature
SDS	Sodium dodecylsulfate
SEM	Standard error of the mean
Ser	Serine
siRNA	Small interfering RNA
SMC	Smooth muscle cell
SRE	Serum Response Element
SRF	Serum Response Factor
TCA	Trichloroacetic acid
TCFs	Ternary complex factors
TBS	Tris buffered saline
TBS-T (TST)	Tris buffered saline with tween 20
TEMED	Tetramethylethylenediamin

Thr	Threonine
Tris	Tris-(hydroxymethyl)-aminomethane
Triton® X-100	Polyethylenglycol-mono-[p-(1,1,3,3-tetramethylbutyl)-phenyl]-ether
TSP-1	Thrombospondin1
UV	Ultraviolet
VEGF	Vascular Endothelial Growth Factor
VEGFR	Vascular Endothelial Growth Factor Receptors
VSMC	Vascular smooth muscle cell
v/v	Volume per volume
WB	Western blot
Y	Tyrosine

7. REFERENCES

Aase, K., von Euler, G., Li, X., Pontén, A., Thorén, P., Cao, R., Cao, Y., Olofsson, B., Gebre-Medhin, S., Pekny, M., Alitalo, K., Betsholtz, C., and Eriksson, U. (2001). Vascular endothelial growth factor-B-deficient mice display an atrial conduction defect. Circulation 104, 358-64.

Achen, M.G., Jeltsch, M., Kukk, E., Mäkinen, T., Vitali, A., Wilks, A.F., Alitalo, K., and Stacker, S.A. (1998). Vascular endothelial growth factor D (VEGF-D) is a for the tyrosine kinases VEGF receptor 2 (Flk1) and VEGF receptor 3 (Flt4). PNAS 95, 548-53.

Adams, R.H. and Alitalo, K. (2007). Molecular regulation of angiogenesis and lymphangiogenesis. Nat Rev Mol Cell Biol 8, 464-78.

Alberti, S., Krause, S.M., Kretz, O., Philippar, U., Lemberger, T., Casanova, E., Wiebel, F.F., Schwarz, H., Frotscher, M., Schütz, G., and Nordheim, A. (2005). Neuronal migration in the murine rostral migratory stream requires serum response factor. PNAS 102, 6148-53.

Allingham, J.S., Klenchin, V.A., and Rayment, I. (2006). Actin-targeting natural products: structures, properties and mechanisms of action. Cell Mol Life Sci 63, 2119-34.

Amano, M., Ito, M., Kimura, K., Fukata, Y., Chihara, K., Nakano, T., Matsuura, Y., and Kaibuchi, K. (1996). Phosphorylation and activation of myosin by Rho-associated kinase (Rho-kinase). J Biol Chem 271, 20246-9.

Amano, M., Mukai, H., Ono, Y., Chihara, K., Matsui, T., Hamajima, Y., Okawa, K., Iwamatsu, A., and Kaibuchi, K. (1996). Identification of a putative target for Rho as the serine-threonine kinase protein kinase N. Science 271, 648-50.

Amano, M., Nakayama, M., and Kaibuchi, K. (2010). Rho-kinase/ROCK: A key regulator of the cytoskeleton and cell polarity. Cytoskeleton (Hoboken) 67, 545-54.

Amin, E., Dubey, B.N., Zhang, S.C., Gremer, L., Dvorsky, R., Moll, ‚J.M., Taha, M.S., Nagel-Steger, L., Piekorz, R.P., Somlyo, A.V., and Ahmadian, M.R. (2013). Rho-kinase: regulation, (dys)function, and inhibition. Biol Chem 394, 1399-410.

Angstenberger, M., Wegener, J.W., Pichler, B.J., Judenhofer, M.S., Feil, S., Alberti, S., Feil, R., and Nordheim, A. (2007). Severe intestinal obstruction on induced smooth muscle-specific ablation of the transcription factor SRF in adult mice. Gastroenterology 133, 1948-59.

Angstenberger, M., (2007). Analyse der in vivo-Funktion des Transkriptionsfaktors SRF in adulten Glattmuskelzellen der Maus. (Dissertation), Faculty of Science, University of Tuebingen.

Arcondéguy, T., Lacazette, E., Millevoi, S., Prats, H., and Touriol, C. (2013). VEGF-A mRNA processing, stability and translation: a paradigm for intricate regulation of gene expression at the post-transcriptional level. Nucleic Acids Res 17, 7997-8010.

Arjonen, A., Kaukonen, R., and Ivaska, J. (2011). Filopodia and adhesion in cancer cell motility. Cell Adh Migr 5, 421-30.

Armstrong, L.C. and Bornstein, P. (2003). Thrombospondins 1 and 2 function as inhibitors of angiogenesis. Matrix Biol 6, 63-71.

Arsenian, S., Weinhold, B., Oelgeschläger, M., Rüther, U., and Nordheim, A. (1998). Serum response factor is essential for mesoderm formation during mouse embryogenesis. EMBO J 17, 6289-99.

Asch, A.S., Silbiger, S., Heimer, E., and Nachman, R.L. (1992). Thrombospondin sequence motif (CSVTCG) is responsible for CD36 binding. Biochem Biophys Res Commun 182, 1208-17.

Augustin, H.G. (2004). Methods in Endothelial Cell Biology, Springer-Verlag Belin Heidelberg New York, p145.

Baarlink, C., Wang, H., and Grosse, R. (2013). Nuclear actin network assembly by formins regulates the SRF coactivator MAL. Science 340, 864-7.

Bae, J.S., Noh, S.J., Kim, K.M., Jang, K.Y., Chung, M.J., Kim, D.G., and Moon, W,S. (2014). Serum response factor induces epithelial to mesenchymal transition with resistance to sorafenib in hepatocellular carcinoma. Int J Oncol 44, 129-36.

Bai, S., Nasser, M.W., Wang, B., Hsu, S.H., Datta, J., Kutay, H., Yadav, A., Nuovo, G., Kumar, P., and Ghoshal, K. (2009). MicroRNA-122 inhibits tumorigenic properties of hepatocellular carcinoma cells and sensitizes these cells to sorafenib. J Biol Chem 284, 32015–27.

Balsalobre, A., Damiola, F., and Schibler, U. (1998). A serum shock induces circadian gene expression in mammalian tissue culture cells. Cell 93, 929-37.

Barnes, B.R., Szelenyi, E.R., Warren, G.L., and Urso, M.L. (2009). Alterations in mRNA and protein levels of metalloproteinases-2, -9, and -14 and tissue inhibitor of metalloproteinase-2 responses to traumatic skeletal muscle injury. Am J Physiol Cell Physiol 297, C1501-8.

Barron, M.R., Belaguli, N.S., Zhang, S.X., Trinh, M., Iyer, D., Merlo, X., Lough, J.W., Parmacek, M.S., Bruneau, B.G., and Schwartz, R.J. (2005). Serum response factor, an

enriched cardiac mesoderm obligatory factor, is a downstream gene target for Tbx genes. J Biol Chem 280, 11816-28.

Bates, D.O. (2010). Vascular endothelial growth factors and vascular permeability, Cardiovasc Res 87, 262-271.

Beckers, C.M., van Hinsbergh, V.W., and van Nieuw Amerongen, G.P. (2010). Driving Rho GTPase activity in endothelial cells regulates barrier integrity. Thromb Haemost. 103, 40-55.

Belaguli, N.S., Zhou, W., Trinh, T.H., Majesky, M.W., and Schwartz, R.J. (1999). Dominant negative murine serum response factor: alternative splicing within the activation domain inhibits transactivation of serum response factor binding targets. Mol Cell Biol 19, 4582-91.

Benedito, R., Roca, C., Sörensen, I., Adams, S., Gossler, A., Fruttiger, M., and Adams, R.H. (2009). The notch ligands Dll4 and Jagged1 have opposing effects on angiogenesis. Cell 137, 1124-35.

Berridge, M.J. (2012). Cell Signalling Biology, Portland Press Limited.

Ergin, B. (2008). FunctionalmoleculargeneticdissectionoftheEtstranscription factors Sap-1 and Elk-1 in immediate-early and neuronal gene expression (Dissertation), Faculty of Science, University of Tuebingen

Bryan, B.A., Dennstedt, E., Mitchell, D.C., Walshe, T.E., Noma, K., Loureiro, R., Saint-Geniez, M., Campaigniac, J.P., Liao, J.K., and D'Amore, P.A. (2010). RhoA/ROCK signaling is essential for multiple aspects of VEGF-mediated angiogenesis. FASEB J 24, 3186-95.

Boulter, E., Garcia-Mata, R., Guilluy, C., Dubash, A., Rossi, G., Brennwald, P.J., and Burridge, K. (2010). Regulation of Rho GTPase crosstalk, degradation and activity by RhoGDI1. Nat Cell Biol 12, 477-83.

Boulter, E., Estrach, S., Garcia-Mata, R., and Féral, C.C. (2012). Off the beaten paths: alternative and crosstalk regulation of Rho GTPases. FASEB J 26, 469-79.

Boureux, A., Vignal, E., Faure, S., and Fort P. (2007). Evolution of the Rho family of ras-like GTPases in eukaryotes. Mol Biol Evol 24, 203-16.

Bourne, H.R., Sanders, D.A., and McCormick, F. (1991). The GTPase superfamily: conserved structure and molecular mechanism. Nature 349, 117-27.

Bubb, M.R., Spector, I., Beyer, B.B., and Fosen, K.M. (2000). Effects of jasplakinolide on the kinetics of actin polymerization. An explanation for certain in vivo observations. J Biol Chem 275, 5163-70.

Buchwalter, G., Gross, C., and Wasylyk, B. (2004). Ets ternary complex transcription factors. Gene 324, 1-14.

Bussmann, J., Lawson, N., Zon, L., and Schulte-Merker, S. (2008). Zebrafish VEGF receptors: a guideline to nomenclature. PLoS Genet 4, e1000064.

Calvino, N. (2003). Connective tissue: Vascular and hematological (blood) support. J Chiropr Med 2, 25-36.

Carmeliet, P., Ferreira, V., Breier, G., Pollefeyt, S., Kieckens, L., Gertsenstein, M., Fahrig, M., Vandenhoeck, A., Harpal, K., Eberhardt, C., Declercq, C., Pawling, J., Moons, L., Collen, D., Risau, W., and Nagy, A. (1996). Abnormal blood vessel development and lethality in embryos lacking a single VEGF allele. Nature 380, 435-9.

Carmeliet, Peter. (2000). Mechanisms of angiogenesis and arteriogenesis. Nat Med 6, 389-95.

Camoretti-Mercado, B., Dulin, N.O., and Solway, J. (2012). SRF function in vascular smooth muscle: when less is more? Circ Res 97, 409-10.

Cébe-Suarez, S., Zehnder-Fjällman, A., and Ballmer-Hofer, K. (2006). The role of VEGF receptors in angiogenesis; complex partnerships. Cell Mol Life Sci 63, 601-15.

Chai, J. and Tarnawski, A.S. (2002). Serum response factor: discovery, biochemistry, biological roles and implications for tissue injury healing. J Physiol Pharmacol 53, 147-57.

Chai, J., Baatar, D., Moon, W., and Tarnawski, A. (2002). Expression of serum response factor in normal rat gastric mucosa. J Physiol Pharmacol 53, 289-94.

Chai, J., Jones, M.K., and Tarnawski, A.S. (2004). Serum response factor is a critical requirement for VEGF signaling in endothelial cells and VEGF-induced angiogenesis. FASEB J, 03-1232fje.

Chai, J. and Modak, M. (2010). Serum response factor: Look into the gut. World J. Gastroenterology 16, 2195-201.

Chavret, C., Houbron, C., Parlakian, A., Giordani, J., Lahoute, C., Bertrand, A., Sotiropoulos, A., Renou, L., Schmitt, A., Melki, J., Li, Z., Daegelen, D., and Tuil, D. (2006). New role for serum response factor in postnatal skeletal muscle growth and regeneration via the interleukin 4 and insulin-like growth factor 1 pathways. Mol Cell Biol 26, 6664–6674.

Cheng, Z., Garvin, D., Paguio, A., Stecha, P., Wood, K., and Fan, F. (2010). Luciferase Reporter Assay System for Deciphering GPCR Pathways. Curr Chem Genomics 21, 84-91

Cherfils, J. and Chardin, P. (1999). GEFs: structural basis for their activation of small GTP-binding proteins. Trends Biochem Sci 24, 306-11.

Cherfils, J. and Zeghouf, M. (2013). Regulation of small GTPases by GEFs, GAPs, and GDIs. Physiol Rev 93, 269-309.

Chhabra, E.S. and Higgs, H.N. (2007). The many faces of actin: matching assembly factors with cellular structures. Nat Cell Biol 9, 1110-21.

Claesson-Welsh, L. (2010). ADAM-mediated shedding, a new flavor in angiogenesis regulation. Arterioscler Thromb Vasc Biol 30, 2087-8.

Clark, K.A. and Graves, B.J. (2014). Dual views of SRF: a genomic exposure. Genes Dev 28, 926-8.

Cohen, A.W., Carbajal, J.M., and Schaeffer, R.C. Jr. (1999). VEGF stimulates tyrosine phosphorylation of beta-catenin and small-pore endothelial barrier dysfunction. Am J Physiol 277, H2038-49.

Cooper, J.A. (1987). Effects of cytochalasin and phalloidin on actin. J Cell Biol 105, 1473-8.

Cooper, S.J., Trinklein, N.D., Nguyen, L., and Myers, R.M. (2007). Serum response factor binding sites differ in three human cell types. Genome Res 17, 136-44.

Cramer, L.P., Siebert, M., and Mitchison, T.J. (1997). Identification of novel graded polarity actin filament bundles in locomoting heart fibroblasts: implications for the generation of motile force. J Cell Biol 136, 1287-305.

Crider, B.J., Risinger, G.M. Jr., Haaksma, C.J., Howard, E.W., and Tomasek, J.J. (2011). Myocardin-related transcription factors A and B are key regulators of TGF-β1-induced fibroblast to myofibroblast differentiation. J Invest Dermatol 131, 2378-85.

Cross, M.J., Dixelius, J., Matsumoto, T., and Claesson-Welsh, L. (2003). VEGF-receptor signal transduction. Trends Biochem Sci 9, 488-94.

Curry, F.R. and Adamson, R.H. (2010). Vascular permeability modulation at the cell, microvessel, or whole organ level: towards closing gaps in our knowledge. Cardiovasc Res 87, 218-29.

Dalton, S. and Treisman, R. (1992). Characterization of SAP-1, a protein recruited by serum response factor to the c-fos serum response element. Cell 68, 597-612.

Dalton, S., Marais, R., Wynne, J., and Treisman, R. (1993). Isolation and characterization of SRF accessory proteins. Philos Trans R Soc Lond B Biol Sci 340, 325-332.

Daly, M.E., Makris, A., Reed, M., and Lewis, C.E. (2003). Hemostatic regulators of tumor angiogenesis: a source of antiangiogenic agents for cancer treatment?. J Natl Cancer Inst 95, 1660-73.

Davis, G.E. and Senger, D.R. (2005). Endothelial extracellular matrix: biosynthesis, remodeling, and functions during vascular morphogenesis and neovessel stabilization. Circ Res 97, 1093-107.

De Gregorio, L., Vincenti, V., Breier, G., Damert, A., Dragani, T.A., and Persico, M.G. (1997). Genetic mapping of the vascular endothelial growth factor (Vegf) gene to mouse chromosome 17. Mamm Genome 8, 451-2.

de Vries, C., Escobedo, J.A., Ueno, H., Houck, K., Ferrara, N., and Williams, L.T. (1992). The FMS-like tyrosine kinase, a receptor for vascular endothelial growth factor. Science 255, 989-991.

Dejana, E., Corada, M., and Lampugnani, M.G. (1995). Endothelial cell-to-cell junctions. FASEB J 9, 910-8.

DerMardirossian, C. and Bokoch, G.M. (2005). GDIs: central regulatory molecules in Rho GTPase activation. Trends Cell Biol 15, 356-63.

Descot, A., Hoffmann, R., Shaposhnikov, D., Reschke, M., Ullrich, A., and Posern, G. (2009). Negative regulation of the EGFR-MAPK cascade by actin-MAL-mediated Mig6/Errfi-1 induction. Mol Cell 35, 291-304.

Dominguez, R. and Holmes, K.C. (2011). Actin structure and function. Annu Rev Biophys 40, 169-86.

Donmez, G., Sullu, Y., Baris, S., Yildiz, L., Aydin, O., Karagoz, F., and Kandemir, B. (2009). Vascular endothelial growth factor (VEGF), matrix metalloproteinase-9 (MMP-9), and thrombospondin-1 (TSP-1) expression in urothelial carcinomas. Pathol Res Pract 205, 854-7.

Donners, M.M., Wolfs, I.M., Olieslagers, S., Mohammadi-Motahhari, Z., Tchaikovski, V., Heeneman, S., van Buul, J.D., Caolo, V., Molin, D.G., Post, M.J., and Waltenberger, J. (2010). A disintegrin and metalloprotease 10 is a novel mediator of vascular endothelial growth factor-induced endothelial cell function in angiogenesis and is associated with atherosclerosis. Arterioscler Thromb Vasc Biol 30, 2188-95.

Dransart, E., Olofsson, B., and Cherfils, J. (2005). RhoGDIs revisited: novel roles in Rho regulation. Traffic 6, 957-66.

Duffy, M.J., McKiernan, E., O'Donovan, N., and McGowan, P.M. (2009). Role of ADAMs in cancer formation and progression. Clin Cancer Res 15, 1140-4.

Duffy, M.J., Mullooly, M., O'Donovan, N., Sukor, S., Crown, J., Pierce, A., and McGowan, P.M. (2011). The ADAMs family of proteases: new biomarkers and therapeutic targets for cancer? Clin Proteomics 8:9.

Ellenbroek, S.I.J. and Collard, J.G. (2007). Rho GTPases: functions and association with cancer. Clin Exp Metastasis 24, 657-72.

Esnault, C., Stewart, A., Gualdrini, F., East, P., Horswell, S., Matthews, N., and Treisman, R. (2014). Rho-actin signaling to the MRTF coactivators dominates the immediate transcriptional response to serum in fibroblasts. Genes Dev 28, 943-58.

Evelyn, C.R., Wade, S.M., Wang, Q., Wu, M., Iñiguez-Lluhí, J.A., Merajver, S.D., and Neubig, R.R. (2007). CCG-1423: a small-molecule inhibitor of RhoA transcriptional signaling. Mol Cancer Ther 6, 2249-60.

Evelyn, C.R., Bell, J.L., Ryu, J.G., Wade, S.M., Kocab, A., Harzdorf, N.L., Showalter, H.D., Neubig, R.R., and Larsen, S.D. (2010). Design, synthesis and prostate cancer cell-based studies of analogs of the Rho/MKL1 transcriptional pathway inhibitor, CCG-1423. Bioorg Med Chem Lett 20, 665-72.

Fang, F., Yang, Y., Yuan, Z., Gao, Y., Zhou, J., Chen, Q., and Xu, Y. (2011). Myocardin-related transcription factor A mediates OxLDL-induced endothelial injury. Circ Res 108, 797-807.

Félétou, M. (2011). The Endothelium, Part 1: Multiple Functions of the Endothelial Cells—Focus on Endothelium-Derived Vasoactive Mediators, Morgan & Claypool Life Sciences

Ferrara, N. and Henzel, W.J. (1986). A highly conserved vascular permeability factor secreted by a variety of human and rodent tumor cell lines. Cancer Res 46, 5629-32.

Fleige, A., Alberti, S., Grobe, L., Frischmann, U., Geffers, R., Müller, W., Nordheim, A., and Schippers, A. (2007). Serum response factor contributes selectively to lymphocyte development. J Biol Chem 282, 24320–8.

Fong, G.H., Rossant, J., Gertsenstein, M., and Breitman, M.L. (1995) Role of the Flt-1 receptor tyrosine kinase in regulating the assembly of vascular endothelium. Nature 376, 66–70.

Fong, G.H., Klingensmith, J., Wood, C.R., Rossant, J., and Breitman, M.L. (1996). Regulation of flt-1 expression during mouse embryogene- sis suggests a role in the establishment of vascular endothelium. Dev Dyn 207, 1–10.

Fong, G.H., Zhang, L., Bryce, D.M., and Peng, J. (1999). Increased hemangioblast commitment, not vascular disorganization, is the primary defect in flt-1 knock-out mice. Development 126, 3015–25.

Fox, S.I. (2010). Human physiology 12th edition, McGraw-Hill.

Franco, C.A., Mericskay M., Parlakian A., Gary-Bobo G., Gao-Li J., Paulin D., Gustafsson E., and Li, Z. (2008). Serum response factor is required for sprouting angiogenesis and vascular integrity. Dev Cell 15, 448-61.

Franco, C.A. and Li, Z. (2009). SRF in angiogenesis: branching the vascular system. Cell Adh Migr 3, 264-7.

Franco, C.A., Blanc, J., Parlakian, A., Blanco, R., Aspalter, I.M., Kazakova, N., Diguet, N., Mylonas, E., Gao-Li, J., Vaahtokari, A., Penard-Lacronique, V., Fruttiger, M., Rosewell, I., Mericskay, M., Gerhardt, H., and Li, Z. (2013). SRF selectively controls tip cell invasive behavior in angiogenesis. Development 140, 2321-33.

Freeman, J.L., Abo, A., and Lambeth, J.D. (1996). Rac "insert region" is a novel effector region that is implicated in the activation of NADPH oxidase, but not PAK65. J Biol Chem 271, 19794-801.

Franzke, C.W., Bruckner-Tuderman, L., and Blobel, C.P. (2009). Shedding of collagen XVII/BP180 in skin depends on both ADAM10 and ADAM9. J Biol Chem 284, 23386-96.

Friedl, P. and Gilmour, D. (2009). Collective cell migration in morphogenesis, regeneration and cancer. Nat Rev Mol Cell Biol 10, 445-57.

Garcia-Mata, R., Boulter, E., and Burridge, K. (2012). The 'invisible hand': regulation of RHO GTPases by RHOGDIs. Nat Rev Mol Cell Biol 12, 493-504.

Geneste, O., Copeland, J.W., and Treisman, R. (2002). LIM kinase and Diaphanous cooperate to regulate serum response factor and actin dynamics. J Cell Biol 157, 831-8.

Gerber, A., Esnault, C., Aubert, G., Treisman, R., Pralong, F., and Schibler, U. (2013). Blood-borne circadian signal stimulates daily oscillations in actin dynamics and SRF activity. Cell 152, 492-503.

Getz, T.M., Dangelmaier, C.A., Jin, J., Daniel, J.L., and Kunapuli, S.P. (2010). Differential phosphorylation of myosin light chain (Thr)18 and (Ser)19 and functional implications in platelets. J Thromb Haemost 8, 2283-93.

Ghajar, C.M., Peinado, H., Mori, H., Matei, I.R., Evason, K.J., Brazier, H., Almeida, D., Koller, A., Hajjar, K.A., Stainier, D.Y., Chen, E.I., Lyden, D., and Bissell, M.J. (2013). The perivascular niche regulates breast tumour dormancy. Nat Cell Biol 15, 807-17.

Gilles, L., Bluteau, D., Boukour, S., Chang, Y., Zhang, Y., Robert, T., Dessen, P., Debili, N., Bernard, O.A., Vainchenker, W., and Raslova, H. (2009). MAL/SRF complex is involved in platelet formation and megakaryocyte migration by regulating MYL9 (MLC2) and MMP9. Blood 114, 4221-32.

Gineitis, D. and Treisman, R. (2001). Differential usage of signal transduction pathways defines two types of serum response factor target gene. J Biol Chem 276, 24531-9.

Giovane, A., Pintzas, A., Maira, S.M., Sobieszczuk, P., and Wasylyk, B. (1994). Net, a new ets transcription factor that is activated by Ras. Genes & development 8, 1502-1513.

Giovane, A., Sobieszczuk, P., Ayadi, A., Maira, S.M., and Wasylyk, B. (1997). Net-b, a Ras-insensitive factor that forms ternary complexes with serum response factor on the serum response element of the fos promoter. Mol Cell Biol 17, 5667-78.

Gooz, M. (2010). ADAM-17: the enzyme that does it all. Crit Rev Biochem Mol Biol 45, 146-69.

Greenberg, M.E. and Ziff, E.B. (1984). Stimulation of 3T3 cells induces transcription of the c-fos proto-oncogene. Nature 311, 433-8.

Groblewska, M., Siewko, M., Mroczko, B., and Szmitkowski, M. (2012). The role of matrix metalloproteinases (MMPs) and their inhibitors (TIMPs) in the development of esophageal cancer. Folia Histochem Cytobiol 50, 12-19.

Guettler, S., Vartiainen, M.K., Miralles, F., Larijani, B., and Treisman, R. (2008). RPEL Motifs Link the Serum Response Factor Cofactor MAL but Not Myocardin to Rho Signaling via Actin Binding. Mol Cell Biol 28, 732-42.

Gupta, M., Korol, A., and West-Mays., J.A. (2013). Nuclear translocation of myocardin-related transcription factor-A during transforming growth factor beta-induced epithelial to mesenchymal transition of lens epithelial cells. Mol Vis 19, 1017-28.

Gupton, S.L. and Gertler, F.B. (2007). Filopodia: the fingers that do the walking. Sci STKE 2007, re5.

Hagberg, C.E., Falkevall, A., Wang, X., Larsson, E., Huusko, J., Nilsson, I., van Meeteren, L.A., Samen, E., Lu, L., Vanwildemeersch, M., Klar, J., Genove, G., Pietras, K., Stone-Elander, S., Claesson-Welsh, L., Ylä-Herttuala, S., Lindahl, P., and Eriksson, U. (2010). Vascular endothelial growth factor B controls endothelial fatty acid uptake. Nature 464, 917-21.

Hakoshima, T., Shimizu, T, and Maesaki, R. (2003). Structural basis of the Rho GTPase signaling. J Biochem 134, 327-31.

Halene, S., Gao, Y., Hahn, K., Massaro, S., Italiano, J.E. Jr., Schulz, V., Lin, S., Kupfer, G.M., and Krause, D.S. (2010). Serum response factor is an essential transcription factor in megakaryocytic maturation. Blood 116, 1942-50.

Heasman, S.J. and Ridley, A.J. (2008). Mammalian Rho GTPases: new insights into their functions from in vivo studies. Nat Rev Mol Cell Biol 9, 690-701.

Heath, R.J.W., Leong, J.M., and Xavier, R.W. (2011). Bacterial and Host Determinants of MAL Activation upon EPEC Infection: The Roles of Tir, ABRA, and FLRT3. PLoS Pathog 7, e1001332.

Heo, S.H., Choi, Y.J., Ryoo, H.M., and Cho, J.Y. (2010). Expression profiling of ETS and MMP factors in VEGF-activated endothelial cells: role of MMP-10 in VEGF-induced angiogenesis. J Cell Physiol 224, 734-42.

Hill, C.S., Wynne, J., and Treisman, R. (1994). Serum-regulated transcription by serum response factor (SRF): a novel role for the DNA binding domain. The EMBO J 13, 5421-32.

Hill, C.S., Wynne., J., and Treisman, R. (1995). The Rho family GTPases RhoA, Rac1, and CDC42Hs regulate transcriptional activation by SRF. Cell 81, 1159-70.

Hipskind, R.A., Rao, V.N., Mueller, C.G., Reddy, E.S., and Nordheim, A. (1991). Ets-related protein Elk-1 is homologous to the c-fos regulatory factor p62TCF. Nature 354, 531-534.

Hitchcock, S.E. (1980). Actin deoxyroboncuclease I interaction. Depolymerization and nucleotide exchange. J Biol Chem 255, 5668-73.

Hoeben, A., Landuyt, B., Highley, M.S., Wildiers, H., Van Oosterom, A.T., and De Bruijn ,E.A. (2004). Vascular endothelial growth factor and angiogenesis. Pharmacol Rev 56, 549-80.

Holtz, M.L. and Misra, R.P. (2008). Endothelial-specific ablation of serum response factor causes hemorrhaging, yolk sac vascular failure, and embryonic lethality. BMC Dev Biol 11:18.

Hotulainen, P. and Lappalainen, P. (2006). Stress fibers are generated by two distinct actin assembly mechanisms in motile cells. J Cell Biol 173, 383-94.

Houston, M.C. (2000). The role of vascular biology, nutrition and nutraceuticals in the prevention and treatment of hypertension. JANA 8, 5–71.

Huet, A., Parlakian, A., Arnaud, M.C., Glandières, J.M,, Valat, P., Fermandjian, S., Paulin, D., Alpert, B., and Zentz, C. (2005). Mechanism of binding of serum response factor to serum response element. FEBS J 272, 3105-19.

Ilan, N. and Madri, J.A. (2003). PECAM-1: old friend, new partners. Curr Opin Cell Biol 15, 515-24.

Iruela-Arispe, M.L., Luque, A., and Lee, N. (2004). Thrombospondin modules and angiogenesis. Int J Biochem Cell Biol 36, 1070-8.

Ishizaki, T., Uehata, M., Tamechika, I., Keel, J., Nonomura, K., Maekawa, M., and Narumiya, S. (2000). Pharmacological properties of Y-27632, a specific inhibitor of rho-associated kinases. Mol Pharmacol 57, 976-83.

Jackson, C.J., and Nguyen, M. (1997). Human microvascular endothelial cells differ from macrovascular endothelial cells in their expression of matrix metalloproteinases. Int J Biochem Cell Biol 10, 1167-77.

Jackson, M., Baird, J.W., Cambray, N., Ansell, J.D., Forrester, L.M., and Graham, G.J. (2002). Cloning and characterization of Ehox, a novel homeobox gene essential for embryonic stem cell differentiation. J Biol Chem 277, 38683-92.

Jiménez, B., Volpert, O.V., Crawford, S.E., Febbraio, M., Silverstein, R.L., and Bouck, N. (2000). Signals leading to apoptosis-dependent inhibition of neovascularization by thrombospondin-1. Nat Med 6, 41-8.

Jin, W., Goldfine, A.B., Boes, T., Henry, R.R., Ciaraldi, T.P., Kim, E.Y., Emecan, M., Fitzpatrick, C., Sen, A., Shah, A., Mun, E., Vokes, V., Schroeder, J., Tatro, E., Jimenez-Chillaron, J. and Patti, M,E. (2011). Increased SRF transcriptional activity in human and mouse skeletal muscle is a signature of insulin resistance. J Clin Invest 121, 918-29.

Jin, Y,, Liu, Y., Lin, Q., Li, J., Druso, J.E., Antonyak, M.A., Meininger, C.J., Zhang, S.L., Dostal, D.E., Guan, J.L., Cerione, R.A., and Peng, X. (2013). Deletion of Cdc42 enhances ADAM17-mediated vascular endothelial growth factor receptor 2 shedding and impairs vascular endothelial cell survival and vasculogenesis. Mol Cell Biol 33, 4181-97.

Kakudo, N., Kushida, S., Suzuki, K., Matsumoto, N., and Kusumoto, K. (2011). Effect of C3 transferase on human adipose-derived stem cells. Hum Cell 24, 165-9.

Kalluri, R. (2003). Basement membranes: structure, assembly and role in tumour angiogenesis. Nat Rev Cancer 3, 422-33.

Kameritsch, P., Khandoga, N., Pohl, U., and Pogoda, K. (2013). Gap junctional communication promotes apoptosis in a connexin-type-dependent manner. Cell Death Dis 4:e584.

Kaneko-Kawano, T., Takasu, F., Naoki, H., Sakumura, Y., Ishii, S., Ueba, T., Eiyama, A., Okada, A., Kawano, Y., and Suzuki, K. (2012). Dynamic Regulation of Myosin Light Chain Phosphorylation by Rho-kinase. PLoS ONE 7, e39269.

Kaplan-Albuquerque, N., Van Putten, V., Weiser-Evans, M.C., and Nemenoff, R.A. (2005). Depletion of Serum Response Factor by RNA Interference Mimics the Mitogenic Effects of Platelet Derived Growth Factor-BB in Vascular Smooth Muscle Cells. Circ Res 97, 427-33.

Karkkainen, M.J., Haiko, P., Sainio, K., Partanen, J., Taipale, J., Petrova, T.V., Jeltsch, M., Jackson, D.G., Talikka, M., Rauvala, H., Betsholtz, C., and Alitalo, K. (2004). Vascular endothelial growth factor C is required for sprouting of the first lymphatic vessels from embryonic veins. Nat Immunol 5, 74-80.

Katoh, K., Kano, Y., and Noda, Y. Rho-associated kinase-dependent contraction of stress fibres and the organization of focal adhesions. J R Soc Interface 8, 305-11.

Keller, T.T., Mairuhu, A.T., de Kruif, M.D., Klein, S.K., Gerdes, V.E., ten Cate, H., Brandjes, D.P., Levi, M., and van Gorp, E.C. (2003). Infections and endothelial cells. Cardiovasc Res 60, 40-8.

Kemp, P.R. and Metcalfe, J.C. (2000). Four isoforms of serum response factor that increase or inhibit smooth-muscle-specific promoter activity. Biochem J 345, 445-51.

Kessenbrock, K., Plaks, V., and Werb, Z. (2010). Cell 141, 52-67.

Kim, K.R., Bae, J.S., Choi, H.N., Park, H.S., Jang, K.Y., Chung, M.J., and Moon, W.S. (2011). The role of serum response factor in hepatocellular carcinoma: an association with matrix metalloproteinase. Oncol Rep 26, 1567-72.

Kim, M.J., Kim, S., Kim, Y., Jin, E.J., and Sonn, J.K. (2012). Inhibition of RhoA but not ROCK induces chondrogenesis of chick limb mesenchymal cells. Biochem Biophys Res Commun 418, 500-5.

Kim, Y., Imdad, R.Y., Stephenson, A.H., Sprague, R.S., and Lonigro, A.J. (1998). Vascular endothelial growth factor mRNA in pericytes is upregulated by phorbol myristate acetate. Hypertension 31, 511-5.

Kimura, K., Ito, M., Amano, M., Chihara, K., Fukata, Y., Nakafuku, M., Yamamori, B., Feng, J., Nakano, T., Okawa, K., Iwamatsu, A., and Kaibuchi, K. (1996). Regulation of myosin phosphatase by Rho and Rho-associated kinase (Rho-kinase). Science 273, 245-8.

Kiran, M.S., Viji, R.I., Kumar, S.V., Prabhakaran, A.A., and Sudhakaran, P.R. (2011). Changes in expression of VE-cadherin and MMPs in endothelial cells: Implications for angiogenesis. Vasc Cell 3:6.

Knöll, B. and Nordheim, A. (2009). Functional versatility of transcription factors in the nervous system: the SRF paradigm. Trends Neurosci 32, 432-42.

Knöll, B. (2010). Actin-mediated gene expression in neurons: the MRTF-SRF connection. Biol Chem 391, 591-7.

Knöll, B. (2011). Serum response factor mediated gene activity in physiological and pathological processes of neuronal motility. Front Mol Neurosci 4:49.

Koch, S., Tugues, S., Li, X., Gualandi, L., and Claesson-Welsh, L. (2011). Signal transduction by vascular endothelial growth factor receptors. Biochem J 437, 169-83.

Koegel, H., von Tobel, L., Schäfer, M., Alberti, S., Kremmer, E., Mauch, C., Hohl, D., Wang, X.J., Beer, H.D., Bloch, W., Nordheim, A., and Werner, S. (2009). Loss of serum response factor in keratinocytes results in hyperproliferative skin disease in mice. J Clin Invest 119, 899-910.

Konjer, N. (2009). The role of the transcription factor SRF in the inhibition of senescence in human and porcine smooth muscle cells. (Dissertation), Faculty of Science, University of Tuebingen.

Kuwahara, K., Barrientos, T., Pipes, G.C., Li, S., and Olson, E.N. (2005). Muscle-specific signaling mechanism that links actin dynamics to serum response factor. Mol Cell Biol 25, 3173-81.

Kwon, C.Y., Kim, K.R., Choi, H.N., Chung, M.J., Noh, S.J., Kim, D.G., Kang, M.J., Lee, D.G., and Moon, W.S. (2010). The role of serum response factor in hepatocellular carcinoma: implications for disease progression. Int J Oncol 37, 837-44.

Laemmli, U.K. (1970). Cleavage of Structural Proteins during the Assembly of the Head of Bacteriophage T4, Nature 227, 680-85.

Lahoute, C., Sotiropoulos, A., Favier, M., Guillet-Deniau, I., Charvet, C., Ferry, A., Butler-Browne, G., Metzger, D., Tuil, D., and Daegelen, D. (2008). Premature aging in skeletal muscle lacking serum response factor. PLoS One 3, e3910.

Lambrechts, A., Van Troys, M., and Ampe, C. (2004). The actin cytoskeleton in normal and pathological cell motility. Int J Biochem Cell Biol 36, 1890-909.

Latasa, M.U., Couton, D., Charvet, C., Lafanechère, A., Guidotti, J.E., Li, Z., Tuil, D., Daegelen, D., Mitchell, C., and Gilgenkrantz, H. (2007). Delayed liver regeneration in mice lacking liver serum response factor. Am J Physiol Gastrointest Liver Physiol 292, G996–G1001.

Lawler, J.W., Slayter, H.S., and Coligan, J.E. (1978). Isolation and characterization of a high molecular weight glycoprotein from human blood platelets. J Biol Chem 253, 8609–16.

Lawler, J. (2002). Thrombospondin-1 as an endogenous inhibitor of angiogenesis and tumor growth. J Cell Mol Med 6, 1-12.

Lawler, P.R. and Lawler, J. (2012). Molecular basis for the regulation of angiogenesis by thrombospondin-1 and -2. Cold Spring Harb Perspect Med 2:a006627.

Lee, N.V. and Iruela-Arispe, M.L. (2008). Thrombospondins and Angiogenesis. Tumor Angiogenesis, Springer Berlin Heidelberg, pp 233-45

Lee, S., Chen, T.T., Barber, C.L., Jordan, M.C., Murdock, J., Desai, S., Ferrara, N., Nagy, A., Roos, K.P., and Iruela-Arispe, M.L. (2007). Autocrine VEGF signaling is required for vascular homeostasis, Cell 24, 691-703.

Leitner, L., Shaposhnikov, D., Descot, A., Hoffmann, R., and Posern, G. (2010). Epithelial Protein Lost in Neoplasm alpha (Eplin-alpha) is transcriptionally regulated by G-actin and MAL/MRTF coactivators. Mol Cancer 9:60.

Li, J., Zhu, X., Chen, M., Cheng, L., Zhou, D., Lu, M.M., Du, K., Epstein, J.A., and Parmacek, M.S. (2005). Myocardin-related transcription factor B is required in cardiac neural crest for smooth muscle differentiation and cardiovascular development. PNAS 102, 8916-21.

Li, J., Bowens, N., Cheng, L., Zhu, X., Chen, M., Hannenhalli, S., Cappola, T.P., and Parmacek, M.S. (2012). Myocardin-like protein 2 regulates TGFβ signaling in embryonic stem cells and the developing vasculature. Development 139, 3531-42.

Li, S., Czubryt, M.P., McAnally, J., Bassel-Duby, R., Richardson, J.A., Wiebel, F.F., Nordheim, A., and Olson, E.N. (2005). Requirement for serum response factor for skeletal muscle growth and maturation revealed by tissue-specific gene deletion in mice. PNAS 102, 1082-7.

Li, S., Chang, S., Qi, X., Richardson, J.A., and Olson, E.N. (2006). Requirement of a Myocardin-Related Transcription Factor for Development of Mammary Myoepithelial Cells. Mol Cell Biol 26, 5797–808.

Li, S., Czubryt, M.P., McAnally, J., Bassel-Duby, R., Richardson, J.A., Wiebel, F.F., Nordheim, A., and Olson, E.N. (2005). Requirement for serum response factor for skeletal muscle growth and maturation revealed by tissue-specific gene deletion in mice. PNAS 102, 1082-7.

Li, X., Tjwa, M., Van, Hove., Enholm, B., Neven, E., Paavonen, K., Jeltsch, M., Juan, T.D., Sievers, R.E., Chorianopoulos, E., Wada, H., Vanwildemeersch, M., Noel, A., Foidart, J.M., Springer, M.L., von Degenfeld, G., Dewerchin, M., Blau, H.M., Alitalo, K., Eriksson, U., Carmeliet, P., and Moons, L. (2008). Reevaluation of the role of VEGF-B suggests a restricted role in the revascularization of the ischemic myocardium. Arterioscler Thromb Vasc Biol 28, 1614-20.

Li, X. (2010). VEGF-B: a thing of beauty, Cell Research 20: 741–744.

Liu, Y., Shepherd, E.G., and Nelin, L.D. (2007). MAPK phosphatases--regulating the immune response. Nat Rev Immunol 7, 202-12.

Lundquist, M.R., Storaska, A.J., Liu, T.C., Larsen, S.D., Evans, T., Neubig, R.R., and Jaffrey, S.R.. (2014). Redox modification of nuclear actin by MICAL-2 regulates SRF signaling. Cell 156, 563-76.

Lutz, R., Sakai, T., and Chiquet, M. (2010). Pericellular fibronectin is required for RhoA-dependent responses to cyclic strain in fibroblasts. J Cell Sci 123, 1511-21.

Ma, Z., Morris, S.W., Valentine, V., Li, M., Herbrick, J.A., Cui ,X., Bouman, D., Li, Y., Mehta, P.K., Nizetic, D., Kaneko, Y., Chan, G.C., Chan, L.C., Squire, J., Scherer, S.W., and Hitzler, J.K. (2001). Fusion of two novel genes, RBM15 and MKL1, in the t(1;22)(p13;q13) of acute megakaryoblastic leukemia. Nat Genet 28, 220-1.

Madaule, P. and Axel R. (1985). Cell 41, 31-40.

Maier, S., Lutz, R., Gelman, L., Sarasa-Renedo, A., Schenk, S., Grashoff, C., and Chiquet, M. (2008). Tenascin-C induction by cyclic strain requires integrin-linked kinase. Biochim Biophys Acta 1783, 1150-62.

Marinissen, M.J. and Gutkind, J.S. (2005). Scaffold proteins dictate Rho GTPase-signaling specificity. Trends Biochem Sci 30, 423-6.

McGee, K.M., Vartiainen, M.K., Khaw, P.T., Treisman, R., and Bailly, M. (2011). Nuclear transport of the serum response factor coactivator MRTF-A is downregulated at tensional homeostasis. EMBO Rep 12, 963-70.

Medjkane, S., Perez-Sanchez, C., Gaggioli, C., Sahai, E., and Treisman, R. (2009). Myocardin-related transcription factors and SRF are required for cytoskeletal dynamics and experimental metastasis. Nat Cell Biol 11, 257-68.

Miano, J.M. (2003). Serum response factor: toggling between disparate programs of gene expression. J Mol Cell Cardiol 35, 577-93.

Miano, J.M., Ramanan, N., Georger, M.A., de Mesy Bentley, K.L., Emerson, R.L., Balza, R.O. Jr, Xiao, Q., Weiler, H., Ginty, D.D., and Misra, R.P. (2004). Restricted inactivation of serum response factor to the cardiovascular system. Proc Natl Acad Sci U S A 101, 17132-7.

Miano, J.M., Long, X., and Fujiwara, K. (2007). Serum response factor: master regulator of the actin cytoskeleton and contractile apparatus. Am J Physiol Cell Physiol 292, C70–C81.

Miano, J.M. (2010). Role of serum response factor in the pathogenesis of disease. Lab Invest 90, 1274-84.

Michiels, C. (2003). Endothelial cell functions. J Cell Physiol 196, 430-3.

Millauer, B., Wizigmann-Voos, S., Schnurch, H., Martinez, R., Moller, N.P.H., Risau, W., and Ullrich, A. (1993). High affinity VEGF binding and developmental expression suggest FLK-1 as a major regulator of vasculogenesis and angiogenesis. Cell 72, 835-846.

Minami, T., Kuwahara, K., Nakagawa, Y., Takaoka, M., Kinoshita, H., Nakao, K., Kuwabara, Y., Yamada, Y., Yamada, C., Shibata, J., Usami, S., Yasuno, S., Nishikimi, T., Ueshima, K., Sata, M., Nakano, H., Seno, T., Kawahito, Y., Sobue, K., Kimura, A., Nagai, R., and Nakao, K. (2012). Reciprocal expression of MRTF-A and myocardin is crucial for pathological vascular remodelling in mice. EMBO J 31, 4428-40.

Minty, A. and Kedes, L. (1986). Upstream regions of the human cardiac actin gene that modulate its transcription in muscle cells: presence of an evolutionarily conserved repeated motif. Mol Cell Biol 6, 2125-36.

Miralles, F., Posern, G., Zaromytidou, A.I., and Treisman, R. (2003). Actin dynamics control SRF activity by regulation of its coactivator MAL. Cell 113, 329-42.

Miralles, F., Hebrard, S., Lamotte, L., Durel, B., Gilgenkrantz, H., Li, Z., Daegelen, D., Tuil, D., and Joshi, R.L. (2006). Conditional inactivation of the murine serum response factor in the pancreas leads to severe pancreatitis. Lab Invest 86, 1020–36.

Misra, R.P. (2010). The Role of Serum Response Factor in Early Coronary Vasculogenesis. Pediatr Cardiol 31, 400-7.

Modak, C. and Chai, J. (2010). Serum response factor: look into the gut. World J Gastroenterol 16, 2195-201.

Mokalled, M.H., Johnson, A., Kim, Y., Oh, J., and Olson, E.N. (2010). Myocardin-related transcription factors regulate the Cdk5/Pctaire1 kinase cascade to control neurite outgrowth, neuronal migration and brain development. Development 137, 2365-74.

Mohammed, M.A., Seleim, M.F., Abdalla, M.S. Sharada, H.N., and Abdel Wahab, A.H.A. (2003). Urinary high molecular weight matrixmetalloproteinases as non-invasive biomarker for detection of bladder cancer. BMC urology, 13:25.

Moon, S.Y. and Zheng, Y. (2003). Rho GTPase-activating proteins in cell regulation. Trends Cell Biol 13, 13-22.

Moon, Y., Bottone, F.G. Jr., McEntee, M.F., and Eling, T.E. (2005). Suppression of tumor cell invasion by cyclooxygenase inhibitors is mediated by thrombospondin-1 via the early growth response gene Egr-1. Mol Cancer Ther 4, 1551-8.

Morgan, T.E., Lockerbie, R.O., Minamide, L.S., Browning, M.D., and Bamburg, J.R. (1993). Isolation and characterization of a regulated form of actin depolymerizing factor. J Cell Biol 122, 623-33.

Morton, W.M., Ayscough, K.R., and McLaughlin, P.J. (2000). Latrunculin alters the actin-monomer subunit interface to prevent polymerization. Nat Cell Biol 2, 376-8.

Mosmann, T. (1983). Rapid colorimetric assay for cellular growth and survival: application to proliferation and cytotoxicity assays. J Immunol Methods 65, 55-63.

Mouilleron, S., Guettler, S., Langer, C.A., Treisman, R., and McDonald, N.Q. (2008). Molecular basis for G-actin binding to RPEL motifs from the serum response factor coactivator MAL. The EMBO J 27, 3198-208.

Mouilleron, S., Langer, C.A., Guettler, S., McDonald, N.Q., and Treisman, R. (2011). Structure of a pentavalent G-actin/MRTF-A complex reveals how G-actin controls nucleocytoplasmic shuttling of a transcriptional coactivator. Sci Signal 4, ra40.

Muehlich, S., Wang, R., Lee, S.M., Lewis, T.C., Dai, C., and Prywes, R. (2008). Serum-induced phosphorylation of the serum response factor coactivator MKL1 by the extracellular signal-regulated kinase 1/2 pathway inhibits its nuclear localization. Mol Cell Biol 28, 6302-13.

Muehlich, S., Hampl, V., Khalid, S., Singer, S., Frank, N., Breuhahn, K., Gudermann, T., and Prywes, R. (2012). The transcriptional coactivators megakaryoblastic leukemia 1/2 mediate the effects of loss of the tumor suppressor deleted in liver cancer 1. Oncogene 31, 3913-23.

Murphy, G. (2011). Tissue inhibitors of metalloproteinases. Genome Biol 12, 233.

Nagase, H., Visse, R., and Murphy, G. (2006). Structure and function of matrix metalloproteinases and TIMPs. Cardiovasc Res 69, 562-73.

Nakamura, E.S., Koizumi, K., Kobayashi, M. and Saiki, I. (2004). Inhibition of lymphangiogenesis-related properties of murine lymphatic endothelial cells and lymph node metastasis of lung cancer by the matrix metalloproteinase inhibitor MMI270. Cancer Sci 95, 25-31.

Nakamura, S., Hayashi, K., Iwasaki, K., Fujioka, T., Egusa, H., Yatani, H. and Sobue, K. (2010). Nuclear import mechanism for myocardin family members and their correlation with vascular smooth muscle cell phenotype. J Biol Chem 285, 37314-23.

Narumiya, S., Tanji, M. and Ishizaki, T. (2009). Rho signaling, ROCK and mDia1, in transformation, metastasis and invasion. Cancer Metastasis Rev 28, 65-76.

Nelson, J.D., Denisenko, O. and Bomsztyk, K. (2006). Protocol for the fast chromatin immunoprecipitation (ChIP) method. Nat Protoc 1, 179-85.

Ngok, S.P. and Anastasiadis, P.Z. (2013). Rho GEFs in endothelial junctions: Effector selectivity and signaling integration determine junctional response. Tissue Barriers. 1:5,e27132.

Ngok, S.P., Geyer, R., Kourtidis, A., Mitin, N., Feathers, R., Der, C., and Anastasiadis, P.Z. (2013). TEM4 is a junctional Rho GEF required for cell-cell adhesion, monolayer integrity and barrier function. J Cell Sci 126, 3271-7.

Nessa, A., Latif, S.A., Siddiqui, N.I., Hussain, M.A., Bhuiyan, M.R., Hossain, M.A., Akther, A., and Rahman, M. (2009). Angiogenesis-a novel therapeutic approach for ischemic heart disease. Mymensingh Med J 18, 264-72.

Nobes, C.D. and Hall, A. (1995). Rho, rac, and cdc42 GTPases regulate the assembly of multimolecular focal complexes associated with actin stress fibers, lamellipodia, and filopodia. Cell 81, 53-62.

Norman, C., Runswick, M., Pollock, R., and Treisman, R. (1988). Isolation and properties of cDNA clones encoding SRF, a transcription factor that binds to the c-fos serum response element. Cell 55, 989-1003.

Nunes, K.P., Rigsby, C.S., and Webb, R.C. (2010). RhoA/Rho-kinase and vascular diseases: what is the link? Cell Mol Life Sci 67, 3823-36.

Nürnberg, A., Kitzing, T., and Grosse, R. (2011). Nucleating actin for invasion. Nat Rev Cancer 11, 177-87.

Nuttall, R.K., Sampieri, C.L., Pennington, C.J., Gill, S.E., Schultz, G.A., and Edwards, D.R. (2004). Expression analysis of the entire MMP and TIMP gene families during mouse tissue development. FEBS Lett 563, 129-34.

Ogawa, S., Oku, A., Sawano, A., Yamaguchi, S., Yazaki, Y., and Shibuya, M. (1998). A novel type of vascular endothelial growth factor, VEGF-E (NZ-7 VEGF), preferentially utilizes KDR/Flk-1 receptor and carries a potent mitotic activity without heparin-binding domain. J Biol Chem 273, 31273-82.

Ohrnberger, S. (2010). Funktionen des Transkriptionsfaktors Serum Response Factor in der Leber der Maus. (Dissertation), Faculty of Science, University of Tuebingen.

Ohrnberger, S., Thavamani, A., Braeuning, A., Lipka, D.B., Kirilov, M., Geffers, R., Autenrieth, S.E., Römer, M., Zell, A., Bonin, M., Schwarz, M., Schütz, G., Schirmacher, P., Plass, C., Longerich, T., and Nordheim, A. (2015). Dysregulated serum response factor triggers formation of hepatocellular carcinoma. Hepatology 61, 979-89.

Okumura, N., Ueno, M., Koizumi, N., Sakamoto, Y., Hirata, K., Hamuro, J., and Kinoshita, S. (2009). Enhancement on primate corneal endothelial cell survival in vitro by a ROCK inhibitor. Invest Ophthalmol Vis Sci 50, 3680-7.

Olsen, J.V., Blagoev, B., Florian Gnad, F., Boris Macek, B., Kumar, C., Mortensen, P., and Mann, M. (2006). Global, In Vivo, and Site-Specific Phosphorylation Dynamics in Signaling Networks, Cell 127, 635–48.

Olson, E.N. and Nordheim, A. (2010). Linking actin dynamics and gene transcription to drive cellular motile functions. Nat Rev Mol Cell Biol 11, 353-65.

Olsson, A.K., Dimberg, A., Kreuger, J., and Claesson-Welsh, L. (2006). VEGF receptor signalling - in control of vascular function. Nat Rev Mol Cell Biol 7, 359-71.

Olofsson, B., Pajusola, K., Kaipainen, A., von Euler, G., Joukov, V., Saksela, O., Orpana, A., Pettersson, R.F., Alitalo, K., and Eriksson, U. (1996). Vascular endothelial growth factor B, a novel growth factor for endothelial cells. PNAS 93, 2576-81.

Orlandini, M., Marconcini, L., Ferruzzi, R., and Oliviero, S. (1996). Identification of a c-fos-induced gene that is related to the platelet-derived growth factor/ vascular endothelial growth factor family. PNAS 93, 11675–80.

Oswald, J., Boxberger, S., Jørgensen, B., Feldmann, S., Ehninger, G., Bornhäuser, M., and Werner, C. (2004). Mesenchymal stem cells can be differentiated into endothelial cells in vitro. Stem Cells 22, 377-84.

Owens, G.K., Kumar, M.S., and Wamhoff, B.R. Molecular regulation of vascular smooth muscle cell differentiation in development and disease. Physiol Rev 84, 767–801.

Paavonen, K., Horelli-Kuitunen, N., Chilov, D., Kukk, E., Pennanen, S., Kallioniemi, O.P., Pajusola, K., Olofsson, B., Eriksson, U., Joukov, V., Palotie, A., and Alitalo, K. (1996). Novel human vascular endothelial growth factor genes VEGF-B and VEGF-C localize to chromosomes 11q13 and 4q34, respectively. Circulation 93, 1079-82.

Parlakian, A., Tuil, D., Hamard, G., Tavernier, G., Hentzen, D., Concordet, J.P., Paulin, D., Li, Z., and Daegelen, D. (2004). Targeted inactivation of serum response factor in the developing heart results in myocardial defects and embryonic lethality. Mol Cell Biol 24, 5281–5289.

Parri, M. and Chiarugi, P. (2010). Rac and Rho GTPases in cancer cell motility control. Cell Commun Signal 8:23.

Pawłowski, R., Rajakylä, E.K., Vartiainen, M.K., and Treisman, R. (2010). An actin-regulated importin α/β-dependent extended bipartite NLS directs nuclear import of MRTF-A. EMBO J 29, 3448-58.

Perrin, B.J. and Ervasti, J.M. (2010). The actin gene family: function follows isoform. Cytoskeleton (Hoboken). 67, 630-4.

Plouët, J., Schilling, J., and Gospodarowicz, D. (1989). Isolation and characterization of a newly identified endothelial cell mitogen produced by AtT-20 cells. EMBO J 8, 3801–3806.

Parmacek, M.S. (2007). Myocardin-related transcription factors: critical coactivators regulating cardiovascular development and adaptation. Circ Res 100: 633-44.

Pellegrin, S. and Mellor, H. (2007). Actin stress fibres. J Cell Sci 120, 3491-9.

Pellegrini, L., Tan, S., and Richmond, T.J. (1995). Structure of serum response factor core bound to DNA. Nature 376, 490-8.

Piekny, A., Werner, M., and Glotzer, M. (2005). Cytokinesis: welcome to the Rho zone. Trends Cell Biol 15, 651-8.

Poser ,S., Impey, S., Trinh, K., Xia, Z., and Storm D.R. (2000). SRF-dependent gene expression is required for PI3-kinase-regulated cell proliferation. Embo J 19, 4955-66.

Posern, G. and Treisman, R. (2006). Actin' together: serum response factor, its cofactors and the link to signal transduction. Trends Cell Biol 16, 588-96.

Poesen, K., Lambrechts, D., Van Damme, P., Dhondt, J., Bender, F., Frank, N., Bogaert, E., Claes, B., Heylen, L., Verheyen, A., Raes, K., Tjwa, M., Eriksson, U., Shibuya, M., Nuydens, R., Van Den Bosch, L., Meert, T., D'Hooge, R., Sendtner, M., Robberecht, W., and Carmeliet, P. (2008). Novel role for vascular endothelial growth factor (VEGF) receptor-1 and its ligand VEGF-B in motor neuron degeneration. J Neurosci 28, 10451-9.

Pradeep, C.R., Sunila, E.S., and Kuttan, G. (2005). Expression of vascular endothelial growth factor (VEGF) and VEGF receptors in tumor angiogenesis and malignancies. Integr Cancer Ther 4, 315-21.

Primakoff, P and Myles, D.G. (2000). The ADAM gene family: surface proteins with adhesion and protease activity. Trends Genet 16, 83-7.

Provenzano, P.P. and Keely, PJ. (2011). Mechanical signaling through the cytoskeleton regulates cell proliferation by coordinated focal adhesion and Rho GTPase signaling. J Cell Sci 124, 1195-205.

Rafferty, B.J., Unger, B.L., Perey, A.C., Tammariello, S.P., Pavlides, S., and McGee, and D.W. (2012). A novel role for the Rho-associated kinase, ROCK, in IL-1-stimulated intestinal epithelial cell responses. Cell Immunol 280, 148-55

Ragu, C., Elain, G., Mylonas, E., Ottolenghi, C., Cagnard, N., Daegelen, D., Passegué E., Vainchenker, W., Bernard, O.A., and Penard-Lacronique, V. (2010). The transcription factor Srf regulates hematopoietic stem cell adhesion. Blood 116, 4464-73.

Reed, M.J., Iruela-Arispe, L., O'Brien, E.R., Truong, T., LaBell, T., Bornstein, P., and Sage, E.H. (1995). Expression of thrombospondins by endothelial cells. Injury is correlated with TSP-1. Am J Pathol 147, 1068-80.

Reiher, F.K., Volpert, O.V., Jimenez, B., Crawford, S.E., Dinney, C.P., Henkin, J., Haviv, F., Bouck, N.P., and Campbell, S.C. (2002). Inhibition of tumor growth by systemic treatment with thrombospondin-1 peptide mimetics. Int J Cancer 98, 682-9.

Ren, B., Yee, K.O., Lawler, J., and Khosravi-Far, R. (2006). Regulation of tumor angiogenesis by thrombospondin-1. Biochim Biophys Acta 1765, 178-88.

Ren, X.D., Kiosses, W.B. and Schwartz, M.A. (1999). Regulation of the small GTP-binding protein Rho by cell adhesion and the cytoskeleton. EMBO J 18, 578–85.

Ridley, A.J. (2012). Historical overview of Rho GTPases. Methods Mol Biol 827, 3-12.

Rieker, C., Schober, A., Bilbao, A., Schütz, G., and Parkitna, J.R. (2012). Ablation of serum response factor in dopaminergic neurons exacerbates susceptibility towards MPTP-induced oxidative stress. Eur J Neurosci 35, 735-41.

Rigor, R.R., Shen, Q., Pivetti, C.D., Wu, M.H., and Yuan, S.Y. (2013). Myosin light chain kinase signaling in endothelial barrier dysfunction. Med Res Rev 33, 911-33.

Robinson, C.J. and Stringer, S.E. (2001). The splice variants of vascular endothelial growth factor (VEGF) and their receptors. J Cell Sci 114, 853-65.

Roskoski Jr., R. (2007). Vascular endothelial growth factor (VEGF) signaling in tumor progression. Crit Rev Oncol Hematol 62, 179-213.

Rossman, K.L., Der, C.J., and Sondek, J. (2005). GEF means go: turning on RHO GTPases with guanine nucleotide-exchange factors. Nat Rev Mol Cell Biol 6, 167-80.

Rottner, K. and Stradal, T.E. (2011). Actin dynamics and turnover in cell motility. Curr Opin Cell Biol 23, 569-78.

Rundhaug, J.E. (2003). Matrix Metalloproteinases, Angiogenesis, and Cancer. Clin Cancer Res 9, 551-554.

Rundhaug, J.E. (2005). Matrix metalloproteinases and angiogenesis. J Cell Mol Med 9, 267-85.

Saha, M., Ingraham, S.E., Carpenter, A., Robinson, M., McHugh, K.E., Singh, S., Robinson, M.L., and McHugh, K.M. (2009). Identification of distinct myocardin splice variants in the bladder. J Urol 182, 766-75.

Saito, S.Y. (2009). Toxins affecting actin filaments and microtubules. Prog Mol Subcell Biol 46:187-219.

Sandbo, N., Kregel, S., Taurin, S., Bhorade, S., and Dulin, N.O. (2009). Critical role of serum response factor in pulmonary myofibroblast differentiation induced by TGF-beta. Am J Respir Cell Mol Biol 41, 332-8.

Sandström, J., Heiduschka, P., Beck, S.C., Philippar, U., Seeliger, M.W., Schraermeyer, U., and Nordheim, A. (2011). Degeneration of the mouse retina upon dysregulated activity of serum response factor. Mol Vis 17:1110-27.

Sarkar, A., Zhang, M., Liu, S.H., Sarkar, S., Brunicardi, F.C., Berger, D.H., and Belaguli, N.S. (2011). Serum response factor expression is enriched in pancreatic β cells and regulates insulin gene expression. FASEB J 25, 2592-603.

Scharenberg, M.A., Chiquet-Ehrismann, R., and Asparuhova, M.B. (2010). Megakaryoblastic leukemia protein-1 (MKL1): Increasing evidence for an involvement in cancer progression and metastasis. Int J Biochem Cell Biol 42, 1911-4.

Schmittgen, T.D. and Livak, K.J. (2008). Analyzing real-time PCR data by the comparative C(T) method. Nat Protoc 3, 1101-8.

Schratt, G., Weinhold, B., Lundberg, N.S., Schuck, S., Berger, J., Schwarz, H., Weinberg, R.A., Rüther, U., and Nordheim, A. (2001). Serum response factor is required for immediate-early gene activation yet is dispensable for proliferation of embryonic stem cells Mol Cell Biol 21, 2933-43.

Schratt, G., Philippar, U., Hockemeyer, D., Schwarz, H., Alberti, S., and Nordheim, A. (2004). SRF regulates Bcl-2 expression and promotes cell survival during murine embryonic development. The EMBO J 23, 1834-44.

Schofield, A.V., Steel, R., and Bernard, O. (2012). Rho-associated coiled-coil kinase (ROCK) protein controls microtubule dynamics in a novel signaling pathway that regulates cell migration. J Biol Chem 287, 43620-9.

Schwarz-Sommer, Z., Huijser, P., Nacken, W., Saedler, H., and Sommer, H. (1990). Genetic Control of Flower Development by Homeotic Genes in Antirrhinum majus. Science 250, 931-936.

Sebe, A., Masszi, A., Zulys, M., Yeung, T., Speight, P., Rotstein, O.D., Nakano, H., Mucsi, I., Szászi, K., and Kapus, A. (2008). Rac, PAK and p38 regulate cell contact-dependent nuclear translocation of myocardin-related transcription factor. FEBS Lett. 582, 291-8.

Sehr, P., Joseph, G., Genth, H., Just, I., Pick, E., and Aktories, K. (1998). Glucosylation and ADP ribosylation of rho proteins: effects on nucleotide binding, GTPase activity, and effector coupling. Biochemistry 37, 5296-304.

Selvaraj, A. and Prywes, R. (2004). Expression profiling of serum inducible genes identifies a subset of SRF target genes that are MKL dependent. BMC Mol Biol 5:13.

Senger, D.R., Galli, S.J., Dvorak, A.M., Perruzzi, C.A., Harvey, V.S., and Dvorak, H.F. (1983). Tumor cells secrete a vascular permeability factor that promotes accumulation of ascites fluid. Science 219, 983-5.

Senger, D.R., Perruzzi, C.A., Feder, J., and Dvorak, H.F. (1986). A highly conserved vascular permeability factor secreted by a variety of human and rodent tumor cell lines. Cancer Res 46, 5629-32.

Shalaby, F., Ho, J., Stanford, W.L., Fischer, K.D., Schuh, A.C., Schwartz, L., Bernstein, A., and Rossant, J. (1997). A requirement for Flk1 in primitive and definitive hematopoiesis and vasculogenesis. Cell 89, 981–90.

Shalaby, F., Rossant, J., Yamaguchi, T.P., Gertsenstein, M., Wu, X.F., Breitman, M.L., and Schuh, A.C. (1995). Failure of blood-island for- mation and vasculogenesis in Flk-1-deficient mice. Nature 376, 62–6.

Shaposhnikov, D., Descot, A., Schilling, J., and Posern, G. (2012). Myocardin-related transcription factor A regulates expression of Bok and Noxa and is involved in apoptotic signalling. Cell Cycle 11, 141-50.

Shaw, P.E., Schroter, H., and Nordheim, A. (1989). The ability of a ternary complex to form over the serum response element correlates with serum inducibility of the human c-fos promoter. Cell 56, 563-572.

Sheibani, N., Newman, P.J., and Frazier, W.A. (1997). Thrombospondin-1, a natural inhibitor of angiogenesis, regulates platelet-endothelial cell adhesion molecule-1 expression and endothelial cell morphogenesis. Mol Biol Cell 8, 1329-41.

Shen, Q., Rigor, R.R., Pivetti, C.D., Wu, M.H., and Yuan, S.Y. (2010). Myosin light chain kinase in microvascular endothelial barrier function. Cardiovasc Res 87, 272-80.

Short, S.M., Derrien, A., Narsimhan, R.P., Lawler, J., Ingber, D.E., and Zetter, B.R. (2005). Inhibition of endothelial cell migration by thrombospondin-1 type-1 repeats is mediated by beta1 integrins. J Cell Biol 168, 643-53.

Small, E.M., Thatcher, J.E., Sutherland, L.B., Kinoshita, H., Gerard, R.D., Richardson, J.A., Dimaio, J.M., Sadek, H., Kuwahara, K., and Olson, E.N. (2010). Myocardin-related transcription factor-a controls myofibroblast activation and fibrosis in response to myocardial infarction. Circ Res 107, 294-304.

Smith, E.C., Thon, J.N., Devine, M.T., Lin, S., Schulz, V.P., Guo, Y., Massaro, S.A., Halene, S., Gallagher, P., Italiano, J.E. Jr., and Krause, D.S. (2012). MKL1 and MKL2 play redundant and crucial roles in megakaryocyte maturation and platelet formation. Blood 120, 2317-29.

Smith, E.C., Teixeira, A.M., Chen, R.C., Wang, L., Gao, Y., Hahn, K.L., and Krause, D.S. (2013). Induction of megakaryocyte differentiation drives nuclear accumulation and transcriptional function of MKL1 via actin polymerization and RhoA activation. Blood 121, 1094-101.

Sotiropoulos, A., Gineitis, D., Copeland, J., and Treisman, R. (1999). Signal-regulated activation of serum response factor is mediated by changes in actin dynamics. Cell 98, 159-69.

Spindler, V., Schlegel, N., and Waschke, J. (2010). Role of GTPases in control of microvascular permeability. Cardiovasc Res 87, 243-53.

Stockton, R.A., Shenkar, R., Awad, I.A., and Ginsberg, M.H. (2010). Cerebral cavernous malformations proteins inhibit Rho kinase to stabilize vascular integrity. J Exp Med 207, 881-96.

Stoll, S.J. and Kroll, J. (2012). HOXC9: a key regulator of endothelial cell quiescence and vascular morphogenesis. Trends Cardiovasc Med 22, 7-11.

Streit, M., Velasco, P., Brown, L.F., Skobe, M., Richard, L., Riccardi, L., Lawler, J., and Detmar, M. (1999). Overexpression of thrombospondin-1 decreases angiogenesis and inhibits the growth of human cutaneous squamous cell carcinomas. Am J Pathol 155, 441-52.

Stringer, J.L., Belaguli, N.S., Iyer, D., Schwartz, R.J., and Balasubramanyam, A. (2002). Developmental expression of serum response factor in the rat central nervous system. Dev Brain Res 138, 81–86.

Stritt, C., Stern, S., Harting, K., Manke, T., Sinske, D., Schwarz, H., Vingron, M., Nordheim, A., and Knöll, B. (2009). Paracrine control of oligodendrocyte differentiation by SRF-directed neuronal gene expression. Nat Neurosci 12, 418-27.

Stuttfeld, E. and Ballmer-Hofer, K. (2009). Structure and function of VEGF receptors. IUBMB Life 61, 915-22.

Suchting, S. and Eichmann, A. (2009). Jagged gives endothelial tip cells an edge. Cell 137, 988-90.

Suehiro, J., Hamakubo, T., Kodama, T., Aird, W.C., and Minami, T. (2010). Vascular endothelial growth factor activation of endothelial cells is mediated by early growth response-3. Blood 115, 2520-32.

Sumpio, B.E., Riley, J.T., and Dardik, A. (2002). Cells in focus: endothelial cell. Int J Biochem Cell Biol 34, 1508-12.

Sun, K., Battle, M.A., Misra, R.P., and Duncan, S.A. (2009). Hepatocyte expression of serum response factor is essential for liver function, hepatocyte proliferation and survival, and postnatal body growth in mice. Hepatology 49, 1645–1654.

Sun, J. (2010). Matrix metalloproteinases and tissue inhibitor of metalloproteinases are essential for the inflammatory response in cancer cells. J Signal Transduct. 2010:985132.

Sun, Q., Chen, G., Streb, J.W., Long, X., Yang, Y., Stoeckert Jr, C.J., and Miano, J.M. (2006). Defining the mammalian CArGome. Genome Res 16, 197-207.

Surma, M., Wei, L., and Shi, J. (2011). Rho kinase as a therapeutic target in cardiovascular disease. Future Cardiol 7, 657-71

Sounni, N.E., Dehne, K., van Kempen, L., Egeblad, M., Affara, N.I., Cuevas, I., Wiesen, J., Junankar, S., Korets, L., Lee, J., Shen, J., Morrison, C.J., Overall, C.M., Krane, S.M., Werb, Z., Boudreau, N., and Coussens, L.M. (2010). Stromal regulation of vessel stability by MMP14 and TGFbeta. Dis Model Mech 3, 317-32.

Swendeman, S., Mendelson, K., Weskamp, G., Horiuchi, K., Deutsch, U., Scherle, P,, Hooper, A., Rafii, S., and Blobel, C.P. (2008). VEGF-A stimulates ADAM17-dependent shedding of VEGFR2 and crosstalk between VEGFR2 and ERK signaling. Circ Res 103, 916-8.

Tabuchi, A., Estevez, M., Henderson, J.A., Marx, R., Shiota, J., Nakano, H., and Baraban, J.M. (2005). Nuclear translocation of the SRF co-activator MAL in cortical neurons: role of RhoA signalling. J Neurochem 94, 169-80.

Takahashi, J.S., Hong, H.K., Ko, C.H., and McDearmon, E.L. (2008). The genetics of mammalian circadian order and disorder: implications for physiology and disease. Nat Rev Genet 9, 764-75.

Tham, E., Gielen, A.W., Khademi, M., Martin, C., and Piehl, F. (2006). Decreased expression of VEGF-A in rat experimental autoimmune encephalomyelitis and in cerebrospinal fluid mononuclear cells from patients with multiple sclerosis. Scand J Immunol 64, 609-22.

Thuy le, T.T., Morita, T., Yoshida, K., Wakasa, K., Iizuka, M., Ogawa, T., Mori, M., Sekiya, Y., Momen, S., Motoyama, H., Ikeda, K., Yoshizato, K., and Kawada, N. (2011). Promotion of liver and lung tumorigenesis in DEN-treated cytoglobin-deficient mice. Am J Pathol 179, 1050-60.

Treisman, R. (1986). Identification of a protein-binding site that mediates transcriptional response of the c-fos gene to serum factors. Cell, 46, 567–574.

Treisman, R. (1987). Identification and purification of a polypeptide that binds to the c-fos serum response element. EMBO J., 6, 2711–2717.

Ueda, T., Kikuchi, A., Ohga, N., Yamamoto, J., and Takai, Y. (1990). Purification and characterization from bovine brain cytosol of a novel regulatory protein inhibiting the dissociation of GDP from and the subsequent binding of GTP to rhoB p20, a ras p21-like GTP-binding protein. J Biol Chem 265, 9373-80.

Urso, M.L., Szelenyi, E.R., Warren, G.L., and Barnes, B.R. (2010). Matrix metalloprotease-3 and tissue inhibitor of metalloprotease-1 mRNA and protein levels are altered in response to traumatic skeletal muscle injury. Eur J Appl Physiol 109, 963-72.

van der Meel, R., Symons, M.H., Kudernatsch, R., Kok, R.J., Schiffelers, R.M., Storm, G., Gallagher, W.M., and Byrne, A.T. (2011). The VEGF/Rho GTPase signalling pathway: a promising target for anti-angiogenic/anti-invasion therapy. Drug Discov Today 16, 219-28.

van Nieuw Amerongen, G.P., Koolwijk, P., Versteilen, A., and van Hinsbergh, V.W. (2003). Involvement of RhoA/Rho kinase signaling in VEGF-induced endothelial cell migration and angiogenesis in vitro. Arterioscler Thromb Vasc Biol 23, 211-7.

Vartiainen, M.K., Guettler, S., Larijani, B., and Treisman, R. (2007). Nuclear actin regulates dynamic subcellular localization and activity of the SRF cofactor MAL. Science 316, 1749-52.

Velasquez, L.S., Sutherland, L.B., Liu, Z., Grinnell, F., Kamm, K.E., Schneider, J.W., Olson, E.N., and Small, E.M. (2013). Activation of MRTF-A-dependent gene expression with a small molecule promotes myofibroblast differentiation and wound healing. PNAS 110, 16850-5.

Verdoni, A.M., Ikeda, S, and Ikeda, A. (2010). Serum response factor is essential for the proper development of skin epithelium. Mamm Genome 21, 64–76

Vincenti, V., Cassano, C., Rocchi, M., and Persico, G. (1996). Assignment of the vascular endothelial growth factor gene to human chromosome 6p21.3. Circulation 93, 1493-5.

Voelkel, N. and Rounds, S. (2009). The Pulmonary Endothelium: Function in Health and Disease, Chapter 19, Wiley-Blackwell.

Wakatsuki, T., Schwab, B., Thompson, N.C., and Elson, E.L. (2001). Effects of cytochalasin D and latrunculin B on mechanical properties of cells. J Cell Sci 114, 1025-36.

Wang, D.Z., Li, S., Hockemeyer, D., Sutherland, L., Wang, Z., Schratt, G., Richardson, J.A., Nordheim, A., and Olson EN. (2002). Potentiation of serum response factor activity by a family of myocardin-related transcription factors. PNAS 99, 14855-60.

Wang, D.Z. and Olson, E.N. (2004). Control of smooth muscle development by the myocardin family of transcriptional coactivators, Curr Opin Genet Dev 14, 558-66.

Wang, N., Zhang, R., Wang, S.J., Zhang, C.L., Mao, L.B., Zhuang, C.Y., Tang, Y.Y., Luo, X.G., Zhou, H., and Zhang, T.C. (2013). Vascular endothelial growth factor stimulates endothelial differentiation from mesenchymal stem cells via Rho/myocardin-related transcription factor--a signaling pathway. Int J Biochem Cell Biol 1447-56.

Wei, K., Che, N., and Chen, F. (2007). Myocardin-related transcription factor B is required for normal mouse vascular development and smooth muscle gene expression. Dev Dyn 236, 416-25.

Weinl, C., Riehle, H., Park, D., Stritt, C., Beck, S., Huber, G., Wolburg, H., Olson, E.N., Seeliger, M.W., Adams, R.H., and Nordheim A. (2013). Endothelial SRF/MRTF ablation causes vascular disease phenotypes in murine retinae. J Clin Invest 123, 2193-206.

Weinl, C., Castaneda Vega, S., Riehle, H., Stritt, C., Calaminus, C., Wolburg, H., Mauel, S., Breithaupt, A., Gruber, A.D., Wasylyk, B., Olson, E.N., Adams, R.H., Pichler, B.J., and Nordheim, A. (2015). Endothelial depletion of murine SRF/MRTF provokes intracerebral hemorrhagic stroke. PNAS 112, 9914-9.

Weinhold, B., Schratt, G., Arsenian, S., Berger, J., Kamino, K., Schwarz, H., Rüther, U., and Nordheim, A. (2000). Srf(-/-) ES cells display non-cell-autonomous impairment in mesodermal differentiation. EMBO J 19, 5835-44.

Werth, D., Grassi, G., Konjer, N., Dapas, B., Farra, R., Giansante, C., Kandolf, R., Guarnieri, G., Nordheim, A., and Heidenreich, O. (2010). Proliferation of human primary vascular smooth muscle cells depends on serum response factor. Eur J Cell Biol 89, 216–224.

Xie, B., Shen, J., Dong, A., Swaim, M., Hackett, S.F., Wyder, L., Worpenberg, S., Barbieri, S., and Campochiaro, P.A. (2008). An Adam15 amplification loop promotes vascular endothelial growth factor-induced ocular neovascularization. FASEB J 22, 2775-83.

Yan, L., Borregaard, N., Kjeldsen. L., and Moses M.A. (2001). The High Molecular Weight Urinary Matrix Metalloproteinase (MMP) Activity Is a Complex of Gelatinase B/MMP-9 and Neutrophil Gelatinase-associated Lipocalin (NGAL): MODULATION OF MMP-9 ACTIVITY BY NGAL. J Biol Chem 276, 37258-65.

Yang, C. and Svitkina, T. (2011). Filopodia initiation: focus on the Arp2/3 complex and formins. Cell Adh Migr 5, 402-8.

Ye, Z., Zhang, C., Tu, T., Sun, M., Liu, D., Lu, D., Feng, J., Yang, D., Liu, F., and Yan X. (2013). Wnt5a uses CD146 as a receptor to regulate cell motility and convergent extension. Nat Commun 4:2803.

Yeh, H.I., Lai, Y.J., Chang, H.M., Ko, Y.S., Severs, N.J., and Tsai, C.H. (2000). Multiple connexin expression in regenerating arterial endothelial gap junctions. Arterioscler Thromb Vasc Biol 20,1753-62.

Yin, K.J., Cirrito, J.R., Yan, P., Hu, X., Xiao, Q., Pan, X., Bateman, R., Song, H., Hsu, F.F., Turk, J., Xu, J., Hsu, C.Y., Mills, J.C., Holtzman, D.M., and Lee, J.M. (2006). Matrix metalloproteinases expressed by astrocytes mediate extracellular amyloid-beta peptide catabolism. J Neurosci 26, 10939-48.

Yoo, P.S., Mulkeen, A.L., and Cha, C.H. (2006). Post-transcriptional regulation of vascular endothelial growth factor: implications for tumor angiogenesis. World J Gastroenterol 12, 4937-42.

Zachary, I. and Gliki, G. (2001). Signaling transduction mechanisms mediating biological actions of the vascular endothelial growth factor family. Cardiovasc Res 49, 568-81.

Zhang, X., Azhar, G., Chai, J., Sheridan, P., Nagano, K., Brown, T., Yang, J., Khrapko, K., Borras, A.M., Lawitts, J., Misra, R.P., and Wei, J.Y. (2001). Cardiomyopathy in transgenic mice with cardiac-specific overexpression of serum response factor. Am J Physiol Heart Circ Physiol 280, H1782-92.

Zhang, X., Azhar, G., Helms, S.A., and Wei, J.Y. (2011). Regulation of cardiac microRNAs by serum response factor. J Biomed Sci 18:15.

Zhao, X., Cho, H., and Evans, R.M. (2013). SRF'ing around the clock. Cell 152, 381-2.

Zhou, H., Falkenburger, B.H., Schulz, J.B., Tieu, K., Xu, Z., and Xia, X.G. (2007). Silencing of the Pink1 gene expression by conditional RNAi does not induce dopaminergic neuron death in mice. Int J Biol Sci 3, 242-50.